

11-7-2012

# Developing an Enhanced Model for Combined Heat and Air Infiltration Energy Simulation

Chadi Younes

*Florida International University*, [chadi.younes@fiu.edu](mailto:chadi.younes@fiu.edu)

**DOI:** 10.25148/etd.FI12112705

Follow this and additional works at: <https://digitalcommons.fiu.edu/etd>

---

## Recommended Citation

Younes, Chadi, "Developing an Enhanced Model for Combined Heat and Air Infiltration Energy Simulation" (2012). *FIU Electronic Theses and Dissertations*. 743.

<https://digitalcommons.fiu.edu/etd/743>

This work is brought to you for free and open access by the University Graduate School at FIU Digital Commons. It has been accepted for inclusion in FIU Electronic Theses and Dissertations by an authorized administrator of FIU Digital Commons. For more information, please contact [dcc@fiu.edu](mailto:dcc@fiu.edu).

FLORIDA INTERNATIONAL UNIVERSITY

Miami, Florida

DEVELOPING AN ENHANCED MODEL FOR COMBINED HEAT AND AIR  
INFILTRATION ENERGY SIMULATION

A dissertation submitted in partial fulfillment of the

requirements for the degree of

DOCTOR OF PHILOSOPHY

in

CIVIL ENGINEERING

by

Chadi Younes

2012

To: Dean Amir Mirmiran  
College of Engineering and Computing

This dissertation, written by Chadi Younes, and entitled Developing an Enhanced Model for Combined Heat and Air Infiltration Energy Simulation, having been approved in respect to style and intellectual content, is referred to you for judgment.

We have read this thesis and recommend that it be approved.

---

Hector Fuentes

---

Arindam Chowdhury

---

Yiding Cao

---

Yimin Zhu

---

Caesar Abi Shdid, Major Professor

Date of Defense: November 7, 2012

The dissertation of Chadi Younes is approved.

---

Dean Amir Mirmiran  
College of Engineering and Computing

---

Dean Lakshmi N. Reddi  
University Graduate School

Florida International University, 2012

© Copyright 2012 by Chadi Younes

All rights reserved.



حَسْبُنَا اللهُ وَنِعْمَ الْوَكِيلُ  
هَذِهِ تِلْكَ الْقِسْمَةُ .

## DEDICATION

I dedicate this dissertation to my parents for their devotion, continuous encouragement and prayers; and to Ruba, Rana & Nawal for their unlimited love and support.

## ACKNOWLEDGMENTS

I wish to thank my major professor, Dr. Caesar Abi Shdid for the guidance and mentorship he provided me throughout my graduate studies. His dedication, guidance and support made this work possible and successful. I am truly fortunate for having the opportunity to work with him.

I also wish to thank the members of my committee for their support and guidance. Drs. Hector R. Fuentes, Arindam Chowdhury, Yiding Cao and Yimin Zhu input on my research was particularly helpful. I would especially like to acknowledge the dedication of Dr. Fuentes to insure the quality and clarity of this manuscript.

I wish to acknowledge the support of the University Graduate School at Florida International University, especially for awarding me the Dissertation Year Fellowship which allowed me to concentrate my time and efforts on completing this dissertation. In addition, I profoundly appreciate the support of the Department of Civil and Environmental Engineering for in the form of graduate assistantships throughout my graduate studies at FIU. I also owe special thanks to the Civil & Environmental Engineering Department personnel and to the FIU libraries staff.

Finally, it is a great pleasure to thank everyone who helped me write my dissertation successfully.

ABSTRACT OF THE DISSERTATION  
DEVELOPING AN ENHANCED MODEL FOR COMBINED HEAT AND AIR  
INFILTRAION ENERGY SIMULATION

by

Chadi Younes

Florida International University, 2012

Miami, Florida

Professor Caesar Abi Shdid, Major Professor

The need for efficient, sustainable, and planned utilization of resources is ever more critical. In the U.S. alone, buildings consume 34.8 Quadrillion ( $10^{15}$ ) BTU of energy annually at a cost of \$1.4 Trillion. Of this energy 58% is utilized for heating and air conditioning.

Several building energy analysis tools have been developed to assess energy demands and lifecycle energy costs in buildings. Such analyses are also essential for an efficient HVAC design that overcomes the pitfalls of an under/over-designed system. DOE-2 is among the most widely known full building energy analysis models. It also constitutes the simulation engine of other prominent software such as eQUEST, EnergyPro, PowerDOE. Therefore, it is essential that DOE-2 energy simulations be characterized by high accuracy.

Infiltration is an uncontrolled process through which outside air leaks into a building. Studies have estimated infiltration to account for up to 50% of a building's energy demand. This, considered alongside the annual cost of buildings energy

consumption, reveals the costs of air infiltration. It also stresses the need that prominent building energy simulation engines accurately account for its impact.

In this research the relative accuracy of current air infiltration calculation methods is evaluated against an intricate Multiphysics Hygrothermal CFD building envelope analysis. The full-scale CFD analysis is based on a meticulous representation of cracking in building envelopes and on real-life conditions. The research found that even the most advanced current infiltration methods, including in DOE-2, are at up to 96.13% relative error versus CFD analysis.

An Enhanced Model for Combined Heat and Air Infiltration Simulation was developed. The model resulted in 91.6% improvement in relative accuracy over current models. It reduces error versus CFD analysis to less than 4.5% while requiring less than 1% of the time required for such a complex hygrothermal analysis. The algorithm used in our model was demonstrated to be easy to integrate into DOE-2 and other engines as a standalone method for evaluating infiltration heat loads. This will vastly increase the accuracy of such simulation engines while maintaining their speed and ease of use characteristics that make them very widely used in building design.

## TABLE OF CONTENTS

CHAPTER	PAGE
Chapter 1 Introduction .....	1
Main Objective .....	9
Specific Objectives .....	9
Justification .....	10
Chapter 2 Background .....	14
Building Energy Simulation Programs.....	16
DOE-2 .....	18
DOE-2 Programs.....	18
How a DOE-2 Simulation Works .....	23
Weighting Factors.....	24
Response Factors .....	28
Heat Balance .....	30
Heat-Gain Weighting Factors .....	34
Determination of Hourly Loads & Space Temperatures.....	37
eQUEST .....	39
Infiltration.....	43
Infiltration in ASHRAE .....	45
Residential Calculation Models .....	47
Empirical Models .....	47
Multizone Models.....	47
Single Zone Models.....	48
Superposition of Wind and Stack Effects.....	48
Infiltration in Commercial Buildings.....	48
Air Infiltration Calculation Techniques & Methods .....	52
Empirical Techniques .....	58
Air Change methods .....	58
Reduction Pressurization Test Data .....	59
Regression Techniques .....	59
Theoretical Methods .....	60
Single-Zone Models.....	62
Multizone Models.....	63
CFD, FFD, AND COMBINED MULTIZONE-CFD METHODS.....	65
Types of Air Infiltration .....	68
Concentrated Air Infiltration.....	69
Doors.....	69
Windows .....	74
Fire Place .....	75
Diffuse Air Infiltration: Heat Recovery .....	77
Building Energy Simulation Infiltration Evaluation Approach .....	85
Current Approach.....	85
Air-Change Method .....	85
Residential Method.....	86
Crack Method .....	87
Sherman – Grimsrud Method & ASHRAE Enhanced Method .....	87

Final Calculation.....	89
Chapter 3 Methodology .....	90
Combined Infiltration, Conduction & Solar Model .....	90
Differential Equation .....	91
Differential Equation Discretization .....	94
Internal Node/Layer .....	94
External Node/Layer of wall.....	96
Outside wall surface .....	97
Inside surface of the wall.....	98
Final Discretization.....	99
Infiltration Mass Flow Rate.....	102
Stack Effect.....	103
Wind Pressure .....	106
Wind Pressure Coefficients.....	108
Wind Direction .....	108
Wind Incidence Angle .....	111
Wind Speed.....	111
Local Shielding Parameters .....	115
Infiltration Mass Flow Rate .....	116
Solar Calculation and Shading.....	120
Solar Calculation.....	120
Declination Angle (DECLN).....	120
Solar Equation of Time (EQTIME).....	121
Solar Constant (SOLCON) .....	122
Atmospheric Excitation Coefficient (ATMEXT) .....	122
Sky Diffuse Factor (SKYDIFF).....	122
Shading Calculation .....	129
Shading Polygons .....	129
Shading Calculation Description .....	130
CFD Modeling of Cracks and Airflow Paths.....	132
Air Leakage Cracks & Paths.....	133
Equations Utilized.....	134
Cracking in Walls .....	135
Existing Literature .....	135
ASHRAE .....	136
In-Wall Leakage Path Crack Dimensions.....	137
Leakage Path Dimensions at Joints and Interfaces .....	138
Simulated Test Case: Location, Properties & Others .....	139
Model Location.....	141
Model Material and Construction Method.....	143
CFD Model .....	144
Model Construction .....	144
Chapter 4 Modeling and Simulation.....	149
Hygrothermal Multiphysics CFD Analysis.....	149
Model Meshing.....	149
CFD Analysis Fundamentals .....	154
Energy.....	154
Solar Radiation .....	155

Weather and ground Conditions .....	157
eQUEST – DOE-2 Hourly Analysis .....	159
Model Properties.....	159
Infiltration Method.....	165
Enhanced Model.....	165
Mass Flow Rate Model.....	167
Infiltration Heat Load .....	167
Chapter 5 Results and Discussion.....	171
Simulation Duration.....	171
Southwest Wall (SW).....	174
Northwest Wall (NW).....	183
Discussion of Results.....	191
Heat Loading Error .....	191
Simulation Speed .....	194
Enhanced Model Ease of Use .....	197
Infiltration Heat Recovery.....	198
Chapter 6 Conclusions and Recommended Future Work.....	205
Fulfilled Research Objectives .....	209
Recommended Future Work.....	210
References.....	212
APPENDICES .....	223
VITA.....	307



## LIST OF FIGURES

FIGURE	PAGE
Figure 2-1: Overlapping triangular pulses defining a function (DOE-2 Engineers manual, 1982) .....	29
Figure 2-2: Flow of Energy through a multilayer wall (DOE-2 Engineers manual, 1982) .....	30
Figure 2-3: Typical Infiltration & Ventilation Airflow .....	45
Figure 3-1: Heat flux flow control volume .....	92
Figure 3-2: Nodes and notation.....	94
Figure 3-3: Node on the outside surface of the wall.....	97
Figure 3-4: Node on the inside surface of the wall.....	98
Figure 3-5: A wall with multiple layers and n nodes.....	100
Figure 3-6: Stack Effect on a building wall .....	104
Figure 3-7: Wind pressure on a typical Gable, Hip roof house (Figure 6-6, ASCE 7-05) .....	107
Figure 3-9: Hourly Temperature and Wind data available from weather file (DOE-2/eQUEST) .....	113
Figure 3-10: Effective air leakage are, ASHRAE Handbook Chapter 25 Table 1 (partially).....	117
Figure 3-12: Daily Solar Geometry (DOE-2 Engineers Manual, 1982).....	125
Figure 3-13: Shading calculations related polygons.....	129
Figure 3-14: Shading calculation strips .....	131
Figure 3-15: Sample 2-D Infiltration CFD Models .....	132
Figure 3-16: Sample 2-D Infiltration CFD Models With Loading Induced Cracks .....	133
Figure 3-17: Crack Shape and Dimensions .....	136
Figure 3-18: Crack Shape and Dimensions .....	136

Figure 3-19: Chosen Location of Building Envelope, Vicinity of Fargo Intl, Fargo, North Dakota .....	142
Figure 3-20: Air Leakage By County (Sherman and McWilliams, 2007).....	142
Figure 3-21: Basic Block with Angled Crack and Electrical Inlet Crack.....	144
Figure 3-22: Basic Block with Angled Crack and Electrical Outlet Crack .....	144
Figure 3-23: A Mixed Crack Wall Created by Assembling 36 of the Basic Building Blocks .....	146
Figure 3-24: A Resulting Representative Concrete Cavity Wall.....	146
Figure 3-25: Wall Section Showing Internal Cavity and In-plane Cracks .....	147
Figure 3-26: Close-up Showing Corner/Joint Cracks.....	147
Figure 3-27: An X-ray of A Resulting 3D Model Showing All In-plane and Joint Cracks .....	147
Figure 4-1: Sample Full Model and Domain Mesh .....	150
Figure 4-2: Sample Full Model Mesh.....	151
Figure 4-3: Meshing of Minute Airflow Cracks .....	151
Figure 4-4: Tessellation of Thin Sections and Proper Mesh Attachment (contact) Between Fluid Outside the Envelope (1), Infiltrating Through Cracks (2), Inside Wall Cavity (3), In Corner Joints (4), and In Inner Domain(5).....	152
Figure 4-5: Meshing of Cavity Brick Walls, Proper Contact Between Solid & Fluid Meshes, and Close Up on a Sample Leakage Crack Mesh.....	153
Figure 4-6: Defining the Radiation Model.....	156
Figure 4-7: Setting the Solar Ray Tracing Model.....	157
Figure 4-8: Sample Hourly Temperature Profile .....	158
Figure 4-9: Applying Ground Temperature on the Defined Ground Boundary with Ground (Soil) Material Properties .....	158
Figure 4-10: Thermostat Settings in eQUEST to Match 72F in CFD Analysis .....	160
Figure 4-11: Defining Cavity Brick Wall in eQUEST .....	160

Figure 4-12: Defining Building Orientation in eQUEST to Match the CFD Analysis ..	161
Figure 4-13: Defining Ground Temperature and Building Coordinates.....	161
Figure 4-14: Building Operation set to 24 Hours Daily .....	162
Figure 4-15: No Holiday Defined, Continuous Building Operation.....	162
Figure 4-16: Defining Electric Baseboards for Heating .....	164
Figure 4-17: Defined HVAC System for The Building Model .....	164
Figure 4-18: Built Enhanced Model Input Interface.....	166
Figure 4-19: Hourly DOE-2/eQUEST Input into the Enhanced Model .....	168
Figure 4-20: Built Interface for the Mass Flow Rate Calculation Model.....	169
Figure 4-21: BUILT Enhanced Model Output Interface .....	170
Figure 5-1: Lateral-Section Temperature Contour Plot Across a CFD Model with Angled (Zig-Zag) Cracks.....	201
Figure 5-2: Lateral-Section Temperature Contour Plot Across a CFD Model with Mixed Cracks .....	201
Figure 5-3: Lateral-Section Temperature Contour Plot Across a CFD Model with Straight Cracks .....	202
Figure 5-4: Lateral-Section Velocity Vector Plot Across a CFD Model with Angled (zig-zag) Cracks.....	202
Figure 5-5: Vertical-Section Velocity Vector Plot Across a CFD Model with Mixed Straight and Angled Cracks .....	203
Figure 5-6: Vertical-Section Combined Velocity Vector and Temperature Contour Plot Across a CFD Model with Straight Cracks, with the Effect of Solar Heating Showing on the Envelope's Southern Wall .....	203
Figure 5-7: Vortex Plot Revealing Air Leakage Across In-wall Cracks (1), Corner Cracks (2) and Ceiling Joint Cracks (3).....	204

## LIST OF TABLES

TABLE	PAGE
Table 2-1: Choice of pulsated term in the heat balance equation .....	34
Table 2-2: Empirical Infiltration techniques (Based on Liddament (1986)) .....	57
Table 2-3: Theoretical Infiltration techniques; Based on Liddament (1986) .....	57
Table 2-4: Air Changes per Hour (ACH) estimated by Construction Tightness (Bobenhausen, 1994) .....	58
Table 2-5: Infiltration Through Entrances – Doors in One Wall Only (Infiltration Through Doors, 1937).....	71
Table 2-6: Infiltration through Entrances – Doors in More Than one Wall (Infiltration Through Doors, 1937).....	72
Table 2-7: Stack Coefficient $C_s$ (ASHRAE Handbook of Fundamentals, 2009) .....	88
Table 2-8: Local shelter classes (ASHRAE Handbook of Fundamentals, 2009).....	88
Table 2-9: Wind Coefficient $C_w$ (ASHRAE Handbook of Fundamentals, 2009) .....	89
Table 3-1: External Pressure Coefficient, $C_p$ (ASCE 7-05, Figure 6-6) .....	108
Table 3-2: Surface Roughness Coefficients (Simu and Miyata, 2006) .....	112
Table 3-3: Normalized shielding coefficients from Deru and Burns (2003) based on Sherman and Modera (1998) .....	116
Table 3-4: ASHRAE 1977 Handbook of Fundamentals.....	123
Table 3-5: Fourier series equation constants .....	124
Table 3-6: Sample ASHRAE Material leakage Data.....	137
Table 3-7: In-Plain Crack Diameter for Brick Cavity Wall.....	137
Table 3-8: Summary of Adopted Crack and Gap Dimensions .....	139
Table 3-9: Averaged Weather Conditions for Fargo Over the Simulation Span Time Period .....	141

Table 5-1: Comparison of Cumulative Extrapolated 31 Day Data versus Actual Cumulative 31 Day Data.....	173
Table 5-2: Hourly Infiltration Heat Load Data for Southwest Wall.....	175
Table 5-3: Cumulative Infiltration Heat Load Data for Southwest Wall.....	179
Table 5-4: Cumulative Monthly Heat Load on Southwest Wall .....	182
Table 5-5: Hourly Infiltration Heat Load Data for Northwest Wall.....	184
Table 5-6: Cumulative Infiltration Heat Load Data for Northwest Wall.....	187
Table 5-7: Cumulative Monthly Heat Load on Northwest Wall .....	190
Table 5-8: Cumulative Monthly Heat Load on Northwest Wall .....	196
Table 5-9: Simulation Speed Comparison .....	195

## LIST OF FLOWCHARTS

CHART	PAGE
Flowchart 1-1: Major Steps Followed to Achieve the Stated Objectives.....	13
Flowchart 2-1: Summary of DOE-2 Program Components and Program Tasks.....	22
Flowchart 2-2: Flow of DOE-2 Core Simulation Process .....	38
Flowchart 2-3: Possible Model Flows In eQUEST .....	42
Flowchart 2-4: Role of Air Infiltration Model in the Energy Design/Analysis Process (Liddament, 1986).....	53
Flowchart 2-5: Hierarchal order of Infiltration Calculation Techniques (Liddament, 1986) .....	56
Flowchart 2-6: Multizone Models Calculation Models (Feustel, 1985 - Modified).....	64
Flowchart 3-1 : Model Incorporation into hourly calculations.....	91
Flowchart 3-2 : Bule Print of the Enhanced Model .....	101
Flowchart 3-3: Wind Pressure calculation based on local factors and building characteristics.....	114
Flowchart 3-4: Mass flow rate calculation and components .....	119
Flowchart 3-5: Crack Properties Determination Process.....	134

## LIST OF CHARTS

CHART	PAGE
Chart 2-1: Air Leakage Rates of Elevator Shaft Walls (2009 ASHRAE® Handbook of Fundamentals).....	49
Chart 2-2: Air Leakage Rate of Door versus Average Crack Width (2009 ASHRAE® Handbook of Fundamentals).....	51
Chart 2-3: Airflow Coefficient for Automatic Doors (2009 ASHRAE® Handbook of Fundamentals).....	51
Chart 2-4: Infiltration Characteristics (Liddament, 1986) .....	54
Chart 2-5: Orifice Flowmeter Coefficient (ASHRAE 1977) (Walton, 1980) .....	62
Chart 2-6: Entrance Coefficients for Single Bank Entrances (Min, 1958).....	73
Chart 2-7: Infiltration versus RPM and indoor-outdoor temperature difference (Revolving Door).....	73
Chart 2-8: The intersection point of the two curves in this chart shows the point where there is no addition or loss of heat (Anon, 1937) - Reproduced.....	77
Chart 3-1: Surface pressure coefficient as a function of wind incidence angle for the Walton model and Swami & Chandra model (Deru and Burns, 2003) .....	109
Chart 3-2: Plot of solar equation of time, minute correction by day of the year .....	122
Chart 5-1: Hourly Infiltration Heat Load at the Southwest Wall by Various DOE-2/eQUEST Methods.....	176
Chart 5-2: Hourly Infiltration Heat Load at the Southwest Wall versus Angled (zig-zag) cracks CFD Output for the wall.....	176
Chart 5-3: Hourly Infiltration Heat Load at the Southwest Wall versus Mixed cracks CFD Output for the wall.....	177
Chart 5-4: Hourly Infiltration Heat Load at Southwest Wall versus Straight cracks CFD Output for the wall.....	177
Chart 5-5: Cumulative Monthly Infiltration Heat Load at Southwest Wall versus Angled (zig-zag) cracks CFD Output for the Wall.....	180

Chart 5-6: Cumulative Monthly Infiltration Heat Load at Southwest Wall versus Mixed cracks CFD Output for the Wall .....	180
Chart 5-7: Cumulative Monthly Infiltration Heat Load at Southwest Wall versus Straight cracks CFD Output for the Wall .....	181
Chart 5-8: Hourly Infiltration Heat Load at Northwest Wall by Various DOE-2/eQUEST Methods.....	185
Chart 5-9: Hourly Infiltration Heat Load at Northwest Wall versus Angled (zig-zag) cracks CFD Output for the Wall .....	185
Chart 5-10: Hourly Infiltration Heat Load at Northwest Wall versus Mixed cracks CFD Output for the Wall .....	186
Chart 5-11: Hourly Infiltration Heat Load at Northwest Wall versus Straight cracks CFD Output for the Wall .....	186
Chart 5-12: Cumulative Monthly Infiltration Heat Load at Northwest Wall versus Angled (zig-zag) cracks CFD Output for the Wall.....	188
Chart 5-13: Cumulative Monthly Infiltration Heat Load at Northwest Wall versus Mixed cracks CFD Output for the Wall .....	189
Chart 5-14: Cumulative Monthly Infiltration Heat Load at Northwest Wall versus Straight cracks CFD Output for the Wall .....	189
Chart 5-15: Comparison of Cumulative Monthly Infiltration Heat Load for the Southwest Wall.....	192
Chart 5-16: Comparison of Cumulative Monthly Infiltration Heat Load for the Northwest Wall.....	192
Chart 5-17: Infiltrating Air Temperature Rise Across the Building Envelope.....	199
Chart 5-18: Infiltrating Air Velocity Drop Across the Building Envelope .....	200



## NOMENCLATURE

A	Area (Area of opening)
$A_e$	Approximate leakage area
ACH	Air changes per hour
ATMEXT	Atmospheric extinction coefficient
$\alpha$	Non-dimensional airflow rate
$1/\alpha$	Surface roughness coefficient
$\beta$	Surface tilt
BSUN	Diffuse solar radiation
C (solid)	Specific heat of solid material
C (air flow)	Flow coefficient
$C_p$ (heat)	Specific heat of air
$C_p$ (wind)	Wind pressure coefficients
$C_p'$	Pressure coefficient corrected for wind direction
Classical	Conventional infiltration calculation method
$\gamma$	Porosity of wall
$\gamma_s$	Surface azimuth
E	East node
EQTIME	Equation of time
$\varepsilon$	Infiltration Heat Exchange Effectiveness
g	gravitational acceleration constant
$g_0, g_1, g_2, g_3, p_1, p_2$	Air – temperature weighting factors
GUNDOG	Hour angle of sunrise/sunset
H	Zone height
I	Intensity of solar radiation
IHR	Hour of the day
K	Heat conductance
k	Flow coefficient
$\dot{m}$	Infiltration air flow rate

## NOMENCLATURE

$n$	Flow exponent
$\rho$	Density of solid material
$\rho_{air}$	Density of air
$\rho_{in}$	Density of inside air
$\rho_{out}$	Density of outside air
$P$	Center node
$P_{o\ in}$	Internal pressure at base of wall
$P_{o\ out}$	Outside pressure at base of wall
$P_w$	Wind Pressure
$P_w + shielding$	Wind pressure including shielding effect
$q_i$	hourly heat gain/loss
$q_d$	Combined conduction and infiltration heat flux
$Q_i$	hourly cooling/heating load
$Q_{inf}$	Air infiltration energy load
$\delta Q$	Heat storage rate in control volume
$R$	Multiplication/Reduction factor
$R$ (ideal gas law)	Specific gas constant
RAYCOS(1)	Solar direction angles
RAYCOS(2)	
RAYCOS(3)	
$RDN$	Direct solar radiation
$RP$	Receiving polygon
$SC$	Shielding coefficient
$SKYDFD$	Sky diffuse factor
$SOLCON$	Solar constant
$SP$	Shading polygon
$T$	Temperature
$\delta T$	Temperature difference

## NOMENCLATURE

$T_i$	Inside(indoor) room temperature
$T_o$	Outside (ambient) air Temperature
$T_R$	The reference temperature
$T_{sa}$	Sol-air temperature
$\tau$	Time
$\Delta\tau$	Time step
$UA_o$	Heat loss factor due to conduction only
$UA$	Actual heat loss factor with airflow included
$V$	Wind speed
$V_{Zref}$	Measured wind speed at reference height
$v_0, v_1, v_2, w_1, w_2$	Heat – gain weightng factors
$W$	West node
$y_{np}$	Height of neutral pressure level
$y$	Height above bottom of zone
$\Psi$	Wind direction from weather file
$Z$	Elevation
$Z_g$	Gradient height of terrain
$Z_{ref}$	Elevation of wind speed measuring point

## **Chapter 1**

### **Introduction**

A wealth of Building Energy Simulation software and tools is available. The United States Department of Energy Building Technologies Program lists under its “Building Energy Software Tools Directory” three hundred and eighty nine building software and tools from 28 different countries. These software and tools range between databases, component and system analysis tools, spreadsheets, and whole-building energy performance simulation programs (Building Technologies Program, 2010).

Traditionally, the two primary reasons for performing building thermal performance calculations are to (1) size and select the required mechanical equipment, or to (2) obtain a prediction of the building’s annual energy consumption and costs. Some programs can handle either of these tasks while others can handle both (Paradis, 2010). Sizing programs are mainly designed to perform hourly calculations of peak heating and cooling loads. Many of these programs are based on algorithms established by ASHRAE. Energy cost programs, on the other hand, are principally set up to predict building annual energy consumption in BTUs, dollars, or pollution/pollution avoidance (Paradis, 2010).

DOE-2 is one of the most widely well-known full building energy simulation models. It also serves, either fully or partially, as the simulation engine of several other renowned software such as eQUEST, PowerDOE, Energy Plus, Energy Pro and others. DOE-2 was developed by James J. Hirsch & Associates (JJH) in collaboration with Lawrence Berkley National Laboratory (LBNL). ([www.DOE2.com](http://www.DOE2.com), 2010).

“DOE-2 is an hourly whole building Energy Analysis program calculating Energy Performance and life cycle cost of operation” (Building Technology program, 2010).

Using a description of a building layout, construction, operating schedules, conditioning system along with user-provided utility rates, and weather data, DOE-2 is capable of performing hourly energy simulations of a building and providing an estimation of the various building utility bills ([www.DOE2.com](http://www.DOE2.com), 2010). Other features include its use in rebate programs, comparison and implementation of energy efficiency standards and compliance certification (Building Technology Program, 2010).

A subsequent development to DOE-2 is eQuest. DOE-2 is eQUEST's "simulation engine". eQUEST provides the sophisticated building energy simulation of DOE-2 in an easy-to-use Graphical User Interface (GUI) and wizards medium. eQUEST can be simply defined as ([www.doe2.com/equest](http://www.doe2.com/equest), 2010):

$$\mathbf{eQUEST = DOE-2 + Wizards + Graphics}$$

DOE-2 & eQUEST have been both time proven and are well known and widely used. DOE-2 is well recognized as an industry standard. It is used by more than 800 major user organizations within the United States and 200 organizations internationally; where each organization includes of up to 20 users or more. Similarly, eQUEST is one of the most widespread building energy simulation programs. eQUEST registers more than 10,000 full program downloads annually (Building Technologies Program, DOE-2 & Building Technologies Program eQUEST, 2010).

The simulation capabilities of DOE-2 and eQUEST and their widespread use make them of high significance and impact. This also highlights the essentiality of accuracy in their building energy simulation. Both eQUEST and its simulation engine DOE-2 have been proven in many aspects by experimentation and are based on ASHRAE in many algorithms. Examples include Kerrisk et al. (1980), Meldem et al.

(1998), Loutzenhiser and Maxwell (2006), Hong et al. (2009), and others. However, some major energy demand components are treated by the software with less complexity and are accounted for using overly simplified approaches and algorithms. It is therefore essential that such shortcomings be improved in order to provide a more accurate building energy simulation. With the prevalent use of these two software packages, any improvement in their calculation model of a major energy load would be of high importance and impact. Therefore, all building energy simulation model improvements developed in this work will be applied using DOE-2 & eQUEST as the demonstration software. However, these improvements should be easily applicable to any alternate building energy simulation software.

Any work to be done shall focus on DOE-2. Since DOE-2 is the simulation engine of eQUEST (also of EnergyPro, PowerDOE, EnergyPlus - in part- and others). Then, any developed improvements to DOE-2 shall be consequentially incorporated into eQUEST.

Improvements to DOE-2 can be of different levels and from many aspects. One aspect could be the improvement of an existing DOE-2 algorithm to correct a built-in flawed. For example, in the Design Day weather feature, users can define their own weather. This would create an hourly weather that is used in the building energy simulation and in the HVAC sizing process. The algorithm, however, doesn't revise the user-inputted weather which could be defining indoor humidity levels exceeding 100 % humidity (indoor rain!). Another improvement approach could be to add to an existing DOE-2 subprogram. Therefore, allowing it to account for more heating/cooling load sources. For instance, the software accounts for shading of a building by adjacent

structures and bodies. Yet, it overlooks the solar radiation reflected onto the building under study from surrounding surfaces. Especially important are surrounding surfaces with a high Surface Reflectance Index (SRI), such as surrounding buildings with white painted (light colored) or mirror glass facades. Such veneers could reflect a considerable portion of the solar radiation incident on them onto the building being simulated. A third DOE-2 improvement approach could be to add or create an entirely new feature into the software. For example, developing green roofs as a material with different variations and properties (R-value, Insulation...etc). This will make green roofs available as a feature for use in the Energy Simulation of Green Buildings.

Infiltration is an uncontrolled process through which outside air leaks into a conditioned space in a building (Brownell, 2002). Air infiltration affects both indoor air quality and building energy consumption. It significantly contributes to the overall heating and cooling loads in a building. The magnitude of the impact of infiltration on the overall heating/cooling load depends on several factors. These include environmental conditions, building design and operation and construction quality (Buchanan & Sherman, 2000). A 40 % of the heating/cooling cost in homes is attributed to infiltration as was shown by field measurement of residential buildings (Caffey, 1979). Estimates by the National Institute of Standards & Technology (NIST) attributed, based on a study of U.S. office buildings, 15 % of the heating loads in office buildings to air infiltration (NIST 1996). Other studies estimated air infiltration to account for up to 25% to 50% of space heating demands for both commercial and domestic buildings (Nevrala & Etheridge, 1977; Kirkwood, 1977). Similarly, Persily (1982) concluded that infiltration

accounts for one-third of the heating and cooling requirements of a building. A comparable conclusion was also affirmed by Sherman & Matson (1993) who studied the Ventilation-Energy liabilities in U.S. dwellings. They inferred that a large fraction of the space conditioning load in U.S. residential buildings is due to infiltration.

The prediction and measurement of infiltration rates for buildings has been the subject of extensive work and research. An example is the Feustel & Kendon (1988) comprehensive review of the multitude of available methods. However, determining the energy consumption due to this infiltration has been the subject of limited research (Bhattacharyya & Claridge, 1992). The energy impact of air infiltration has been classically evaluated as a product of the infiltrating air mass flow rate, the air specific heat capacity and the inside-outside temperature gradient. The classical expression for heat loss due to infiltration is given by equation 1-1.

$$Q_{inf} = \dot{m} C_p (T_i - T_o) \quad (1 - 1)$$

Where:

- $Q_{inf}$  = Air infiltration energy load (W)
- $\dot{m}$  = Air infiltration mass flow rate (kg/s)
- $T_i$  = Inside(indoor) room temperature ( $^{\circ}$ C)
- $T_o$  = Outside (ambient) air Temperature ( $^{\circ}$ C)
- $C_p$  = Specific heat of air (J/kg $^{\circ}$ C)

The classical method and current design methods assume that solar radiation, conduction and air infiltration are independent and behave independently. Those methods overlook the interaction between these three phenomena. However, such an assumption is



unrealistic and embracing it can result in extensive errors in the evaluation of design loads and annual energy consumption by a building (Liu & Claridge, 1992).

Cold air infiltrating into a room or a building through porous material can attain a temperature closer to the room temperature than the outside air temperature (Claridge et al, 1995). Especially through brick, concrete masonry, concrete and other material commonly used in building construction. Heat exchange occurs between the infiltrating air and the building envelope allowing the air to absorb/release energy and become closer to the indoor space temperature; a phenomenon known as “Heat Recovery”. While, as shown in equation (1-1), the general assumption is that the amount of energy required for heating/cooling infiltrating air is the same as that required for heating/cooling the outside air to indoor conditions (Bhattacharyya & Claridge, 1992). It has been shown by Anderlind (1985) that the infiltration energy load can attain a maximum value of equation (1-1); however it is generally smaller due to heat exchange occurring in the walls between the walls and the infiltrating air. This has also been confirmed experimentally by Claridge, Liu and Bhattacharyya (1990, 1992, 1995, 1996 and 1999), Anderlind (1985) and Guo & Liu (1985).

Anderlind (1985) introduced a reduction factor to the classical equation (equation 1-1) to account for the heat recovery. Thus, modifying the classical equation as shown in equation 1-2 below:

$$Q_{inf} = R \dot{m} C_p (T_i - T_o) \quad (1 - 2)$$

Where:

- R = a multiplier ranging between 0 and 1 , depending on the structure and construction of the walls

Claridge and Bhattacharyya (1992) put forward the Infiltration Heat Exchange Effectiveness (IHEE). Where, IHEE ( $\varepsilon$ ) represents the fraction of energy consumption that was recovered during the Heat Recovery process. The expression for  $\varepsilon$  is given in equation 1-3:

$$\varepsilon = 1 - \frac{Q_{inf}}{\dot{m} C_p (T_i - T_o)} \quad (1 - 3)$$

Where:

- $\varepsilon$  = Infiltration Heat Exchange Effectiveness
- $Q_{inf}$  = Air infiltration energy load (W)
- $\dot{m}$  = Air infiltration mass flow rate (kg/s)
- $T_i$  = Inside(indoor) room temperature ( $^{\circ}\text{C}$ )
- $T_o$  = Outside (ambient) air Temperature ( $^{\circ}\text{C}$ )

Several building energy simulation software account for the impact of infiltration by utilizing a variety of models. However most of the models utilized are either overly simplified or at best suffer from several deficiencies and fail to capture the full physics of the phenomenon. As a sample software, DOE-2 in its building energy simulation accounts for infiltration. In the DOE-2 Engineers Manual, the major impact of infiltration on the building energy load is well acknowledged and infiltration is defined as “One of the largest components contributing to heating loads” (DOE-2 Engineers Manual, 1982). However, in defining the models used to simulate the energy impact of infiltration it is prominently stated that Infiltration in building Energy Analysis is “Usually treated by

very simple approximate models” (DOE-2 Engineers Manual, 1982). In modeling infiltration, DOE-2 employs five different models:

- Air Change Method
- Crack Method
- Residential (Achenbach – Coblenz) Method.
- Sherman & Grimsrud
- ASHRAE Enhanced

These models are (respectively) overly simplified, purely empirical and based on curve fitting, or deficient in considering the various factors contributing to air infiltration.

Like the majority of building energy simulation software available, DOE-2 infiltration models overlook a variety of aspects that significantly contribute to the infiltration energy load. This inadequacy becomes more critical when considering the significant contributions of infiltration to the heating/cooling load in buildings, as discussed earlier. Among the aspects unaccounted for by the DOE-2 infiltration models are:

- Infiltration heat recovery
- Neglecting the resistance to intra-room airflow
- Infiltration through doors : manual, automatic, revolving and others
- Infiltration through windows
- Infiltration through doors and windows sealings
- Infiltration due to a fireplace
- Others

## **Main Objective**

The main objective of this research is to build a comprehensive infiltration energy load model that integrates the interaction between solar radiations, conduction and infiltration into building energy load calculations along with a better evaluation of the infiltration airflow rate; and to apply this model onto prominent building energy simulation software. The model developed in this research will be referred to throughout this research as the Enhanced Model.

## **Specific Objectives**

The main objective of this work are to improve the accuracy of building energy simulations by incorporating into their calculations the impact of the interaction between solar radiation, conduction and infiltration in contrast with current methods that consider these three phenomena to act independently. Also, to provide a better evaluation of the infiltration airflow rate, for use in the infiltration load calculations, based on local conditions, terrain and building characteristics. Therefore this study performs a comprehensive review of infiltration and how it is accounted for in current models and in prominent building energy simulation software. It also determines the latest research on studying the interaction among these three phenomena and to decide on a model to build upon, further develop and later apply onto prominent building energy simulation software. Next it develops a dynamic model for evaluating the infiltration airflow rate (to be used in the infiltration energy load model) that accounts for wind speed, wind direction, topography, terrain, building characteristics, and others. The third objective is to build a comprehensive infiltration energy load model that integrates (1) heat recovery, (2) interaction between conduction, solar radiation and infiltration and (3) incorporates

the developed airflow rate model. The fourth objective is to verify the relative accuracy of the developed Enhanced Model versus a hygrothermal multiphysics computational fluid dynamics (CFD) model. This is done by comparing the simulation output of the Enhanced Model for a demonstrative building to the results of a finite elements CFD analysis of the same building. The final objective is to demonstrate the improvement in infiltration load calculation relative accuracy (versus complex CFD analysis) by comparing the obtained Enhanced Model's simulation output to the regular DOE-2 output for the same building. Flowchart 1-1 highlights the major steps followed to achieve the stated objectives.

### **Justification**

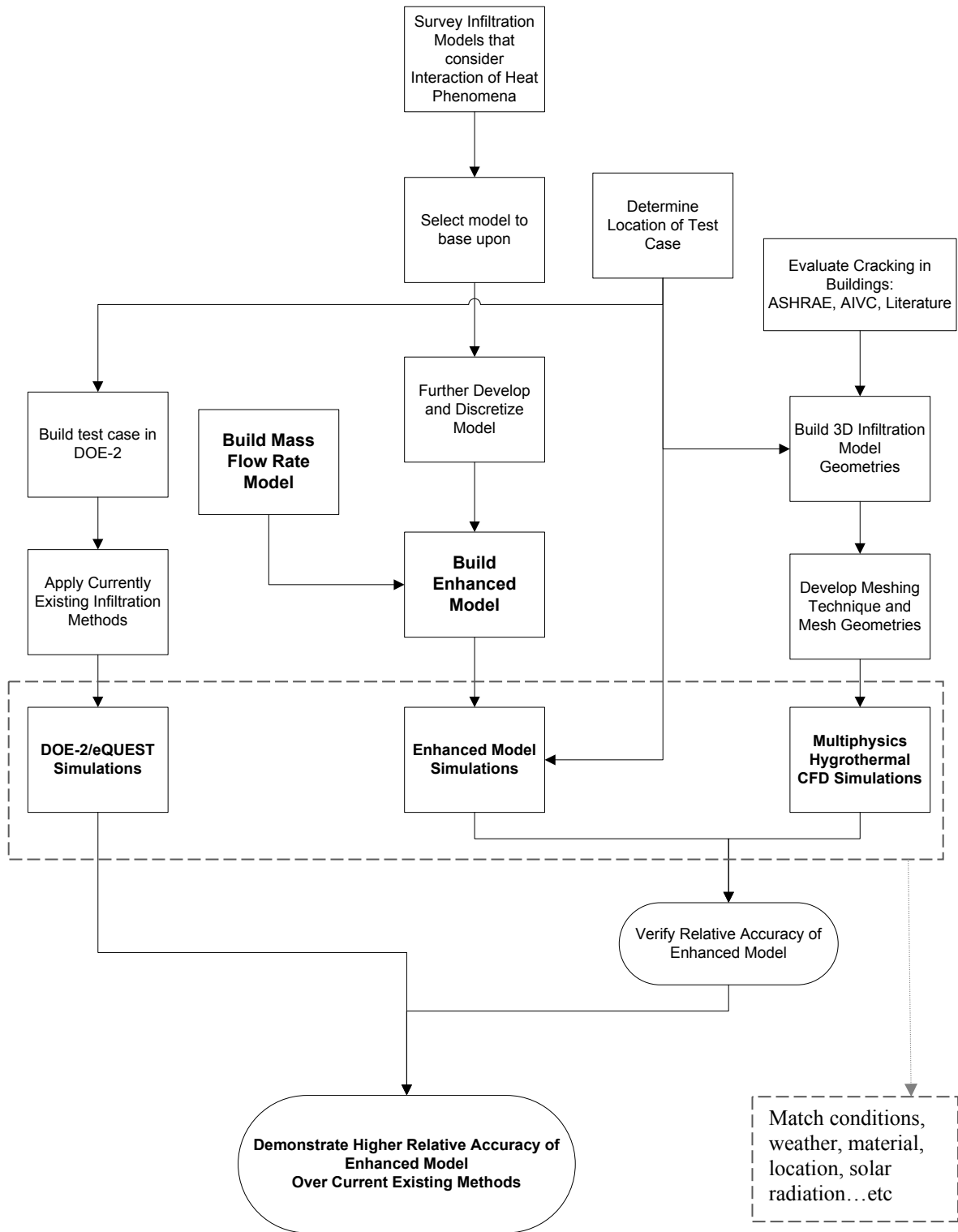
The significance of the work lies in building a comprehensive model that incorporates into building energy load calculations, the interaction between solar radiation, infiltration and conduction, while considering factors such as building height, topography, terrain roughness, wind speed and direction, and others. The developed Enhanced Model is a tool that helps designers to quickly, accurately and efficiently simulate infiltration heat loads. The the current dilemma of accuracy versus efficiency is overcome by reducing by six orders the simulation time necessary for obtaining an accurate simulation while compromising relative accuracy by 2 % only. The classical method for evaluating the infiltration energy loads which considers infiltration to act independently from conduction in the building envelope and other phenomena has been proven to result in significant errors in building energy loads estimation. Building energy simulation software are of wide spread use and high impact, yet most still deploy the classical infiltration load calculation method or other overly simplified methods.

Therefore, it would be of large significance and impact to apply the obtained Enhanced Model onto building energy simulation software, which could significantly improve their simulation accuracy, most importantly to an industry standard and widespread software such as DOE-2. Aside from DOE-2 and the software that it is a simulation engine for, the built model shall be easy to incorporate into other building energy simulation software. The resulting improvement in building energy simulation accuracy will allow several benefits including:

- More accurate HVAC (Heating Ventilation and Air Conditioning) equipment sizing. Oversized equipment will not efficiently perform and result in higher operating costs. Also HVAC over sizing leads to increased initial costs, larger than required meters, low system distribution pressures during peak demand, and others (Regester and Reinauer, 1981)
- Improved energy audits and more accurate energy utility estimation costs. In sustainable building design, during the parametric comparison of various design alternatives, this allows a more confident selection of the most energy efficient building design.
- Controllable ventilation rates that fallout onto a healthier building. Since the infiltration energy load can be more accurately calculated, controlled natural ventilation through infiltration can be Permitted (Brownell, 2002).
- Allowing an optimal distribution of insulation, due to enhanced knowledge of conduction losses.

- Making available the application of dynamic insulation: Replacing ventilation systems with “breathing walls” that provide fresh yet thermally condition air (through heat recovery) (Brownell, 2002).

The various outcomes of the Enhanced Model amount to a better evaluation of the energy requirements of a building. This, results in a building with less energy demand, lower lifecycle costs, and increased occupant comfort.



Flowchart 1-1: Major Steps Followed to Achieve the Stated Objectives



## **Chapter 2**

### **Background**

The Energy Information Agency reports that 99.402 Quadrillion ( $10^{15}$ ) BTU's of energy were consumed in the United States in 2008. This includes energy used in residential, commercial, industrial and transportation applications. All at a total cost of \$1,396.69 Billion (U.S. Energy Information Administration, 2010). Buildings consume 36% of all the energy produced (Brownell, 2002); the equivalent of 35.784 quadrillion BTU's. Of all the energy consumed annually by buildings, 58 % is utilized for heating and air conditioning (Brownell, 2002). This represents 20.75 Quadrillion BTU's a year. That, by proportion, stands for \$ 291.56 Billion spent annually on heating and cooling of buildings. As a result, even minor factors influencing the heating/cooling of buildings become of significant importance, much less factors such as infiltration that can contribute to more than a third of the heating/cooling load of a building.

The large and constant need of energy for heating and cooling in buildings results from undesired thermal losses in these structures. The primary forms of thermal loss are: (1) conduction losses through the building envelope, (2) heat loss due to ventilation, and (3) unwanted heat loss due to air leakages known as infiltration. With infiltration representing up to 40% of the heating/cooling load cost (Caffey, 1979) and the magnitude and cost of energy consumption discussed earlier; the importance of accurate simulation and modeling of infiltration energy loads becomes evident and highly necessary.

This literature review includes a discussion of DOE-2 and its various components. Since a common basic structure is shared by DOE-2 and several other hourly building energy simulation software, the following discussion can be made applicable to understanding the layout and inner workings of similar energy simulation software. An overview of the component programs LOADS, SYSTEMS, PLANTS and ECONOMICS common to several hourly building energy simulation software and their interaction is presented. Included also is a discussion of weighting factors and response factors and their use in DOE-2. An explanation of DOE-2 basic principles and the underlying philosophy of load calculations is also presented. The progress of a DOE-2 Energy simulation is illustrated through especially developed flow charts. Similarly, the review includes a general overview of eQUEST, its component wizards and principles. The literature review also contains a discussion of the presentation of Infiltration in ASHRAE according to the ASHRAE 2009 and 2007 Handbooks. The final section of this literature review is dedicated to a comprehensive review of infiltration. The various methods of evaluating infiltration energy loads and their classification as well as the two major categories of air leakage and infiltration, concentrated and diffuse are discussed. Presented is a breakdown and a discussion of each, including the role of heat recovery and all relevant research done.

## **Building Energy Simulation Programs**

A diverse body of building energy analysis programs is available. This includes a wide array of spreadsheets, databases, component and system analysis tools, and whole building energy simulation programs. The U.S. Department of Energy Building Technologies program directory lists a set of 389 of these tools and software with varying capabilities and origins (Building Technology Program, 2010). Two prominent entries on this list are DOE-2 and eQUEST. Both software are full hourly Building Energy Simulation software, with DOE-2 representing the simulation engine of eQUEST. They are both widely recognized, time proven, widely used and considered to be an “Industry Standard” (Building Technologies Program, 2010). 800 large organizations in the United States and 200 other international organizations use DOE-2 for building energy simulation. Similarly, eQUEST averages more than 10,000 full program downloads annually (Building Technologies Program, 2010). The widespread use of these two software makes them of high impact and emphasizes the importance of their simulation accuracy. Consequently, improvements made to DOE-2 (and accordingly eQUEST) would reflect in considerable energy and cost savings.

The majority of the following discussions will involve DOE-2 since it concurrently represents the simulation engine of eQUEST. Included in the literature review is an explanation of the basics of DOE-2. This entails an overview of the software’s basic equation, essential and core operations, main programs and subprograms, and the interaction between its various components.

## **Origins of Energy Simulation Programs: Historic Overview**

Early on efforts for the use of computers in building mechanical/electrical service design were first acknowledged by the industry in 1965 (Lau & Ayres, 1979). Automated Procedures for Engineering Consultants Inc. (APEC) was created by a group of mechanical engineering consultants. They developed their first program The “APEC Heating and Cooling Peak Load Calculation (HCC) program (HCC-Heating/Cooling Load Calculation program, 1967). The program was used in the design of heating, ventilating and air conditioning systems in buildings. The work on the program was concluded in 1967. It was designed to calculate peak heating and cooling loads and air quantities. The calculations were performed based on input summer and winter design days climatic data. This primal program alleviated design engineers from tedious hand calculations as well as provided essential data for the selection of suitable heating and cooling equipment and the design of air distribution systems (Lau and Ayres, 1979)

The American Society of Heating, Refrigerating and Air Conditioning engineers (ASHRAE) formed in 1976 the ASHRAE Task Group on Energy Requirements (TGER). As a result, building heat transfer sub-routines, algorithms, and HVAC system and component simulation procedure for computerized energy calculations were established (Lau and Ayres, 1979). The availability of such procedures permitted the development of the first generation of Loads/Energy programs. This Includes the National Bureau of Standards (Kusuda, 1974) and the U.S. Post Office (Lokmanhekin, 1971) who developed public domain energy software. Simultaneously energy calculation computer software developed by the private sector thrived (Lau and Ayres, 1979).

The major systems involved in building energy analysis are particularly thermal loads calculation, system simulation and central plant simulation (Lau and Ayres, 1979). Building Energy Analysis programs are commonly structured in such composition and order with sub-programs performing each of these sub-steps. A number of building energy programs, such as DOE-2, expands further to include economic analysis. Accordingly, building energy simulation programs are usually composed of four fundamental analysis programs: LOADS, SYSTEMS, PLANT, and ECONOMICS (shortly known as LSPE), as shown in Flowchart 2-1. Various software simply differ in the degree of mathematical complexity of their chosen models and the extent they match real world conditions (Lau and Ayres, 1979).

## **DOE-2**

The DOE-2 Engineers Manual (1982) illustrates the philosophy of the DOE-2 computer program. It describes and explains “What happens to the input data”. The following section describes the inner operations of DOE-2 and is mostly based on the latest DOE-2 engineers manual available; DOE-2 ENGINEERS Manual, Version 2.1 A, November 1982.

## **DOE-2 Programs**

A building’s energy consumption is governed by its shape, thermal properties of its constituting materials, size, location & orientation, and the positions of walls, floors, roofs, windows and doors. Also contributing are the transient affects of shading, occupancy patterns, lighting schedules, equipment operation, ambient conditions, and temperature and humidity conditions. Finally, is the role of the building HVAC systems and their efficiencies. A Building Description Language (BDL) was therefore written for

use in DOE-2. This language helps in describing a building and its various properties that contribute to the energy consumption calculations. Following, is a general description of the various processor and program components of DOE-2 and their role.

### **BDL Processor**

The BDL Processor successively checks every BDL instruction. It verifies each instruction's form, syntax and content. Additionally, the BDL Processor checks input values and verifies that they fall within the input range. The BDL Processor also retrieves from various libraries user specified data (e.g. Materials Library). Also, it calculates the Response Factors. These factors characterize the transient heat flow through exterior walls and roofs and are used by the LOADS program. Moreover, it calculates the custom weighting factors, if required by the user, which account for thermal lag in heating and cooling. Finally, the BDL processor assembles and prepares the LOADS, SYSTEM, PLANT and ECONOMICS (LSPE) simulators input files.

### **LOADS Program**

The LOADS Program uses an array of algorithms to calculate hourly heating and cooling loads. LOADS performs a separate calculation for heat gains and losses through walls, roofs, floors, windows and doors. It utilizes the response factors generated by the BDL processor to calculate heat transfer through the building skin by conduction and radiation. The impacts of thermal mass, insulation placement, sun angle, cloud cover, building location and orientation are all considered in the weighting factors generated by the BDL processor and used in LOADS. In LOADS, each generated weighting factors set is placed in a designated file to be consequently used by LOADS and SYSTEMS programs. Loads due to infiltration are also calculated based on the difference between

the inside and outside conditions using the “Crack Method” or “Air Change Method”. Heat gains due to lighting, equipment and occupants are also calculated in LOADS based on user-assigned schedules and occupancy hours.

It is essential to note that all LOADS computations are performed based on a fixed temperature for each space. The LOADS output is then modified in the SYSTEMS program to produce the factual thermal loads based on variable hourly internal zone temperatures.

### **SYSTEMS Program**

The SYSTEMS program includes a set of algorithms for simulating the performance of secondary HVAC systems. These systems control building zones temperatures and humidity. An array of preprogrammed space conditioning systems is available for the user to pick from. To use the SYSTEMS program, the user has to select one of these preprogrammed systems and provide the necessary input data.

The LOADS output along with the user defined airflow rate, thermostat settings, equipment operation schedules and other user-defined system characteristics are used by SYSTEMS to calculate hour-by-hour energy requirements of the secondary HVAC system. Finally, SYSTEMS program recalculates all the thermal loads previously calculated in the LOADS program (based on a fixed space temperature), adjusting them based on variable zone temperature conditions.

### **PLANT Program**

Boilers, absorption chillers, compression chillers, cooling towers, hot water storage tanks, solar heaters and other Plant components have their operation modeled in the PLANT Program. This program contains all the equations essential for calculating the performance of various primary energy equipment. Hourly outputs of LOADS and SYSTEMS Programs are also used by PLANT Program to calculate the electrical and thermal energy consumption of the building. Finally, the life cycle cost of Plant equipments is calculated by PLANT using subroutines contained in the program.

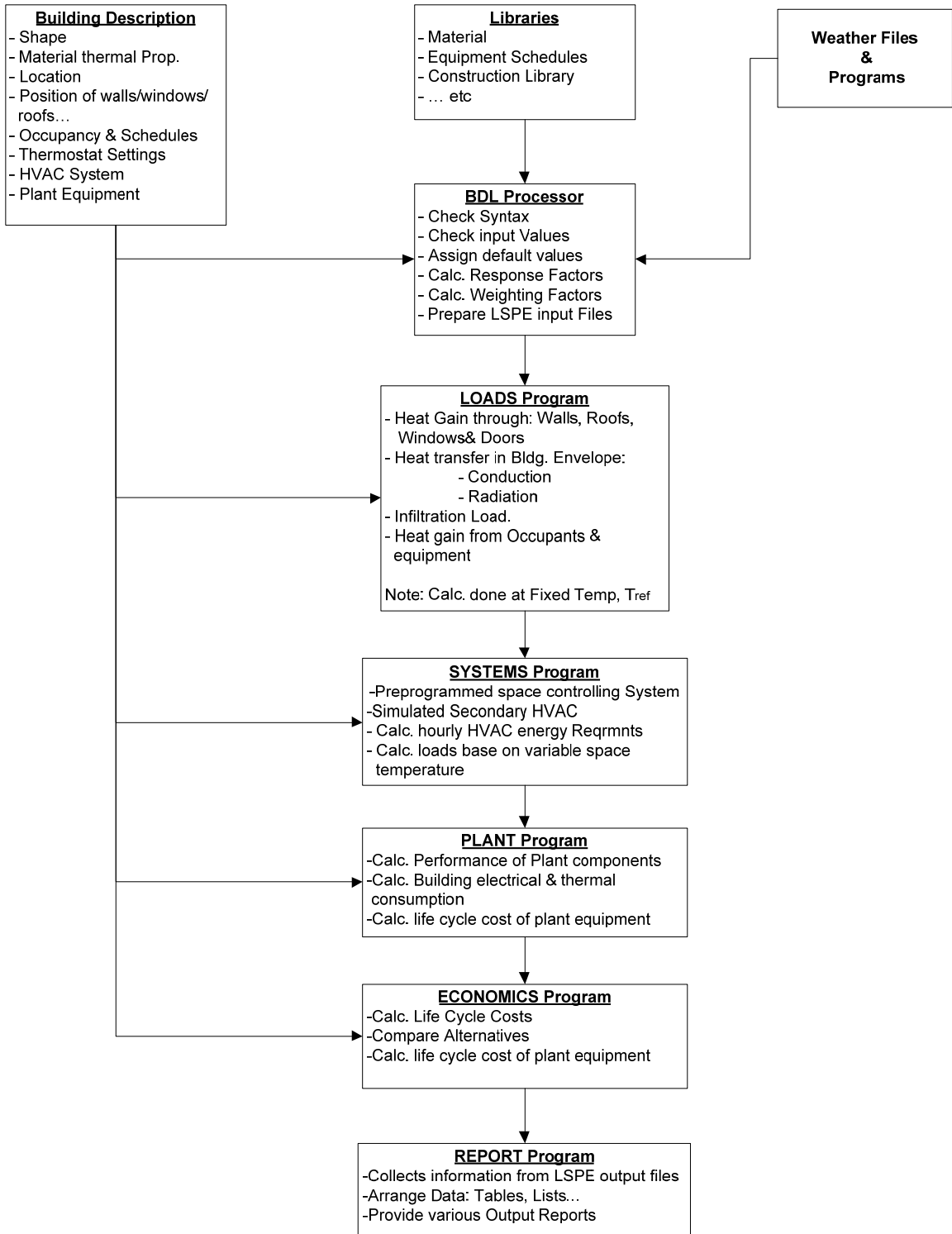
### **ECONOMIC Program**

The ECONOMIC Program utilizes user-input utility rates, interest rates, building and equipment costs and others, along with the output of previous programs. It is used to calculate the life-cycle costs of a building. ECONOMICS Program can also perform economic comparisons of possible project alternatives.

### **REPORT Program**

Data and information from the output files of all the LSPE programs are collected by REPORT. The output data are then arranged by REPORT into lists, tables and others. Various types (by complexity and detail level) of reports are provided by REPORT, including reports with extensive details and hourly values





**Flowchart 2-1: Summary of DOE-2 Program Components and Program Tasks**

## How a DOE-2 Simulation Works

The fundamental concept at the core of a DOE-2 simulation is that input brought together with a Transfer Function results in the output. The Input represents heat gain or loss, the output is the cooling/heating load and the Transfer Function is the weighting factors. This concept can be represented by the relationships in equations 2-1 and 2-2.

$$\text{Output} = (\text{Transfer Function}) \times \text{Input} \quad (2 - 1)$$

$$\therefore \text{Heating/Cooling Load} = (\text{Weighting Factors}) \times \text{Heat Gain/Loss} \quad (2 - 2)$$

Where: The use of weighting factors represents a compromise between the use of complex methods, such as full energy balance, and overly simplified methods, such as steady state.

The core thermal simulation process of DOE-2 can be summed up in two major phases. The first phase happens in the LOADS program and is heavily dependent on processes performed by the BDL Processor (i.e. weighting factors calculation, response factors calculation and others). The second major phase of simulation occurs in the SYSTEMS Program and produces the actual space air temperatures, corresponding thermal loads, and others.

In the calculations of Phase I, LOADS assumes a fixed reference air temperature for each space,  $T_{\text{ref}}$ . Then, using a list of available algorithms and user-defined building-specific data, LOADS calculates instantaneous heat gains/losses due to solar radiation, lighting, people and occupants, equipment, conduction in walls and so on. LOADS then

deploys the relationship represented in equation 2-1 and the various sets of weighting factors calculated by the BDL Processor to calculate the resulting space cooling/heating loads resulting from each of the heat gains previously mentioned. This represents the energy needed to maintain the temperature of the space fixed at  $T_{ref}$  in response to the recorded heat gain/loss. Phase II is then subsequently performed in the SYSTEMS Program. In this phase, cooling/heating loads from Phase I are combined with HVAC system data and air temperature weighting factors. As a result, the actual space air temperatures, total heat extraction, and thermal loads (based on variable space temperature) are determined. The output of Phase II is then used by subsequent components of the software. For example, it is used by ECONOMICS Program to calculate various utility costs and lifecycle costs.

### **Weighting Factors**

Weighting Factors are utilized by DOE-2 in calculating thermal loads and room air temperatures (York and Tucker, 1980). They represent a z-transfer function relating the heat gained to the resulting cooling load. The weighting factors method is one of several methods that are commonly used in building energy simulation. It was first introduced by Mitalas and Stephenson (Stephenson & Mitalas, 1967; Mitalas and Stephenson, 1967). This method represents a compromise between overly simplified methods, such as steady-state computations that disregard thermal mass storage; and overly complicated methods like energy balance calculations. As a result, the weighting factor method is - according to DOE-2 ENGINEERS Manual - an efficient, simple,

flexible and fast method that at the same time considers all important parameters affecting building energy analysis.

The use of weighting factors in DOE-2 entails 2 general assumptions. First, since heat gains due to various sources are calculated individually and then summed up (by superposition) to obtain the total load; all modeled processes are assumed to be adequately represented by linear differential equations. As a result, linear approximations of nonlinear processes, such as natural convection and radiation, must be made. Second, it is assumed that all system properties influencing the weighting factors are constant. Namely, these system properties are not functions of time or temperature. Therefore, any varying system properties are represented by an averaged value. These Two major assumptions signify some limitations arising from the use of weighting factors and the weighting factor method.

DOE-2 operates using either precalculated weighting factors or custom weighting factors. Precalculated weighting factors, as the name implies, have been precalculated for typical building rooms. They are stored in DOE-2 and can be selected for use. These factors are largely based on ASHRAE original weighting factors for rooms with Light, Medium and Heavy construction; characterized by 30, 70, and 130 lb/ft<sup>2</sup> construction weights respectively (Lokmanhekim, 1975; ASHRAE Handbook and Product Directory, 1977). For floor weights other than those stated, interpolation and extrapolation is used to obtain the required precalculated weighting factors. The use of these precalculated weighting factors entail a set of assumptions in addition to the two general assumptions of linearity and constant system properties (associated with the general use of the weighting factors method). Foremost, the user is accepting the “Typical Construction” of

the “Standard Rooms” that were used in the precalculated weighting factors calculation. Among others, this includes: Wall construction and thermal properties, window area and orientation, furniture quantity and properties, incident solar radiation properties and distribution, walls radiative properties (absorptivity, reflectivity and others), and interior film coefficients. Therefore, precalculated weighting factors are approximate descriptions of building rooms and their use is rarely encouraged.

Custom weighting factors are especially calculated for every room by DOE-2 based on the room's actual description. Custom weighting factors can be of two categories, either Heat-Gain or Air-Temperature weighting factors. A Separate set of custom heat-gain weighting factors is calculated for each source of heat gain. Namely, solar radiation, lighting, task lighting, occupant people and equipment in a room, and heat conduction into a room. Similarly, air-temperature gain weighting factors that relate a specific room's air temperature to the net energy load on the room are calculated. Since custom weighting factors are particularly calculated for each room, they represent a major improvement over precalculated weighting factors. Their use is therefore recommended. Furthermore, the use of custom weighting factors is a must when modeling buildings with heavy construction, indirect gain, passive solar buildings, and in buildings where a significant part of the load is due to solar energy.

Custom weighting factors represent z-transfer functions that relate the hourly cooling/heating load to instantaneous heat gains/losses (heat-gain weighting factors); and a room air temperature to net energy loads on a room (air-temperature weighting factors).

This relationship can be illustrated using equations 2-3 and 2-5 below for heat-gain and air-temperature weighting factors respectively

**Heat-Gain Weighting Factors:**

$$\frac{Q(z)}{q(z)} = \frac{v_0 + v_1 z^{-1} + v_2 z^{-2}}{1 + w_1 z^{-1} + w_2 z^{-2}} \quad (2 - 3)$$

$$\therefore Q_\tau = v_0 q_\tau + v_1 q_{\tau-1} + v_2 q_{\tau-2} - w_1 Q_{\tau-1} - w_2 Q_{\tau-2} \quad (2 - 4)$$

Where:

- $q_i = q_0, q_1, q_2 \dots = \text{hourly heat gain (Input)}$
- $Q_i = Q_1, Q_2, Q_3 \dots = \text{hourly cooling load (Output)}$
- $v_0, v_1, v_2, w_1, w_2$  are Heat – gain weightitng factors (Transfer function)

**Air-Temperature Weighting Factors:**

$$\frac{Q(z)}{t(z)} = \frac{g_0 + g_1 z^{-1} + g_2 z^{-2} + g_3 z^{-3}}{1 + p_1 z^{-1} + p_2 z^{-2}} \quad (2 - 5)$$

$$\therefore Q_\tau = g_0 t_\tau + g_1 t_{\tau-1} + g_2 t_{\tau-2} + g_3 t_{\tau-3} - p_1 Q_{\tau-1} - p_2 Q_{\tau-2} \quad (2 - 6)$$

But  $Q_\tau$  can already be determined from the Heat-Gain weighting factors, equation 2-4, thus use equation 2-6 to determine  $t_\tau$ :

$$\Rightarrow t_{\tau} = \frac{1}{g_0} [Q_{\tau} + p_1 Q_{\tau-1} + p_2 Q_{\tau-2} - g_1 t_{\tau-1} - g_2 t_{\tau-2} - g_3 t_{\tau-3} p_2 Q_{\tau-2}] \quad (2-7)$$

Where:

- $g_0, g_1, g_2, g_3, p_1, p_2$  are Air – temperature weightng factors
- $t_{\tau} = T(z) - T_R$  (2-8)

Where:

- $T(z)$  = z-transform of the actual air space temperature
- $T_R$  = The Reference temperature used in LOADS calculations

Custom weighting factors are calculated by applying a unit pulse onto a network representing the heat balance for each room; with the heat balance incorporating response factors that characterize the heat flow through the room walls. The calculation of the weighting factors is performed at the onset of the simulation, using heat balance, by repeating the hourly simulation for the first day 3 times. Once the weighting factors stabilize (due to the repeated calculation) they are used from there on - repeatedly - to calculate hourly cooling (heating) loads from heat gains (losses) instead of performing an hourly full heat balance calculation.

### **Response Factors**

With the inside temperature (user specified) and outside temperature (from weather file or other) known, the problem becomes finding the heat flux at both the inside and outside surfaces of the wall. DOE-2 considers a once dimensional heat flow across a wall. The equation is then defined by equation 2-9.

$$\frac{\delta^2 T}{\delta x^2} = \frac{1}{\alpha} \frac{\delta T}{\delta t} \quad (2-9)$$

Where:

- $T$  = Temperature
- $t$  = time
- $x$  = distance from the outside surface
- $\alpha$  = diffusivity =  $k/C\rho$
- $C$  = Specific heat
- $\rho$  = Density

The solution to this equation defining the heat flow in the wall is obtained in DOE-2 by superimposing a series of simple cases in order to obtain the general solution. These simple cases represent triangular pulse excitations (Figure 2-1). As a result a series of response factors are obtained.

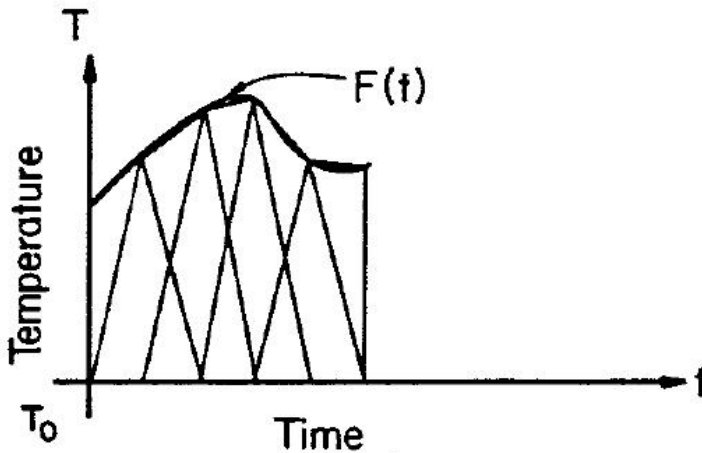


Figure 2-1: Overlapping triangular pulses defining a function (DOE-2 Engineers manual, 1982)



These response factors represent the heat flux response to temperature excitations. DOE-2 deploys three different series of response factors defined in DOE-2 Engineers manual as follows; and with reference to Figure 2-2.

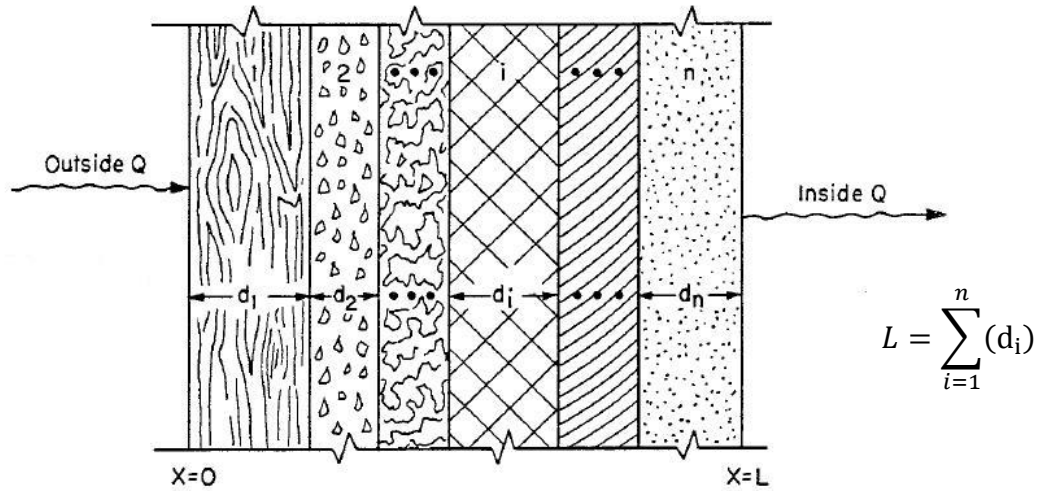


Figure 2-2: Flow of Energy through a multilayer wall (DOE-2 Engineers manual, 1982)

- **X** Response Factor Series: Represents the response (heat flow out of the outside surface) at  $x = 0$  to a triangular temperature excitation at  $x = 0$
- **Z** Response Factor Series: Represents the response (heat flow out of the inside surface) at  $x = L$  to a triangular temperature excitation at  $x = L$
- **Y** Response Factor Series: Represents the response (heat flow out of the inside surface) at  $x = L$  to a triangular temperature excitation at  $x = 0$  (outside surface)

### Heat Balance

A heat balance network for each room is established. The heat balance is pulsated in order to determine the custom weighting factors for the room. The weighting factors

are then used, to calculate hourly cooling/heating loads and space temperatures. The heat balance is constructed on the interior surface of the walls in the room. Four processes are considered in the heat balance of the room: conduction through the walls and furniture, Convection from interior surfaces to the room, radiation between the room's interior surface, and impinging radiation on the interior surfaces. Infiltration is considered in DOE-2 to be a direct communication between the air in the room and the outside; and therefore is not considered by DOE-2 as part of the heat balance equation.

Following, is an overview of the expressions representing each of the heat balance equation components. The equations generally resemble the standard conduction, convection and radiation equation; yet they involve z-transfer functions due to the nature of the data.

### **Conduction through walls**

Conduction heat flow,  $Q_{Di}(z)$ , to the inside surface is represented by equation 2-10 below.

$$Q_{Di}(z) = K_{Di}(z) T_i(z) - K'_{Di}(z) T'_i(z) \quad (2 - 10)$$

Where:

- $Q_{Di}(z)$  = z-transform of conduction heat flow into the interior surface of the wall i
- $T_i(z)$  = z- transform of the wall's inside surface temperature
- $T'_i(z)$  = z- transform of the wall's outside surface temperature
- $K_{Di}$  &  $K'_{Di}$  = z-transfer function representing the conduction heat flow coefficient

The thermal resistances ( $R_i$ ) of the wall layers are directly represented in  $K_{Di}$  &  $K'_{Di}$  transfer functions in the case of Quick Walls (walls with no thermal storage). Or, they are represented through the, previously discussed, response factors that are constituents of  $K_{Di}$  &  $K'_{Di}$  in the case of delayed walls (walls with thermal storage).

### Convection

The convection component of the heat balance equation representing convective heat transfer between the wall surfaces is expressed by equation 2-11.

$$Q_{ci}(z) = K_{ci}(z) [T_a(z) - T'_i(z)] \quad (2 - 11)$$

Where:

- $Q_{ci}(z)$  = z-transform of convective heat flow from the room air to the wall, i, surface.
- $T_a(z)$  = z- transform of the air temperature
- $T'_i(z)$  = z- transform of the wall , i, surface temperature
- $K_{ci} = h_{ci}A_i$  = z-transfer function of the convective heat transfer process of the wall i. (2 - 12)

Where:

- $h_{ci}$  = convective heat transfer coefficient for wall, i
- $A_i$  = Area of wall, i

### Radiative Heat Exchange Between walls

The Radiative heat exchange between walls in a room is expressed in equation 2-13.

$$Q_{Rim}(z) = K_{Rim}(z) [T_m(z) - T_i(z)] \quad (2 - 13)$$

Where:

- $Q_{Rim}(z)$  = z-transform of the radiative heat flow from surface, i, to another surface, m.
- $T_m(z)$  &  $T_i(z)$  = z- transforms of the corresponding surface temperatures
- $K_{Rim}(z) = 4 (\epsilon_i) \sigma (T_R^3) (F_{im}) A_i$  (McAdams, 1954) (2 – 14)

Where:

- $\epsilon_i$  = Surface emissivity (usually assumed by DOE-2 as:  $\epsilon_i = 0.9$ )
- $\sigma$  = Stefan –Boltzman constant
- $T_R$  = Surface reference temperature (usually assumed by DOE-2 as:  
 $T_R = 530$  °K/70 °F)
- $A_i$  = Area of radiating surface
- $F_{im}$  = View factor between the 2 surfaces (if to surfaces don't see each other then  $F_{im} = 0$ ) =  $\frac{A_m \text{ (receiving surface)}}{A_T \text{ (Transmitting surface)}}$  (2 – 15)

With all the terms Accounted for, the resulting heat balance equation is therefore give by equation 2-16.

$$Q_{Di}(z) = Q_{Ci}(z) + \sum_{m=1}^N Q_{Rim}(z) + Q_{Si}(z) \quad (2 – 16)$$

Where N = Number of surfaces in a room.

By replacing each of the previous terms in the heat balance, the equation becomes 2-17:

$$K_{Di}(z) T_i(z) - K'_{Di}(z) T'_i(z) = K_{Ci}(z) [T_a(z) - T'_i(z)] + \sum_{m=1}^N K_{Rim}(z) [T_m(z) - T_i(z)] + Q_{Si}(z) \quad (2 – 17)$$

To determine the custom weighting factors, as described previously, the heat balance equation is pulsed. The term to be pulsed is chosen based on the type of custom weighting factors required. The “pulsated term” choice is illustrated in Table 2-1.

Heat-Gain Weighting Factors	Air-Temperature weighting Factors
<p style="text-align: center;"><u>Pulse <math>Q_{Si}</math></u></p> $\sum_{m=1}^N Q_{Si}(0) = 1$ $Q_{Si}(k\Delta) = 0 \text{ for } k > 0$ $T_a(k\Delta) = 0 \text{ for } k \geq 0$	<p style="text-align: center;"><u>Pulse <math>T_a</math></u></p> $T_a(0) = 1$ $T_a(k\Delta) = 0 \text{ for } k > 0$ $Q_{Si}(k\Delta) = 0 \text{ for } k \geq 0$

Table 2-1: Choice of pulsed term in the heat balance equation

### Heat-Gain Weighting Factors

The determination of the heat-gain custom weighting factors from the heat balance equation is illustrated below. Air-temperature weighting factors are determined in a similar manner by pulsating the corresponding term. To obtain the heat-gain weighting factors, the heat balance equation is rearranged as shown in equation 2-18 and with a unit pulse of  $Q_{Si}(z)$ .

$$\begin{aligned}
Q_i(k\Delta) = & A_i h_{ci} \sum_{m=1}^N D_{im} \left[ A_m Z_m(k) \sum_{n=1}^N D_{mn} B_n(0) \right] \\
& - A_i h_{ci} \sum_{m=1}^N D_{im} \left\{ \frac{1}{h_{cm}} \sum_{n=1}^N Z_m(j) Q_m[(k-j)\Delta] \right\} \quad (2-18)
\end{aligned}$$

Where:

- $Q_i(k\Delta)$ : Represents the cooling load from each wall at time  $k\Delta$ , expressed in terms of previous values of  $Q(k\Delta)$
- $D$  &  $B$ : Characteristic matrices resulting from incorporating the various wall layers into the heat balance equation.

The cooling loads  $Q(k\Delta)$  at each  $k\Delta$  represent the coefficients of the temperature  $z$ -transfer function described earlier. Therefore  $T(z)$  is expressed as shown in equation 2-19 below:

$$\begin{aligned}
T(z) = & \underbrace{Q(0)}_{d_0} + \underbrace{Q(\Delta)z^{-1}}_{d_1} + \underbrace{Q(2\Delta)z^{-2}}_{d_2} + \dots \quad (2-19)
\end{aligned}$$

$$\therefore T(z) = d_0 + d_1 z^{-1} + d_2 z^{-2} + \dots \quad (2-20)$$

However  $Q(z)$  has been already expressed in equation 2-3 as:

$$\frac{Q(z)}{q(z)} = \frac{v_0 + v_1 z^{-1} + v_2 z^{-2}}{1 + w_1 z^{-1} + w_2 z^{-2}}$$

$\therefore T(z)$  is expressed in a similar format resulting in :

$$T(z) = d_0 + d_1 z^{-1} + d_2 z^{-2} + \dots = \frac{v_0 + v_1 z^{-1} + v_2 z^{-2}}{1 + w_1 z^{-1} + w_2 z^{-2}} \quad (2-21)$$

Therefore, by combining coefficients of the same power we obtain:

$$v_0 = d_0$$

$$\begin{aligned}
v_1 &= d_1 + d_0 w_1 \\
v_2 &= d_2 + d_1 w_1 + d_0 w_2 \\
&\dots etc.
\end{aligned}
\tag{2 - 22}$$

Solving the resulting system of 5 equations with 5 unknowns yields the values of the Heat-Gain weighting factors. The heat-gain weighting factors can now be used to determine the cooling/heating loads from instantaneous heat gains/losses using equation 2-4 shown earlier. This is the way by which cooling loads are calculated in DOE-2.

$$\therefore Q_\tau = v_0 q_\tau + v_1 q_{\tau-1} + v_2 q_{\tau-2} - w_1 Q_{\tau-1} - w_2 Q_{\tau-2} \tag{2 - 4}$$

Where:

- $q_i = q_0, q_1, q_2 \dots = \text{hourly heat gain}$
- $Q_i = Q_1, Q_2, Q_3 \dots = \text{hourly cooling load}$
- $v_0, v_1, v_2, w_1, w_2$  are Heat – gain weightitng factors

The air-temperature weighting factors are determined in a similar manner as the heat gain weighting factors. Once determined,  $g_0, g_1, g_2, g_3, p_1, \& p_2$ , can be used to determine the space temperature using equation 2-7 shown below.

$$t_\tau = \frac{1}{g_0} [Q_\tau + p_1 Q_{\tau-1} + p_2 Q_{\tau-2} - g_1 t_{\tau-1} - g_2 t_{\tau-2} - g_3 t_{\tau-3} p_2 Q_{\tau-2}] \tag{2 - 7}$$

Where:  $t_\tau = T(z) - T_R$

### **Custom Weighting Factors “Modification” by Heat Load Type**

DOE-2 considers heat gain due to (1) Solar radiation in the room, (2) People and equipment, (3) Lighting & task lighting, (4) Heat conduction through the walls, and (5) Heat conduction through furniture. Therefore, a variety of models is utilized in the heat

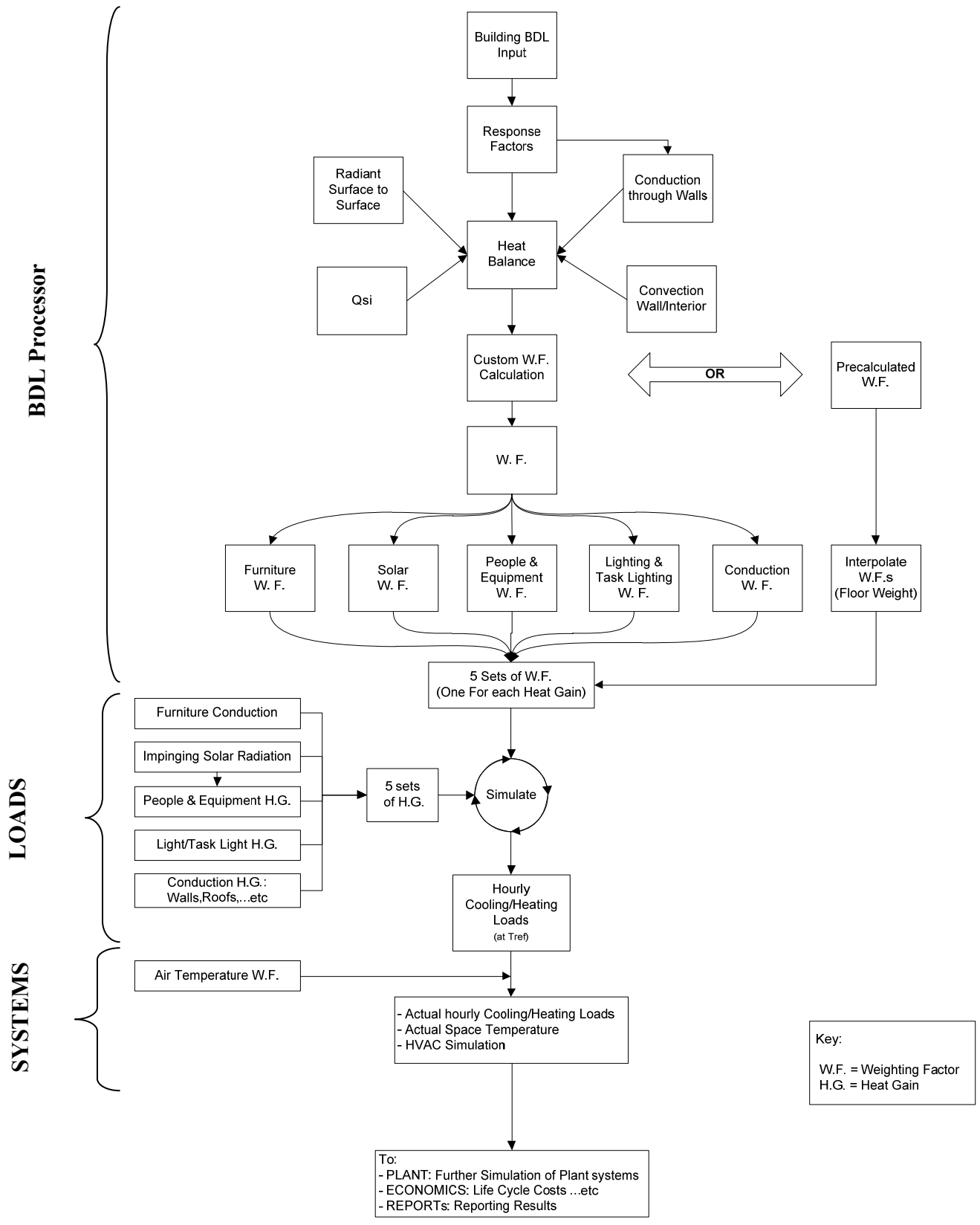
load calculation, one for each category of heat gain. The custom weighting factors are therefore, for each category of heat gain (input), tailored to provide a transfer function specific for calculating the required hourly cooling load (output). As a result, 5 different sets of custom weighting factors are obtained, corresponding to each of the above stated categories of heat gain.

### **Determination of Hourly Loads & Space Temperatures**

LOADS deploys a variety of algorithms and subroutines to calculate the hourly heat gains, by category. The respective weighting factors are applied to each set of heat gain to result in sets of hourly cooling/heating loads. These cooling/heating loads (due to each separate category) are then summed up to result in a Total Hourly Cooling/Heating Load. This is the method by which DOE-2 calculates hourly cooling/heating loads. SYSTEMS then applies the air-temperature weighting factors onto the calculated hourly heat gains/losses and cooling/heating loads to correct for using a fixed room temperature,  $T_{ref}$ , in LOADS calculations; and to calculate the actual hourly space temperatures. SYSTEMS also simulates the distribution equipment that provide heating, ventilation, and/or air conditioning in the building.

The use of the fixed reference temperature in DOE-2 in LOADS alleviates the computational time and load. Also, it results in a tight coupling between the calculations of the cooling/heating loads in LOADS program and the HVAC equipment calculation in SYSTEMS. The disadvantage of using a fixed reference temperature, however, is that it introduces slight approximations. The DOE-2 core simulation process is depicted in Flowchart 2-2





Flowchart 2-2: Flow of DOE-2 Core Simulation Process

## eQUEST

eQUEST, the Quick Energy Simulation Tool, is a graphical user interface based tool that facilitates for users the creation of DOE-2 building models. It includes building creation wizards that generate the DOE-2 model based on the user input. The wizards also help in automatically running parametric simulations for comparing alternative designs. Another important aspect of eQUEST is providing graphical outputs with key charts, values, and tables; along with the detailed regular DOE-2 output files. The following section contains an overview of the eQUEST wizards and distinctive properties that make it a very popular building energy simulation tool. Information in the following synopsis are obtained from the “Q eQUEST Introductory Tutorial, version 3.63” by James J. HIRSCH & Associates, April 2009; the “Q eQUEST Modeling Procedures Quick Reference Guide” by James J. HIRSCH & Associates, May 2007; and other software documentation on the eQUEST website ([www.equest.com](http://www.equest.com)).

eQUEST includes three main wizards, the Schematic Design Wizard (SD Wizard), the Design Development (DD Wizard), and the Energy Efficiency Measure Wizard (EEM Wizard). Both the SD and DD wizards are used in creating a building model. The EEM wizard is used, on the other hand, for evaluating and comparing design alternatives. The main difference between the SD and DD wizards is the degree of complexity of the models being created. The SD wizard is most suitable for smaller and simpler structures or for obtaining rough estimates in the early design phase of a structure. It has within it predefined generic shapes that can be manipulated by the user to define a simple building’s plan and layout. Users can instead import drawing files

containing the building layout. Another limitation on the SD wizard is the number of HVAC systems that can be simulated. This is limited to a maximum of 2 HVAC templates per shell, with a maximum of 2 building shells allowed with this wizard. The SD wizard offers choice of simplified building schedules and allows defining no more than 2 seasons per year.

The Design Development wizard is designed to be used for large and more complicated buildings. Also, for buildings with complex HVAC system assignments and/or intricate internal loads and schedules. The DD wizard has no limit on the number of different HVAC systems that can be used. Schedules and season options in the DD wizard are also more intricate and detailed. The DD wizard is preferably used during late stages of a building design, a phase where most of the building data essential for a more detailed building energy simulation are available.

Energy Efficiency Measures wizard (EEM) provides a quick and easy tool for comparing the energy performance of various design alternatives. EEM permits defining and comparing up to 9 alternatives at the same time. This wizard makes available for designers a valuable means of comparing the impact and evaluating the tradeoff of alternative designs. For example, the designer is able to evaluate the cost tradeoff of adding extra insulation versus the resulting savings on reduced heating/cooling costs. Similarly individual alternatives (up to 9) can be compared individually versus each other, or collectively (i.e. modifying two or more alternative versus a third for example). Examples of the possible alternative comparison runs include:

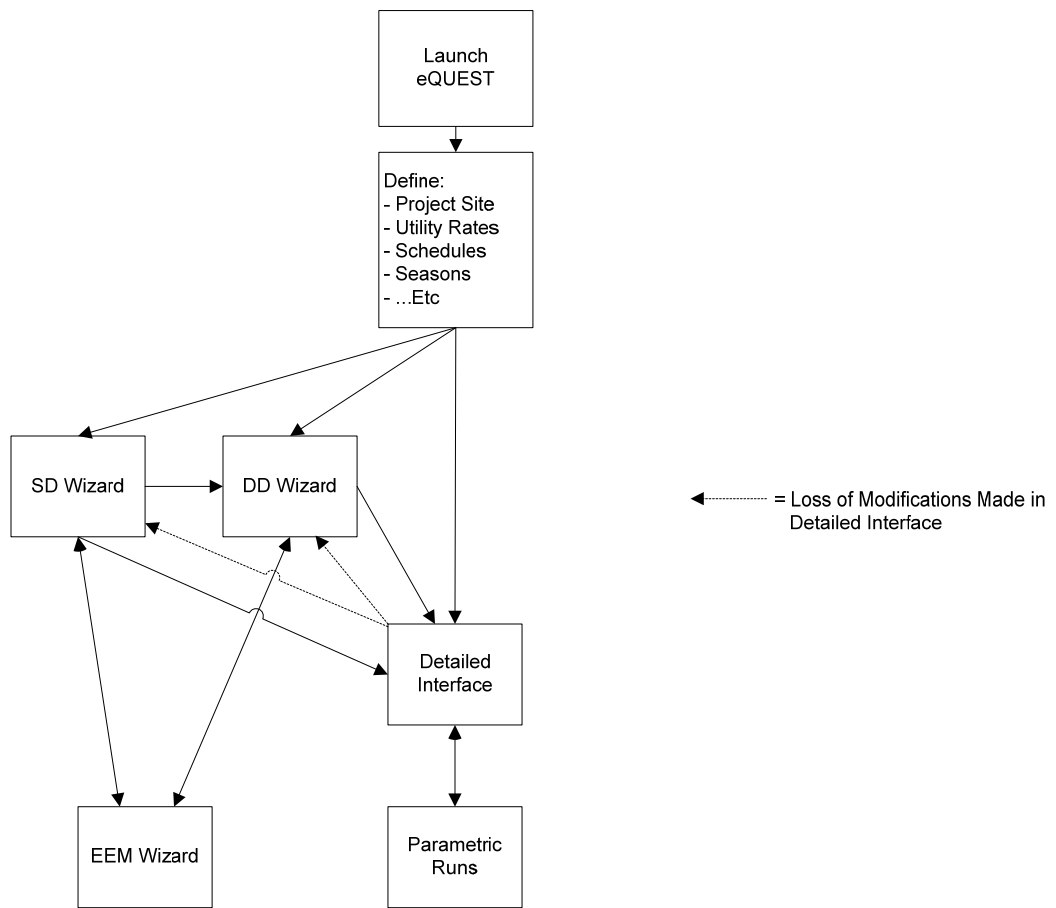
- Modifying/adding roof insulation
- Introducing top day lighting

- Installing high efficiency lighting
- Installing high efficiency chillers
- Switching to high performance glass
- Others

In addition to the wizards, eQUEST allows users to modify and edit models directly without using a wizard. This is known as the Detailed Interface. The detailed interface allows modifying specific/individual components. It also allows copying, creating, and linking of objects. Furthermore, it allows modifications to the building geometry and/or individual components. The detailed interface also includes an abundance of methods to define shades, including fixed shades and shades that rotate with the change of a building's orientation. Another aspect of the detailed interface is allowing users to adjust HVAC zone assignments. Comparison of alternatives is available in the detailed interface and is defined as Parametric Runs. These runs are similar to the EEM wizard used with the SD and DD wizards. However, parametric runs offer more detailed and comprehensive methods of investigating design alternatives. Some examples of possible parametric runs in the detailed interface include:

- Varying the properties of HVAC systems (performance curve, head ...etc)
- Varying the solar/optical characteristics of user-defined glass types
- Varying the windows glass type assignments
- Modifying the walls and roofs insulation
- Changing the building orientation
- Modifying operating schedules of light, equipment and people occupancy

- Modifying the geometry of building components (walls, roofs, shades...etc)
- The impact of adding skylights
- The impact of utilizing daylight controls
- The impact of installing/adding shades
- Others



**Flowchart 2-3: Possible Model Flows In eQUEST**

## **Infiltration**

Infiltration is a significant aspect of heat loss calculation. The determination of the thermal load resulting from the passage of outside air into the interior of a building is necessary. This thermal load is traditionally viewed as principally dependent on the flow rate of the infiltrating air and the inside-outside air temperature gradient. The driving pressure of outside airflow into the building is mostly caused by one of 2 forces or a combination of both. This driving pressure is either caused by the influence of outside gusting winds or the pressure difference across the building envelope resulting from the difference between inside and outside air temperatures (Jackman, 1974). In most situations, a combination of both persists as the driving force. The pressure gradient on the face of a building resulting from gusting wind is mostly the controlling infiltration driving force in low rise buildings (under 3-story rise buildings). In high rise buildings, the driving force of infiltration is primarily the stack effect. The difference in air temperature across the building envelope and height results in air buoyancy differences and as a result a pressure difference between the inside and outside of the building is established. During the heating season, for example, warm air rises inside a high rise building creating an inside positive pressure at the top and a lower pressure in the bottom floors, thus resulting in air infiltration at the bottom of the building (Brownell, 2002). The two infiltration driving mechanisms do not act independently. The air leakage driving force is usually an inside-to-outside pressure difference caused by a combination of both mechanisms (Blomsterberg and Harrije, 1979). Air infiltration, along with ventilation, has a major influence on a building's internal environment. Most importantly, infiltration has

a profound impact on the energy demand of a building. Relatively high infiltration rates excessively burden a building's heating and/or air conditioning system. This results in unnecessary waste and over-consumption of energy; or in surpassing the heating and cooling ability of the HVAC system in a building and resulting in a thermally uncomfortable interior environment (Liddament, 1986).

Studies estimate that infiltration accounts for 25% to 50% of the heating load in both residential and commercial buildings (Nevrala and Ethridge, 1977; Kirkwood, 1977). Caffey (1979) attributed 40% of the heating/cooling load in houses to infiltration. Similarly, Persily (1982) concluded that one third of the heating and cooling loads in a building are due to infiltration. The National Institute of Standards and Technology (1996) estimates that 15% of the heating loads in commercial building to be due to air infiltration. Similarly, other studies assert the significant impact of air infiltration on thermal loads in a building.

The following sections include a review of ASHRAE definitions, guidelines, and procedure for dealing with infiltration as well as an overview of infiltration calculation methods and their categorizations. A review of different infiltration types, the corresponding sources and gateways, and the impact of each is also presented. Finally, a discussion of major problems and inadequacies with the currently adopted infiltration load calculation models.

## Infiltration in ASHRAE

Infiltration is primarily addressed in Chapter 16 of the 2009 ASHRAE Handbook of Fundamentals® “Ventilation and Infiltration”.. According to ASHRAE infiltration, along with ventilation, is classified under “Air Exchange” of outdoor air with a building's indoor air. Ventilation is defined as the intentional introduction of outside air into the inside of a building. Ventilation can be natural, through naturally planned openings in a building envelope, or forced (mechanical) ventilation. On the other hand, infiltration (air leakage) is defined by ASHRAE as “The flow of outdoor air into a building through cracks and other unintentional openings and through the normal use of exterior doors for entrance and egress”. Infiltration is either driven by natural or artificial pressure differences.

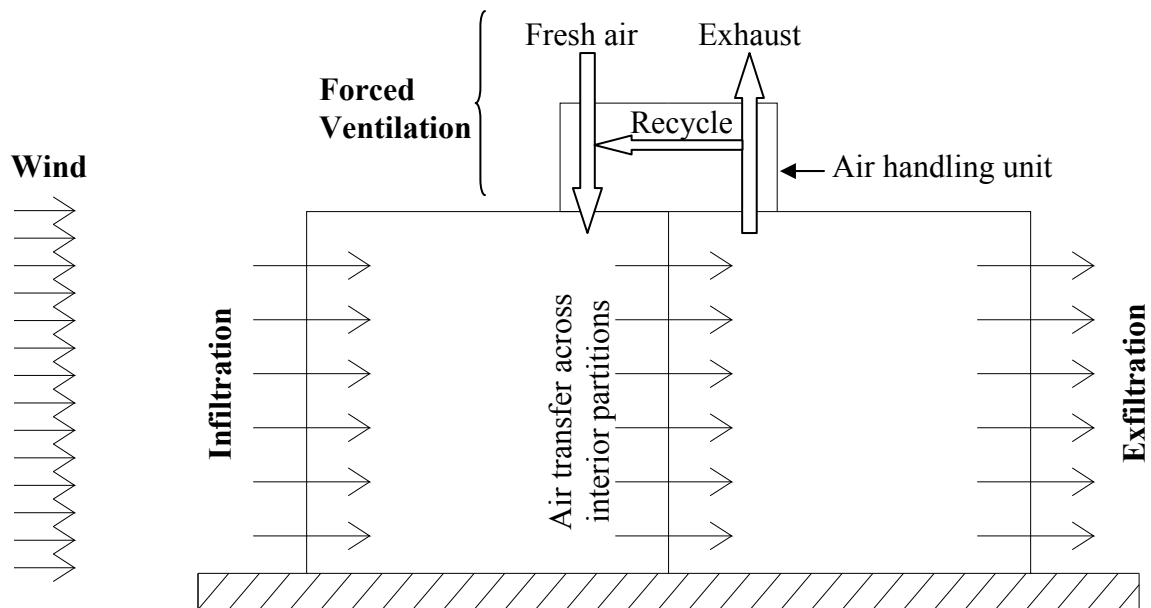


Figure 2-3: Typical Infiltration & Ventilation Airflow



ASHRAE emphasizes the discussion of infiltration majorly in residential houses, while in commercial buildings the focus in ASHRAE is on ventilation. However, it clearly advises that infiltration in commercial buildings should not be ignored. This is in agreement with the previously discussed literature overview where studies showed infiltration to account for 40 % of the heating/cooling load in residential buildings versus 15 % in commercial buildings (Caffey, 1979; NIST, 1996).

ASHRAE, with reference to Dickerhoff et al. (1982) and Harrje and Bur (1982), estimates the percentage distribution of infiltration air leakage by building components as follows:

- Walls: 18% to 50%, with an average of 35%.
- Ceiling Details: 3% to 30%, with an average of 18%. This leakage undermines the purpose of insulation in attics, residential houses, and ceiling insulation in buildings.
- Forced-air and/or Cooling systems: 3% to 28%, with an average of 18%. This category represents air leaks in conditioning/heating air paths and ducts.
- Windows and Doors: 6% to 22%, with a 15% average. The infiltration air leakage in windows is a matter of the window type rather than age (Weidt et al., 1979). It is important to note that this percentage represents the infiltration through doors and windows seals and cracks, not due to the opening of doors by passing individuals, for instance.
- Fire Place: 0% to 30%, with an average of 12%. Similar to the case of doors and windows, this percentage represents the air leakage through a “cold fireplace”; not a running fire place with open dampers, plugs, caps or such.

- Vents in conditioned spaces: 2% to 12% with an average of 5%. This refers to undamped or improperly damped small exhaust vents in a conditioned space.

Other infiltration (air leakage) sources count for 1% or less of the total leakage.

### **Residential Calculation Models**

ASHRAE references a list of simplified models for use in the calculation of infiltration in residential buildings. The referenced calculation models vary between simple estimation models and more advanced models. The model categories include:

#### **Empirical Models**

These residential infiltration models are found on statistical fits of infiltration rate data collected from specific houses. The data used is collected from pressurization tests on houses and reduced to a low order equation. These models define, at most, a very simple relationship between infiltration rate, some air tightness factor and a weather condition. The referenced models include Sherman (1987), Kronvall (1980), Reeves et al. (1979) and Shaw (1981).

#### **Multizone Models**

Multizone models consider the building to be a series of interconnected zones, assuming a well mixed air within each. They are based on a mass balance requiring a balance between the inflow and outflow in each of the interconnected zones. Among the Multizone methods referenced in ASHRAE Fundamentals Handbook are: Allard and Herrlin (1989), Etheridge and Alexander (1980), Herrlin (1985), Liddament and Allen (1983), and Walton and Dols (2003). Multizone models require a user input describing

the leakage in the building envelope, wind pressure on the building envelope, zone temperatures, and ventilation air flow rates. Estimates from available literature are usually used and assumed as input.

### **Single Zone Models**

These models are developed and based on the principal of accounting for the building interior as a single zone with no internal resistance of air flow. Some of the ASHRAE referenced models are: Cole et al. (1980), Sherman & Grimsrud (1980), Warren and Webb (1980), and Walker and Wilson (1998). All single zone models require inputs of wind speed, temperature, wind shelter and leakage distribution over the building envelope. These models are extremely sensitive to the required input data, which in turn are rather difficult to determine.

### **Superposition of Wind and Stack Effects**

Infiltration is caused by two driving forces, wind and stack effect. Superposition models calculate the infiltration due to each driving force separately and then combine the two results.

### **Infiltration in Commercial Buildings**

Commercial and institutional building envelopes, according to ASHRAE, are commonly assumed to be rather airtight. Conversely, ASHRAE emphasizes that according to Persily & Grot (1986), if measured air leakage flow rates are normalized by building envelope area (rather than building volume), the results obtained show envelope air tightness levels in commercial buildings resembling those of typical residential

American houses. Office building envelopes are therefore found to be leakier than expected. There are several negative consequences to infiltration in commercial buildings. This includes reduced thermal comfort, degradation of indoor air quality, increase in energy consumption, moisture damage, and others.

Important to evaluating air leakage in commercial buildings, according to ASHRAE, are leakages associated with internal partitions, elevators, stairs, shaft walls, doors and others. As a result, included in ASHRAE Handbook of Fundamentals are charts that help, for example, in quantifying the air leakage through elevator shafts and similar components.

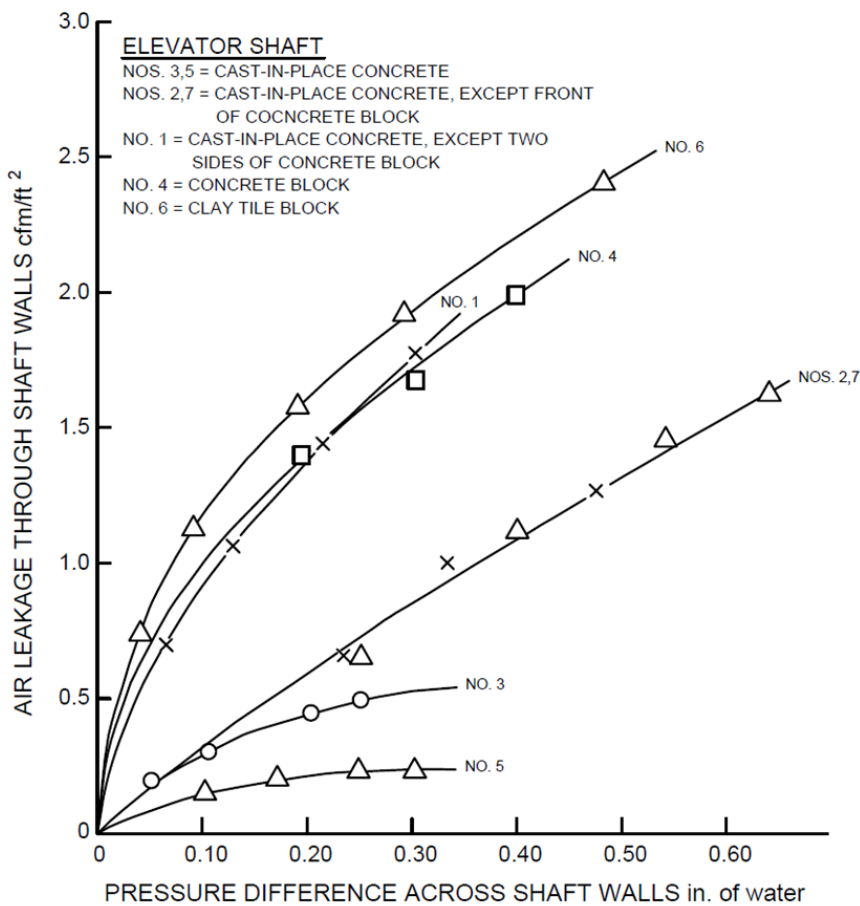


Chart 2-1: Air Leakage Rates of Elevator Shaft Walls (2009 ASHRAE® Handbook of Fundamentals)

Infiltration through doors depends on several factors such as the type and use of the door, room and building. Also critical are the air speed and pressure differentials across the door. In residential and small buildings, infiltration through doors is more defined by air leakage through cracks and openings between the door and its frame; primarily due to the infrequent use of the doors. However, as the frequency of the door use increases, the infiltration calculation becomes dependant on the air flow through the door (when open). Automatic doors (swinging, sliding, or rotating), for example, represent a major venue of air infiltration. These doors stay open much longer than manual doors and allow significant amounts of air infiltration. In the case of a facing pair of doors, air flow becomes an even more significant issue to be considered in heating and cooling load calculations. In ASHRAE fundamentals, for doors, an air flow rate chart is provided (Figure 2-5) and air flow coefficients charts (Figure 2-6) along with the relevant equations necessary for calculating the resulting air flow.

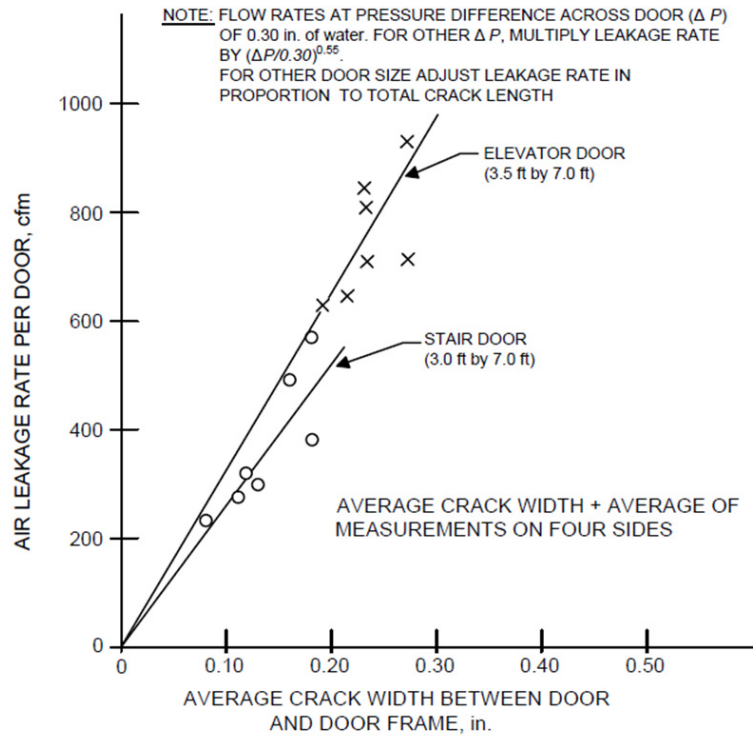


Chart 2-2: Air Leakage Rate of Door versus Average Crack Width (2009 ASHRAE® Handbook of Fundamentals)

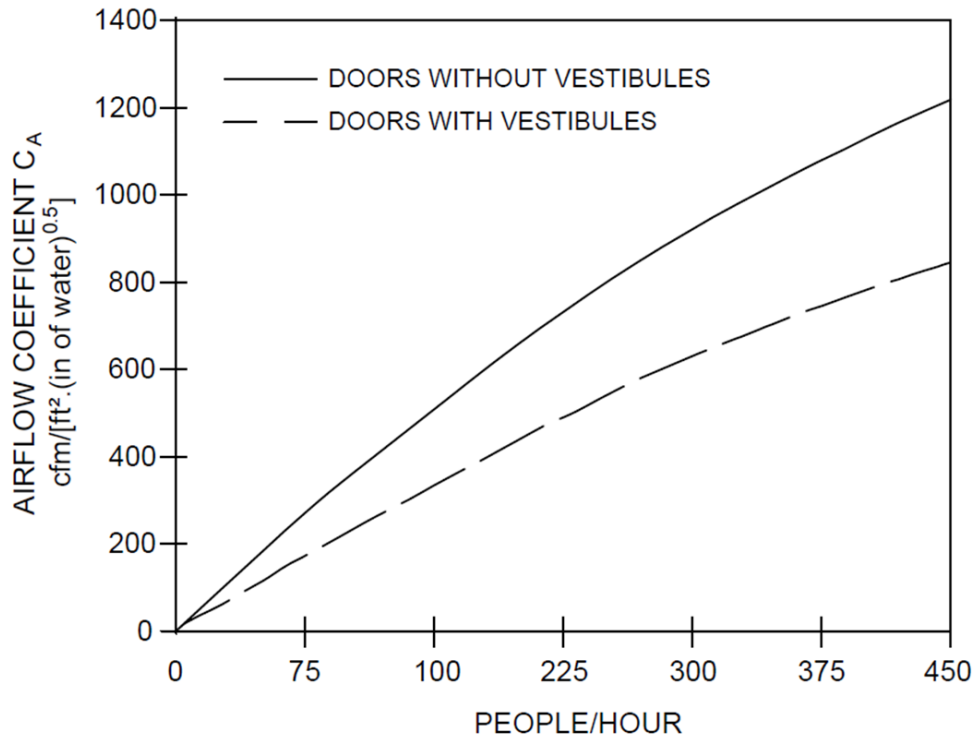


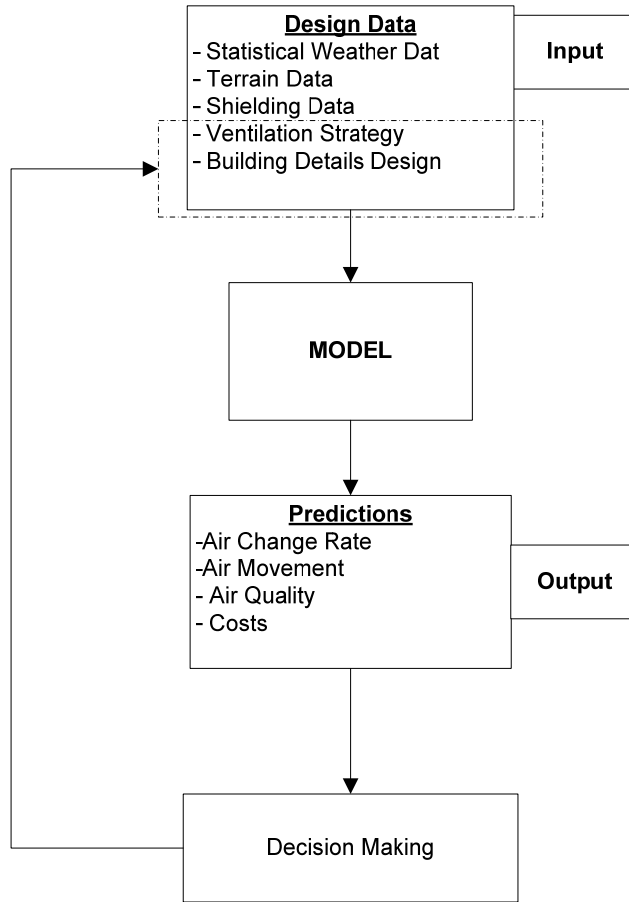
Chart 2-3: Airflow Coefficient for Automatic Doors (2009 ASHRAE® Handbook of Fundamentals)

## **Air Infiltration Calculation Techniques & Methods**

Even though air infiltration is an important facet of building physics, it still involves substantial uncertainty. This is mostly due to the difficulty of measuring infiltration in buildings, which limits the experimental database available for use in developing infiltration evaluation techniques and methods. Another reason is the wide variety of available construction techniques and practices, each of which is distinguished by diverse infiltration characteristics (Liddament, 1986). Several models and algorithms have been developed for evaluation infiltration. Among these are Walton (1984), Jackman (1974), Reeves (1979), Crall (1983), Warren (1982) and several others. Following, is a general review and classification of the available infiltration techniques and methods.

Infiltration calculation models are essential in the building thermal design process. They are used in calculating the resulting air change rates, energy requirements, and, ultimately, costs. Flowchart 2-4 shows the role these models play in the design process. The output of a model can be used to modify the building properties and optimize the design.

Air infiltration calculation is primarily a measure for calculating the rate of air change in a building under given conditions (Liddament, 1986). The air change rate is a measure of the number of times the volume of air within a fixed airspace (room, building or other) is replaced by infiltrating outside air. The number of air changes per hour in a fixed space is defined by equation 2-23.



**Flowchart 2-4: Role of Air Infiltration Model in the Energy Design/Analysis Process (Liddament, 1986)**



$$N = \frac{60 Q}{V} \quad (2 - 23)$$

Where:

- N = Number of air changes per hour
- Q = Volumetric flow rate of infiltration air
- V = Volume of Space

Air infiltration is primarily affected by the building overall tightness, the influence of climate (primarily wind speed and air temperature) on the driving mechanisms, and the location of the building (topography). The concurrent influence of these factors on infiltration can be represented in the following graphical form, Figure 2-7 (Liddament, 1986).

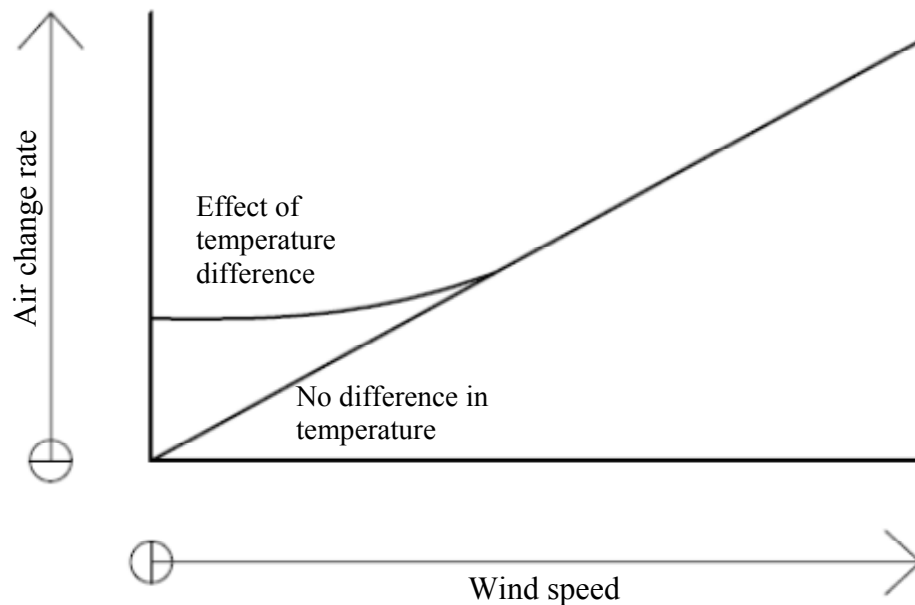
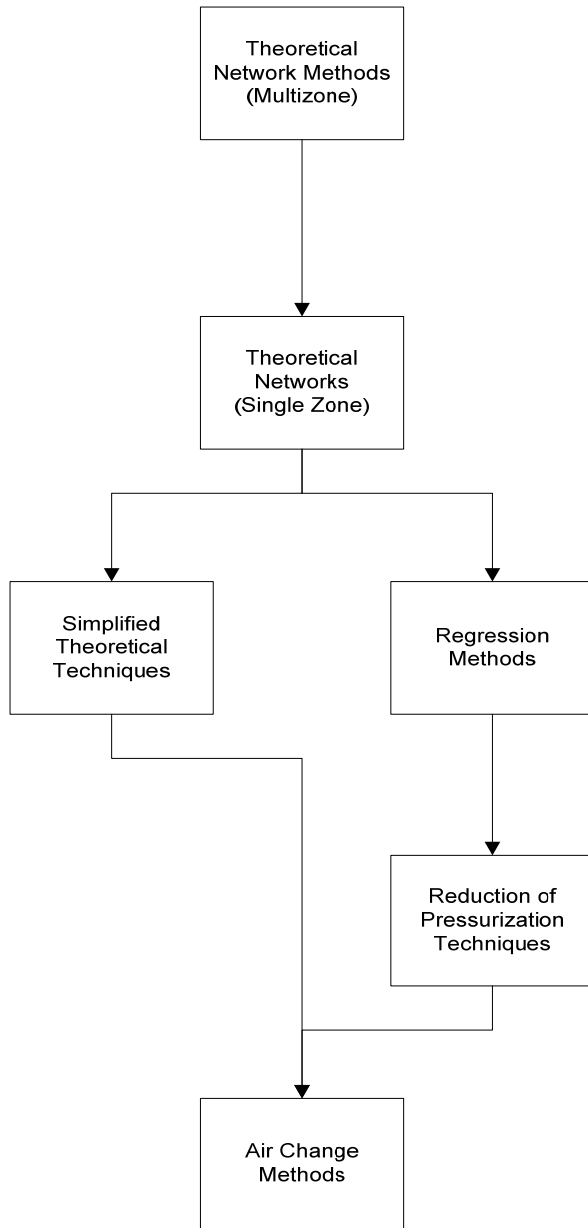


**Chart 2-4: Infiltration Characteristics (Liddament, 1986)**

The various infiltration, and ventilation, calculation techniques fall into five general categories listed below.

- |  |   |                    |
|--|---|--------------------|
| 1. Air Change Methods                    | } | Empirical Models   |
| 2. Reduction of Pressurization Test Data |   |                    |
| 3. Regression techniques                 |   |                    |
| 4. Theoretical Network Methods           | } | Theoretical Models |
| 5. Simplified Theoretical Methods        |   |                    |

Air change methods, reduction of pressurization test data and regression techniques are all empirical models, while the remaining 2 methods are classified as numerical methods. These various categories can be organized in a hierarchal order in terms of complexity and range of applicability. Theoretical network multizone methods top the hierarchy in complexity; while air change methods are considered the least complex with the least range of applicability. Shown in Flowchart 2-5 is the infiltration calculation methods hierarchy as defined by Liddament (1986) along with a summary of the data requirements, advantages, and disadvantages of each in Tables 2-2 and 2-3.



**Flowchart 2-5: Hierarchical order of Infiltration Calculation Techniques (Liddament, 1986)**

## Summary of Calculation Techniques

### (A) Empirical Models

Technique	Data Requirements	Advantages	Disadvantages
Air Change Methods	Basic Bldg Design Details <ul style="list-style-type: none"> <li>- Size</li> <li>- Height</li> <li>- etc</li> </ul>	<ul style="list-style-type: none"> <li>- Ease of use</li> <li>- No computing facilities required</li> </ul>	Doesn't provide detailed infiltration predictions
Reduction of Pressurization test data	Pressurization test data	<ul style="list-style-type: none"> <li>- Ease of use</li> <li>- No computing facilities required</li> </ul>	<ul style="list-style-type: none"> <li>- Applies only to existing buildings (that have been pressure tested)</li> <li>- Doesn't indicate the affects of weather, sheltering and/or terrain</li> </ul>
Regression Methods	Infiltration measurement data with parallel wind and temperature records	<ul style="list-style-type: none"> <li>- Fairly easy to use</li> <li>- Gives weather dependent infiltration prediction</li> </ul>	<ul style="list-style-type: none"> <li>- Only applies to existing buildings (Tracer gas tested)</li> <li>- Regression data can give unreliable results</li> </ul>

Table 2-2: Empirical Infiltration techniques (Based on Liddament (1986))

### (B) Theoretical Models

Technique	Data Requirements	Advantages	Disadvantages
Network Models	<ul style="list-style-type: none"> <li>- Bldg Description                             <ul style="list-style-type: none"> <li>- Size</li> <li>- Height</li> <li>- Etc</li> </ul> </li> <li>- Surrounding Shield data</li> <li>- Terrain</li> <li>- Flow data (location and description of leaks)</li> </ul>	<ul style="list-style-type: none"> <li>- Predicts air distribution pattern</li> <li>- Determine internal pressure</li> <li>- Responds to weather&amp; terrain variations</li> <li>- If moderate, it can be run on regular computers</li> </ul>	<ul style="list-style-type: none"> <li>- Substantial data required to describe flow</li> <li>- Considerable computational power required</li> </ul>
Simplified Theoretical Models	<ul style="list-style-type: none"> <li>- Building air leakage characteristics</li> <li>- Shielding &amp; terrain data</li> </ul>	<ul style="list-style-type: none"> <li>- Compromise between theoretical models complexity &amp; inaccurate empirical techniques</li> </ul>	<ul style="list-style-type: none"> <li>- Applies to single zone only</li> <li>- No information on air movement</li> </ul>

Table 2-3: Theoretical Infiltration techniques; Based on Liddament (1986)

## Empirical Techniques

### Air Change methods

The air change method depends on a tabulation of average air changes per hour, as shown in sample Table 2-4. The values in such tables are based on construction tightness. The tightness of the construction depends, largely, on workmanship. Typically, residential construction falls in the low end of the “Medium” category shown in Table 2-4 (Bobenhausen, 1994).

<b>Tightness of Envelope Construction</b>	<b>Average Winter Air Changes per Hour</b>
<b>Tight</b>	0.2 to 0.6 ACH
<b>Medium</b>	0.6 to 1.0 ACH
<b>Loose</b>	1.0 to 2.0 ACH

Table 2-4: Air Changes per Hour (ACH) estimated by Construction Tightness (Bobenhausen, 1994)

The calculation of heat loss due to infiltration using Air Change Methods is expressed by equation 2-24 (Bobenhausen, 1994)

$$q_{inf} = (C) \times (ACH) \times 0.018 \quad (2 - 24)$$

Where:

- $q_{inf}$  = Infiltration heat loss (Btu/°F.hr)
- C = Space volume (ft<sup>3</sup>)
- ACH = Air Change rate per hour
- 0.018: Air heat capacity (Btu/°F.ft<sup>3</sup>)

## Reduction Pressurization Test Data

The reduction of pressurization test data method is a very simplified technique for calculating the average infiltration in a building. This method, as stated in Table 2-3, is limited to the evaluation of infiltration in pre-existing buildings. It depends on pressure data test results. This method doesn't offer any information on the impact of wind, temperature, terrain, or shielding on the infiltration levels in the building (Liddament, 1986). The mathematical expression of this method is shown in equation 2-25.

$$Q_{inf} = \frac{Q_{50}}{20} \quad (2 - 25)$$

Where:

- $Q_{inf}$  = Infiltration rate/hr
- $Q_{50}$  = Measured air change rate at 50 Pa, from building pressure testing

## Regression Techniques

Regression techniques are based on curve fitting of statistical data. Accumulated long term infiltration data measurements are coupled with some climatic data into an empirical equation. The resulting expression can be of increasing complexity, starting with a linear relationship. The general format of the resulting relationship is shown in equation 2-26 and has been reported by several researchers including Jordon, et al. (1963), Tamura and Wilson (1964), Elkins and Wensman (1971), Hill and Kusuda (1975), and others.

$$Q_{inf} = a' + b'\Delta T + C'V^2 \quad (2 - 26)$$

Where:

- $Q_{inf}$  = Infiltration rate ( $t^{-1}$ )
- $\Delta T$  = Internal/external temperature difference

- $V$  = Wind speed
- $a'$  ,  $b'$  , &  $c'$  are regression coefficients

### Theoretical Methods

Existing theoretical models vary in their degree of complexity in calculating infiltration. Correspondingly, the choice of a specific method depends on the building type and internal application (Liddament, 1986). The simplest form of theoretical models is single zone models. More complex methods are multizone models that breakdown a building into a series of interconnected zones. The underlying concept of all theoretical methods is mass balance. Infiltrating air displaces an equivalent volume of internal air; thus maintaining a mass flow balance (Liddament, 1986). Theoretical models require a description of the flow mechanism. The representation of the air flow varies between large openings and small cracks. In large openings, such as windows, doors and large cracks, the flow is usually turbulent. The flow is therefore commonly represented by an orifice equation as in equation 2-27.

$$Q = C_d A \left[ \frac{2}{\rho} \Delta P \right]^{\frac{1}{2}} \quad (2 - 27)$$

Where:

- $Q$  = air flow rate ( $m^3/s$ )
- $C_d$  = Discharge coefficient
- $\rho$  = Air density
- $A$  = Area of opening

Alternatively, in small cracks like those found in mortar or among tightly fitting components the flow tends to be laminar and controlled by the affect of viscosity. Such flow can be characterized by equation 2-28 (Liddament, 1986).

$$Q = \frac{\Delta P}{\mu L} [\pi r^4] \quad (2 - 28)$$

Where:

- $\mu$  = dynamic viscosity
- $L$  = Length of the flow path
- $r$  = Radius of opening

In application, the flow mechanism is defined by an equation combining both flow schemes as in equation 2-29

$$Q = k (\Delta P)^n \quad (2 - 29)$$

Where:

- $k$  = Flow coefficient
- $n$  = Flow exponent ( $0.5 \leq n \leq 1$ ) characteristic of the flow regime
- $\Delta P$  = Pressure gradient across the crack/opening

An understanding of the value of ( $k$ ) can be acquired by referring to the equation of flow through an orifice (equation 2-30) (Walton, 1984)

$$Q = c . A . \rho . \sqrt{2 . \frac{\Delta P}{\rho}} \quad (2 - 30)$$

Where:

- $C$  = Flow coefficient
- $A$  = Area of opening
- $\rho$  = Air density



The flow coefficient,  $C$ , holds a value of 0.6 for a wide range of Reynold's Number, as shown in Figure 2-8. Therefore,  $C$  is usually assumed to be 0.6.

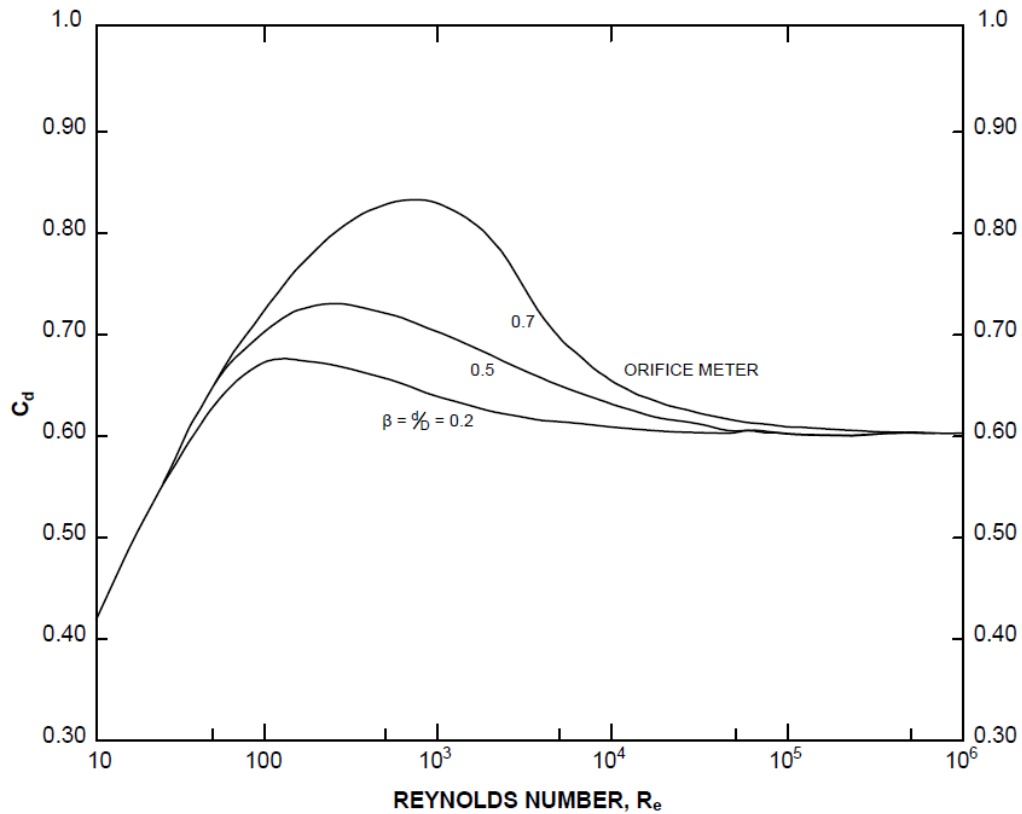


Chart 2-5: Orifice Flowmeter Coefficient (ASHRAE 1977) (Walton, 1980)

### Single-Zone Models

Single zone models, as discussed previously, calculate infiltration by considering the whole building interior as one enclosed space. Essential to the single zone method calculation are (Liddament, 1986):

- Flow paths and flow characteristics ( $k$  &  $A$  values)
- Building height
- Internal/External temperature gradient
- Area wind speed
- Any local shielding conditions

- Terrain roughness factors
- Mechanical ventilation system properties

The total infiltration into a space is then quantified using equation 2-29 and following equation 2-31 below (Liddament, 1986)

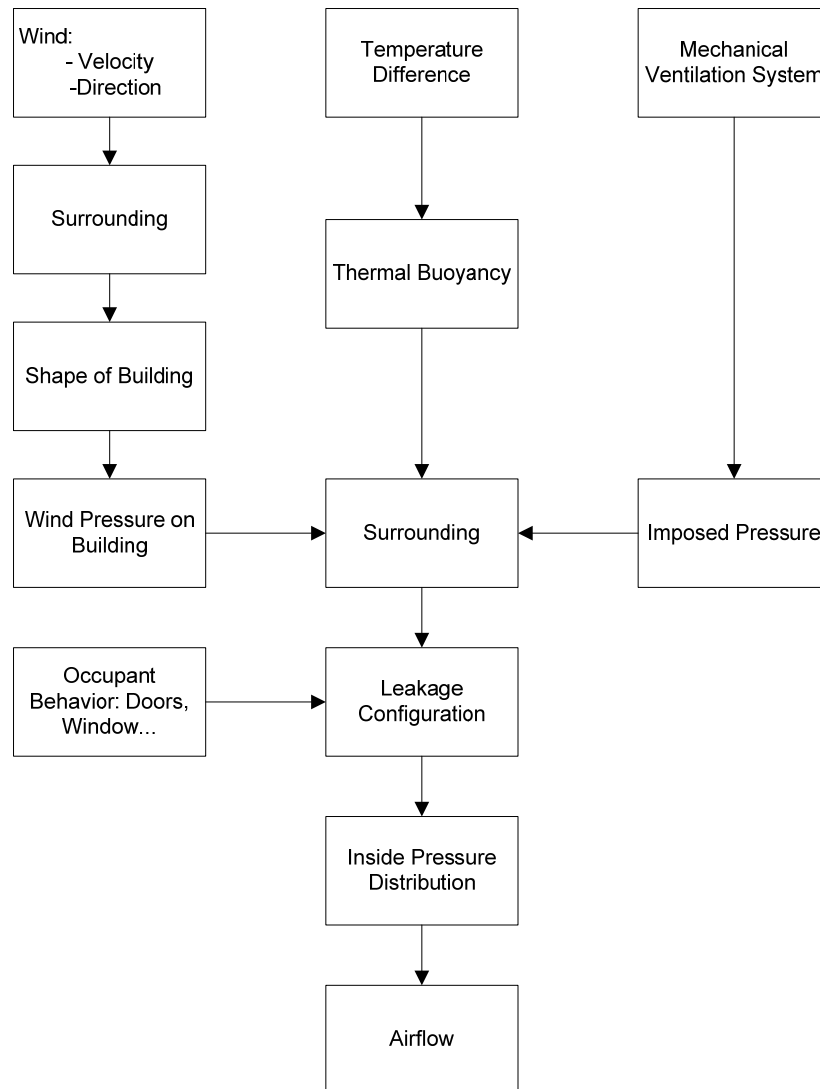
$$Q_{in} = \sum_{i=1}^j Q_i \quad (2 - 31)$$

Where:

- $j$  = Total number of flow paths
- $Q_i > 0$  : Infiltration Flow
- $Q_i < 0$  : Exfiltration Flow

### **Multizone Models**

Multizone models differ from single zone models by accounting for internal partitions. These partitions obstruct the internal movement of air. Similar to single zone models, multizone models require knowledge of flow paths details and characteristics, building geometry and others. Added to the mass balance in these methods are airflow equations representing the air flow/leakage across internal zones and partitions (Liddament, 1986). However, according to Etheridge (1998), internal room air flow is of secondary effect on infiltration. The influences of wind gust and room air buoyancy induced pressures are the prominent infiltration driving force. Therefore, for each case, the amount of effort involved in using multizone models has to be weighed against the significance of accounting for the impact of internal partitions on the infiltration load calculations. A general depiction of a multizone calculation model layout is presented in Flowchart 2-6.



**Flowchart 2-6: Multizone Models Calculation Models (Feustel, 1985 - Modified)**

Single and multizone theoretical models represent an improvement over empirical methods. However, these methods require substantial data input and considerable computations. Multizone models also require a large amount of input and in many cases need for their variables values that are hard to obtain, such as wind and stack pressure coefficients and others. A building needs to be tested in order to obtain such coefficients, and therefore at a design stage obtaining such factors becomes problematic and a major

source of simulation error. When these values are substituted for by scarce tabulated data, the level of simulation inaccuracy is elevated. This is due to the fact that generic coefficients are being used that do not represent local conditions, building characteristics, and other important building related factors. Furthermore, despite accounting for important infiltration related aspects, such as wind and stack pressure, using coefficient or some other form; existing multizone models still ignore other important factors that influence infiltration loads such as heat recovery and solar radiation.

### **CFD, FFD, AND COMBINED MULTIZONE-CFD METHODS**

Multizone models, in addition to having the capability of simulating infiltration, can calculate the amount of mass flow between different zones within a building (inter-zonal airflow). Such information is essential for the design of heating/cooling and ventilation systems in buildings (Haghighat and Li, 2004). However, the underlying assumption in most multizone models is the presumption of perfect mixing of indoor air. This assumption of well-mixed zones permits these models to predict indoor conditions and the Hygrothermal performance of the building envelope (Steeman et al., 2009). Multizone models also assume a uniform temperature for each zone and neglect airflow momentum preservation inside a zone. These assumptions affect modeling accuracy and can result in errors (Wang and Chen, 2006). As a result was the promotion of Computation Fluid Dynamics (CFD) methods in modeling infiltration airflow. These methods reduce the number of assumptions otherwise necessary when using multizone methods. CFD methods are also capable of providing detailed airflow values, temperatures, and pollutant distribution conditions (Wang and Chen, 2006; Stamou and Katsiris, 2006). There are 3 general groups of CFD methods: Direct Numerical

Simulation (DNS), Large Eddy Simulation (LES), and Reynolds Averaged Navier-Stokes (RANS) methods (Stamou and Katsiris, 2006).

Encountered flows can be turbulent and characterized with eddies falling into a wide range of lengths and time scales. Using a very fine grid resolution is required by DNS methods. Therefore though theoretically a direct solving of the Navier-Stokes equations is permissible, the use of DNS methods can be self-prohibitive. Alternatively, a filtering of eddies and Reynolds averaging can be performed. When filtering is applied, eddies smaller than the filter size (grid size is usually taken as filter size) are removed. Consequently large eddies are modeled using the filtered equations using what is known as LES (Large Eddy Simulation) CFD methods; small eddies are then separately modeled independent of the geometry of flow. Other methods rely on applying transport equations for quantities of mean flow only. These methods are known as RANS (Reynolds Averaged Navier-Stokes) CFD methods. The majority of CFD models utilize RANS Methods (Stamou and Katsiris, 2006).

One of the major draw backs of using CFD methods is simulation time. A single simulation of a building at even steady-state conditions can take from several hours up to several days. CFD methods are consequently unfeasible for use in hourly dynamic simulations of a building for the span of a full year (Wang and Chen, 2006). CFD is a very versatile and important tool for the study of flow and contaminant transport, yet when the simulated flow is complex and/or its domain is large a large and complex load of computation results. This could become severely prohibitive to the use of CFD in full building energy simulations (Zuo and Chen,2010). Therefore, the use of CFD has generally been reserved to air flow studies in single rooms (Mora et al., 2003).

Combined multizone-CFD methods have been proposed in which CFD would be used for zones in which a uniform well-mixed condition assumption cannot be held, and a multizone model would be used for the remaining zones. As a result, since CFD would be applied to limited zones in a building, the computation load and required simulation time would be reduced compared to when applying the CFD method to the full building (Wang and Chen, 2006). Some proposed coupled multizone-CFD methods include Clark et al (1995), Negrao (1998) and Jayarman et al (2004). Another approach to reducing the computation complexity of CFD approaches are the proposed Fast Fluid Dynamics (FFD) methods such as Stam (1999). The same Navier-Stokes equations solved by CFD are solved by FFD methods. However, FFD methods utilize an alternative set of numerical methods in solving the governing differential equations which allow the model solution to proceed faster than when using a typical CFD method (Zou and Chen, 2010). Nevertheless, FFD methods are still not rapid enough for a real-time building simulation (Zou and Chen, 2010); setting aside performing an hourly simulation for a full building over a full 1 year time span.

## **Types of Air Infiltration**

Air infiltration results in higher energy consumption, thermal un-comfort and can cause moisture accumulation problems in walls and other infiltration flow paths. Air leakage can occur through two venues. Leakage can occur through large opening, through large cracks such as cracks in windows and door frames and seals and other large leakage points. Or, the air leakage can be spread over small cracks all over the building envelope. In reality, air infiltration occurs through a combination of both venues (Anerlind, 1985). Leakage through large openings, large leakage points, and cracks through which air follows short paths is referred to as “Concentrated” leakage. On the other hand, infiltration through small cracks in walls and others, in which air travels several feet before reaching the interior, is denoted as “Diffuse” leakage (Anderlind, 1985). Traditionally the energy load due to air infiltration is calculated as a product of the infiltration mass flow rate and the inside-outside enthalpy difference. This method of calculating infiltration loads might be well acceptable when calculating the load due to concentrated air infiltration. In diffuse infiltration, heat exchange (along the infiltrating air flow path) between the infiltrating air and the walls (or medium) results in a somewhat conditioning of the infiltrating air. Therefore, calculating the energy load due to diffuse infiltration using the classical infiltration calculating entails a considerable overestimation of the energy impact of this type of infiltration.

The subsequent sections include an overview of the quantification of the impact of both modes of infiltration, concentrated and diffuse. The infiltration through large openings such as doors, windows, fireplaces, and others will be discussed. Similarly, a recount of the impact of diffuse infiltration will be included.

## Concentrated Air Infiltration

### Doors

Building entrance doors have always been a predicament for heating and air conditioning engineers. The problem is especially significant in stores and commercial buildings with an excessively heavy traffic of people utilizing the doors. During the summer cooling season entrance doors admit unwanted hot air from the outside; and during the heating season they let in cold air (Simpson, 1936). As in other forms of infiltration, air leakage through doors is driven by a pressure difference across the door. This pressure gradient is due to wind, stack effect or the ventilation system (Zmeuranu et al., 2001). Air infiltration through entrance doors cannot be considered as a good ventilation air. For example, during summer the air infiltrating through a door is a superheated and dust loaded air that has swept over hot pavements (Simpson, 1936). The air flow through doors influences, in addition to the heat load, the air circulation patterns and air contaminants distribution in a building (Wilson and Kiel, 1990). The amount of air infiltrating through doors is a summation of (1) the air infiltrating through cracks and openings between the door and its framing; and (2) the air infiltrating through open door as a function of the door area, open time, people traffic, temperature, and others. The amount infiltrating through a door, under a given pressure differential, varies from one door to another depending on (Min et al., 1985; Schuturm et al., 1961, Vastistas et al., 2006):

1. Entrance type : single bank door, vestibule...etc
2. Door dimensions
3. Doors arrangement:



- Opposite doors
  - Parallel doors
4. Direction of door swings:
    - All swing out
    - All swing in
    - One swings out & one swing in
  5. Door rotational speed (for rotating doors)
  6. Open time
  7. Vestibule depth (if any)
  8. Size of door cracks
  9. Rates and patterns of traffic across the door
  10. Tightness of other building parts and components

Several experimental studies have been performed in order to determine the infiltration through various forms of doors. The outcomes of such studies are charts and tables reporting the volumetric inflow of air as a function of the number of persons passing through the door per hour. Examples include Yuill (2000), Mc Quisten et al. (2000), Yuill (1996), Min et al. (1958) Simpson (1936) and others. Samples of such door charts and tables are shown in Tables 2-5 and 2-6 and Figures 2-9 and 2-10. Some works establish a neutral level in a door below which there is air inflow and air flow above such as Vatistas et al. (2007)

No. of Passages per Hour upto	Single Swing Doors		Swing Doors - Vestibules		Revolving Doors	
	Infiltration per Passage ft <sup>3</sup>	Heat Gain per Passage per Degree Temp Diff. BTU	Infiltration ft <sup>3</sup> Per Passage	Heat Gain BTU per °F Per Passage	Infiltration ft <sup>3</sup> Per Passage	Heat Gain BTU per °F Per Passage
100	110	1.98	83	1.49	30	0.54
200	110	1.98	83	1.49	30	0.54
300	110	1.98	83	1.49	30	0.54
400	110	1.98	83	1.49	29	0.52
500	110	1.98	83	1.49	29	0.52
600	110	1.98	82	1.47	28	0.50
700	110	1.98	82	1.47	27	0.49
800	110	1.98	82	1.47	26	0.47
900	109	1.96	82	1.47	25	0.45
1000	109	1.96	82	1.47	24	0.43
1100	109	1.96	82	1.47	23	0.41
1200	108	1.95	82	1.47	21	0.38
1300	108	1.95	82	1.47	19	0.34
1400	108	1.95	81	1.46	18	0.32
1500	108	1.95	81	1.46	17	0.31
1600	108	1.95	81	1.46	16	0.29
1700	107	1.93	81	1.46	15	0.27
1800	105	1.89	80	1.44	14	0.25
1900	104	1.87	80	1.44	13	0.23
2000	100	1.80	79	1.42	12	0.22
2100	96	1.73	79	1.42	11	0.20

**Table 2-5: Infiltration Through Entrances – Doors in One Wall Only (Infiltration Through Doors, 1937)**

No. of Passages per Hour upto	Single Swing Doors		Swing Doors - Vestibules		Revolving Doors (6ft x 6ft)		Revolving Doors (7ft x 7ft)	
	Infiltration per Passage ft <sup>3</sup>	Heat Gain per Passage per Degree Temp Diff. BTU	Infiltration ft <sup>3</sup> Per Passage	Heat Gain BTU per °F Per Passage	Infiltration ft <sup>3</sup> Per Passage	Heat Gain BTU per °F Per Passage	Infiltration ft <sup>3</sup> Per Passage	Heat Gain BTU per °F Per Passage
100	110	1.98	83	1.49	30	0.54	48	0.86
200	110	1.98	83	1.49	30	0.54	48	0.86
300	110	1.98	83	1.49	30	0.54	48	0.86
400	110	1.98	83	1.49	29	0.52	47	0.85
500	110	1.98	83	1.49	29	0.52	46	0.83
600	110	1.98	82	1.47	28	0.50	4	0.81
700	110	1.98	82	1.47	27	0.49	43	0.78
800	110	1.98	82	1.47	26	0.47	41	0.74
900	109	1.96	82	1.47	25	0.45	39	0.70
1000	109	1.96	82	1.47	24	0.43	36	0.65
1100	109	1.96	82	1.47	23	0.41	33	0.59
1200	108	1.95	82	1.47	21	0.38	30	0.54
1300	108	1.95	82	1.47	19	0.34	28	0.50
1400	108	1.95	81	1.46	18	0.32	25	0.45
1500	108	1.95	81	1.46	17	0.31	23	0.41
1600	108	1.95	81	1.46	16	0.29	21	0.38
1700	107	1.93	81	1.46	15	0.27	19	0.34
1800	105	1.89	80	1.44	14	0.25	18	0.32
1900	104	1.87	80	1.44	13	0.23	17	0.30
2000	100	1.80	79	1.42	12	0.22	16	0.29
2100	96	1.73	79	1.42	11	0.20	15	0.27

**Table 2-6: Infiltration through Entrances – Doors in More Than one Wall (Infiltration Through Doors, 1937)**

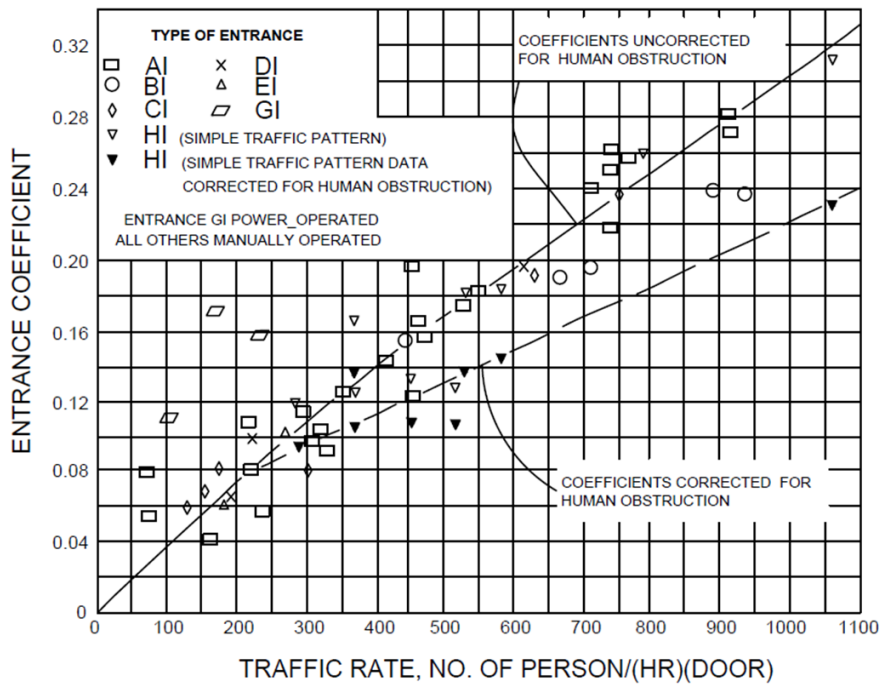


Chart 2-6: Entrance Coefficients for Single Bank Entrances (Min, 1958)

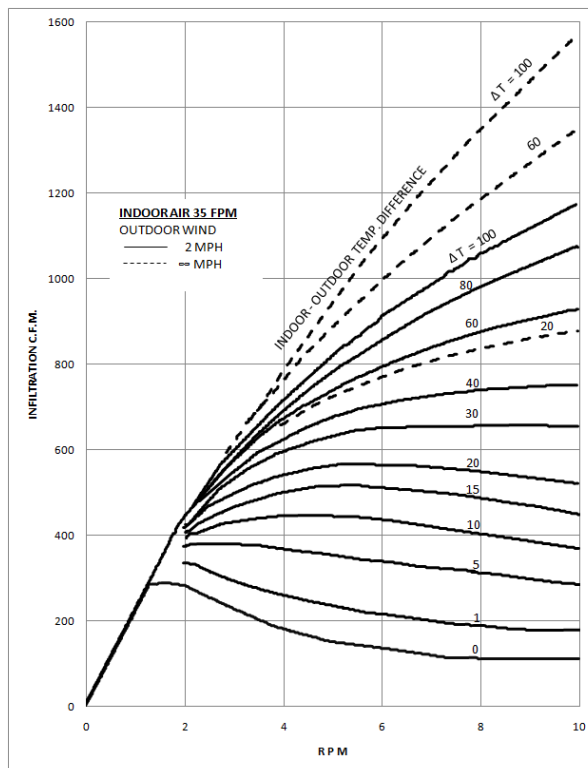


Chart 2-7: Infiltration versus RPM and indoor-outdoor temperature difference (Revolving Door)

To reduce the energy load due to infiltration through doors, some designers resort to using air blowers. These blowers are installed above a door and blow in hot/cold air to compensate for the cold/hot infiltrating air. Such mechanisms also depend on charts and tables, similar to those shown above, to calculate the amount of air that needs to be introduced. Calculations are also done by equations similar to equation 2-32 (Fuller, 1949).

$$A_1 = \frac{A_g(T_1 - T_2)}{(LT - T_1)} \quad (2 - 32)$$

Where:

- $A_1$  = Volume of Air introduced by blower
- $A_2$  = Volume of inrushing outside air (from table/chart)
- $T_3$  = Outside temperature
- $T_4$  = Inside temperature
- $LT$  = Temperature of the Introduced (blown in) air.

## **Windows**

Air infiltration through windows is of less bearing on the cooling/heating load of buildings than the infiltration through walls or open doors. The major energy impact of windows is rather through radiative heat flow. Studies of heat transfer in double glazed windows indicate that 70% of the heat flow is through radiation (Arasteh et al., 1985; Selkowitz, 1979). Nevertheless, the ramifications of air infiltration through windows are considerable. Significant damages to the building material can result from air leakage at the wall/window interface. This includes mold, fungal growth and damages to interior finishings, seals, insulation and even structural elements (ASHRAE Handbook – HVAC

Applications, 2007). As with other venues of infiltration, air infiltration through windows is a function of: the inside-outside pressure difference, air speed, inside-outside air temperature difference, mechanical air balance, and the sealing characteristics of the window (Klems, 1983; Weidt and Weidt, 1980). In windows, the rate of infiltration is mostly affected by the construction quality, material used, weather stripping material and the method of operation (if any) (ASHRAE Handbook – HVAC Application, 2007).

The estimation of air infiltration through windows has 2 possible approaches; either calculating the air infiltration through a “particular” window, or evaluating the total infiltration through an average window. In the latter approach, all windows in a building level are considered to be identical and the net impact of window air leakage on the building is then calculated (Klem, 1983). Both methods deploy a form of the previously discussed orifice equation. Yet, when considering the averaging second approach, half of the windows are assumed to be in infiltration mode and the remaining windows are assumed to be experiencing exfiltration. Therefore a multiplication by half (1/2) factor is added to the orifice equation as shown in equation 2-33 (Klems, 1983).

$$Q = \frac{1}{2} k (\Delta P_w)^n \quad (2 - 33)$$

Where:  $P_w$  account for both the stack and wind driven pressure across the window.

### **Fire Place**

Fire places are used in many houses for heating during the heating season. A burning fire place adds a definite amount of heat to a room, especially in the vicinity of the fire place. However, fire places result also in a considerable air flow and the escape of warm air from the room up through the fire place flue (Anon, 1937). In order to maintain a mass balance, the warm air being lost through the flue of a fire place must be replaced.

The only source of replacement air is the outside. Therefore, a volume of cold outside air will infiltrate into the house equivalent to the volume of warm air lost through the flue. Thus, even though the space temperature rises in the vicinity of a running fire place, the temperature of all the other rooms in the house will drop (Anon, 1937). Fire places, even when not burning, are venues for air leakage and even with the dampers (fire place throat) and the J-vent closed. In an experimental study, Dickson (1988) found that in a non-burning fire place a single opening (J-vent or throat) increases the infiltration rate from 0.15/0.2 ACH (air changes per hour) to 0.2/0.4 ACH in the whole house and from 0.15 ACH to 1 ACH in the room containing the fire place. This increase in air change rate adversely impacts the heating load since indoor warm air is now being replaced faster by large volumes of cold air that needs to be heated in order to maintain the set indoor room temperature. Also, under the common practiced “fault” of leaving both the fire place and the J-vent open the infiltration rate in the room hikes up to 2 ACH, seriously impacting the heating energy load. Finally, a burning fire place creates an infiltration rate of 5 ACH in the room and an increase of up to 1 ACH for the whole house (Dickson, 1988).

The net energy impact of a running fire place depends on the amount of heat being delivered by the fire place onto the house versus the amount of heat required to warm up the infiltrating cold air. In many situations the latter exceeds the former and as a result it would be more energy efficient to not run the fire place. This conclusion is evident in Figure 2-11 (Anon, 1937). Below a certain fire place heat production rate cutoff point, the energy needed to heat up the infiltrating air (due to the running fireplace) exceeds the amount of heat produced by the fire place. In Figure 2-11, for example, if the

fire place is producing less than  $\sim 16,000$  Btu/hr it would be more efficient to shut it off, since heating up the infiltrating air (due to the running fire place) is consuming more heat energy than being put out by the fire place.

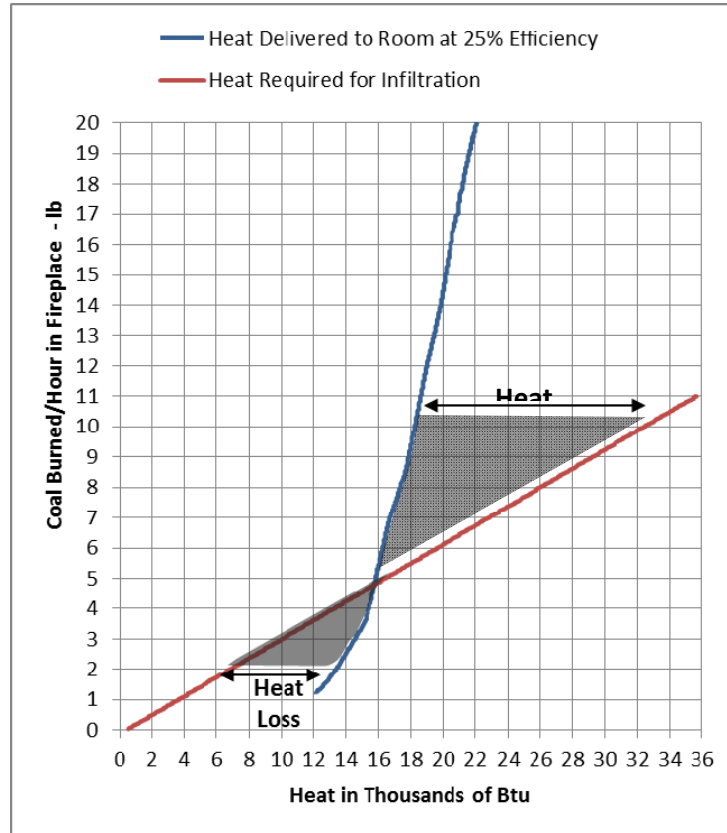


Chart 2-8: The intersection point of the two curves in this chart shows the point where there is no addition or loss of heat (Anon, 1937) - Reproduced

### Diffuse Air Infiltration: Heat Recovery

Diffuse air infiltration occurs through minute cracks and paths in the walls and the overall building envelope. In diffuse infiltration, in contrast with concentrated infiltration, infiltrating air travels through the wall for several feet before reaching the interior. Air infiltration through cracks surrounding doors and windows is classified as concentrated infiltration. Even though the air is infiltrating through small openings and cracks, it doesn't travel a relatively long distance in the wall and therefore this infiltration is considered concentrated not diffuse. Diffuse leakage of air through a wall shifts the



temperature distribution of the wall from a straight line distribution (if 1 layer on is considered, for example) to a curved distribution; thus changing the temperature distribution in the wall (Anderlind, 1985). A heat exchange occurs between the wall and the infiltrating air, a phenomena known as heat recovery. Heat recovery plays a significant role in evaluation the heating/cooling loads due to air leakage (Anderlind, 1985).

Early observations of heat recovery include Harrje (1977) and Beyea et al. (1977) who found that actual attic temperatures exceeded those predicted by typical insulation resistance models. Several other studies also reported the observed impact of heat recovery in reducing heating/cooling energy loads. Claridge et al. (1985) reported a calculated overall house energy loss factors 50% above those obtained through regression analysis of recorded experimental house data; indicating a “Heat Recovery” in infiltration energy. Other similar work includes Claridge and Bhattacharyya (1990) who measured infiltration loads equivalent to as low as 20% of those calculated using classical infiltration calculation methods. Classical methods for calculating the additional energy load due to infiltration, including computer models and hourly simulation programs, assume a load increase due to infiltration equal to the infiltrating air mass flow rate times the inside-outside air enthalpy difference. The classical expression for infiltration is shown in equation 2-34.

$$Q_{inf} = \dot{m} C_p (T_i - T_o) \quad (2 - 34)$$

Classical methods generally ignore the interaction between infiltration and conduction. The heat load is therefore calculated as a summation of the heat loss due to conduction and the heat loss due to infiltration (Claridge and Bhattacharyya, 1990;

Claridge and Liu, 1996). A handful of combined heat loss models were therefore proposed to account for this interaction between conduction and infiltration; including Anderlind (1985), Liu (1987), Bailly (1987) and Arquís (1986). However, the model provided by Anderlind was considered to provide the most intuitive and logical expression (Liu, 1992). Anderlind considered the classical infiltration expression to give the maximum heat loss due to infiltration and therefore defined a reduction factor “R”. R is defined as varying between 0 and 1 ( $0 < R < 1$ ). For a purely concentrated flow infiltration R approaches 1 and as a result the heat loss is given by the classical expression (equation 2-34). Conversely, for purely diffuse flow infiltration R approached 0. However, in reality, infiltration through a building envelope is a combination of both concentrated and diffuse flows. Therefore, R varies between 0 and 1 based on the flow distribution. The general expression given by Anderlind is shown in equation 2-35.

$$Q_{inf} = R[\dot{m} C_p (T_i - T_o)] \quad (2 - 35)$$

Where:

$$- \quad 0 < R < 1 \quad \left\{ \begin{array}{l} R \rightarrow 0 : \text{Diffuse Flow} \\ R \rightarrow 1 : \text{Concentrated Flow} \end{array} \right.$$

Claridge and Bhattacharyya (1990) introduced a new non-dimensional factor representing the effectiveness of heat recovery resulting from the heat exchange between infiltrating/exfiltrating air and the walls. This factor is known as the “Infiltration Heat Exchange Effectiveness” or IHEE ( $\epsilon$ ). In simple terms, IHEE ( $\epsilon$ ) is a measure of the success of the building in “recovering” the otherwise lost (gained) heat due to infiltration of outside air (Claridge and Bhattacharyya, 1990). Research on IHEE has shown  $\epsilon$  to increase as (Claridge and Bhattacharyya, 1990; Bhattacharyya and Claridge, 1996):

- Flow rate decreases

- Flow path length increase
- Crack/hole size diminished

The general expression of IHEE is given by equation 2-36 (Claridge et al. 1995).

$$IHEE = \varepsilon = \frac{UA_0 + \dot{m}C_p - UA_{actual}}{\dot{m}C_p} \quad (2 - 36)$$

Where:

- $UA_0$  = heat loss factor due to conduction only
  - $C_p$  = Specific heat of air
  - $\dot{m}$  = Air infiltration mass flow rate
  - $UA_{actual}$  = Actual heat loss factor with airflow included
- } Infiltration Only

Consequently, the infiltration heat loss is expressed as in equation 2-37

$$Q_{inf} = (1 - \varepsilon)[\dot{m} C_p (T_i - T_o)] \quad (2 - 37)$$

The value of IHEE ( $\varepsilon$ ) depends largely on the relative distribution of air leakage between concentrated and diffuse leakage (Claridge and Bhattacharyya 1990). The range of  $\varepsilon$  was originally assumed to be  $0 \leq \varepsilon \leq 1$ .

The dependence of ( $\varepsilon$ ) on air flow rate is expressed in terms of a non-dimensional factor  $\alpha$ , defined in equation 2-38. For no air leakage flow ( $\dot{m} C_p = 0$ )  $\alpha = 0$ ; and  $\alpha = 1$  for an infiltration loss coefficient ( $\dot{m} C_p$ ) equal to the conductive loss coefficient( $UA_0$ ). Therefore, the dependence of ( $\varepsilon$ ) on air flow rate was approximated by equation 2-39 (Bhattacharyya and Claridge, 1990).

$$\alpha = \frac{\dot{m}C_p}{UA_0} \quad (2 - 38)$$

$$\varepsilon = \varepsilon(0) + m\alpha \quad (2 - 39)$$

Further research by Claridge and Liu (1992) highlighted the dependence of heat recovery on an additional component, solar radiation. The combined impact and interaction between conduction, infiltration and solar radiation in walls and attics was studied. With the role of solar radiation included; the influence of flow rate and air leakage configuration (diffuse versus concentrated) on IHEE were still consistent with the previously stated observations. However, solar radiation further impacted the actual energy loss due to air leakage compared to the classical equation. The combined effect of solar radiation and infiltration helped carry more solar energy to the interior, further reducing the energy loss due to infiltration compared to the classically calculated value (in the case of the heating season for example). In the cooling season, however, the same phenomenon helps increase the cooling load by carrying more solar energy inside. A reversed effect is observed due to exfiltration. Summer exfiltration helps enhance heat recovery in the walls by expelling to the outside incident solar radiation; however exfiltration has a reduced affect on IHEE (Claridge and Liu, 1996; Claridge and Liu, 1992). Due to the introduced impact of solar radiation  $\varepsilon$  was found to now be capable of exceeding 1 or going below 0 (contrary to the initial assumption  $0 \leq \varepsilon \leq 1$ ). Claridge and Liu (1996) suggested a modified heat recovery factor  $\varepsilon$ , incorporating the affect of solar radiation shown in equations 2-40 and 2-42.

$$\varepsilon_t = \frac{UA_{classical} - UA_{actual}}{UA_{classical}} \quad (2 - 40)$$

Where:

- $\varepsilon_t$  = Ration of recovered energy to the energy loss calculated using classical method
- $UA_{classical} = UA_0 + \dot{m}C_p$  (2 - 41)

$$Q_{inf} = UA_0(T_r - T_{sa}) + (1 - \varepsilon)[\dot{m} C_p (T_i - T_o)] \quad (2 - 42)$$

Where:

- $T_{sa}$  = Appropriate sol air temperature

Neglecting the interaction of conduction and solar radiation with infiltration explains a large portion of the overestimation/underestimation of building energy consumption due to air leakage. Models considering the simultaneous interaction of infiltration, conduction, and solar radiation (in an idealized situation) have shown a 38% to 100% saving on heating energy and up to 33% saving on cooling energy compared to a leaky house with no heat recovery (Liu and Claridge, 1992).

Buchanan and Sherman (1998 and 2002) performed 2D and 3D computational fluid dynamics (CFD) simulations for studying the fundamentals of infiltration heat recovery. They found infiltration heat recovery to be of substantial affect. At low leakage rates, the classical method vastly over predicted the loss by 80% to 95%. Even at high leakage rates, the infiltration energy load was overestimated by 20% by the classical calculation method. Flow and energy transport were modeled using Navier-Stokes and the energy equations 2-43 and 2-44.

$$\frac{\varphi \rho}{\varphi t} + \frac{\varphi \rho U_i}{\varphi X_i} = 0 \quad (2 - 43)$$

$$\frac{\varphi \rho T}{\varphi t} + C_p \frac{\varphi \rho U_i T}{\varphi X_i} = k \frac{\varphi^2 \rho T}{\varphi X_i^2} + \frac{\varphi \rho}{\varphi t} + U_i \frac{\varphi \rho}{\varphi X_i} \quad (2 - 44)$$

Buchanan and Sherman's CFD model results compared within 10% in one case with Claridge and Bhattacharyya. Buchanan and Sherman (2000) also developed a simplified "macro-scale" mathematical model for infiltration heat recovery. The model is

based on steady state one dimensional convection-diffusion. However, the purpose of the model is reported by the authors to be for giving a rough idea of the effect of heat infiltration recovery and “not (for) incorporation into network codes for dynamic building simulation” and “doesn’t capture the full physics of the problem”. (Buchanan and Sherman, 2000).

Brownell (2002) conducted experimental tests to collect data for verification of the Buchanan and Sherman model (1998, 2000) using a methodology resembling that of Bhattacharyya and Claridge (1990, 1995). The experimental data extended the range of the non-dimensional flow rate  $\alpha$  measured. Claridge and Bhattacharyya (1990) expressed  $(\epsilon)$  in a linear relationship with  $\alpha$ . However, Brownell data demonstrated a non-immediately linear relationship (Brownell, 2002). The experimental data of Brownell agreed within 10% with Buchanan and Sherman (2000) in some aspects, yet the agreement was not quite good in the remaining sections; especially at high flow rates (Brownell, 2002).

Understanding the heat recovery phenomenon and its impact is of large significance; especially in the field of building science, building physics, and hygrothermal engineering. A better understanding of infiltration heat recovery allows a better estimation of the heating and cooling requirements of a building. This in turn reflects in a more accurate sizing of the required HVAC system. Also, allows a better management of required building tightness criteria. Engineers might, for example, rely on more natural ventilation by allowing a certain amount of air leakage; while depending on heat recovery in the walls to keep the building energy loads in hand. Or, in other cases, seek tighter construction (for example when  $\epsilon$  is low or below zero). Furthermore, a

better understanding of this phenomenon helps better understand attic (and radiant barriers) and insulation behavior (Bhattacharyya, 1999).

The wide spread use of building energy simulation software makes important the integration of the heat recovery phenomenon impact into the calculation models of energy simulation software. As discussed earlier, most building energy simulation software predominantly deploy the classical methods in calculating infiltration energy loads. It is therefore essential to alter infiltration calculation models in building energy software from classical infiltration theories to models that take into account the interaction between conduction, solar energy, and infiltration. Thus incorporating the impact of heat recovery in their building energy loads calculations. Various literature discussed in this review have emphasized the large effect of heat recovery has on the calculation of air infiltration energy loads. It is therefore crucial that infiltration heat recovery be incorporated into the principal energy building energy analysis software. Especially, into DOE-2 (discussed in this review) due to its wide spread use, intricacy, and its role as the simulation engine of various prominent building energy analysis software.

## **Building Energy Simulation Infiltration Evaluation Approach**

### **Current Approach**

Infiltration, as discussed in previously, is a major contributing factor to the heating/cooling load of a building. However, it is the component that most building energy simulation software struggle to model. Infiltration is primarily dependent on the building construction, tightness of the building envelope, building surrounding and local topography, wind speed, wind direction, local weather and others. Thus to avoid these complexities, infiltration is usually modeled using overly simplified and approximate models in building energy simulation software. Such models also ignore the impact of heat recovery in the building envelope on the infiltration load, and the interaction between solar radiation, conduction and infiltration despite of the proven key impact of the interaction of these phenomena. Among these prominent building energy simulation software is DOE-2. Three models were majorly employed by DOE-2 for evaluating the energy impact of infiltration: (1) Air change, (2) Crack Method and the (3) Residential (Achenbach – Coblentz) model. Recently added were also the (4) Sherman-Grimmsrud method and (5) ASHRAE Enhanced Method. These methods are shortly described below with reference to DOE-2 Engineers Manual, Version 2.1A (1982) and DOE-2.2 Volum2: Dictionary (2009).

### **Air-Change Method**

The air change method is based on evaluating infiltration based on the number of infiltration-caused air changes per hour. This method is based on a reference wind speed of 10 mph accompanied by a wind speed correction factor. The air change method basic equation is described by equation 2-45.



$$\begin{aligned} \text{Infiltration (cfm)} &= (\text{wind speed})(\text{Air changes/hr}) \times \text{Volume of space} \\ &+ (\text{cfm/space square foot})(\text{Space Area}) \quad (2 - 45) \end{aligned}$$

In equation 2-45, only one of the two parts of the equation is utilized at one time while the other is set to zero, depending on the user input. If the first part of the equation is utilized it allows a linear wind speed correction to the local wind speed. However, neither term provides any correction/consideration for the prevalent temperature difference across the building envelope.

### **Residential Method**

The residential method has no theoretical justification but rather represents a statistical fit to collected residential infiltration data (Achenbach and Coltz, 1963; Ross and Grimsrud 1978, Peterson 1979). The general expression of the residential method is given by equations 2-46 and 2-47.

$$\text{Air changes/hr} = A + (B)(\text{Wind Speed}) + (C)(|T_{\text{zone}} - T_{\text{Dry bulb}}|) \quad (2 - 46)$$

$$\text{Infiltration (cfm)} = (\text{Air changes/hr}) \times (\text{Volume}) \left( \frac{1}{60} \right) \quad (2 - 47)$$

Where: A, B & C are curve fit coefficients

The default values of A, B and C are (Peterson, n.d.):

$$A = 0.252$$

$$B = 0.0251$$

$$C = 0.0084$$

## Crack Method

The crack method considers, yet inadequately, the impacts of wind velocity and the stack effect. The infiltration driving pressure caused by each of these two phenomena is evaluated separately as shown by equations 2-48 & 2-49.

$$P_{Wind} = (Constant)(wind\ speed)^2(\cos(wind\ direction)) \quad (2 - 48)$$

$$P_{Stack} = (Constant)(P_{atm})\left(\frac{1}{T_{Dry\ bulb}} - \frac{1}{T_{zone}}\right) (Height\ above\ NPL) \quad (2 - 49)$$

Where: NPL = Neutral Pressure Level

$$\therefore Total\ Driving\ Pressure: P_{Total} = P_{stack} + P_{Wind} \quad (2 - 50)$$

$$\Rightarrow Infiltration = (constant) \times P_{Total} \times Area \quad (2 - 51)$$

## Sherman – Grimsrud Method & ASHRAE Enhanced Method

The Sherman-Grimsrud method and ASHRAE Enhanced method both apply only to single zones. The Sherman-Grimsrud incorporates the neutral level concept and leakage area distribution between floor, ceiling and other components. The ASHRAE-Enhanced method was defined by Walter and Wilson (1998). It depends on leakage coefficients obtained using house pressurization tests. This method is highly dependant on these coefficients that are rather difficult to determine (DOE-2 Dictionary, 2009). DOE-2 employs for these coefficients default values given in a calculation example presented in the ASHRAE Handbook of Fundamentals with no other coefficient references or value lists. The infiltration air flow rate with this method is calculated using equations 2-52 and 2-53 (ASHRAE Fundamentals, 2009).

$$Q_{stack} = c C_s \Delta t^n \quad (2 - 52)$$

$$Q_w = c C_w (S U)^{2n} \quad (2 - 53)$$

Where:

- $Q_s$  = Stack airflow rate, cfm
- $Q_w$  = Wind airflow rate, cfm
- $C$  = flow coefficient
- $C_s$  = Stack coefficient
- $C_w$  = Wind coefficient
- $n$  = pressure exponent
- $\Delta t$  = temperature difference between indoors and outdoors,
- $S$  = Shelter factor

	House Height (Stories)		
	One	Two	Three
Stack Coefficient	0.0150	0.0299	0.0499

Table 2-7: Stack Coefficient  $C_s$  (ASHRAE Handbook of Fundamentals, 2009)

Shelter Class	Local Shelter Classes
	Description
1	No Obstruction or Local Shielding
2	Typical shelter for an isolated rural area
3	Typical shelter caused by other buildings across street from building under study
4	Typical shelter for urban buildings on larger lots where sheltering obstacles are more than one building height away
5	Typical shelter produced by buildings or other structures immediately adjacent (closer than one house height)

Table 2-8: Local shelter classes (ASHRAE Handbook of Fundamentals, 2009)

Shelter Class	House Height (Stories)		
	One	Two	Three
1	0.0119	0.0157	0.0184
2	0.0092	0.0121	0.0143
3	0.0065	0.0086	0.0101
4	0.0039	0.0051	0.0060
5	0.0012	0.0016	0.0018

Table 2-9: Wind Coefficient  $C_w$  (ASHRAE Handbook of Fundamentals, 2009)

### Final Calculation

Once the infiltration flow rate is determined using any of the previously discussed five methods; the resulting sensible and latent infiltration loads are calculated using equations 2-54 and 2-55.

#### *Sensible Infiltration Load*

$$= (\text{constant}) \times \rho_{\text{air}} \times (\text{Flow Rate}) \times (T_{\text{Ambient}} - T_{\text{zone}}) \quad (2 - 54)$$

$$\text{Latent Infiltration Load} = (\text{constant}) \times \rho_{\text{air}} \times (\text{Flow Rate})$$

$$\times (\text{Outside humidity} - \text{Indoor Humidity}) \quad (2 - 55)$$

Several other building energy simulation software utilize these or other similar methods, especially that DOE-2 represents a simulation engine and a base for many other building energy simulation software.

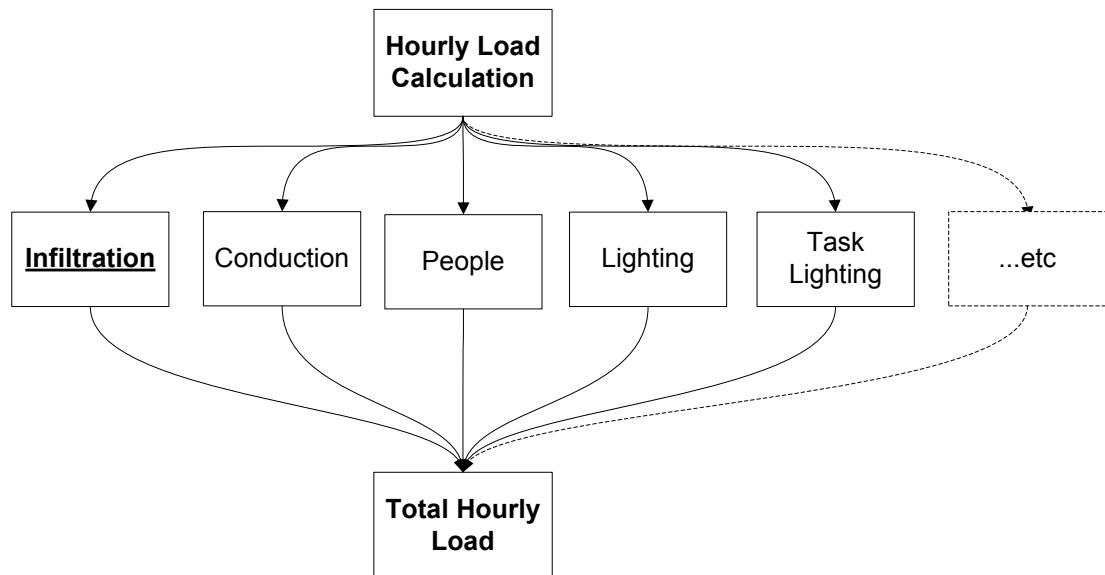
## **Chapter 3**

### **Methodology**

#### **Combined Infiltration, Conduction & Solar Model**

Infiltration, conduction and incident solar radiation act jointly allowing heat recovery to occur in the building envelope and to impact the energy load due to infiltration. Several models have been suggested to enhance infiltration calculations and incorporate heat recovery into infiltration energy load calculations. Earlier models such as Anderlind (1985), Kohonen (1985), Kohonen and Nirtanen (1987) and others tend to be based on some linear reduction factor, depend on steady temperatures and a steady inside/outside enthalpy difference, and ignore the role and impact of solar radiation. Solar radiation has been shown by Liu (1992), through experimental testing, to contribute to infiltration heat recovery and affect the intensity of heat exchange efficiency (IHEE). A later model to incorporate the impact of heat recovery is the model by Sherman and Buchanan (1998). Similar to previous models, this model disregards the experimentally proven role of incident solar energy. CFD models created by the authors to verify the method suffered from convergence issues. A 3-D CFD grid reduction from 140,000 to 33,000 nodes was performed in order to obtain CFD model convergence, yet no verification was performed for grid dependency of the solution. Later experimental work (Brownell, 2002) revealed feeble agreement with the Sherman and Buchanan (1998) model results. Finally, according to the authors the model is not for incorporation into network codes and “doesn’t capture the full physics of the problem” (Sherman and Buchanan, 1998).

The model that will be used and built upon in this methodology was proposed by Liu and Claridge and presented in Liu (1992), Liu and Claridge (1992), Liu and Claridge (1995), Claridge and Liu (1996). The model presented is based on a second order non-linear dynamic differential equation. This model accounts for variable temperatures, changes in infiltration flow rate ( $\dot{m}$ ), accounts for the role of solar radiation, and finally considers the interdependence and interaction between solar radiation, conduction and infiltration. The model will be presented below based on Liu (1992) and using simplifications from Patankar (1980). This infiltration energy load model will be incorporated into the hourly calculations of hourly building energy simulation software for the calculation of infiltration energy load as shown in Flowchart 3-1.



**Flowchart 3-1 : Model Incorporation into hourly calculations**

### **Differential Equation**

The underlying concept of the differential equation is that the energy gained is equal to the difference between the “in” and “out” energy flux flows. There are 2

assumptions inherent into the use of this equation. Primarily is the assumption that air and solid material have an identical temperature at any position and that the infiltration flow is represented by the air mass flow rate  $\dot{m}$ . The controlling differential equation is then defined by equation 3-1 and with reference to the control volume shown in Figure 3-1.

$$Q_x - Q_{x+dx} + Q_{a,x} - Q_{a,x+dx} = \delta Q \quad (3 - 1)$$

Where:

- $Q_x$  = Heat flux entering the control volume due to conduction
- $Q_{x+dx}$  = Heat flux leaving the control volume due to conduction
- $Q_{a,x}$  = Energy carried in by airflow
- $Q_{a,x+dx}$  = Energy carried out by airflow
- $\delta Q$  = Heat storage rate in control volume

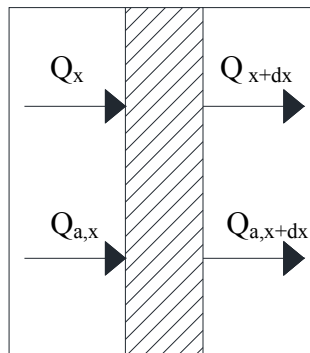


**Figure 3-1: Heat flux flow control volume**

The terms in equation 3-1 can each be represented as:

$$Q_x = -k \frac{\delta T}{\delta x} \delta \tau \quad (3 - 2)$$

$$Q_{x+dx} = -k \frac{\delta T}{\delta x} \delta \tau - k \frac{\delta^2 T}{\delta^2 x} \delta x \delta \tau \quad (3 - 3)$$

$$Q_{a,x} = \dot{m} C_p T \delta \tau \quad (3 - 4)$$

$$Q_{a,x+dx} = \dot{m} C_p T \delta \tau + \dot{m} C_p \frac{\delta T}{\delta x} \delta x \delta \tau - C_p T \frac{\delta \dot{m}}{\delta x} \delta x \delta \tau \quad *1 \quad (3 - 5)$$

$$\delta Q = \frac{\delta T}{\delta \tau} (\rho C + \gamma \rho_a C_p) \delta x \delta \tau \quad *2 \quad (3 - 6)$$

Note:

- <sup>\*1</sup> There isn't much change in airflow rate with path, this term can be ignored

- <sup>\*2</sup> Air heat capacity is << Solid heat capacity, thus this term can be ignored

Where:

- $\dot{m}$  = Air infiltration rate
- $C_p$  = Specific heat of air
- $C$  = Specific heat of solid
- $\rho$  = Density of solid material
- $\rho_a$  = Density of air
- $\gamma$  = Porosity of wall
- $k$  = Conductivity of solid material
- $T$  = Temperature
- $\tau$  = Time



Replacing all the terms in equations 3-2 to 3-6 in equation 3-1 and reducing it results in equation 3-7 shown below, a one dimensional, second order non-linear equation.

$$\rho C \frac{\delta T}{\delta \tau} = k \frac{\delta^2 T}{\delta^2 x} - \dot{m} C_p \frac{\delta T}{\delta x} \quad (3 - 7)$$

The above equation is a second order nonlinear dynamic differential equation and therefore has no analytical solution. A numerical solution will therefore be used for the differential equation and the equation will be discretized as follows. The discretization will utilize expressions from Patankar (1980).

### Differential Equation Discretization

The differential equation is discretized for a set of nodes. The central node is denoted as P. The node on its east is denoted as E and the node on the west is denoted as W. The midpoint of the distance between the nodes P & E is denoted as e and that between P and W is denoted as w. These nodes and notations are shown on Figure 3-2.

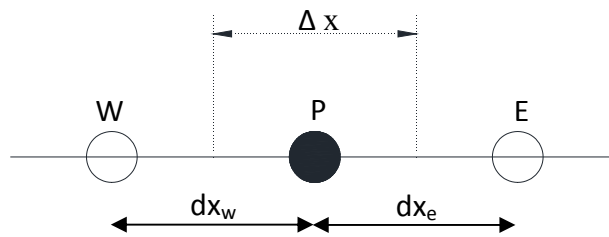


Figure 3-2: Nodes and notation

### Internal Node/Layer

A control volume is taken over  $\Delta x$  between w and e and a double integration of equation 3-7 over time and space is performed as shown in equation 3-8.

$$\int_{\tau}^{\tau+\Delta\tau} \int_x^{x+\Delta x} \rho C \frac{\delta T}{\delta \tau} dx d\tau = \int_{\tau}^{\tau+\Delta\tau} \int_x^{x+\Delta x} k \frac{\delta^2 T}{\delta x^2} dx d\tau - \int_{\tau}^{\tau+\Delta\tau} \dot{m} C_p \frac{\delta T}{\delta x} dx d\tau \quad (3-8)$$

For a small enough control volume,  $\frac{\delta T}{\delta \tau}$ ,  $\rho$ ,  $C$ ,  $\dot{m}$ ,  $C_p$  &  $k$  are constant within the control volume. Therefore, integrating over space ( $\Delta x$ ), equation 3-8 results in equation 3-9.

$$\int_{\tau}^{\tau+\Delta\tau} \rho C \frac{\delta T}{\delta \tau} \Delta x d\tau = \int_{\tau}^{\tau+\Delta\tau} \left[ \left( k \frac{\delta T}{\delta x} \right)_e - \left( k \frac{\delta T}{\delta x} \right)_w \right] d\tau - \int_{\tau}^{\tau+\Delta\tau} \dot{m} C_p (T_e - T_w) d\tau \quad (3-9)$$

Utilizing term simplification from Pantakar (1980) equation 3-9 can be expressed as:

$$\int_{\tau}^{\tau+\Delta\tau} \rho C \frac{\delta T}{\delta \tau} \Delta x d\tau = \int_{\tau}^{\tau+\Delta\tau} \left[ \left( \frac{k}{\delta x} \right)_e (T_E - T_P) - \left( \frac{k}{\delta x} \right)_w (T_P - T_W) \right] d\tau - \int_{\tau}^{\tau+\Delta\tau} \dot{m} C_p (T_e - T_w) d\tau \quad (3-10)$$

Integrating equation 3-10 over time results in equation 3-11

$$\rho C \Delta x (T_P - T_P^0) = \left( \frac{k}{\delta x} \right)_e (T_E - T_P) \Delta \tau - \left( \frac{k}{\delta x} \right)_w (T_P - T_W) \Delta \tau - \dot{m} C_p (T_E - T_W) \Delta \tau \quad (3-11)$$

Where:

- $T_P^0$  = Previous temperature of center node
- $T_P$  = Current temperature of center node
- $T_E$  = Current temperature at east node
- $T_W$  = Current temperature at west node

Rearranging equation 3-11 results in equation 3-12:

$$T_p \left[ \frac{\rho C \Delta x}{\Delta \tau} + \left( \frac{k}{\delta x} \right)_e + \left( \frac{k}{\delta x} \right)_w \right] + T_w \left[ - \left( \frac{k}{\delta x} \right)_w - \dot{m} C_p \right] + T_e \left[ - \left( \frac{k}{\delta x} \right)_e + \dot{m} C_p \right] = \frac{\rho C \Delta x}{\Delta \tau} T_p^0 \quad (3 - 12)$$

Following simplifications from Liu (1992), let:

$$a_w = - \left( \frac{k}{\delta x} \right)_w - \dot{m} C_p$$

$$a_e = - \left( \frac{k}{\delta x} \right)_e + \dot{m} C_p \quad (3 - 13)$$

$$a_p^0 = \frac{\rho C \Delta x}{\Delta \tau}$$

$$a_p = a_p^0 - a_w - a_e$$

Therefore equation 3-13 becomes:

$$a_w T_w + a_p T_p + a_e T_e = a_p^0 T_p^0 \quad (3 - 14)$$

Since conductivity is non-homogeneous and can vary between nodes, then define  $K_w$  and  $K_e$  as (Patankar, 1988) (Equations 3-15 and 3-16):

$$K_w = \frac{2}{\frac{\Delta x_w}{\delta x_w k_w} + \frac{\Delta x_p}{\delta x_p k_p}} \quad (3 - 15)$$

$$K_e = \frac{2}{\frac{\Delta x_p}{\delta x_p k_p} + \frac{\Delta x_e}{\delta x_e k_e}} \quad (3 - 16)$$

### External Node/Layer of wall

The outside surface of the wall receives the incident solar radiation and is also exposed to ambient air temperature. Similarly the inside surface of the wall is exposed to

the indoor ambient temperature. Therefore, separate discretizations are presented for nodes on the outside surface and inside surfaces of a wall.

### Outside wall surface

A node on the outside surface of the wall is subject to solar radiation, outside air temperature and the infiltrating air. The node P is taken on the surface of the wall and the control volume has half the volume of the regular control volume, as shown in Figure 3-3. The energy balance equation for the external node is therefore defined by equation 3-17.

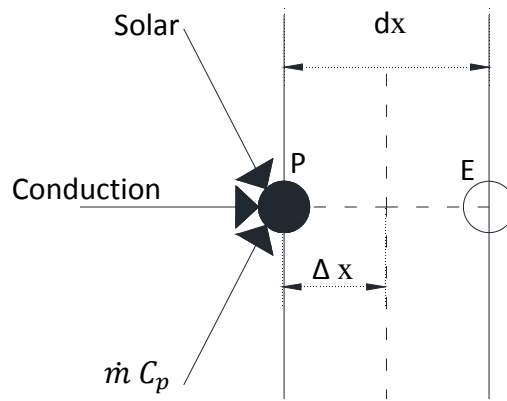


Figure 3-3: Node on the outside surface of the wall

$$T_P \dot{m} C_p - \frac{1}{2} (T_P - T_E) \dot{m} C_p + I + h_o (T_a - T_P) + \left( \frac{k}{\delta x} \right)_e (T_E - T_P) = \left( \frac{\rho C \Delta x}{2 \Delta \tau} \right)_e (T_P - T_P^0) \quad (3 - 17)$$

Where:

- $T_P$  = Temperature of outside surface
- $T_E$  = Temperature of east node
- $I$  = Solar radiation absorbed by the wall

- $h_0$  = Heat transfer coefficient by outside boundary layer of the wall
- $T_a$  = Ambient air temperature
- $\Delta\tau$  = Time step

Therefore equation 3-17 is expressed as:

$$a_p T_p + a_e T_E = a_p^0 T_p^0 + S \quad (3 - 18)$$

$$a_e = -\left(\frac{k}{\delta x}\right)_e + \frac{1}{2} \dot{m} C_p$$

$$a_p^0 = \frac{\rho C \Delta x}{2 \Delta \tau} \quad (3 - 19)$$

$$a_p = a_p^0 - a_e + h_0$$

$$S = I + h_0 T_a$$

### Inside surface of the wall

A node on the inside surface of the wall is influenced by the indoor room air temperature and the temperature of the node on the west of it. The energy balance equation of the interior node is given by equation 3-20.

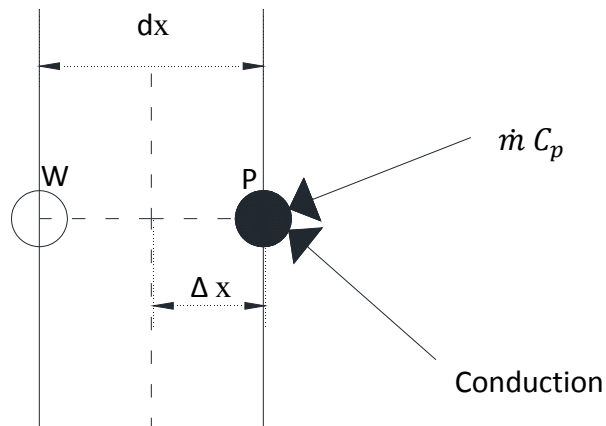


Figure 3-4: Node on the inside surface of the wall

$$\left(\frac{k}{\delta x}\right)_w (T_W - T_P) + \frac{1}{2}(T_W + T_P)\dot{m} C_p - (T_P - T_r)h_i - \dot{m} C_p T_P = \left(\frac{\rho C \Delta x}{2 \Delta \tau}\right) T_P^0 \quad (3 - 20)$$

Rearranging equation 3-20 (as previous), then:

$$a_p T_P + a_w T_W = a_p^0 T_P^0 + S \quad (3 - 21)$$

$$a_w = -\left(\frac{k}{\delta x}\right)_w - \frac{1}{2} \dot{m} C_p$$

$$a_p^0 = \frac{\rho C \Delta x}{2 \Delta \tau} \quad (3 - 22)$$

$$a_p = a_p^0 - a_e + h_i$$

$$S = h_i T_r$$

Where:

- $T_r$  = Room temperature
- $h_i$  = Heat transfer coefficient by inside boundary layer of the wall

### Final Discretization

A wall with n-1 layers has n nodes. Each node type has a specific equation as defined above, with special equations for each of the:

- Node on the outside surface of the wall
- Interior nodes (for interior layers)
- Node on the inside surface of the wall

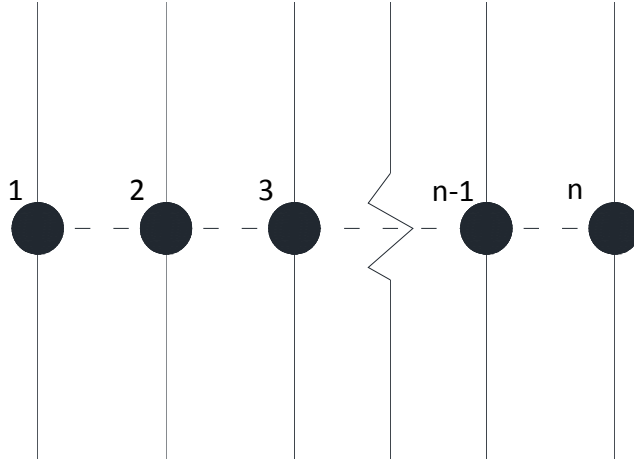


Figure 3-5: A wall with multiple layers and n nodes

All the equations (one for each node) are assembled into the matrix in equation 3-23. The solution for the matrix is the temperature of each node.

$$\begin{pmatrix} a_p^1 & a_e^1 & 0 & 0 & \dots & 0 \\ a_w^2 & a_p^2 & a_e^2 & 0 & \dots & 0 \\ \vdots & \vdots & \vdots & \vdots & \vdots & \vdots \\ & & & & a_w^n & a_p^n \end{pmatrix} \begin{pmatrix} T_1^1 \\ T_2^1 \\ \vdots \\ T_n^1 \end{pmatrix} = \begin{pmatrix} a_p^0(1)T_1^0 \\ a_p^0(2)T_2^0 \\ \vdots \\ a_p^0(n)T_n^0 \end{pmatrix} \quad (3-23)$$

Once the layer temperatures are determined, the combined conduction and infiltration heat flux in the case of infiltration are determined using equation 3-24.

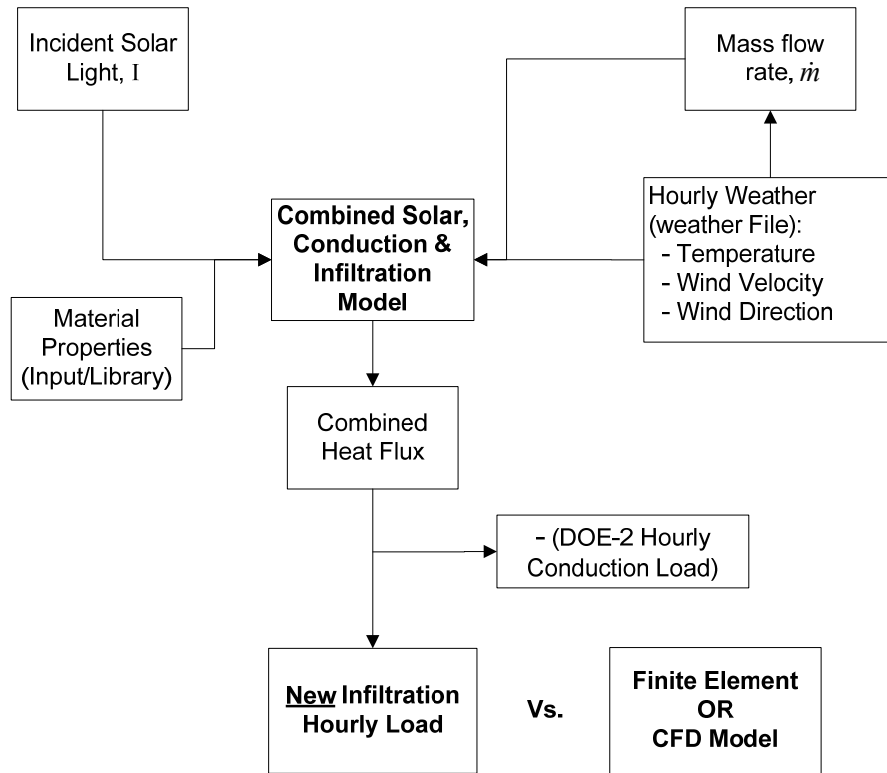
$$q_d(i) = (h_i + \dot{m} C_p)(T_r(i) - T_n(i)) \quad (3-24)$$

Where:

- $\dot{m}$  = Infiltration mass flow rate
- $h_i$  = Heat transfer coefficient of inside boundary layer of the wall
- $C_p$  = Specific heat capacity of air
- $T_r$  = Room temperature
- $T_n(i)$  = Node temperature

From this combined conduction and infiltration hourly heat flux, the hourly infiltration energy loads can be obtained by subtracting hourly conduction loads

obtained from DOE-2 (calculated using the weighting factors method discussed in Chapter 2). The model's framework is presented in Flowchart 3-2.



**Flowchart 3-2 : Buleprint of the Enhanced Model**



## **Infiltration Mass Flow Rate**

In order to evaluate the energy load of air infiltration, it is essential to determine the infiltration flow rate. This indicates the amount (volume) of air infiltrating into a building, based on which the energy load due to this infiltration flow rate can be determined. Air infiltration into a building is driven by pressure differences that emerge across the building envelope under various ambient conditions. Several traditional methods evaluate the infiltration flow rate using fixed constants or percentages. An example is the Air Change method, a widely used method. In the air change method the volume of infiltrating air per hour is defined as a fraction of the total volume of a room. For instance, an air change rate of 0.2 ACH (air changes/hour) implies that the volume of infiltrating air is equal to 20 % of the room/space volume. Such methods assign a fixed value to the infiltration flow rate and do not take into account various dynamic factors that control and fluctuate the infiltration flow rate. Weather conditions, air temperature, wind speed, wind direction and several other dynamic factors influence the air infiltration flow rate and therefore defining this flow rate using a fixed constant is a major source of inaccuracy. Consequently, it is essential to devise a methodology for calculating hourly infiltration airflow rates based on prevalent weather/climatic conditions and local characteristics.

Infiltration airflow is driven by a pressure gradient across the building envelope. The driving pressure is composed of two primary components: Wind Pressure and Stack Pressure (Stack Effect). The stack pressure is a function of the building height and ambient air temperatures (indoor and outdoor); while the wind pressure is mainly affected by the wind velocity, wind direction, local terrain & topography, and building shape

characteristics. Evaluating infiltration airflow by considering the stack effect and local wind pressure allows various dynamic driving factors and building specific characteristics to be considered rather than using a generic fixed constant or even a statistical fit. Following is a discussion of the methodology utilized for evaluating the stack pressure and wind pressure.

### **Stack Effect**

The roots of the stack effect lie in the temperature differences across the building envelope. As expressed by the ideal gas law (equation 3-25), air density is a function of temperature. Therefore the different temperatures on the inside and outside of a building result in a difference between the inside and outside air densities.

$$\rho = \frac{P}{R T} \quad (3 - 25)$$

Where:

- $\rho$  = air density
- P = air pressure
- R = Specific gas constant
- T = Temperature

In turn, this difference in air density across the building envelope results in air buoyancy differences and different air pressures on the inside and outside of the building. This pressure difference across the building envelope results in a pressure gradient over the height of the building known as the “stack effect” which partially drives the flow of infiltrating air. The “stack pressure” gradient varies with the height of the building since

as defined by equation 3-26, at a specific air density ( $\rho$ ), the air pressure value varies with the height of the air column.

$$P = \rho g h \quad (3 - 26)$$

Where:

- $g$  = gravitational acceleration constant
- $h$  = height of air column

The neutral pressure level ( $y_{npl}$ ) is defined as the height at which the interior pressure equals the outside pressure as shown in Figure 3-6.

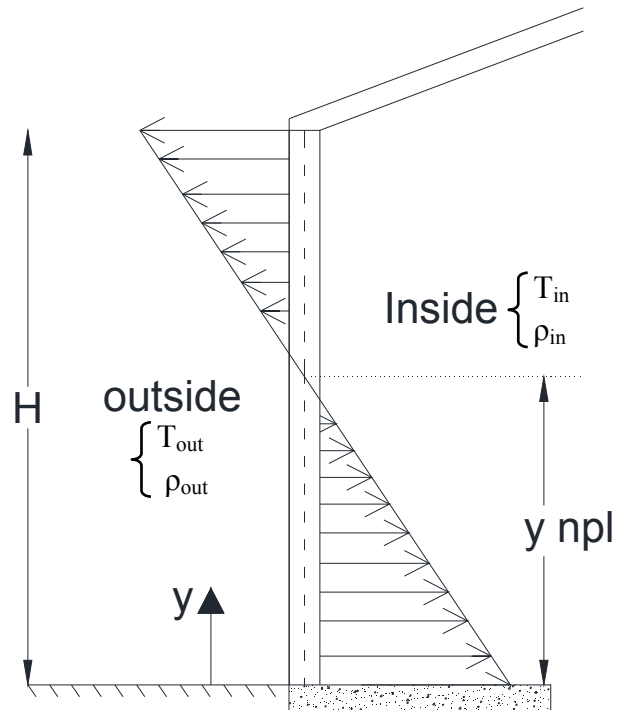


Figure 3-6: Stack Effect on a building wall

The stack pressure can be defined by equations 3-27 to 3-32. The underlying assumption is that the air is well mixed on both sides of the building envelope.

$$P_{in}(y) = P_{o\ in} - \rho_{in} g y \quad (3 - 27)$$

Similarly

$$P_{out}(y) = P_{o\ out} - \rho_{out} g y \quad (3 - 28)$$

$$\Delta P_s(y) = P_{in}(y) - P_{out}(y) \quad (3 - 29)$$

$$\therefore \Delta P_s(y) = (P_{o\ in} - \rho_{in} g y) - (P_{o\ out} - \rho_{out} g y) \quad (3 - 30)$$

$$\Delta P_s(y) = (P_{o\ in} - P_{o\ out}) - g y (\rho_{in} - \rho_{out}) \quad (3 - 31)$$

Define:

$$y' = \frac{y}{H} = \frac{\text{Height above bottom of the zone}}{\text{Zone Height}} \quad (\text{Deru \& Burns, 2003})$$

$$\therefore \Delta P_s(y') = (P_{o\ in} - P_{o\ out}) - y' [g H (\rho_{in} - \rho_{out})] \quad (3 - 32)$$

Where:

- $P_{o\ in}$  = Internal pressure at base of wall
- $P_{o\ out}$  = Outside pressure at base of wall
- $y$  = Distance from bottom of wall
- $H$  = Total zone height
- $y' = Y/H$  = Ration of height above bottom of zone to total zone height
- $\rho_{in}$  = Density of inside air
- $\rho_{out}$  = Density of outside air
- $g$  = gravitational constant

For simplification, a reference pressure is taken on the outside surface at the bottom of the wall. Therefore  $P_{o\ out}$  is taken as  $P_{o\ out} = 0$ .  $P_{o\ in}$  is therefore defined with respect to the reference pressure as follows:

$$P_{o\ in} = \rho_{in} R T_{in} \quad (3 - 33)$$

$$P_{o\ out} = \rho_{out} R T_{out} \quad (3 - 34)$$

$$\Rightarrow P_{o\ in} = (\rho_{in} - \rho_{out}) R (T_{in} - T_{out}) \quad (\text{for } P_{o\ out} \text{ as reference pt}) \quad (3 - 35)$$

Where:

- R = Specific gas constant
- T = Zone temperature in °K

### **Wind Pressure**

The flow of air around a building creates a wind pressure on the building. The pressure intensity, distribution, and nature over the building envelope vary by location. A generic illustration of wind pressure distribution over a low rise building is shown in Figure 3-7. The wind pressure intensity depends on the air density, wind speed and building shape characteristics expressed as a pressure coefficient,  $C_p$ . The general expression of the wind pressure intensity is given by equation 3-36.

$$P_w = \frac{1}{2} \rho_{air} C_p V^2 \quad (3 - 36)$$

Where:

- $P_w$  = Wind pressure
- $\rho_{air}$  = Outside air density
- $V$  = Wind speed

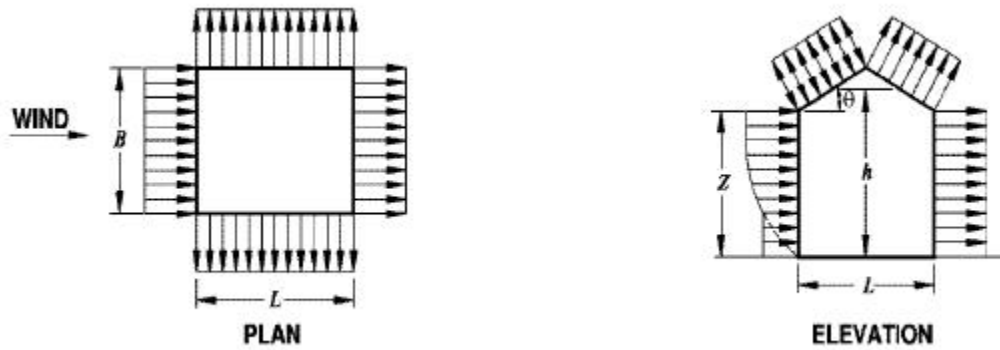


Figure 3-7: Wind pressure on a typical Gable, Hip roof house (Figure 6-6, ASCE 7-05)

The wind speed is usually recorded by weather stations at a height of 10 meters (~30 feet) over a flat terrain. However, this might not reflect the actual terrain, surroundings at the building location or the actual height of the building. Therefore, it is essential to incorporate a set of corrections to adjust the wind speed to local conditions and topography at the building site.

Wind pressure coefficients,  $C_p$ , are non-dimensional coefficients that represent the wind pressure distribution over a body and from which the wind pressure at a specific location over the building envelope can be calculated based on the local wind velocity and using equation 3-36. The general expression of the  $C_p$  coefficient is given by equation 3-37. Pressure coefficients are generally calculated from data obtained through experimental testing, wind tunnel or full scale tests, on various building shapes and heights.

$$C_p = \frac{P - P_o}{\frac{1}{2} \rho_{air} V^2} \quad (3 - 37)$$

Following is a discussion of the methodology used for calculating all the components of the wind pressure expression (equation 3-36). Included is a discussion of all the

corrections performed to account for wind direction, local shielding, terrain roughness and building shape properties.

### Wind Pressure Coefficients

Wind pressure coefficients can be obtained from several sources and databases. However, the wind pressure coefficients can vary largely over the surface of a structure. This would make wind pressure computations for infiltration airflow rate calculations overly complicated and computationally expensive. Therefore, average  $C_p$  values will be used for each surface. These values can be obtained from ASCE 7, Figure 6-6 shown in Table 3-1 below.

Wall Pressure Coefficients, $C_p$		
Surface	L/B	$C_p$
Windward Wall	All values	0.8
Leeward Wall	0 - 1	- 0.5
	2	- 0.3
	$\geq 4$	- 0.2
Side Wall	All Values	- 0.7

Table 3-1: External Pressure Coefficient,  $C_p$  (ASCE 7-05, Figure 6-6)

### Wind Direction

$C_p$  values are primarily based on a wind direction normal to the receiving surface. However, under normal conditions wind directions vary and are not necessarily normal to the receiving surface. In order to correct the pressure coefficients for variations in wind direction the Swami and Chandra (1988) model will be used. Other possible choices are Walton (1982) and COMISGroup Fuestel and Rayner-Hooson (1990). However, the Swami and Chandra model is more intricate than the Walton (1982) model, yet less

complex than the Fuestel and Rayner-Hooson (1990) model. The general expression of Swami and Chandra (1988) is given by equation 3-38, along with a comparison plot against Walton (1982) in Figure 3-9 (Deru and Burns, 2003).

$$C_p' = \frac{C_p}{C_p(\theta = 0)} \ln \left[ \begin{aligned} &1.248 - 0.703 \sin \frac{\theta}{2} - 1.175 \sin^2 \theta + 0.131 \sin^3(2\theta G) \\ &+ 0.769 \cos \frac{\theta}{2} + 0.07G^2 \sin^2 \frac{\theta}{2} + 0.717 \cos^2 \frac{\theta}{2} \end{aligned} \right] \quad (3-38)$$

Where:

- $\theta$  = Wind incidence angle
- $G = \ln(S) = \ln(l_1/l_2)$

S = Side ratio, ration of the length of adjacent walls ( $l_1$  &  $l_2$ )

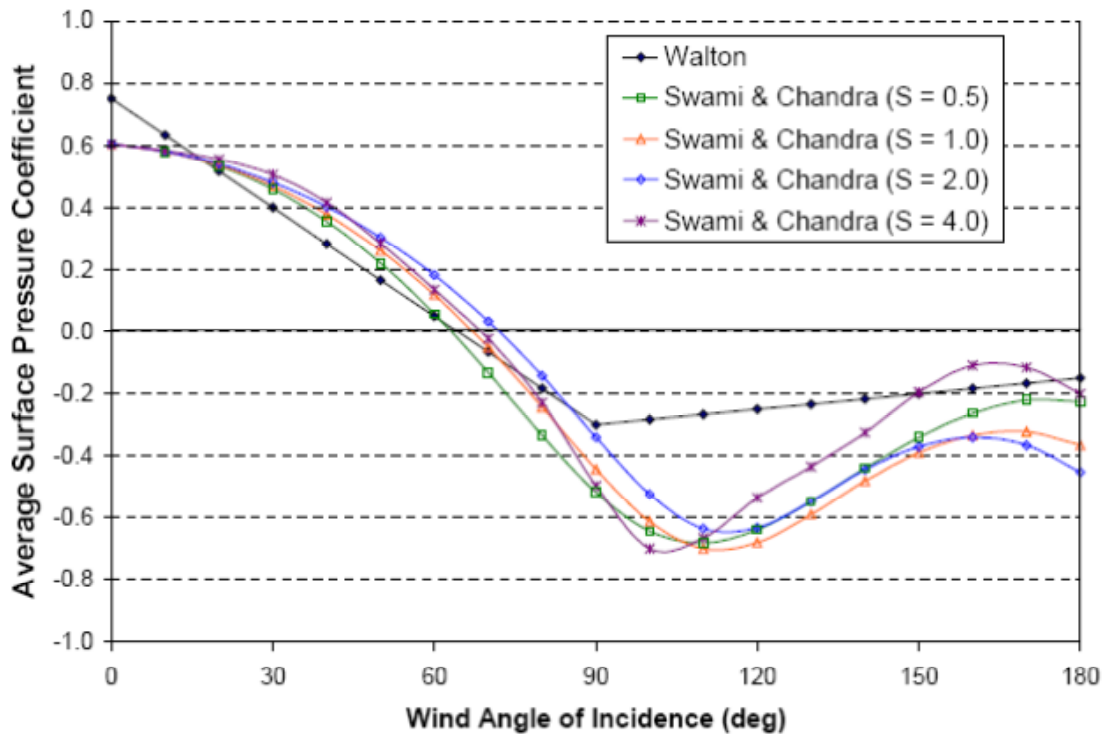


**Chart 3-1: Surface pressure coefficient as a function of wind incidence angle for the Walton model and Swami & Chandra model (Deru and Burns, 2003)**

Note: As shown in Figure 3-9, when S varies from 0.5 to 4.0, the difference in pressure coefficients at each wind direction and for different S values is relatively small.



Therefore, in order to simplify calculation S will be taken as: S =1 (Deru and Burns, 2003), consequently  $G = \ln(S) = 0$ . Thus equation 3-38 can therefore be expressed as:

$$C'_p = \frac{C_p}{C_p(\theta = 0)} = \ln \left[ \begin{array}{l} 1.248 - 0.703 \sin \frac{\theta}{2} - 1.175 \sin^2 \theta \\ + 0.769 \cos \frac{\theta}{2} + 0.717 \cos^2 \frac{\theta}{2} \end{array} \right] \quad (3 - 39)$$

The above relationship was developed for vertical surfaces and walls. Therefore, an expression is needed to determine the pressure coefficients for tilted surfaces such as gabled roofs. Deru and Burns (2003) proposed, for inclined surfaces, to calculate  $\theta$  using equation 3-40, and to use a normal surface pressure coefficient of 1.0 (rather than 0.8 as in ASCE 7 Figure 2-2).

$$\cos \theta = \sin \beta \cos(\gamma_s - \psi) \quad (3 - 40)$$

Where:

- $\beta$  = Surface tilt
- $\gamma_s$  = Surface azimuth (South =  $0^\circ$ , East =  $-90^\circ$ )
- $\psi$  = Wind direction from weather file ( North =  $0^\circ$ , East =  $90^\circ$ )

Results obtained using this method match published experimental results from Aikens (1976) for flat roofs and ASHRAE Handbook of fundamentals data for sloped roofs (Deru and Burns, 2003). Therefore this model will be adopted in this methodology for use in the case of tilted roofs.

### Wind Incidence Angle

The wind incidence angle will be obtained from DOE-2 location weather data. However, in DOE-2, wind angles are reported by sector number. The full 360° is divided into 24 sectors of 15° each. Therefore, in order to determine the wind direction, the wind incident angle will be taken to be at the middle of the DOE-2 reported sector. Therefore, the wind incident angle can be calculated using equation 3-41.

$$\theta_{deg} = (\text{Weather file Sector \#})(15^\circ) + \frac{15^\circ}{2} \quad (3 - 41)$$

### Wind Speed

Wind speed measurements are usually performed in airports or local weather stations with an open terrain. The measurements are usually performed at a height of 30 ft (~10 m). Buildings, however, exist in various terrains that could differ in roughness from a flat terrain, and at heights that could differ from the 30 ft wind speed measurement height. In order to determine local wind speeds the power law is used. The recorded mean wind speed will be used along with coefficients that account for variation in terrain roughness, building height, and measuring station height in order to calculate the local wind speed. The general expression of the power law is given in equation 3-42.

$$V = (V_{Z_{ref}}) \left( \frac{Z}{Z_{ref}} \right)^{1/\alpha} \quad (3 - 42)$$

Where:

- Z= Elevation
- $Z_{ref}$  = Elevation of measuring point
- $V_{Z_{ref}}$  = Measured wind speed at  $Z_{ref}$
- V = Wind speed at elevation Z

-  $1/\alpha$  = Coefficient corresponding to surface roughness

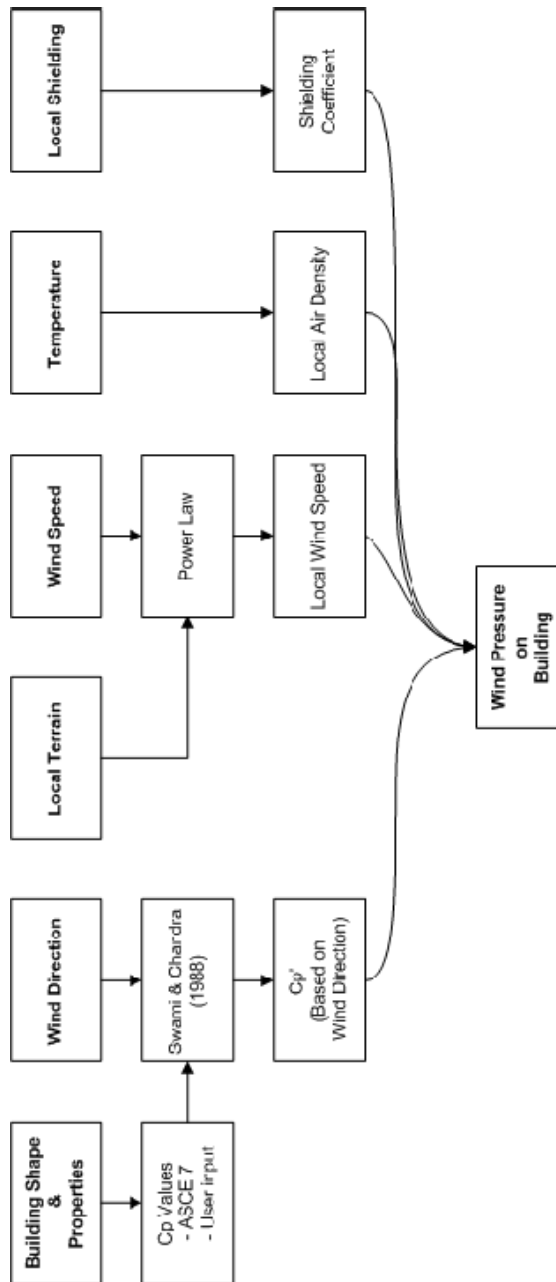
Class	3 Sec Gust Speed		Mean Hourly Speed		Description
	$1/\alpha$	$Z_g$ ft(m)	$1/\alpha$	$Z_g$ ft(m)	
I	1/11.5	700(213)		700(213)	Open water body/ocean
II	1/9.5	900(274)	0.16	900(274)	Open terrain, flat terrain with isolated obstacles
III	1/7	1200(366)	0.28	1200(366)	Suburban terrains, towns
IV		1500(457)	0.4	1500(457)	Centers of large cities

Table 3-2: Surface Roughness Coefficients (Simu and Miyata, 2006)

The general form of the power law can be used to calculate the wind speed at different heights for the same location. However, to calculate the wind speed at a location different from the wind speed measurement location and at a different height and surface roughness, a compound form of the power law will be used. The used expression is given by equation 3-43.

$$V = (V_{Z_{Open}}) \left( \frac{Z_g \text{ Open}}{Z_{Open}} \right)^{1/\alpha \text{ open}} \left( \frac{Z}{Z_g} \right)^{1/\alpha} \quad (3 - 43)$$





Flowchart 3-3: Wind Pressure calculation based on local factors and building characteristics

## Local Shielding Parameters

Local obstructions surrounding a building can actively shield it from the full impact of wind. For instance, large adjacent buildings, lines of trees, or such can shield the building under consideration consequently reducing the wind pressure incident on it. A single row of high-density wind shielding can result in a 60% reduction in infiltration airflow when present within four tree heights from a building (Stathopoulos et al., 1994). Therefore due to its proven impact, it is essential to take into account the affect of shielding in reducing the wind pressure,  $P_w$ , on a building and consequently the affect of shielding on infiltration airflow rate. Sherman and Modera (1986) developed coefficients that can be applied onto  $P_w$  to account for shielding effects and accordingly reduced infiltration flow rates. Deru and Burns (2003) normalized those coefficients by the shielding coefficient of Class I (minimum shielding) for use in situations in which only the effects of local shielding are required. In this methodology, these shielding coefficients will be used and will be applied onto the wind pressure  $P_w$  as shown in equation 3-44.

$$P_w = \frac{1}{2} \rho_{air} C_p' V^2$$
$$P_{w+Shielding} = (SC)P_w \quad (3 - 44)$$

Where:

- $P_{w+Shielding}$  = Wind pressure with shielding effects taken into account
- $SC$  = Normalized shielding coefficient
- $C_p'$  = Pressure coefficient corrected for wind direction
- $V$  = Local wind speed corrected using the power law

Class	SC	Description
I	1.0	No obstructions or local shielding
II	0.880	Light local shielding with few obstructions
III	0.741	Moderate local shielding , some obstructions within 2 house heights
IV	0.571	Heavy shielding obstructions around most of the perimeter
V	0.315	Very heavy shielding, large surrounding obstructions within 2 house heights

Table 3-3: Normalized shielding coefficients from Deru and Burns (2003) based on Sherman and Modera (1998)

### Infiltration Mass Flow Rate

The infiltration flow rate through the building envelope can be represented by and orifice equation. The general expression for flow through an orifice is given by equation 3-45.

$$\dot{m} = C_D A \sqrt{2 \rho \Delta P} \quad (3 - 45)$$

Where:

- $\dot{m}$  = Mass flow rate
- $A$  = Opening Area
- $\rho$  = Leaking air density
- $\Delta P$  = Total driving pressure

Complex leakage through complex holes and small openings has been shown to have a slightly different dependence on the pressure difference. Therefore the flow rate is expressed in equation 3-46 (Deru and Burns, 2003).

$$\dot{m} = C A_e \sqrt{2 \rho} (\Delta P)^n \quad (3 - 46)$$

Where:

- $C$  = Flow Coefficient

- $A_e$  = Approximate leakage Area
- $\rho$  = Density of infiltrating air
- $n$  = Flow exponent ( $0.5 < n < 1$ )

In order to calculate the infiltration mass flow rate using equation 3-46, the various equation entries must be finalized and determined as shown below:

**Effective leakage area:** Material effective leakage area can be obtained from ASHRAE Handbook: Table 1 page 25.15. The effective leakage area for various materials has been determined in ASHRAE at a pressure difference of 0.016 in of water and a  $C_D$  value of 1. These values have been obtained through a study by Colliver et al.(1992).

**Table 1 Effective Air Leakage Areas (Low-Rise Residential Applications Only)**

	Units (see note)	Best Estimate	Mini- mum	Maxi- mum		Units (see note)	Best Estimate	Mini- mum
Ceiling					Piping/Plumbing/Wiring penetrations			
General	in <sup>2</sup> /ft <sup>2</sup>	0.026	0.011	0.04	Uncaulked	in <sup>2</sup> ea	0.9	0.3
Drop	in <sup>2</sup> /ft <sup>2</sup>	0.0027	0.00066	0.003	Caulked	in <sup>2</sup> ea	0.3	0.1
Ceiling penetrations					Vents			
Whole-house fans	in <sup>2</sup> ea	3.1	0.25	3.3	Bathroom with damper closed	in <sup>2</sup> ea	1.6	0.3
Recessed lights	in <sup>2</sup> ea	1.6	0.23	3.3	Bathroom with damper open	in <sup>2</sup> ea	3.1	0.9
Ceiling/Flue vent	in <sup>2</sup> ea	4.8	4.3	4.8	Dryer with damper	in <sup>2</sup> ea	0.46	0.4
Surface-mounted lights	in <sup>2</sup> ea	0.13			Dryer without damper	in <sup>2</sup> ea	2.3	1.9
Chimney	in <sup>2</sup> ea	4.5	3.3	5.6	Kitchen with damper open	in <sup>2</sup> ea	6.2	2.2
Crawl space					Kitchen with damper closed	in <sup>2</sup> ea	0.8	0.1
General (area for exposed wall)	in <sup>2</sup> /ft <sup>2</sup>	0.144	0.1	0.24	Kitchen with tight gasket	in <sup>2</sup> ea	0.16	
8 in. by 16 in. vents	in <sup>2</sup> ea	20			Walls (exterior)			
Door frame					Cast-in-place concrete	in <sup>2</sup> /ft <sup>2</sup>	0.007	0.0
General	in <sup>2</sup> ea	1.9	0.37	3.9	Clay brick cavity wall, finished	in <sup>2</sup> /ft <sup>2</sup>	0.0098	0.0
Masonry, not caulked	in <sup>2</sup> /ft <sup>2</sup>	0.07	0.024	0.07	Precast concrete panel	in <sup>2</sup> /ft <sup>2</sup>	0.017	0.0
Masonry, caulked	in <sup>2</sup> /ft <sup>2</sup>	0.014	0.004	0.014	Lightweight concrete block, unfinished	in <sup>2</sup> /ft <sup>2</sup>	0.05	0.0
Wood, not caulked	in <sup>2</sup> /ft <sup>2</sup>	0.024	0.009	0.024	Lightweight concrete block, painted or stucco	in <sup>2</sup> /ft <sup>2</sup>	0.016	0.0
Wood, caulked	in <sup>2</sup> /ft <sup>2</sup>	0.004	0.001	0.004	Heavyweight concrete block, unfinished	in <sup>2</sup> /ft <sup>2</sup>	0.0036	
Trim	in <sup>2</sup> /lftc	0.05			Continuous air infiltration barrier	in <sup>2</sup> /ft <sup>2</sup>	0.0022	0.0
Jamb	in <sup>2</sup> /lftc	0.4	0.3	0.5	Rigid sheathing	in <sup>2</sup> /ft <sup>2</sup>	0.005	0.0
Threshold	in <sup>2</sup> /lftc	0.1	0.06	1.1	Window framing			
Doors								
Attic/crawl space, not weatherstripped	in <sup>2</sup> ea	4.6	1.6	5.7				
Attic/crawl space	in <sup>2</sup> ea	2.8	1.2	2.0				

**Figure 3-9: Effective air leakage are, ASHRAE Handbook Chapter 25 Table 1 (partially)**

For different reference pressures, air flow rates and flow coefficients, the values of effective leakage area can be corrected using equations 3-47 from the ASHRAE Handbook.

$$A_{r,2} = A_{r,1} \left( \frac{C_{D,1}}{C_{D,2}} \right) \left( \frac{\Delta P_{r,2}}{\Delta P_{r,1}} \right)^{n-0.5} \quad (3 - 47)$$



Where:

- $A_{r,1}$  = Air leakage area at reference pressure difference  $\Delta P_{r,1}$
- $A_{r,2}$  = Air leakage area at reference pressure difference  $\Delta P_{r,2}$
- $C_{D,1}$  = discharge coefficient used to calculate  $A_{r,1}$
- $C_{D,2}$  = discharge coefficient used to calculate  $A_{r,2}$
- $n$  = Flow exponent

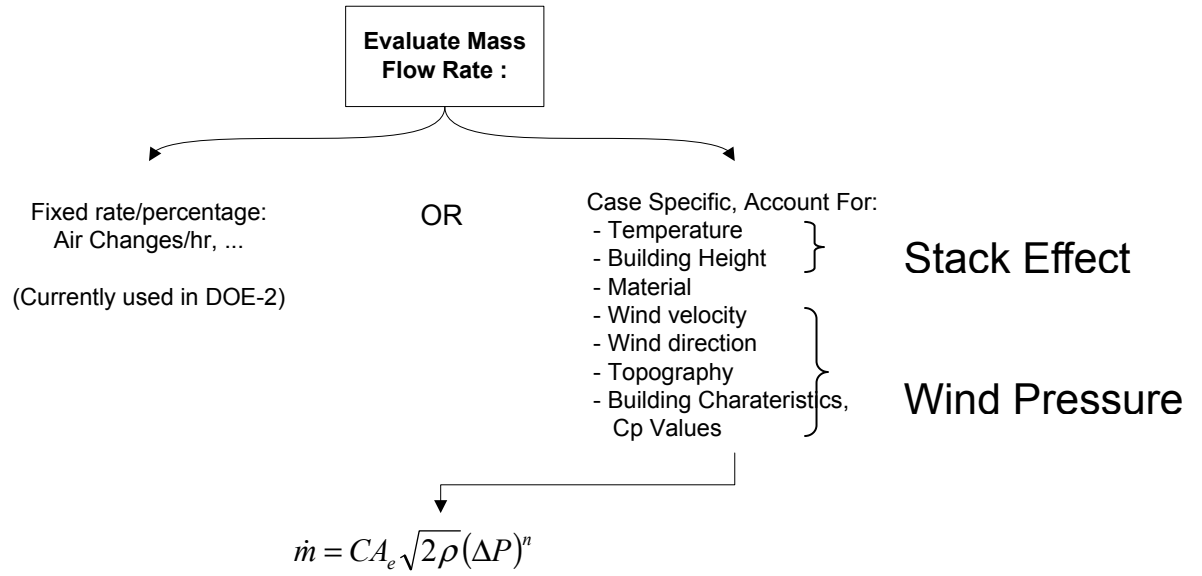
**Flow Exponent:** The flow exponent ranges between 0.5 & 1.0 ( $0.5 \leq n \leq 1$ ). Where 0.5 is in the case of turbulent flow and 1.0 is for the case of laminar flow. Diffusive air infiltration is characterized by a laminar flow and therefore  $n = 1$  will be adopted in this methodology.

**Pressure gradient,  $\Delta P$ :** the driving pressure gradient is a combination of the Stack Effect and Wind Pressure. Thus  $\Delta P$  is calculated as follows:

$$\Delta P = P_{Stack} + P_{Wind+shielding}$$

$$\Delta P = P_{0 in} - \Delta P_{S,0} - Y' P_{S,H} + (SC)P_w$$

$$\Delta P = \left| P_{0 in} - \Delta P_{S,0} - Y' P_{S,H} + \frac{1}{2} C_p' V^2 \right| \quad (3 - 48)$$



**Flowchart 3-4: Mass flow rate calculation and components**

## **Solar Calculation and Shading**

Integrating heat recovery and the interaction between solar radiation, conduction and infiltration into building energy simulation requires an evaluation of the intensity of solar radiation incident on the building. The incident solar radiation depends on several factors including: building location, season, day, time of the day, building orientation, cloud cover and others. Both direct normal solar radiation (incident radiation perpendicular to receiving space) and diffuse solar radiation (diffuse non-perpendicular radiation) must be considered. Shading should also be taken into account. A shade could reduce or eliminate the incident solar radiation onto a surface, this should be accounted for and therefore shading calculations are to be considered also. The solar and shading calculation model is based on the DOE-2 existing calculation model as defined on DOE-2 Engineers Manual Version 2.1 A (November 1982), along with Threlkand and Jordon (1958), Stephenson (1965), and ASHRAE Handbook of Fundamentals.

### **Solar Calculation**

A brief description of the deployed solar calculation model is provided below. Essential to the methodology is, primarily, defining the following fundamental quantities.

#### **Declination Angle (DECLN)**

The solar declination angle represents the angle formed between the earth's equatorial plane and the earth-sun line. Since the earth axis tilts to a maximum of  $23.5^{\circ}$  and is perpendicular to the equatorial plane, the declination angle ranges between  $+23.5^{\circ}$  (June) and  $-23.5^{\circ}$  (December).

## Solar Equation of Time (EQTIME)

The equation of time is a correction term used to calculate the apparent solar time from local clock time. It is important to consider the solar equation of time since it takes into account the varying perturbations in the earth's orbit and rotation rate. The equation of time is given by equation 3-49 (Duffet-Smith, 1988) and plotted in Figure 3-11 over a year span.

$$\Delta t = \frac{(\mu - \vartheta) + (\lambda - \alpha)}{w_E} \quad (3 - 49)$$

Where:

- $\mu$  : Sun mean anomaly (relating the position & time of an object in orbit)

$$\mu = nt = \sqrt{\frac{G(M_x + m)}{a^3}} t \quad (\text{Murry \& Dermott, 1999}) \quad (3 - 50)$$

Where:

- $n$  = mean motion (measure of angular orbiting speed)
- $a$  = length of orbit's semi-major axis
- $M_x$  &  $m$  = mass of orbiting objects
- $G$  = Gravitational constant

$\therefore$  For the sun:

$$\mu = \frac{360}{365.242191} d_{day} \quad (\text{Duffet - smith, 1988}) \quad (3 - 51)$$

- $\vartheta$  = Sun's true anomaly (defines angular position of a mass in orbit)
- $\lambda$  = Angle from vernal equinox to the sun in the elliptical plane
- $\alpha$  = Angle from vernal equinox to the sun in equatorial plane
- $w_E$  = Earth's axial rotation rate: 1 rev/day = 0.001389  $\pi$ /min

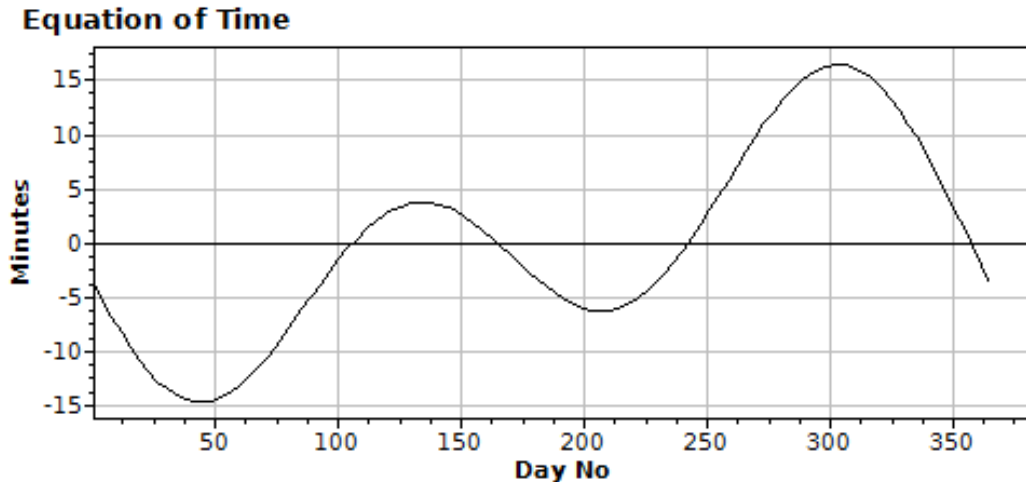


Chart 3-2: Plot of solar equation of time, minute correction by day of the year

### Solar Constant (SOLCON)

The solar constant represents the intensity of solar radiation falling on a surface at the top of the atmosphere normal to the sun rays. It is obtained from a curve fit of measured solar data.

### Atmospheric Excitation Coefficient (ATMEXT)

This coefficient corrects for the reduction of solar energy by the atmosphere. ATMEXT is also obtained from curve fitting of measured data (as in Threlkland and Jordan (1958) and Stephenson (1985)).

### Sky Diffuse Factor (SKYDIFF)

The sky diffuse factor is obtained from curve fitting of measured experimental data (as in Threlkland and Jordan (1958) and Stephenson (1985)) and allows the calculation of diffuse radiation obtained from normal solar radiation.

Monthly values of the above listed entities are shown in Table 3-4 (ASHRAE, 1977). The listed values are for the 21<sup>st</sup> day of each month.

	<b>DECLN (deg)</b>	<b>EQTIME (hrs)</b>	<b>SOLCON</b>	<b>ATMEXT</b>	<b>SKYDFE</b>
<b>January</b>	- 20.00	- 0.19	390	0.142	0.058
<b>February</b>	- 1.08	- 0.23	385	0.144	0.060
<b>March</b>	0.0	- 0.123	376	0.156	0.071
<b>April</b>	11.6	0.020	360	0.180	0.097
<b>May</b>	20.0	0.060	350	0.196	0.121
<b>June</b>	23.45	- 0.025	345	0.205	0.134
<b>July</b>	20.6	- 0.103	344	0.207	0.136
<b>August</b>	12.3	- 0.051	351	0.201	0.122
<b>September</b>	0.0	0.113	365	0.174	0.042
<b>October</b>	- 10.5	0.255	378	0.160	0.073
<b>November</b>	- 19.8	0.235	387	0.149	0.063
<b>December</b>	- 23.45	0.033	391	0.142	0.057

Table 3-4: ASHRAE 1977 Handbook of Fundamentals

For ease of use in software, these five quantities have been expressed in a truncated Fourier series equation (equation 3-52).

$$\left. \begin{array}{l} \tan(DCLN) \\ EQTIME \\ SOLCON \\ ATMEXT \\ SKYDFE \end{array} \right\} = A_0 + A_1 \cos(w) + A_2 \cos(2w) + A_3 \cos(3w) \\
 + B_1 \sin(w) + B_2 \sin(2w) + B_3 \sin(3w) \quad (3 - 52)$$

Where:

- $w = \frac{2\pi}{366} (Doy)$
- Doy = Day of the year

	<b>A<sub>0</sub></b>	<b>A<sub>1</sub></b>	<b>A<sub>2</sub></b>	<b>A<sub>3</sub></b>	<b>B<sub>1</sub></b>	<b>B<sub>2</sub></b>	<b>B<sub>3</sub></b>
<b>Tan (DECLN)</b>	- 0.00527	-0.4001	-0.003996	-0.00424	0.0672	0.0	0.0
<b>EQTIME</b>	$0.696 \times 10^{-4}$	0.007006	-0.0533	-0.00157	-0.122	-0.156	-0.00556
<b>SOLCON</b>	368.44	24.52	-1.14	-1.09	0.58	-0.18	0.28
<b>ATMEXT</b>	0.1717	0.0344	0.0032	0.0024	-0.0043	0.0	-0.0008
<b>SKYDFE</b>	0.0905	-0.0410	0.0073	0.0015	-0.0034	0.0004	-0.0006

**Table 3-5: Fourier series equation constants**

Using the 5 quantities discussed above, the solar calculations are performed using the following major steps (Method deployed by DOE-2).

**1. Determine the sunrise hour angle (GUNDOG)**

$$GUNDOG = \cos^{-1}[-\tan(STALAT) \times \tan(DECLN)]$$

$$(hr \text{ angle of sunrise}) = \cos^{-1}[-\tan(latitude) \times \tan(Declination)] \quad (3 - 53)$$

Where:

- DECLN = Solar declination angle
- STALAT = Latitude

**2. For each hour of the day : Calculate Hour Angle (HORANG)**

$$HORANG = \left( \frac{2\pi(rd)}{24(hr)} \right) \left( IHR - 12 + ITIMZ + EQTIME - \frac{1}{2} \right) - STALON \quad (3 - 54)$$

$$= \left( \frac{2\pi(rd)}{24(hr)} \right) \left[ (hr \text{ of day} - 12) + (timing \text{ zone}) + (eqtn \text{ of time}) - \frac{1}{2} \right]$$

- Longitude

Note: Subtracting (1/2) is because all calculations are performed at the middle of the hourly interval.

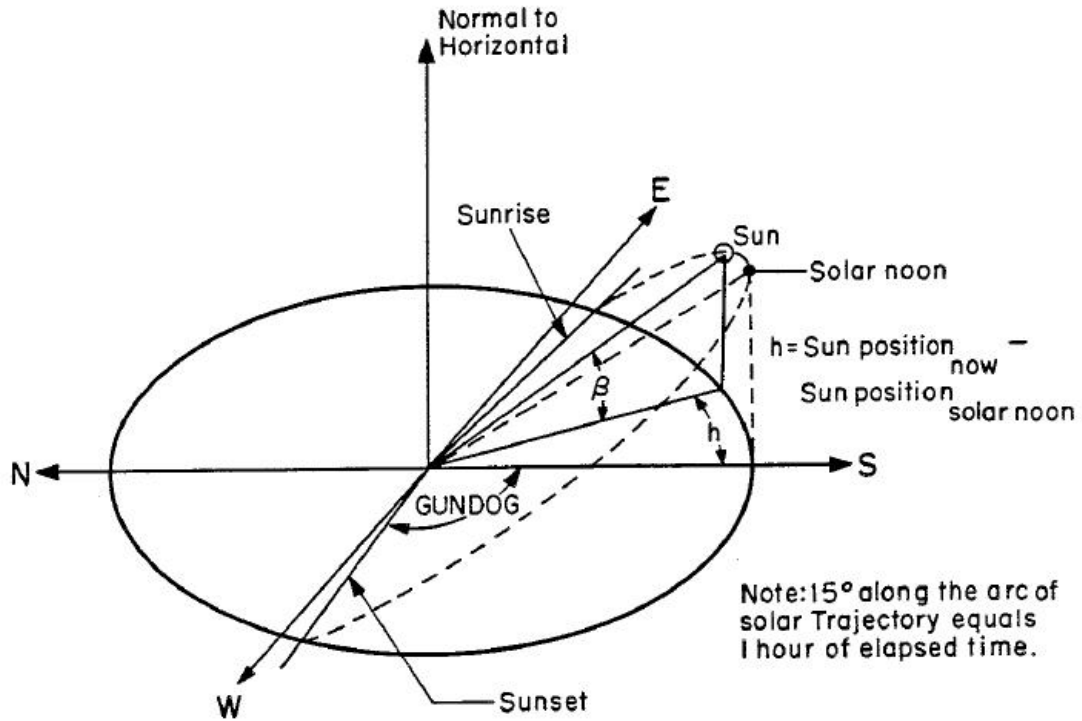


Figure 3-10: Daily Solar Geometry (DOE-2 Engineers Manual, 1982)

**3. Determine if sun is up or down for the current hour**

- Find the boundary of current interval nearest to noon (= TEST)

$$\left. \begin{aligned} \text{If } IHR < 12, TEST &= HORANG + \frac{2\pi \text{ rad/day}}{48 \text{ half hrs/day}} \\ \text{If } IHR > 12, TEST &= HORANG - \frac{2\pi \text{ rad/day}}{48 \text{ half hrs/day}} \end{aligned} \right\} \quad (3 - 55)$$

Where: IHR = Hour of the day

- If  $|TEST| > |GUNDOG| \Rightarrow$  Sun is down for the entire hour

*If |Boundary of current interval| > |Sunrise/Sunset hour angle |*

*$\Rightarrow$  Sun is down for the entire hour*

**4. Determine if the sun is up fully or partially for current hour**



- Find the difference between the hour angle and the boundary of the current interval:

$$DIFF = |GUNDOG| - |TEST| \quad (3 - 56)$$

$$(Difference) = (Sunrise/Sunset \text{ hour angle})$$

$$- (Interval \text{ boundary closest to noon})$$

- If  $0 < DIFF < \frac{2\pi \text{ rd/day}}{24 \text{ hrs/day}} = 0.2618 \Rightarrow$  Sunrise/Sunset in current interval

$\therefore$  Fraction of sun up (FSUNUP) =

$$\begin{cases} FSUNUP = 1 & \text{if sun is fully up} \\ FSUNUP = \frac{24 \text{ (hrs)}}{2\pi \text{ (rd)}} DIFF & \text{if Sunset/Sunrise} \end{cases} \quad (3 - 57)$$

## 5. Determine the Solar Direction Cosines

Three solar direction cosines define the position of the building with respect to the sun and sun rays. They are defined as RAYCOS (1), RAYCOS(2) and RAYCOS(3), in equations 3-58, 3-59, and 3-60.

$$\begin{aligned} RAYCOS(1) = & [\cos(HORANG) \cos(DECLN) \sin(STALAT) \\ & - \sin(DECLN) \cos(STALAT)] \sin(BAZIM) \\ & - \sin(HORANG) \cos(DECLN) \cos(BAZIM) \quad (3 - 58) \end{aligned}$$

$$\begin{aligned} RAYCOS(2) = & [\cos(HORANG) \cos(DECLN) \sin(STALAT) \\ & - \sin(DECLN) \cos(STALAT)] \cos(BAZIM) \\ & - \sin(HORANG) \cos(DECLN) \sin(BAZIM) \quad (3 - 59) \end{aligned}$$

$$\begin{aligned} RAYCOS(3) = & \sin(STALAT) \sin(DECLN) \\ & + \cos(STALAT) \cos(HORANG) \cos(DECLN) \quad (3 - 60) \end{aligned}$$

Where : BAZIM = Building Azimuth angle measured from the north.

## 6. Determine solar data

Solar data are usually included in weather files. However, if not available in the weather file, the solar data are determined using the 5 previously discussed quantities; primarily the Solar constant (SOLCON), Atmospheric extinction (ATMEXT) and Sky diffusion (SKYDFF) factors. Both direct (RDN) and Diffuse (BSUN) solar radiations can now be determined. RDN and BSUN are defined in equations 3-61 and 3-62.

$$RDN = SOLCON \times CLRNES \times e^{-\frac{ATMEXT}{RAY \cos(\theta)}} \quad (3 - 61)$$

$$BSUN = \left( \frac{SKYDFF}{CLRNES^2} \right) RDN \quad (3 - 62)$$

Where : CLRNES = Clearness number. The atmospheric clearness number reflects the attenuation of solar radiation by the atmospheric conditions. Twelve local monthly clearness numbers are available. The clearness numbers are usually included in the weather file. However when not included/appropriate, twelve (monthly) ASHRAE defined numbers can be used for each locality.

## If Cloudy Conditions

### 7. Determine Cloud Cover

Cloud cover presence reduces the incident solar energy intensity. Therefore on cloudy days a correction factor is defined to account for this reduction. The cloud cover correction factor (CLDCOV) is obtained by an empirical function of the third order and as a function of the clouds amount present (defined between 1 and 10)

## 8. Determine Normal and Diffuse Radiation (Cloudy condition)

With all the necessary factors established, the amount of direct and diffuse solar radiation is determined. Taken into account are the cloud cover, atmosphere clearness, hour of the day, location and direction of the building and all the other discussed factors. The amounts of incident direct and diffuse solar radiation are therefore defined by equations 3-63, 3-64 and 3-65.

**Total Solar Radiation:** SOLRAD (considering possible cloud cover)

$$SOLRAD = [RDN \times RAYCOS(3) + BSUN]CLDCOV \times FSUNUP \quad (3 - 63)$$

**Direct Normal Solar Radiation:** RDNCC (considering possible cloud cover)

$$RDNCC = RDN(1 - CLDAMT/10) \times FSUNUP \quad (3 - 64)$$

**Diffuse Solar Radiation:** BSCC (considering possible cloud cover)

$$BSCC = SOLRAD - [RDNCC \times RAYCOS(3)] \quad (3 - 65)$$

## Shading Calculation

Adjacent buildings, overhanging structures, and other miscellaneous objects and structures present in the vicinity of the building under study cast shadows onto it. These shadows affect the intensity of solar radiation incident on various parts of a building. It is therefore essential to perform shading calculations and account for the shading effect of surrounding sun obstructions. Presented below is a general description of the shading calculation method. This method is also utilized by DOE-2 and presented in the DOE-2 Engineers Manual (1982).

### Shading Polygons

In the shading calculations three major polygons are defined. Those polygons are the Shading Polygon (SP), Receiving Polygon (RP), and Shadow Polygon. The surface on which the shadows fall is denoted as the receiving polygon, the surface casting the shadow is defined as the shading polygon, and the shape of the shadow falling on the receiving polygon is defined as the shadow polygon (Figure 3-13).

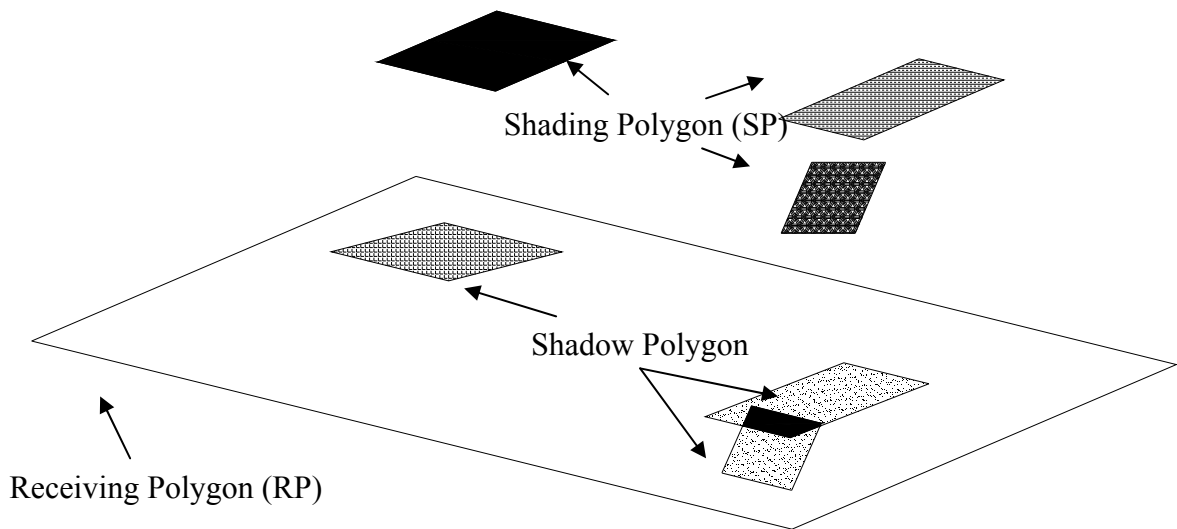


Figure 3-11: Shading calculations related polygons

The shading calculations for each receiving surface area are performed 24 times a day (once for each hour) for 1 day of each month. The underlying assumption is that there is no major variation in the shading properties of a single hour over a period of 1 month.

### **Shading Calculation Description**

The intensity of light falling on the RP polygon (depending on the SP polygon transmittance) is expressed as a function  $f(x, y)$ . As a result, the total amount of solar light incident on the RP polygon is defined by equation 3-66.

$$\text{Light Amount} = \iint f(x, y) dx dy \quad (3 - 66)$$

However, considering that for an individual shade the intensity  $f(x, y)$  is constant, then the amount of incident light can be defined in equation 3-66.

$$\text{Light Amount} = f(x, y) \times \text{Area of Shadow Polygon} \quad (3 - 67)$$

In order to determine the shadow polygon area the following procedures are followed:

1. The receiving polygon is divided into a large number of bars/strips.
2. The points of intersection of the shadow polygon with the midlines of each strip are saved, thus defining the contour of the shadow polygon. As a result, the shadow polygon is transformed into a set of rectangular strips as shown in Figure 3-14.

Therefore, the incident sunlight intensity is equal to the product of the constant  $f(x, y)$  by the area of the covered portion of each rectangular strip.

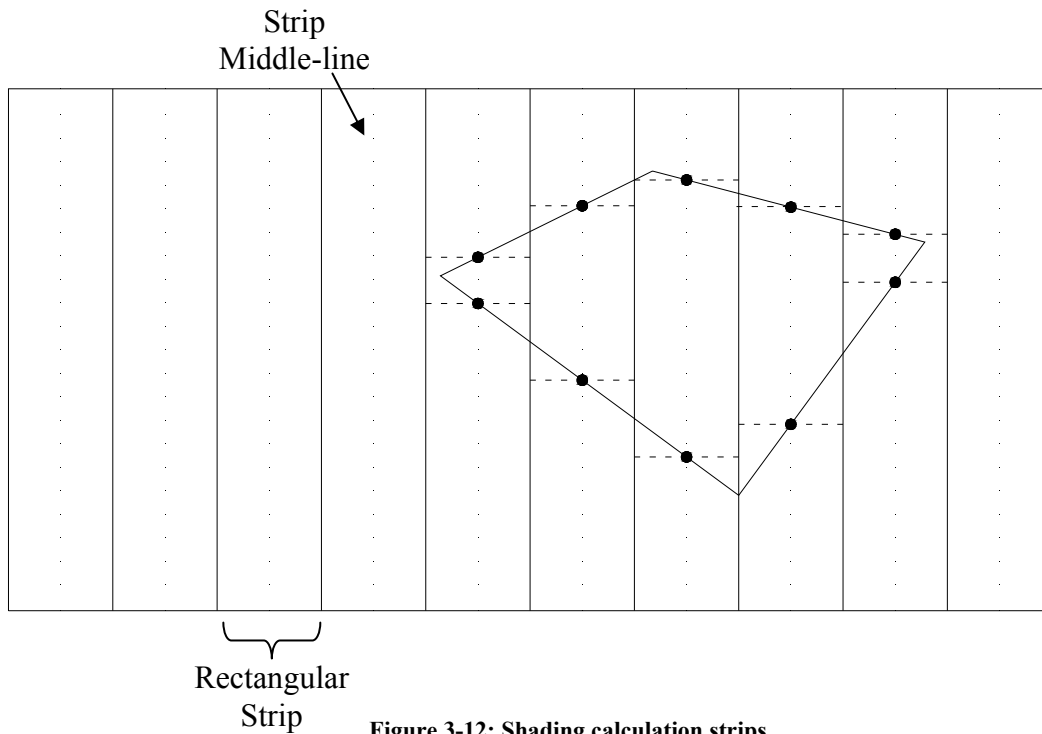


**Figure 3-12: Shading calculation strips**

Similar to the solar calculation, the position of the sun is checked (using the sun cosine angles defined previously) to verify that the sun is up, the location of sun, and the capability of the SP polygon to cast a shadow on the RP polygon. The SP polygon is then projected on to the RP polygon based on the sun position as defined by the sun cosine angles RAYCOS (1), RAYCOS(2), and RAYCOS(3). Also, any portions of the shading polygon dipping below the RP polygon are clipped off; since these part of the SP polygon cannot cast a shade on the RP polygon.

### CFD Modeling of Cracks and Airflow Paths

Air flows across the building envelope through a multitude of cracks and flow paths. These air leakage paths fall into 2 categories in terms of location. Air leakage paths can either be within the plane of a face/wall or at interfaces/joints. Examples of interfaces include wall-wall (corners), wall to ceiling, wall to floor, and others. Existing models of air flow through the building envelope have mostly had either a generalized representative area utilized in calculations of infiltration. On the other hand, CFD models of infiltration are few and have solely modeled a small 2-D section of a building envelope (wall) with a clearly defined single airflow path as shown in Figures 3-15 below. Examples Include Chebil et. Al (2003) and Boussa et. Al(2001). In generalized non-building envelope related fluid flow through cracks simulations researchers have modeled cracks by inducing them in a model using an applied structural load rather than predefining the flow path's properties An example is shown in Figure 3-16 below. This technique is mostly used in nuclear leakage safety research as in Danko and Bahrami (2004).

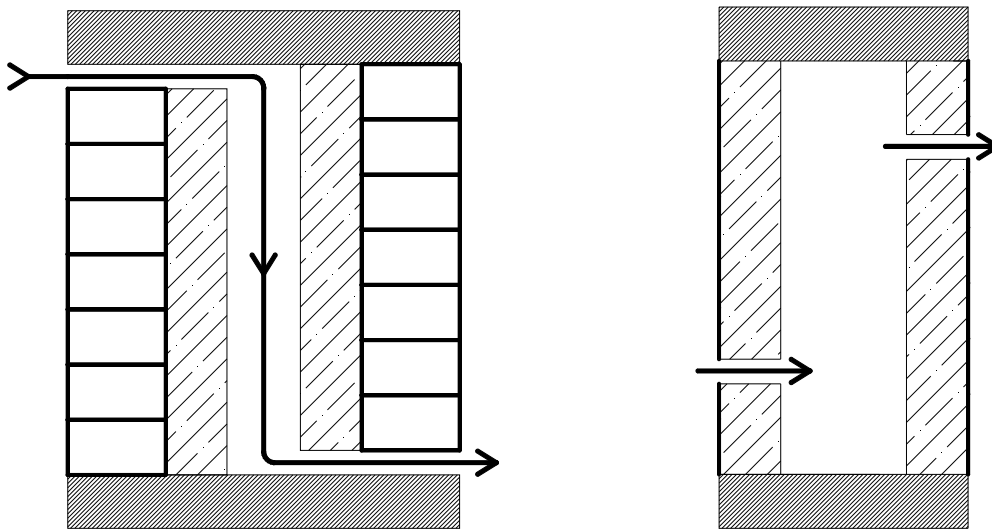
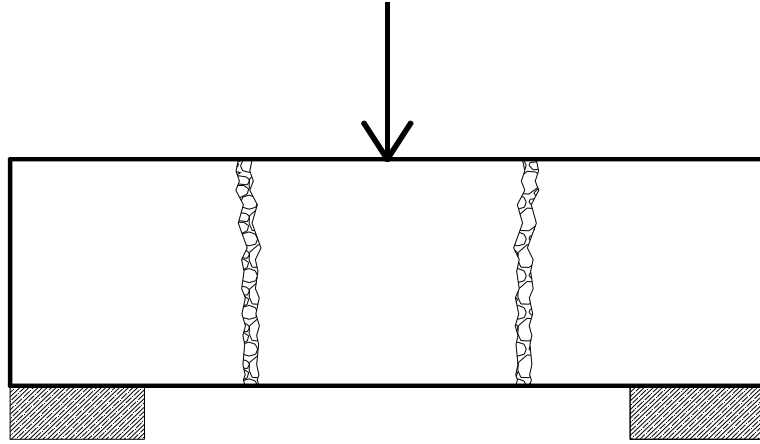


Figure 3-13: Sample 2-D Infiltration CFD Models



**Figure 3-14: Sample 2-D Infiltration CFD Models With Loading Induced Cracks**

In this research a full 3D representative building envelope will be modeled. Therefore, it is essential to identify all possible shapes and locations of air leakage paths for use in building the CFD model. Using a combination of data from available literature, the AIVC (Air Infiltration & Ventilation Center), and ASHRAE it is possible to identify the most common crack shapes in building envelopes and their corresponding path dimensions. The following sections provide an insight into this process and the corresponding resulting 3-D building envelope models.

### **Air Leakage Cracks & Paths**

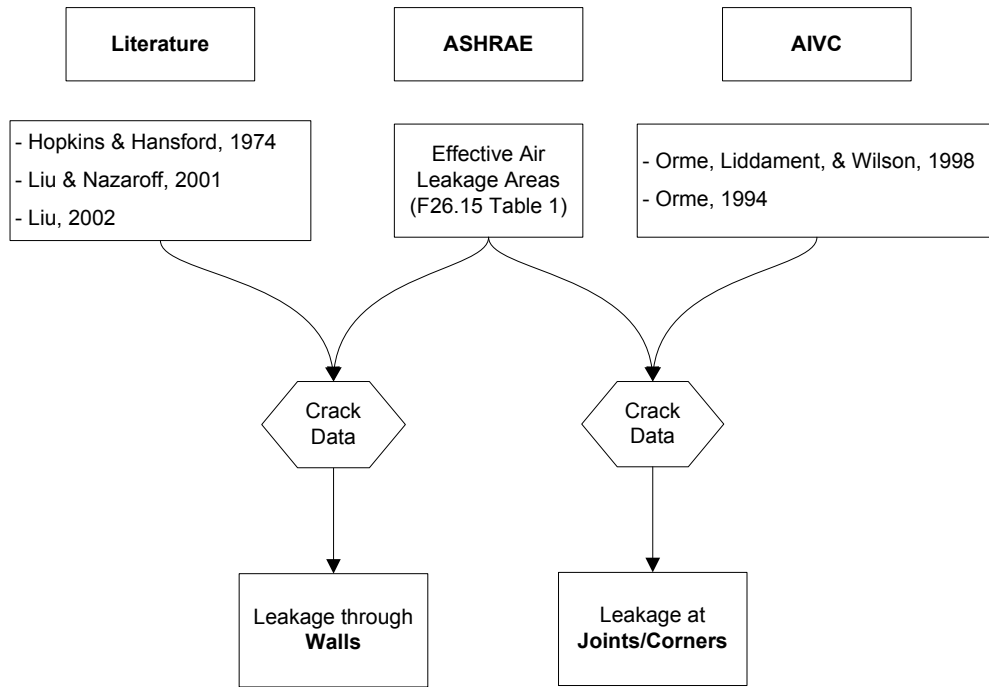
Emulating building cracks and air leakage paths entails 3 main stages:

1. Quantification of the amount of cracks existing in building envelopes within a representative area or span
2. Identification of possible shapes of cracks/flow paths
3. Identification of the dimensions/dimensional ratios of these flow paths in both:
  - a. Plain of a wall (Face)
  - b. At envelope joints, interfaces, and corners



It is import to note that the data determined should be a realistic representation and applicable to the construction methods and materials being used whether brick, concrete, wood or other.

For each type of crack, the data adopted was obtained through a cross matching of at least 2 different sources. Flowchart 3-5 provides a representation of this process.



**Flowchart 3-5: Crack Properties Determination Process**

**Equations Utilized**

In some situations crack dimensional properties are not readily presented but rather back calculated from airflow rates and noted flow coefficient values. The situation is as such in the available AIVC databases. Consequently, Equations 3–68 through 3-71 shown below are utilized for calculating equivalent leakage areas (ELA) from the data provided.

$$Q = C (\Delta P)^n \tag{3 – 68}$$

$$ELA_4 = C 4^{n-0.5} \sqrt{\frac{\rho_{air}}{2}} \quad (3 - 69)$$

$$ELA_4 = Q_4 \sqrt{\frac{\rho_{air}}{8}} \quad (3 - 70)$$

$$d_{crack} = \sqrt{\frac{4 ELA}{\pi}} \quad (3 - 70)$$

Where :  $Q = \text{Air Flow rate (m}^3/\text{Sec)}$

$C = \text{Flow Coefficient (m}^3/\text{Sec.Pa}^n)$

$ELA_4 = \text{Equivalent Leakage Area at 4 Pa (0.016 in water)}$

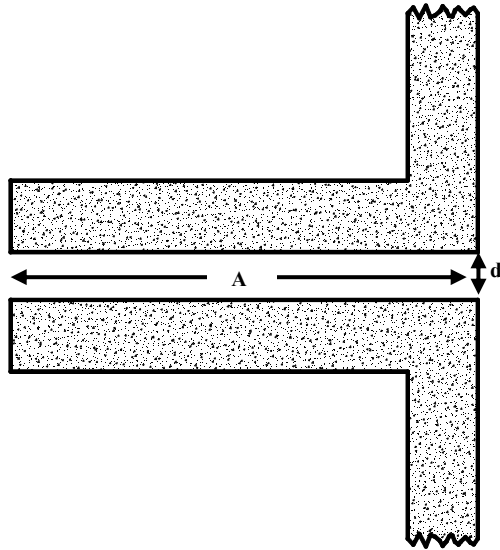
$n = \text{Flow Coefficient}$

$\rho = \text{Air Density (Kg/m}^3)$

## Cracking in Walls

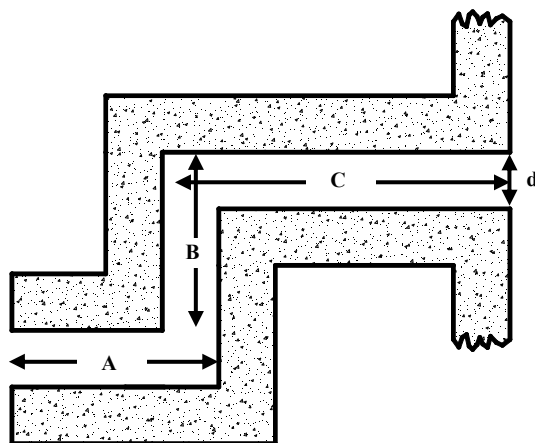
### Existing Literature

A through literature review performed in search for air leakage cracks dimensional characteristics. In most literature, air leakage is presented using an overall estimated leakage area for the building envelope rather than crack specific dimensions. Few sources provided dimensional characteristics for cracks in the plain of a wall; primarily Hopkins & Hansford (1974), Liu & Nazaroff (2001), and Liu (2002). The results shown in Figures 3-17 and 3-18 below are obtained from Hopkins & Hansford and have been cross matched and verified versus crack properties indicated in other literature as shown in flowchart 3-5. Two predominant crack shapes are observed to be reported in literature, straight cracks (Figure 3 – 17) and Angled Cracks (Figure 3-18). Therefore, these two shapes of cracks will be adopted in the following simulations.



	A (mm)	d (mm)
1	25	1, 3, <u>5</u> , 8 mm
2	19	
3	50	
4	6	

Figure 3-15: Crack Shape and Dimensions



mm	A	B	C	d
1	20	29	24	3.5
2	25	29	32	<u>5</u>

Figure 3-16: Crack Shape and Dimensions

## ASHRAE

In ASHRAE Fundamentals (2001) Chapter 26 Table 1 “Effective Air Leakage Area (Low Rise Applications only) “provides leakage areas for common construction material and building components. The data is provided as per a unit length or a unit area of the corresponding material/component. Backward calculations using equation 3-71 allow obtaining a crack dimension. An example of the data provided in ASHRAE is

shown in Table 3-6 below. A representative crack dimension/ft<sup>2</sup> of a sample material can be calculated using the data provided in ASHRAE.

	Unit	Best Estimate	Minimum Estimate	Maximum Estimate
<b>Cast-in-Place Concrete</b>	in <sup>2</sup> /ft <sup>2</sup>	0.007	0.007	0.026
<b>Precast Concrete</b>	in <sup>2</sup> /ft <sup>2</sup>	0.017	0.004	0.024

**Table 3-6: Sample ASHRAE Material leakage Data**

### **In-Wall Leakage Path Crack Dimensions**

The simulated test case will utilize brick cavity walls. The choice of this type of construction is dependent on the chosen geographical location of the building envelope to be simulated. The choice of location and building material will be discussed in following section in this Chapter. Using data discussed in the 2 previous sections calculations for crack diameter characteristics are performed and summarized in Table 3-7 below. By matching the results obtained from literature sources versus ASHRAE data the representative crack diameter for in-plain brick cavity wall is taken as 5 mm for every ft<sup>2</sup> of the wall surface. The length of the crack, both for straight and angled cracks, depends on the thickness of the wall. Proportions for crack span lengths presented in literature for angled cracks will be observed in dimensioning crack span length in the CFD test case.

ASHRAE (in <sup>2</sup> /ft <sup>2</sup> )			Literature	
Best Estimate	Max Estimate	Use	Straight Crack	d = 5 mm
0.0098	0.033	0.033	Angled Crack	d = 5 mm
⇒				
				d = 5.12 mm (0.205 in <sup>2</sup> )

Comparing Results from Both Sources ⇒ use crack diameter **d = 5 mm**

**Table 3-7: In-Plain Crack Diameter for Brick Cavity Wall**

## Leakage Path Dimensions at Joints and Interfaces

As previously discussed, tabulated data from ASHRAE data and AIVC databases are used to determine the dimensions of leakage paths at corners and Interfaces (i.e. wall-ceiling). A summary of the calculations and cross verification between the 2 sources is shown in Table 3-8 below.

	AIVC			ASHRAE (in <sup>2</sup> /ft <sup>2</sup> )
	C	m <sup>3</sup> /Sec.Pa <sup>n</sup>	n	Soleplate, Floor/wall, uncaulked
	0.53		0.6	
ELA	0.22 in <sup>2</sup> /ft <sup>2</sup>			0.26 in <sup>2</sup> /lfc <sup>1*</sup>
Gap (mm)	0.5 mm (0.019 in)			0.25 mm (0.01 in) <sup>2*</sup>

Comparing Results from Both Sources ⇒ use Gap at corner/interface = **0.5 mm**

1\*: lfc = Linear Foot of Crack

2\*: Gap = 0.25 mm per single crack however multiple cracks can exist on a corner/interface.

The ASHRAE result is per linear foot of crack (lfc). However, in a building multiple cracks exist usually at an interface. Assuming 2 cracks exist per corner/interface, the result from ASHRAE will match that of AIVC. Consequently the crack opening dimension (gap) at corners and interfaces is taken to be:

Wall-Wall / Wall – Ceiling: Gap = 0.5 mm

Notes:

1. At floor – wall interface the leakage gap opening is considered to be negligible. The bearing weight of the wall helps keep crack opening at the floor – wall interface negligible.

2. The floor and ceiling are considered (in the current simulations) to be of material with minimal leakage properties. Emphasis is given to the leakage through cracks within the wall plain and at interfaces.
3. One (1) crack per wall is provided to account for leakage area resulting from an electrical outlet. According to the adopted building code at the chosen location of the test case geometry the electrical outlet should be no less than 12 inches from the top/bottom of the wall. According to ASHRAE, the estimated equivalent leakage area for an electrical outlet is  $0.3 \text{ in}^2$  each. Consequently, the diameter of the cracks representing leakage through electrical outlets is 15.5 mm (0.61 inches) each.

	<b>Crack Diameter / Gap Opening (mm)</b>
<b>In-wall</b>	d = 5.12 mm
<b>Wall – Wall (Corner)</b>	Gap = 0.5 mm
<b>Wall – Ceiling</b>	Gap = 0.5 mm
<b>Wall - Floor</b>	Gap = 0 mm
<b>Electrical Outlet</b>	d = 15.5 mm

**Table 3-8: Summary of Adopted Crack and Gap Dimensions**

### **Simulated Test Case: Location, Properties & Others**

A sample location and construction method/material are selected for the building envelope to be simulated. The construction material, location and other properties of the building envelope should be emulated in both eQUEST and the ANSYS CFD simulation.

The selection of the building envelope geographic location and construction characteristics is done with consideration to the following:

**1. Highlight Infiltration**

The selected building location should be as to provide ambient conditions that highlight infiltration. This is specifically in terms of weather and temperature conditions at the selected location. For example, selecting a location in a cold weather region provides conditions that promote infiltration as discussed in previous sections.

**2. Highlight Heat Recovery**

In addition to selecting a location with convenient weather conditions that highlight infiltration, the selected location should be characterized by building construction methods and materials that promote heat recovery

**3. Hourly Data Availability**

Essential to both the ANSYS and eQUEST simulations is the availability of hourly weather data. Therefore, the chosen location should have an hourly weather file available containing all necessary hourly data.

**4. Agreement with Published Statistical Data**

Statistical averaged infiltration rate maps are available for the United States. The maps depict the variation in the severity of air infiltration across building envelopes by county. The choice of a sample location for simulation should agree with published maps in terms of statistically recorded infiltration levels. The chosen location should be in a county with typically high recorded infiltration rates.

## Model Location

The selected test case location is the City of Fargo, North Dakota. The location agrees with the up stated location guidelines. Provided below are detailed information of the location of choice.

- **Location:** Hector International Airport area, Fargo, North Dakota (Figure 3 –19).  
Weather Station is located on site.
- Location matches published statistical infiltration data as shown in Figure 3 – 20 below (Sherman and McWilliams, 2007).
- **Latitude :** 46°, 52', 38" ; **Longitude:** 96°, 47', 22"
- **Weather:** Long, cold, windy & snowy winters
- **Season Chosen :** Heating season
- **Simulation Duration:** 1 month, January. General weather conditions for January are shown in Table 3 – 9.

Month	Jan	Feb
Record high °F (°C)	54 (12.2)	66 (18.9)
Average high °F (°C)	15.9 (-18.9)	22.8 (-5.1)
Average low °F (°C)	-2.3 (-19.1)	5.4 (-14.8)
Record low °F (°C)	-48 (-44)	-47 (-44)
Sunshine hours	140	155

Table 3-9: Averaged Weather Conditions for Fargo Over the Simulation Span Time Period





Figure 3-17: Chosen Location of Building Envelope, Vicinity of Fargo Intl, Fargo, North Dakota

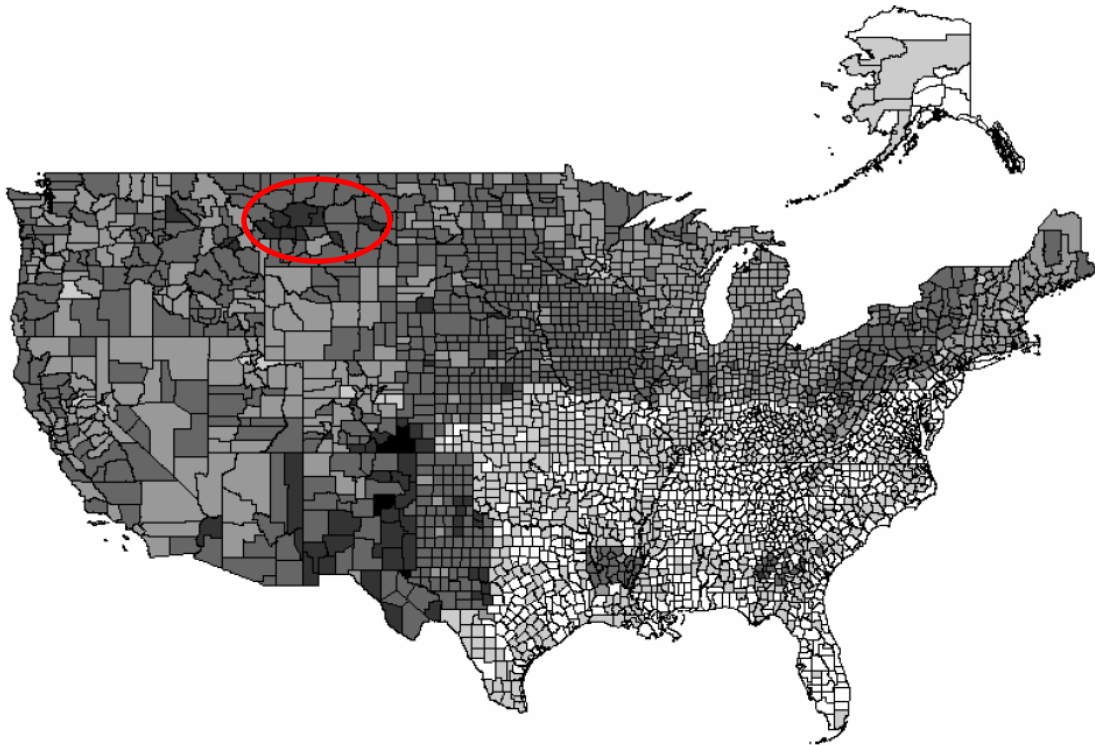


Figure 3-18: Air Leakage By County (Sherman and McWilliams, 2007)

## **Model Material and Construction Method**

The material and construction selected for the simulated test case resemble the construction methods and materials observed in the selected location. Following are the construction details of the model:

- **Material:** Brick and Concrete
- **Walls :** Running Board, Brick Cavity Walls
- **Wall Dimensions:** 6ft x 6 ft each
- **Crack Shapes:**
  - Wall Plain : Straight cracks & Angled Cracks
  - Joints/Interfaces : Open Gap (All-through Crack)
- **Metal Ties :** No Metal Ties

Following adopted construction codes the total number of required metal ties for a 6ftx6ft wall are 2 ties per wall. Therefore it is elected to ignore the metal ties in the construction of the envelope walls. Calculation Details are shown below:

### Horizontal Ties:

Building Code: Ties placed horizontally at 3 ft intervals → 1 Line of Ties / 6 ft wide wall.

### Vertical Ties:

Building Code: Ties placed horizontally at 2 ft intervals → 2 Line of Ties / 6 ft Tall wall.

Therefore: Total = 2 Ties/ Whole 6ft x 6ft wall → Ignore

## CFD Model

### Model Construction

The 3D Building Envelope was built following the guidelines of the calculated crack diameter. That is in terms of diameter of cracking per foot squared. Therefore, individual 1 ft x 1 ft x 10 in basic building blocks were modeled each with built-in crack with a diameter corresponding to one of the calculated cracking diameters. This resulted in 4 types of 1 ft x 1 ft x 10 in Basic Building Blocks:

- Block with a straight through crack
- Block with an angled crack
- Block with a straight through crack + Electrical outlet/inlet crack
- Block with an angled crack + Electrical outlet/ inlet crack

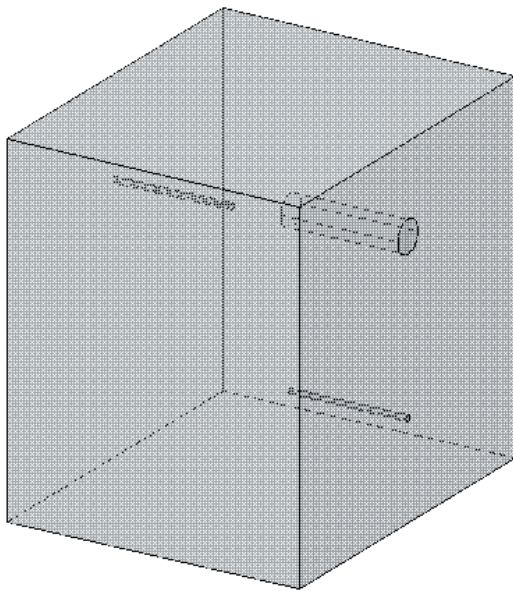


**Figure 3-19: Basic Block with Angled Crack and Electrical Inlet Crack**

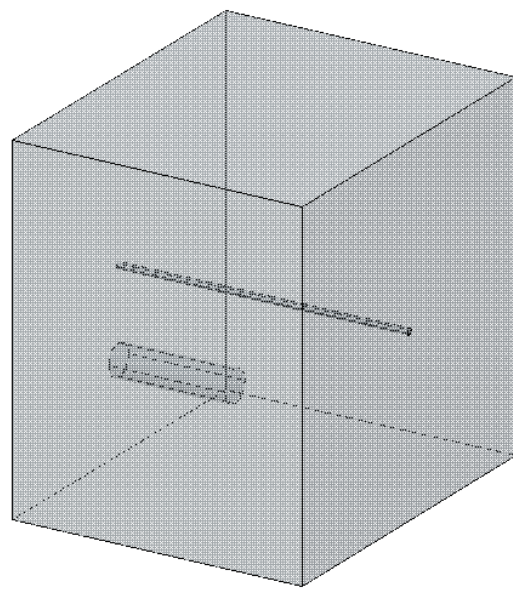


**Figure 3-20: Basic Block with Angled Crack and Electrical Outlet Crack**

The individual basic building blocks were used to assemble the 3 required wall types to be simulated:

- Wall with Straight Cracks
- Walls with Angled Cracks
- Wall with mixed alternating straight Cracks and angled Cracks.

An example assembled wall consisting of mixed cracks (angled cracks + straight cracks) is shown in Figure 3-23. Individual blocks are then merged to create a uniform wall and then a cavity is introduced inside the wall to create the desired representative brick cavity wall. An example is shown in Figure 3 – 24. The resulting individual walls can then be used to assemble the 3 required CAD geometries for the CFD simulation:

- 3D Envelope with Straight Cracks
- 3D Envelope with Angled Cracks
- 3D Envelope with mixed alternating straight Cracks and angled Cracks.

The combined effects of conduction, solar radiation and infiltration significantly impact the energy load due to infiltration. Once this interaction the actual energy load due to infiltration deviates from that determined using the classical method of calculating infiltration energy load as merely a product of the inside/outside enthalpy difference by the specific heat of the infiltrating air. In this methodology an existing model that considers this interaction is built upon and further developed to calculate the energy load due to infiltration. The obtained model is then applied onto eQUEST/DOE-2 building energy simulation software. Though the developed model would be easily applicable to any other hourly building energy simulation software, these software packages were chosen due to their widespread use and their status as an industry standard.

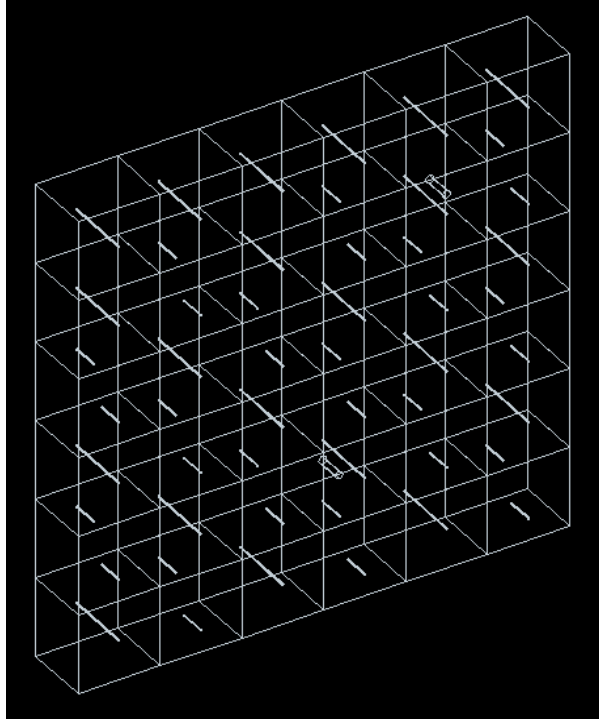


**Figure 3-21: A Mixed Crack Wall Created by Assembling 36 of the Basic Building Blocks**

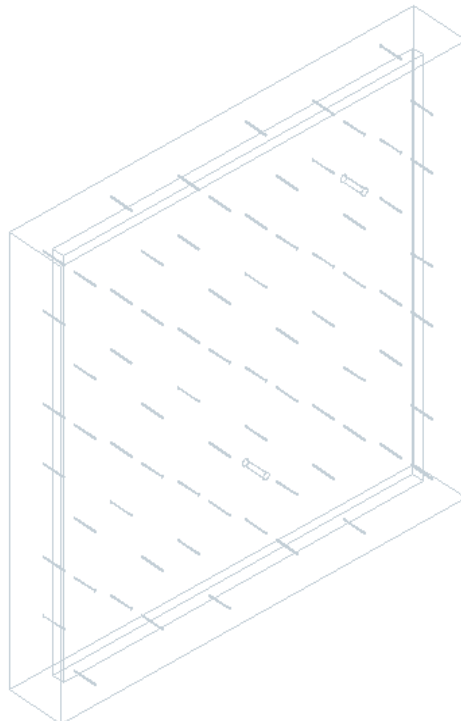


**Figure 3-22: A Resulting Representative Concrete Cavity Wall**



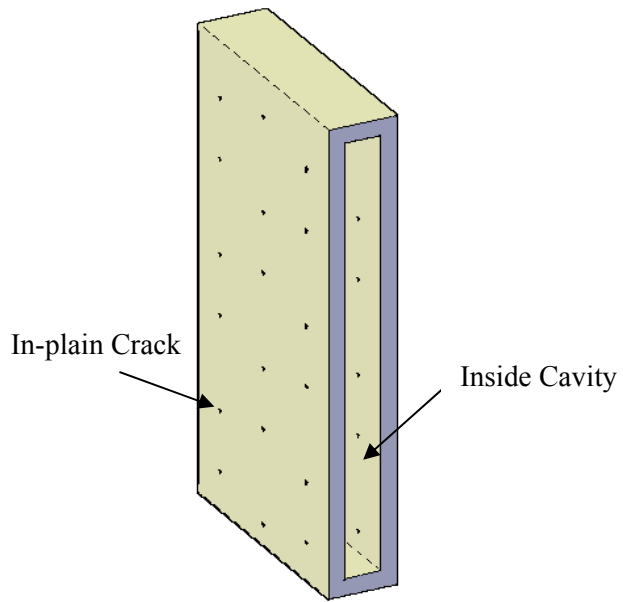


**Figure 3-23: Wall Section Showing Internal Cavity and In-plane Cracks**

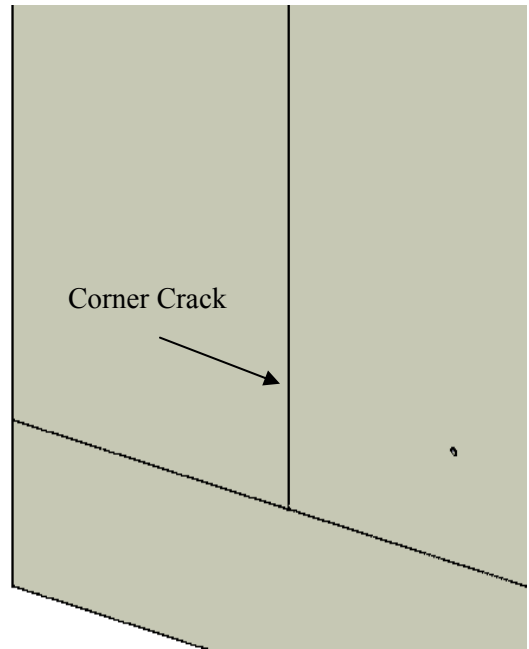


**Figure 3-24: Close-up Showing Corner/Joint Cracks**

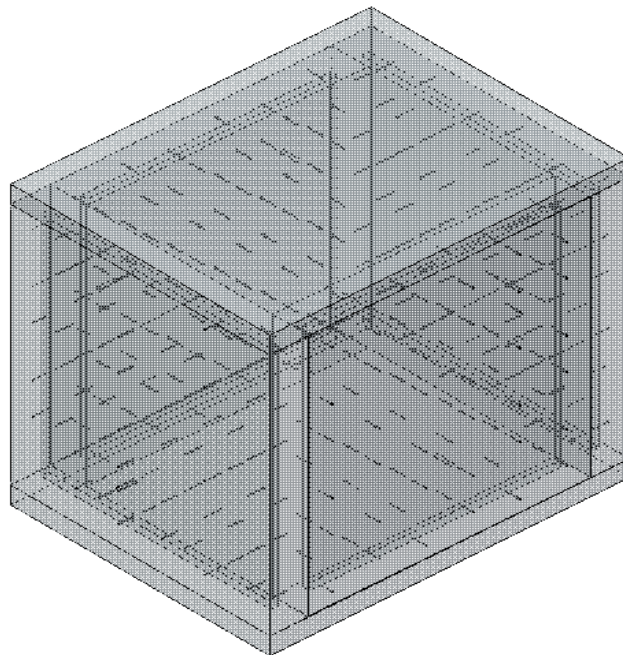


**Figure 3-25: An X-ray of A Resulting 3D Model Geometry Showing All In-plane and Joint Cracks**

The majority of building energy simulation software utilize a form of the classical method or some other crude method for calculating the energy loads due to infiltration; despite acknowledging its considerable effect on building energy demand. With the wide spread use of building energy simulation software and the major impact that infiltration can have on the energy loads in a building; it is essential to develop such a model that represents the true physics of the problem and more accurately represents the energy loads on a building due to infiltration. Once the Infiltration energy load is calculated for a demonstrative structure using eQUEST/DOE-2 “+” the model developed applied upon, the simulation results will be compared to those obtained using a finite element CFD analysis of the same structure. Based on the comparison results with the finite element analysis, the developed model’s accuracy will be established and consequently any necessary modifications to improve its accuracy will be determined.

## **Chapter 4**

### **Modeling and Simulation**

The methodology and modeling methods discussed in Chapter 3 were utilized and followed in the building and simulation of all models. This includes the DOE-2/eQUEST analyses, CFD hygrothermal simulations, and the developed Enhanced Model. In this Chapter we present an overview of the modeling and simulation process of each of the aforementioned model types.

#### **Hygrothermal Multiphysics CFD Analysis**

##### **Model Meshing**

A good quality mesh is essential for obtaining a good solution and avoiding simulation errors. A mesh with poor element quality, high levels of element skewness, low orthogonality, and other issues adversely affects the accuracy and stability of the numerical solution.

In meshing the CFD infiltration models it is essential to pay close attention to additional critical factors beside the regular general mesh quality considerations. Particularly important are the following:

- Element size: particularly within in-wall cracks and joint cracks in order to insure the meshing of all airflow paths.
- Proper contact between fluid in cracks and inner domain fluid
- Contact between fluid in corner joints and inner domain fluid
- Contact between fluid in ceiling joint cracks and inner domain fluid



- Proper mesh attachment between the mesh of fluid in cracks and the mesh of fluid in joint/corner cracks where applicable (the first 1 foot on each side of the two 7'-8" walls).
- Proper tessellation of the mesh to avoid having a missing mesh or mesh gaps in thin sections. This is most critical in corner and ceiling joints.

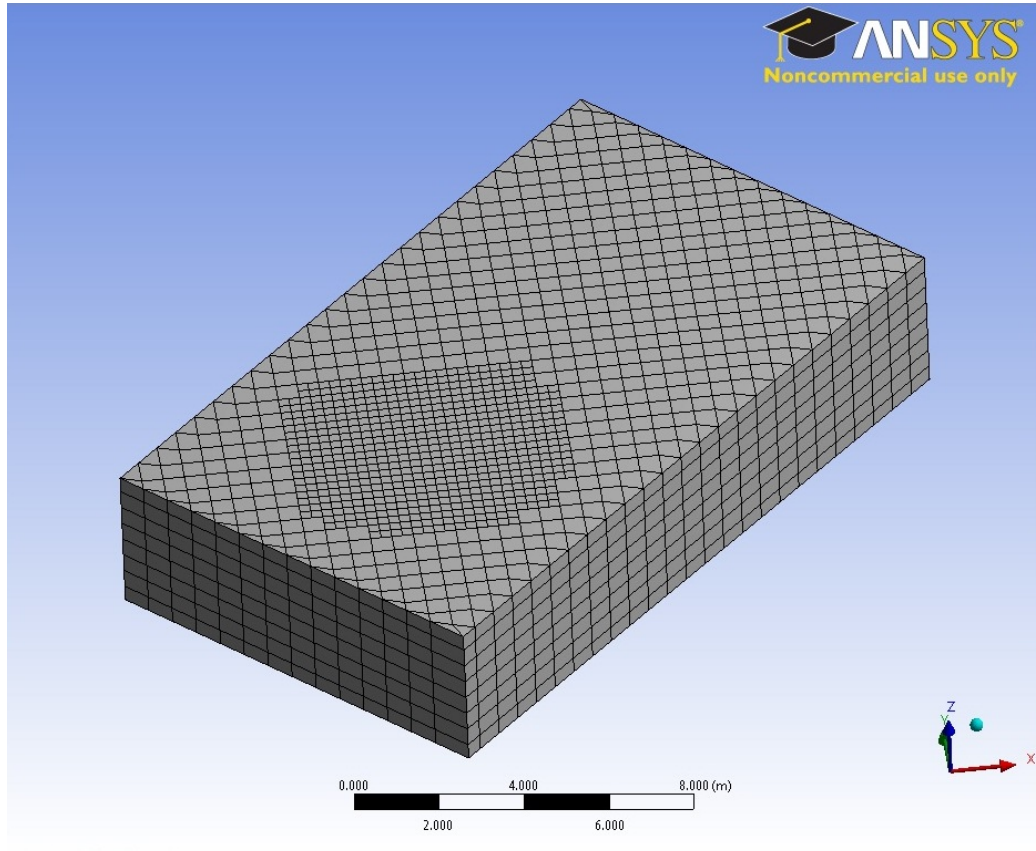


**Figure 4-1: Sample Full Model and Domain Mesh**

Assembly meshing is utilized in meshing the CFD models. Assembly meshing allows considering the meshing of the entire model as a single process rather than meshing each model by parts. This is particularly important due to the complex crack shapes and overlapping face geometries that exist in the infiltration models. Assembly meshing thus allows creating a good quality conformal mesh in this situation. The assembly meshing method utilized is CutCell meshing available in Ansys Fluent.

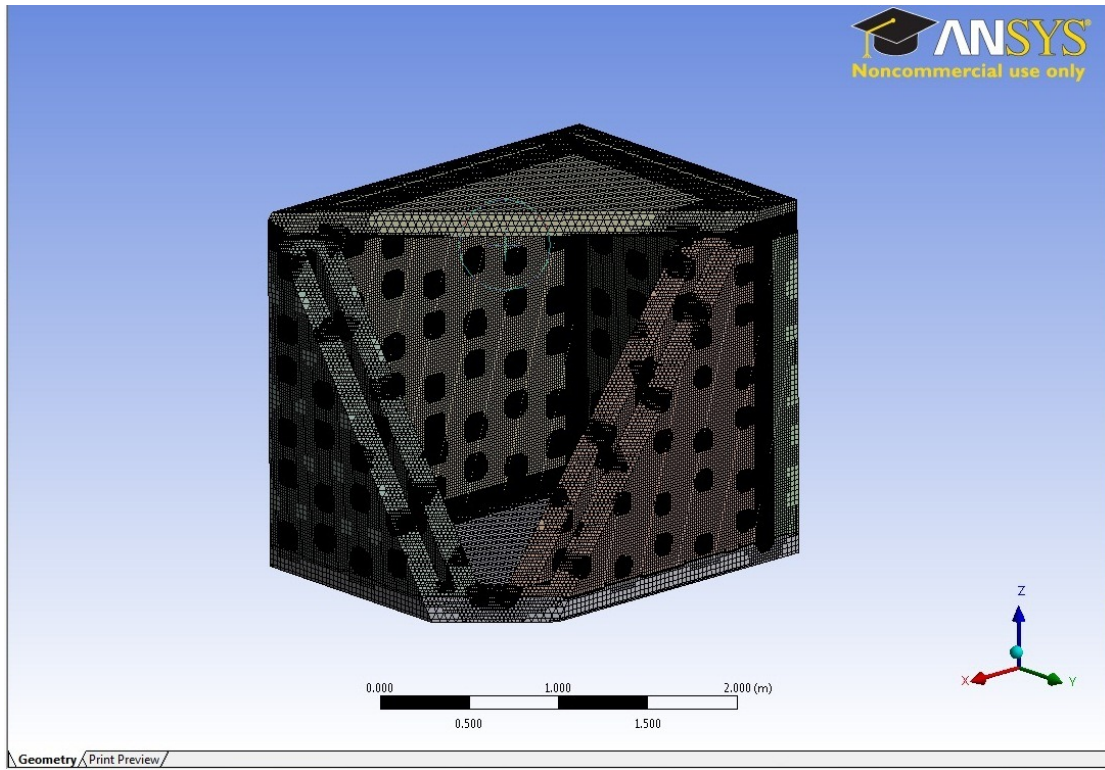


Figure 4-2: Sample Full Model Mesh

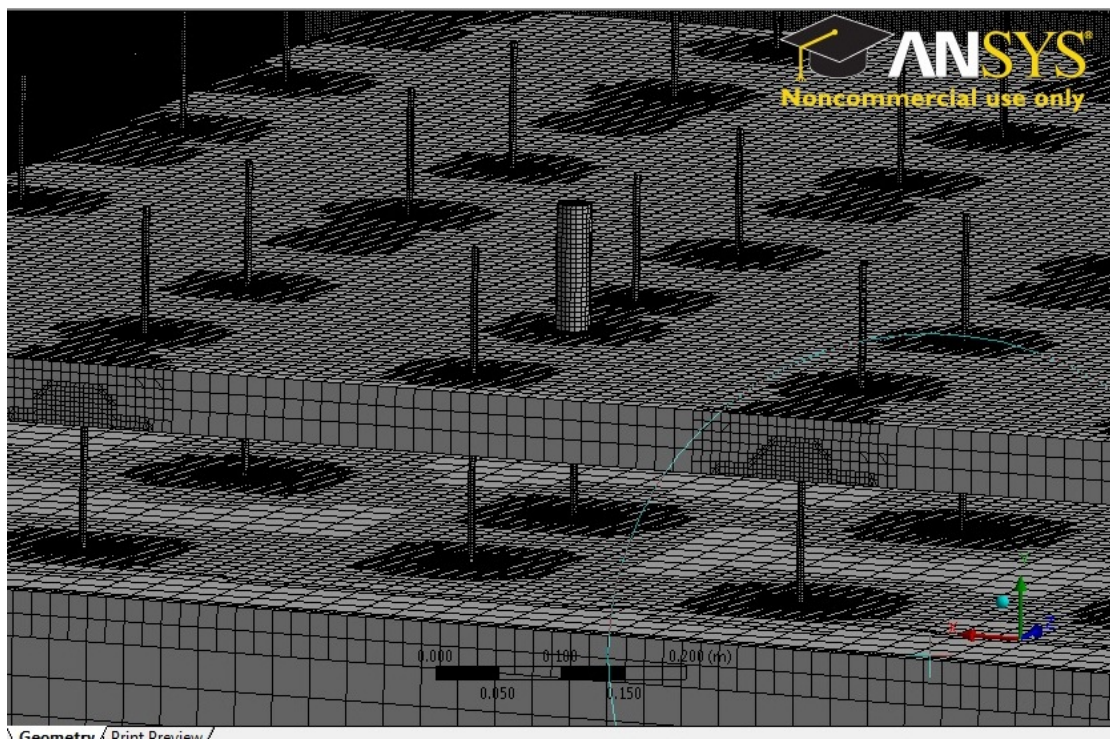
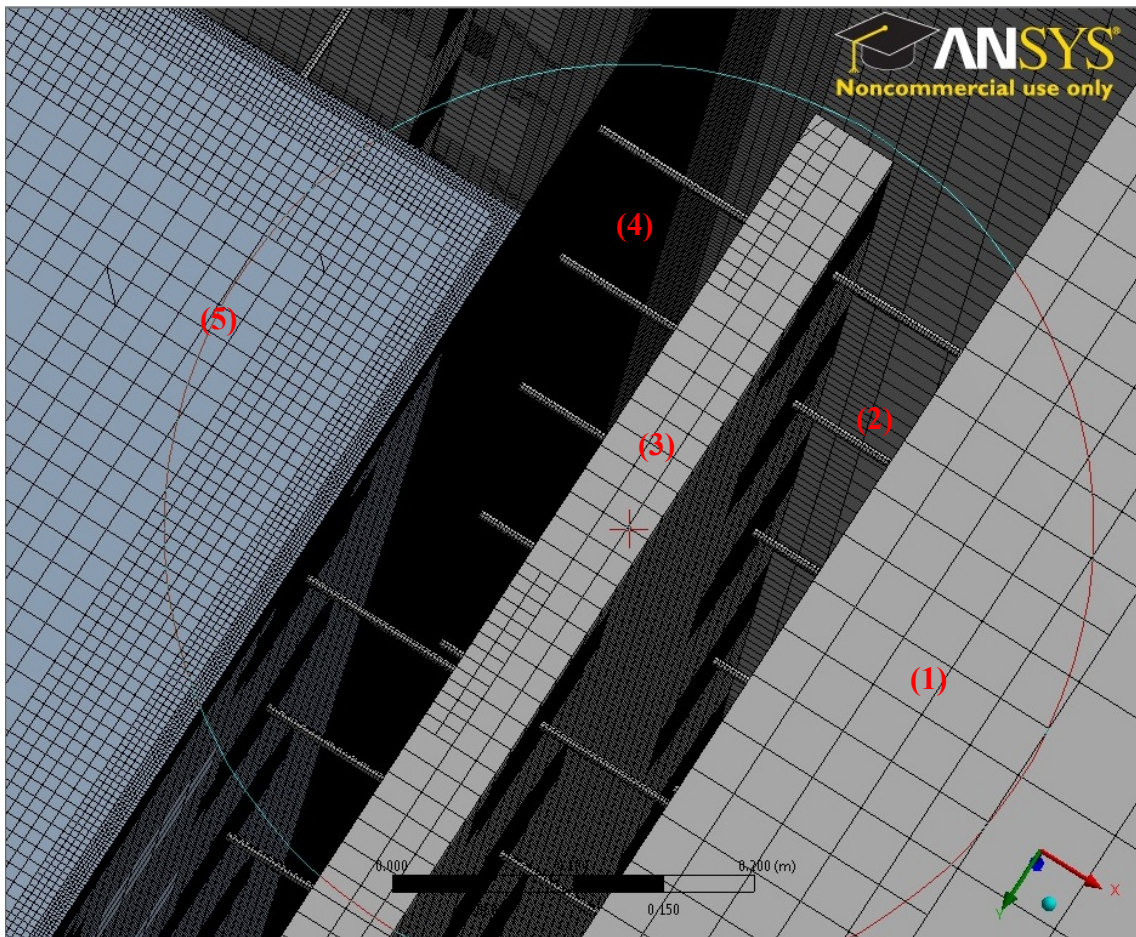


Figure 4-3: Meshing of Minute Airflow Cracks



CutCell meshing is a Cartesian meshing method that performs patch independent volume meshing and utilizes advanced size functions (Ansys 14.0 Help, 2011). Furthermore, the advanced features included along with the CutCell meshing method allow addressing the major meshing concerns stated earlier. In particular, through applying advanced sizing functions on both edges and at proximity & curvature. Thin sections and contacts were also defined and tessellation was utilized to insure mesh continuity in thin sections. Figures 4-1 thru Figure 4-5 highlight the mesh quality and the achieved connections and tessellations at points of interest common throughout each of the CFD models.



**Figure 4-4: Tessellation of Thin Sections and Proper Mesh Attachment (contact) Between Fluid Outside the Envelope (1), Infiltrating Through Cracks (2), Inside Wall Cavity (3), In Corner Joints (4), and In Inner Domain(5)**

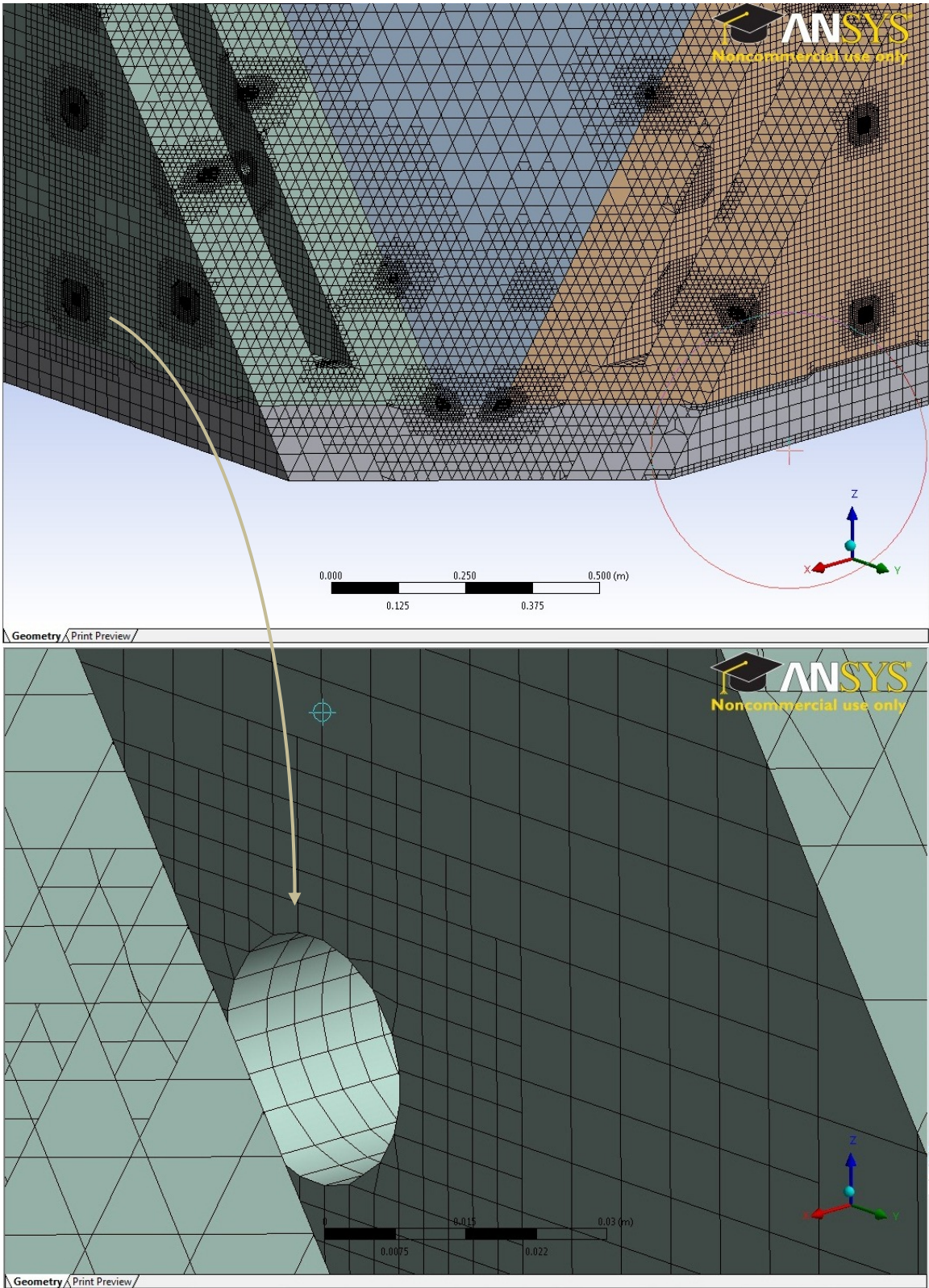


**Figure 4-5: Meshing of Cavity Brick Walls, Proper Contact Between Solid & Fluid Meshes, and Close Up on a Sample Leakage Crack Mesh**

## CFD Analysis Fundamentals

The computational fluid dynamics multiphysics hygrothermal simulation of building air infiltration incorporates wind flow (and pressure), heat transfer, solar tracking (and irradiation), and site-dependent variable weather conditions and factors. The following sections discuss the main factors above as reflected and applied in each of the CFD simulations.

The transient simulation is of time steps of 1 hour (3600 seconds) and spans to 744 time steps. This is equivalent to 1 month of real time. The time step span and simulation duration are taken as such to be consistent with the DOE-2/eQUEST and the Enhanced Model simulations. Similarly are the location, weather properties, and other factors.

### Energy

The underlying equation of the multiphysics CFD simulation is the energy equation shown in equation 4-1. The energy equation allows considering the effect all of the following heat phenomena:

- Convection in fluid
- Conduction in solids
- Thermal radiation
- External heat gains

$$\underbrace{\frac{\delta(\rho E)}{\delta t}}_{\text{Unsteady State}} + \underbrace{\nabla \cdot [\vec{v}(\rho E + P)]}_{\text{Convection}} = \underbrace{\nabla \cdot [k_{eff} \Delta T]}_{\text{Conduction}} - \underbrace{\sum h_i \vec{J}_i}_{\text{Species diffusion}} + \underbrace{\bar{\bar{\tau}}_{eff} \cdot \vec{v}}_{\text{Viscous dissipation}} + \underbrace{S_h}_{\text{Solar Radiation (Volumetric source)}} \quad (4-1)$$



Where:

- $k_{\text{eff}}$  = effective conductivity
- $\vec{J}_i$  = diffusion flux of species
- Viscous dissipation: represents viscous heating, mostly seen in lubricants and other high viscosity fluids. This term is not activated in our simulations.
- $E = h - \frac{p}{\rho} + \frac{v^2}{2}$
- $h$  = Sensible enthalpy for ideal gas

A coupled momentum and pressure solver scheme is utilized. In addition, second order discretization is applied for momentum, energy, viscous dissipation rate, and turbulent kinetic energy. Pressure is treated by the Presto scheme available in Ansys Fluent. This scheme is usually utilized for swirling flows. Therefore, it is deemed suitable in particular due to the large existing number of minute cracks with variable shapes and flow paths.

### **Solar Radiation**

Accounting for solar radiation is essential for a multiphysics hygrothermal model. Solar radiation is also incorporated into the underlying energy equation as seen previously in equation 4-1. Solar loading is applied onto the CFD models through the solar ray tracing algorithm available in Fluent. The solar ray tracing functionality (Figure 4-6) allows at each time step of the simulation (1 hour) the computation of incident solar radiation on the various surfaces of the building envelope. The resulting heat flux is consequently coupled into the simulation using the volumetric energy source ( $S_h$ ) in the energy equation.

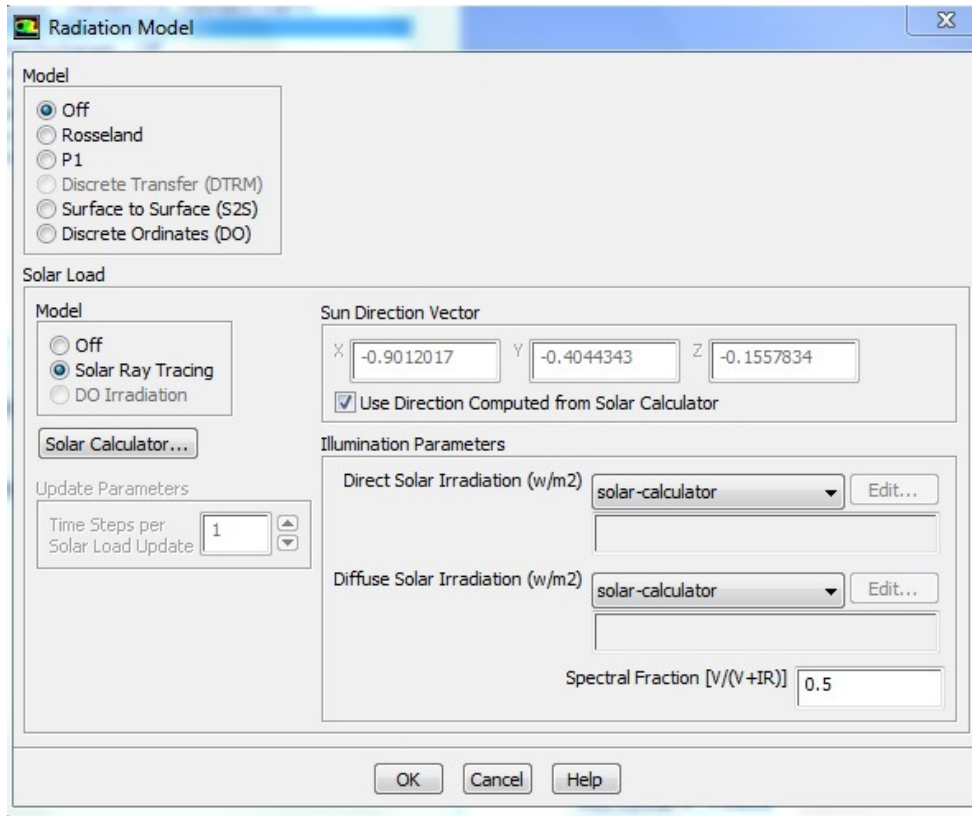


**Figure 4-6: Defining the Radiation Model**

The solar calculator is used in conjunction with the solar ray tracing model to provide the hourly input necessary for the model. The global position (latitude, longitude, and time zone), desired start time and date, mesh orientation, solar irradiation method, and sunshine factor are all defined (Figure 4-7). The algorithm then calculates the sun direction vectors, sunshine fraction, and direct and diffuse solar irradiation necessary for the solar ray tracing algorithm computations. The choice of sunshine fraction was set to theoretical maximum due to the geographical location being considered and the increased ground reflectivity associated with the surrounding snow cover. Since January is the sampled month for these simulations, a snow cover is expected to be present in Fargo, North Dakota. This is confirmed by looking on recorded weather data.

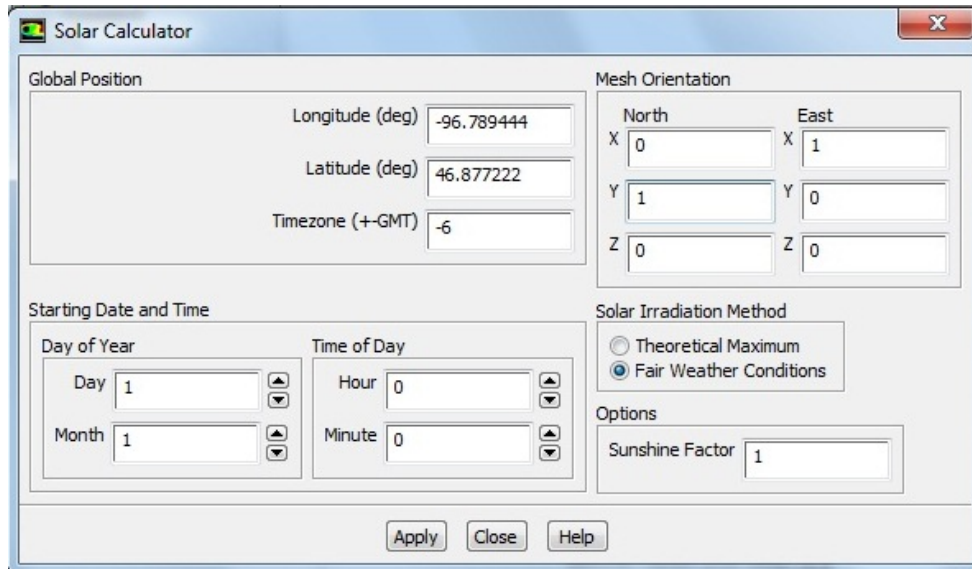


Figure 4-7: Setting the Solar Ray Tracing Model

## Weather and ground Conditions

Weather variables considerably influence the hygrothermal performance of a building envelope. Air temperature, air density, and wind velocity are the major influencing factors. These variables affect both the stack and wind pressures which constitute the driving force of air infiltration. To insure consistency in the CFD models in comparison with the other models in this research the wind velocity is taken as the fixed averaged wind velocity for the time span of the transient simulation. The averaged wind velocity is therefore taken as 6.3 m/s based on the recorded weather file for Fargo, North Dakota.

Variable hourly air temperatures from the Fargo weather file are applied to the CFD models as for DOE-2/eQUEST and the Enhanced Model. This is done in Fluent through custom defined temperature profiles. An example is shown in Figure 4-8. The air temperature associated with each corresponding hour of simulation time is applied at the fluid velocity inlet boundary of the CFD models.



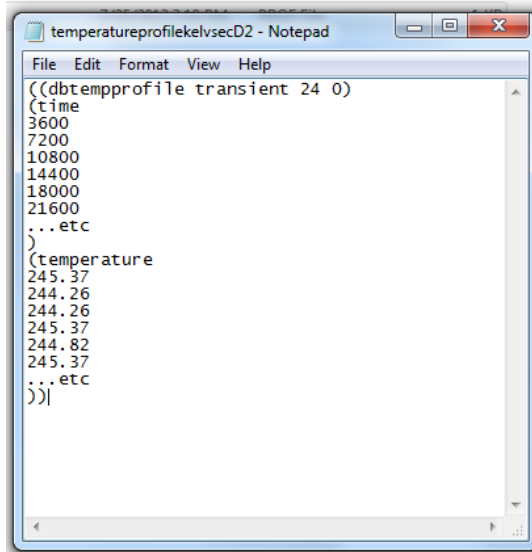


**Figure 4-8: Sample Hourly Temperature Profile**

Ground temperature is also considered due to its effect on the heat balance in a building envelope and on near-ground air layers' temperature. The ground temperature is applied at the boundary constituting the bottom of the building envelope's floor slab and on the ground surrounding the model (Figure 4-9).

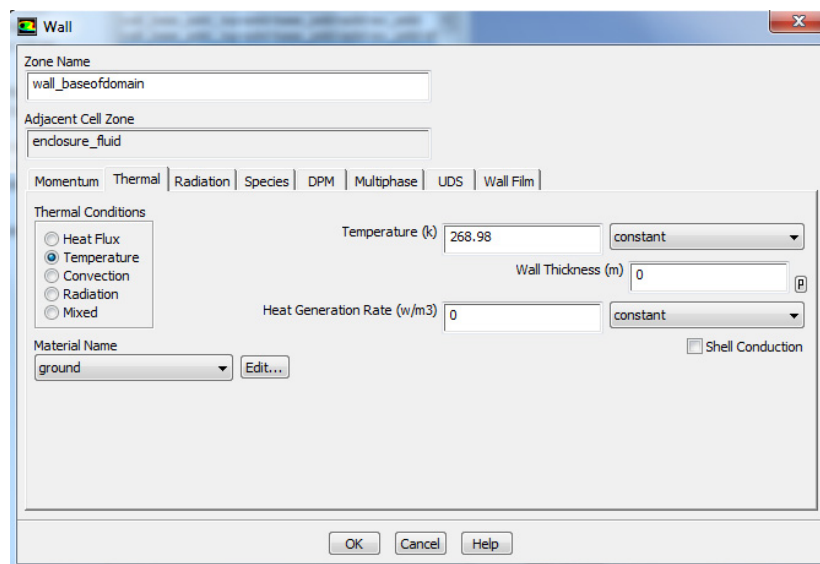


**Figure 4-9: Applying Ground Temperature on the Defined Ground Boundary with Ground (Soil) Material Properties**

## **eQUEST – DOE-2 Hourly Analysis**

### **Model Properties**

In order to isolate the effect of infiltration, the eQUEST model must be built to match the CFD finite elements models in all aspects and properties. These include:

- Indoor air temperature
- Wall properties and construction
- Material properties
- Building envelope orientation
- Solar conditions and illumination/irradiation
- Ground temperature and weather conditions: wind velocity, ambient temperature, wind angle...etc.
- Building occupancy patterns
- Infiltration multipliers
- Heat source with no mechanical ventilation (no forced airflow)

The following sections briefly discuss the properties implemented in the BDL definition of the building envelope in eQUEST. These measures are to insure consistency in simulation properties between the CFD and eQUEST models, and to isolate the effect of air infiltration in each.

### **Indoor Temperature**

The design indoor temperature settings are set to maintain a 72°F (295.37 °K) indoor temperature at all times (Figure 4-10). This is in accordance with the “Fixed Value” of indoor fluid temperature of 295.37°K specified in the Fluent CFD analyses.

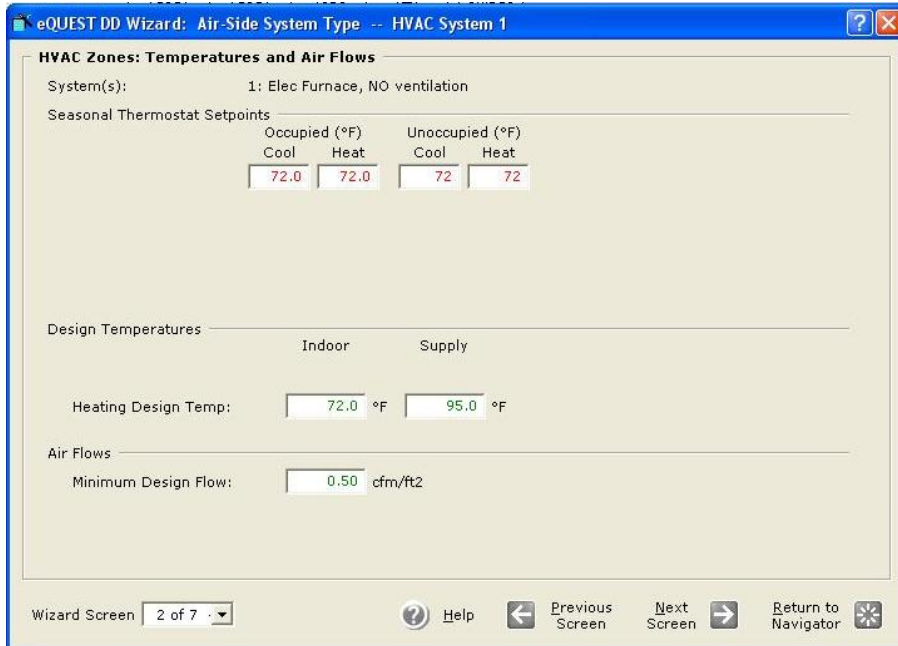


Figure 4-10: Thermostat Settings in eQUEST to Match 72F in CFD Analysis

## Walls and Construction

Identical to the wall construction used in CFD analysis, brick walls are defined in eQUEST. The walls are of the same dimensions, thickness, and layers (Figure 4-11). The material properties of each of the layers are also held the same.

	Material Name	Thickness (ft)	Conductivity (Btu/h-ft-°F)	Density (lb/ft3)	Spec. Heat (Btu/lb-°F)	R-Value (h-ft2-°F/Btu)
1	Com Brick 4in (BK01)	0.333	0.4167	120.00	0.200	n/a
2	Air Lay <3/4in Vert (AL11)	n/a	n/a	n/a	n/a	0.900
3	Com Brick 4in (BK01)	0.333	0.4167	120.00	0.200	n/a
4		n/a				
5		n/a				
6		n/a				
7		n/a				
8		n/a				
9		n/a				
10	n/a	n/a				

Figure 4-11: Defining Cavity Brick Wall in eQUEST

## Orientation

In the BDL description of the eQUEST models the building envelope is defined to be at an azimuth of 315° (- 45°) from the north as shown in Figure 4-12.

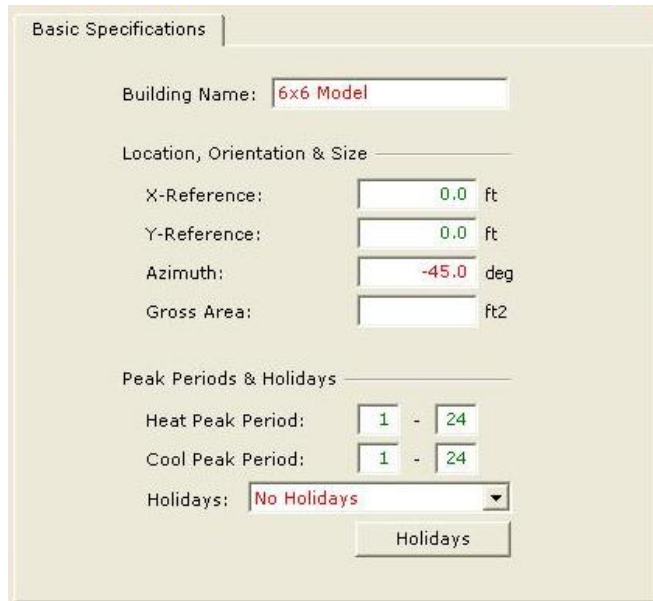


Figure 4-12: Defining Building Orientation in eQUEST to Match the CFD Analysis

### Weather conditions

Weather conditions applied to the eQUEST models are also identical through custom profiles in the CFD analyses. The same Fargo Intl. weather file that is utilized to define the wind flow velocity, hourly temperature profiles, and other variables in the CFD analysis is applied to the eQUEST simulations. This insures that the component factors of both the stack and wind pressures which drive air leakage in the building envelope are uniform across all simulations and models. Identical ground temperatures are also defined in eQUEST (Figure 4-13).

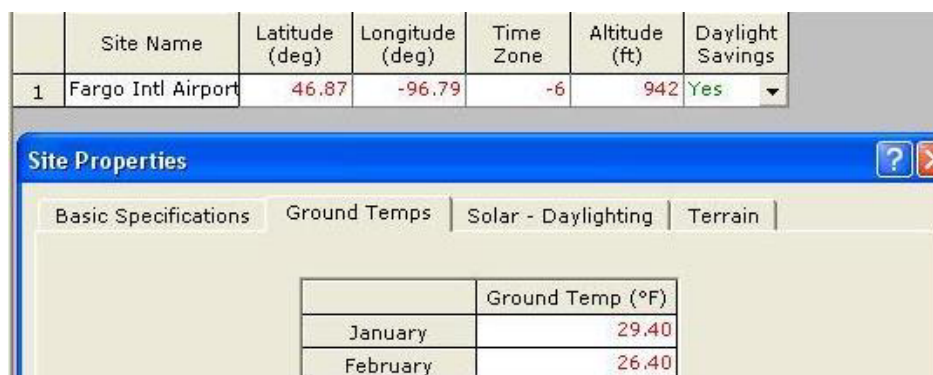


Figure 4-13: Defining Ground Temperature and Building Coordinates

## Building Occupancy

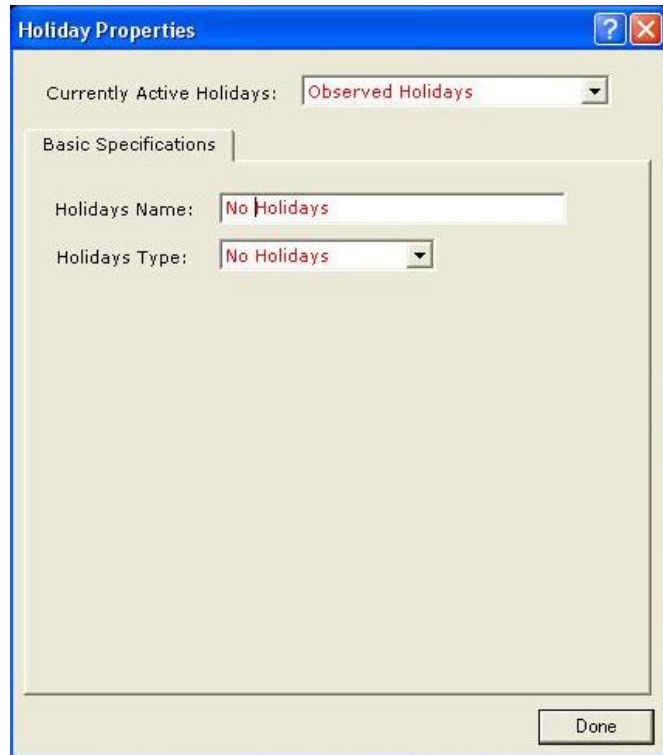
The DOE-2 engine allows considering the energy impact of building occupancy type, schedules, and number of occupants. However, in the CFD analysis air leakage is considered under ambient weather conditions and material leakage properties in the absence of any building occupancy effects. Consequently the same conditions are applied onto eQUEST as shown in Figure 4-14. For the same reasons no building closure or holidays are considered in eQUEST as shown in Figure 4-15.



The 'Building Operation Schedule' dialog box shows the following settings:

- Entire Year: 1/1-12/31
- Use: 24-Hour Operation, Typ (dropdown menu)
- Opens At: (empty)
- Closes At: (empty)
- Mon: Open 24 (dropdown menu)
- Tue: Open 24 (dropdown menu)
- Wed: Open 24 (dropdown menu)
- Thu: Open 24 (dropdown menu)
- Fri: Open 24 (dropdown menu)
- Sat: Open 24 (dropdown menu)
- Sun: Open 24 (dropdown menu)
- Hol: Open 24 (dropdown menu)

Figure 4-14: Building Operation set to 24 Hours Daily



The 'Holiday Properties' dialog box shows the following settings:

- Currently Active Holidays: Observed Holidays (dropdown menu)
- Basic Specifications tab selected
- Holidays Name: No Holidays (text field)
- Holidays Type: No Holidays (dropdown menu)
- Done button at the bottom right

Figure 4-15: No Holiday Defined, Continuous Building Operation

### **Simulation Time**

As in the multiphysics CFD analysis, the simulation span in eQUEST is taken to be one month. The simulation duration spans from January 1 to January 31 in hourly intervals (744 hours).

### **Multipliers and Reduction Factors**

eQUEST applies infiltration schedules by default. These schedules consist of reduction factors that are applied to hourly calculated sensible infiltration heat loads. The multipliers reduce the calculated loads by up to 50 % depending on the time of the day and weekly schedule. No reductions are applied to infiltration heat loads obtained from the CFD analyses. Therefore, the built-in eQUEST reduction multipliers are overridden and disabled.

### **HVAC System**

In order to maintain the indoor air temperature at 72°F it is essential to provide a form of heat input. In selecting the HVAC system it is important to define a system that will not create a forced airflow inside the building envelope, will not mechanically introduce outside air, and will not mechanically expel air from the inside of the building envelope. The heating system is therefore defined in accordance with these constraints. The defined system consists of electric baseboards with no ventilation (Figures 4-16 and 4-17). No mechanical fans or other forms of forced air inflow or outflow are designed into the systems.

**HVAC System Definition**

System Type Name: HVAC System 1

Cooling Source: No Cooling

Heating Source: Baseboards Only

System Type: Elec Baseboards (only) with NO zone v

System per Area: System per Shell

Figure 4-16: Defining Electric Baseboards for Heating

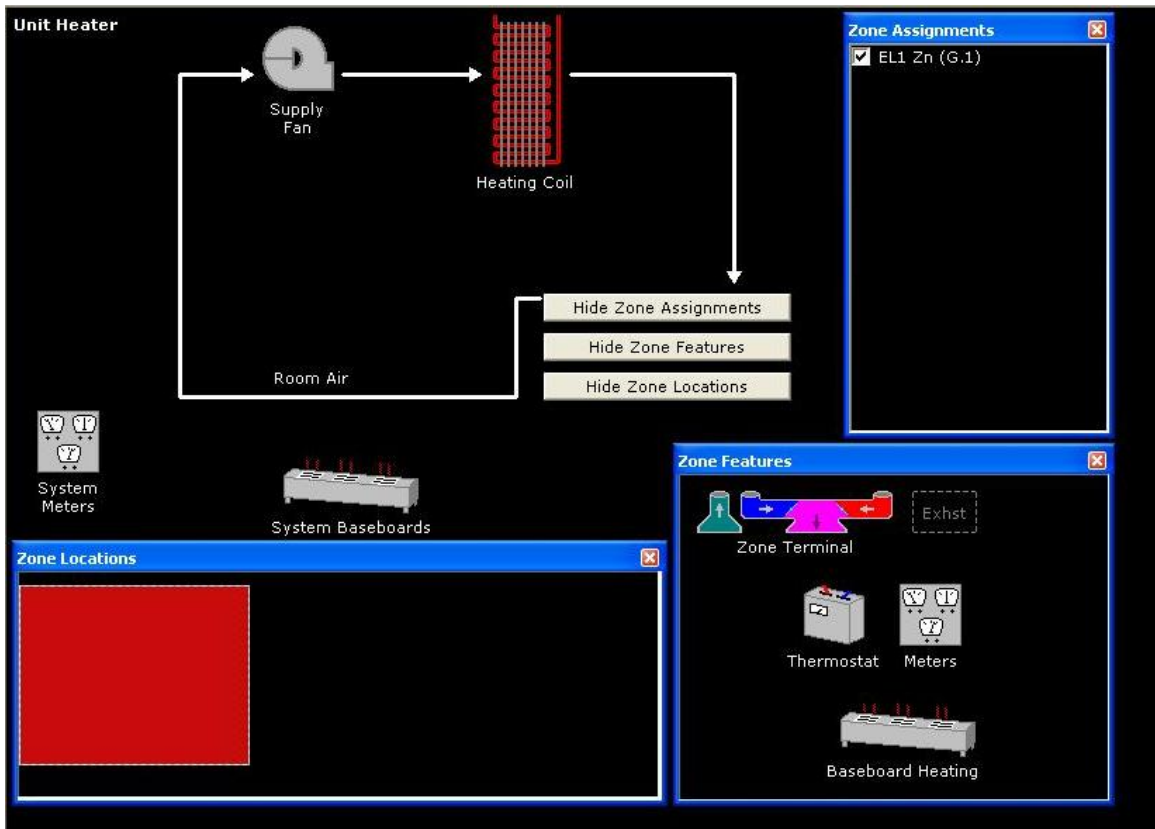


Figure 4-17: Defined HVAC System for The Building Model

## **Infiltration Method**

As discussed earlier, the calculated infiltration loads in eQUEST are to be utilized and evaluated in comparison with those obtained through CFD analyses and through the proposed Enhanced Model. The infiltration methods available in DOE-2/eQUEST have been discussed elaborately in Chapter 2. The air change method is the default method used in performing a building energy analysis in eQUEST. It is only through “Detailed Interface” manipulations that the advanced user is able to specify an alternate method. Therefore, this method is by default the method applied in many of the energy simulations performed in eQUEST. For this reason it is selected as one of the methods to utilize in our analyses and comparisons. The air change method is applied through 2 separate sets of simulations. Each set reflects one of the two alternative components of the air change equation. One set through specifying the number of air changes per hour (defined as ACH hereafter) and a second through specifying the infiltration airflow (defined as Basic Air Change method hereafter). ASHRAE Enhanced method is one for the latest additions to eQUEST and is considered to be among the most complex infiltration methods available in DOE-2/eQUEST. Therefore, it is selected as the third method to be used in simulations and analyses.

## **Enhanced Model**

The developed Enhanced Model (Figure 4-18) is created as described in detail in Chapter 3. A Visual Basic program interface is built containing all the developed equations and algorithms. The Enhanced Model takes as input the following:

- Building wall dimensions
- Building material properties



- Material air leakage data
- Other possible air leakage paths : plumbing openings or electrical outlets
- Wind data : wind speed, wind pressure coefficient (Cp), and wind angle
- Shielding class for the location based on surrounding terrain
- Initial iteration startup values for surface temperature.

**Engineering & Computing**

FLORIDA INTERNATIONAL UNIVERSITY

**Enhanced Infiltration Heat Flux Model**

**Building Envelop Construction**

Wall Properties

Number of walls (i)

Wall Length (L) (ft)

Wall Height (h) (ft)

Wall Thickness (t)

Wall Construction

	Brick		Air	Brick	
	Outer Layer	Middle Layer	Inner Layer	Outer Layer	Inner Layer
k (w/m K) or h	0.72	14.212	0.72	0.72	0.72
Layer Thickness (in)	4	2	4	4	4
Specific Heat (J/Kg)	837.36			837.36	
Density ρ (Kg/m <sup>3</sup> )	1922.2			1922.2	

Air Leakage Area

Joints & Corners

Corner Crack width (in)

Wan-Cemng Joint Crack width (in)

Walls

Brick ELA (in<sup>2</sup>/ft<sup>2</sup>)

Electrical Inlet/outlet

Lumber Inlets / w.al

ELA Inlet (in<sup>2</sup>)

Outlet Height (ft)

Wall layers Nomenclature

Wind & Location Input Data

Wind Data

Wind Velocity (ft)

Pressure Coefficient

Incidence Angle

Correct Cp Value

Terrain Data

Shielding Class

Shielding Coefficient:

Class	Terrain
I	no obstructions or local shielding
II	light local shielding with few obstructions
III	moderate local shielding, some obstructions within two house heights
IV	heavy shielding, obstructions around most of the perimeter
V	very heavy shielding, large obstructions surrounding the perimeter within two house heights

Initial Iteration Data & Calculation Constants

Surface	Cavity Wall Layers				
	Outer Layer	Center	Inner Layer		
	Brick	Air	Brick	Brick	
Temperature (k)	outside	Internal	centerline	Internal	Indoor
Temperature (k)	255	257.2	266.2	279.7	295.37
Density (Kg/m <sup>3</sup> )	1.225	1.225	1.225	1.225	1.225
(w/m <sup>2</sup> K) - air film	14.212	14.212	14.212	14.212	14.212
Cp (air specific heat) (JKg K)	1006.43	1006.4	1006.43	1006.4	1006.43

Flow Exponent, n

Flow Coefficient, C

Time step, Δt (sec)

Model General Calculation Flow Diagram

eQUEST Input

Mass Flow Rate Model

Combined Heat Model

Model Comparison

Figure 4-18: Built Enhanced Model Input Interface

The Enhanced Model reads into its hourly calculations hourly output from the DOE-2/eQUEST engine. The read values are essential for calculating both the hourly infiltration mass flow rate and for the heat model calculations. The read hourly values are ambient air temperature, air density, incident solar radiation, and hourly conduction heat load. For comparison it also reads the hourly sensible infiltration heat loads calculated in eQUEST. These hourly variables are highlighted in red in Figure 4-19.

### **Mass Flow Rate Model**

The first major component of the Enhanced Model is the proposed Mass Flow Rate model. Having a realistic evaluation of the infiltration mass flow rate is extremely essential for a model that evaluates the heat impact of this leakage flow. This importance was discussed elaborately in Chapters 2 and 3. The methodology and details of the developed Mass Flow Rate Model are also shown in Chapter 3. Figure 4-20 presents an example of the hourly output of the mass flow rate model.

### **Infiltration Heat Load**

Hourly output from the Mass Flow Rate Model along with aforementioned hourly eQUEST data are read into the combined Enhanced Model. Following the equations developed in Chapter 3, the heat model calculates hourly infiltration heat loads while accounting for heat storage in the wall mass, variable hourly airflow rates; and the interaction between conduction, infiltration and incident solar radiation. A representation of the model's interface and hourly calculations is shown in figure 4-21. The Enhanced Model output is then examined in comparison with the multiphysics CFD simulation output to verify the accuracy of the Enhanced Model's calculations. Its output is also compared with the hourly infiltration heat load output of the various considered DOE-

2/eQUEST built-in infiltration methods. Details of the output of the 3 methods and other corresponding models along with a detailed analysis of all output data is presented in detail in Chapter 5.

Input Data Obtained from eQUEST / DOE-2													
Input in the BLUE columns Below Output Data Obtained from eQUEST Hourly output													
hour	Ambient Air Temp (F)	Ambient Air Temp (K)	Air density (lb/ft <sup>3</sup> )	Air density (kg/m <sup>3</sup> )	Incident solar rad, i (Btu/hr ft <sup>2</sup> )	Incident solar rad, i (W/m <sup>2</sup> )	CFW Air/wall (ft <sup>3</sup> )	Q sensible Air Infil (tcfu/hr)	Qinfiltration/ wall (tcfu/hr)	Qinfiltration/ wall (W)	Q conduction/ wall (W)	Q conduction/ wall (W)	Q conduction/ wall (W)
1	-2	254.26	0.076	1.225	0	0.000		-455.689	-95.019	-27.841	-646.415	-189.400	
2	-2	254.26	0.076	1.225	0	0.000		-455.689	-96.462	-28.263	-660.214	-193.443	
3	-8	250.93	0.076	1.225	0	0.000		-493.664	-97.021	-28.427	-670.601	-196.486	
4	-13	248.15	0.076	1.225	0	0.000		-525.309	-114.348	-33.504	-678.010	-198.657	
5	-18	245.37	0.076	1.225	0	0.000		-556.954	-114.778	-33.630	-683.778	-200.347	
6	-21	243.71	0.076	1.225	0	0.000		-575.941	-144.002	-42.192	-689.291	-201.962	
7	-21	243.71	0.076	1.225	0	0.000		-575.941	-135.070	-39.576	-695.526	-203.789	
8	-23	242.59	0.076	1.225	0	0.000		-588.599	-155.579	-45.585	-702.611	-205.865	
9	-22	243.15	0.076	1.225	54.2809	171.119		-582.27	-153.906	-45.094	-710.373	-208.139	
10	-21	243.71	0.076	1.225	196.542	619.595		-575.941	-127.499	-37.357	-718.362	-210.480	
11	-19	244.82	0.076	1.225	245.941	775.324		-563.283	-128.972	-37.789	-723.336	-211.937	
12	-16	246.48	0.076	1.225	243.951	769.051		-544.296	-103.943	-30.455	-719.052	-210.662	
13	-13	248.15	0.076	1.225	207.499	654.136		-525.309	-105.814	-31.003	-702.112	-205.719	
14	-11	249.26	0.076	1.225	152.511	480.788		-512.651	-114.755	-33.623	-674.712	-197.691	
15	-10	249.82	0.076	1.225	87.2197	274.958		-506.322	-113.107	-33.140	-641.567	-187.979	
16	-11	249.26	0.076	1.225	26.0191	82.025		-512.651	-135.504	-39.703	-608.190	-178.200	
17	-16	246.48	0.076	1.225	5.29463	16.691		-544.296	-176.348	-51.670	-580.315	-170.032	
18	-18	245.37	0.076	1.225	0	0.000		-556.954	-187.373	-54.900	-562.815	-164.905	
19	-18	245.37	0.076	1.225	0	0.000		-556.954	-195.764	-57.359	-557.545	-163.361	
20	-21	243.71	0.076	1.225	0	0.000		-575.941	-185.036	-54.216	-562.700	-164.871	
21	-21	243.71	0.076	1.225	0	0.000		-575.941	-192.719	-56.467	-575.113	-168.508	
22	-20	244.26	0.076	1.225	0	0.000		-569.612	-150.560	-44.114	-592.018	-173.461	
23	-21	243.71	0.076	1.225	0	0.000		-575.941	-201.307	-58.983	-611.047	-179.037	
24	-21	243.71	0.076	1.225	0	0.000		-575.941	-192.719	-56.467	-630.497	-184.736	
25	-22	243.15	0.076	1.225	0	0.000		-582.27	-211.145	-61.865	-649.596	-190.332	
26	-18	245.37	0.076	1.225	0	0.000		-556.954	-210.411	-61.651	-667.883	-195.690	

Figure 4-19: Hourly DOE-2/eQUEST Input into the Enhanced Model

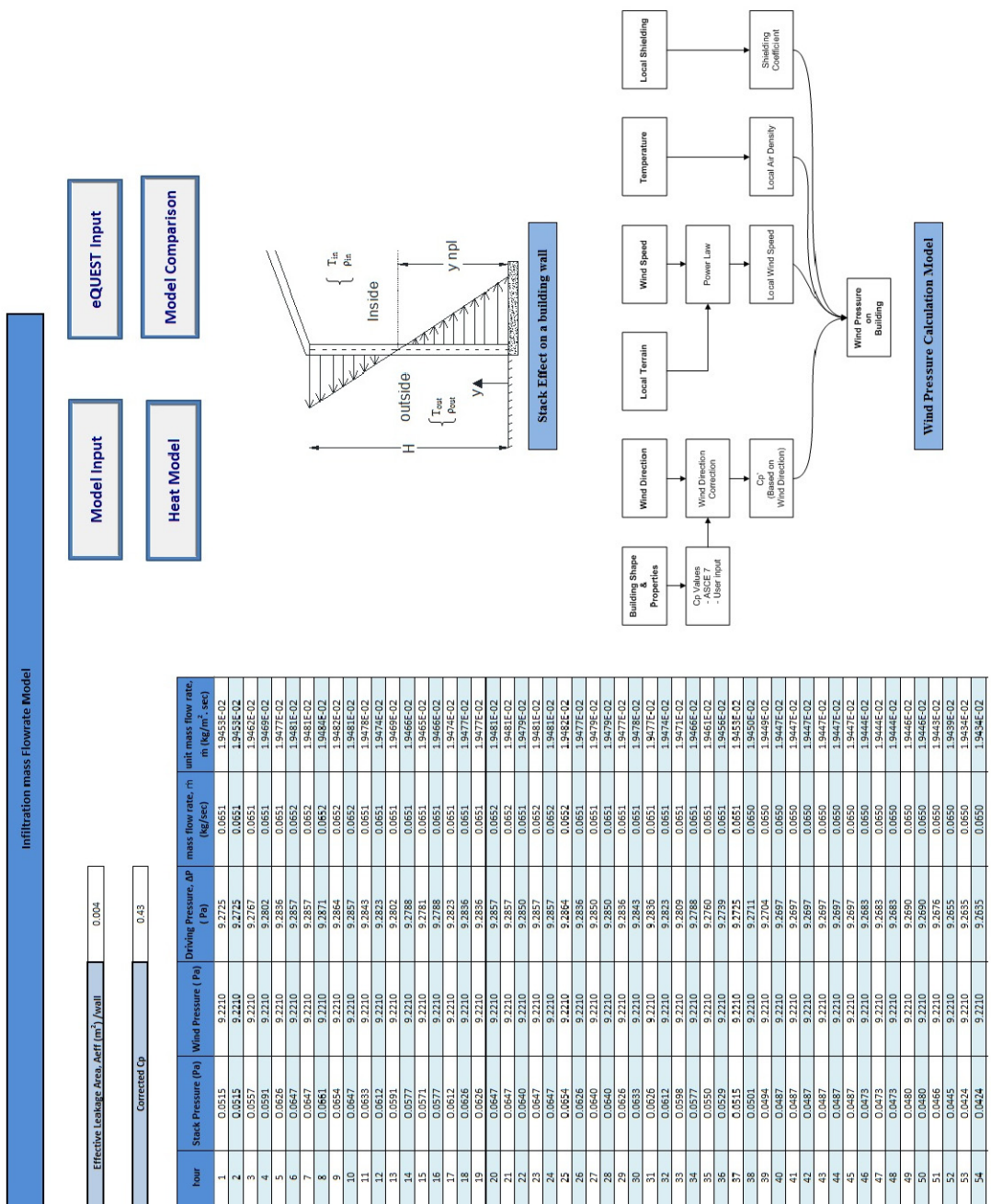


Figure 4-20: Built Interface for the Mass Flow Rate Calculation Model



Infiltration mass flowrate Model

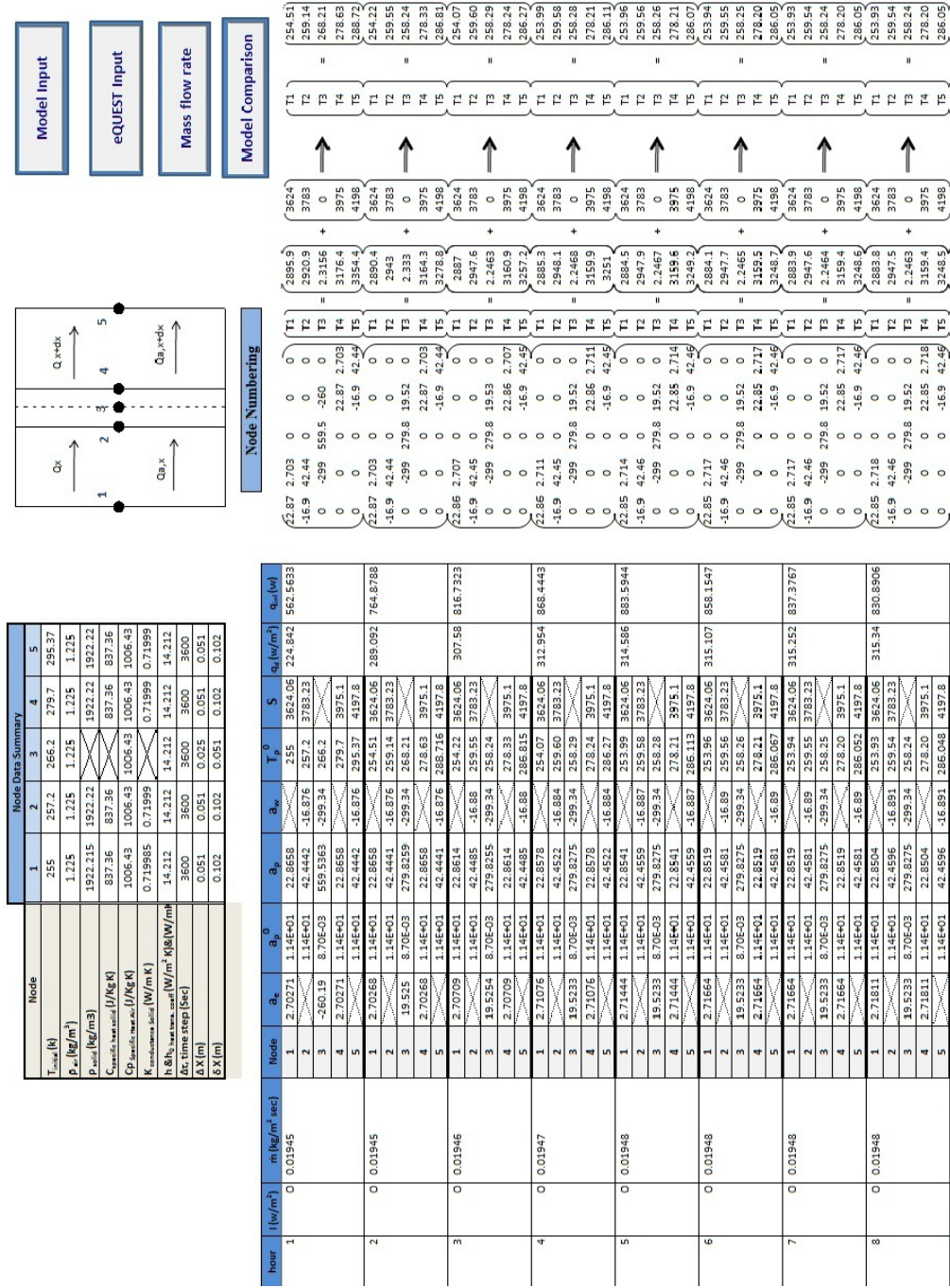


Figure 4-21: BUILT Enhanced Model Output Interface

## **Chapter 5**

### **Results and Discussion**

The main objective of this research is to develop a model that better evaluates the energy impact of air infiltration in building envelopes. The method has to account for the combined interaction effect of heat conduction in the building walls, air flow through leakage paths and the effect of incident solar loading. The developed method is to be applied onto prominent building energy simulation engines in an aim to demonstrate its effectiveness and improve these engines' infiltration energy load calculations accuracy. Consequently, this improves the accuracy of their overall building energy simulations and energy audit calculations.

The Enhanced Model methodology and calculation flow was discussed in detail in Chapters 3 and 4. Similarly, the built multiphysics CFD models and their simulation process along with that of the eQUEST simulations were discussed in previous Chapters.

The hourly output of each of: The Enhanced Model, and the basic DOE-2/eQUEST is presented and analyzed in this chapter. In conjunction, the hourly output obtained from CFD analyses is presented and incorporated into the analysis of the results and the verification of the Enhanced Model's method and output.

Analysis of obtained output data will be presented on a wall by wall basis. Subsequently the overall envelope results are presented and analyzed.

#### **Simulation Duration**

The adopted simulation duration is 744 hours (time steps in CFD analysis). This corresponds to one full month of the year. Performing a full month simulation in eQUEST and the Enhanced Model is a fast process and non resource intensive. However,

the multiphysics CFD analysis for each of the CFD models is very resource intensive in terms of computing power. These simulations require extensive time durations to perform all necessary calculations and iterations. This issue is especially critical considering that each of the simulated CFD models contains more than 13 million elements and that simulations need to span a flow time of 31 days.

A full 31 day simulation was performed on the CFD model with Angular (zig-zag) leakage cracks. The data obtained from the first 372 time steps (15 days of flow time) was extrapolated to predict cumulative infiltration data for 744 time steps (31 days of flow time). The extrapolated 31 day data was then compared against the actual simulation output of 31 days. As shown in Table 5-1. The cumulative full month (744 hours) extrapolated output based on 15 days of flow time simulation (372 time steps) fell within -0.41 % and 1.58% of the actual 744 time steps cumulative output for all the components in the building envelope. Therefore, due to the extensive computing time necessary for performing a full 744 time steps CFD analysis it was decided to perform 372 time steps (15 days) of flow time simulations for each of the remaining CFD models. The 15 day output is then extrapolated to obtain the full month cumulative output for each model. Based on the previously stated evaluation of extrapolated output data for the Angled (zig-zag) cracks model, extrapolation of data for the remaining CFD models is deemed accurate and reliable.

	Convection SW	Conduction SW	Convection SE	Conduction SE	Convection NW	Conduction NW	Convection NE	Conduction NE
$\Sigma$ 15 Days (Watt)	376974.76	53548.29	334047.91	22274.12	350876.15	39623.03	435004.53	26155.81
Extrapolated 31 Days (Watt)	779081.18	110666.47	690365	46033.19	725144.05	81887.60	8990099.36	54055.34
$\Sigma$ 31 Days (Watt)	775389.53	111122.08	688256.55	45341.89	722123.95	82164.68	896080.88	53215.70
% Difference	Overestimate by 0.48%	Underestimate by 0.41%	Overestimate by 0.31%	Overestimated by 1.52%	Overestimate by 0.42%	Overestimate by 0.34%	Overestimate by 0.33%	Overestimate by 1.58%

Table 5-1: Cumulative Extrapolated 31 Day Data versus Actual Cumulative 31 Day Data for CFD Analyses



## Southwest Wall (SW)

Hourly data presented in Table 5-2 are for the calculated hourly infiltration heat load for:

1. EQUEST
  - a. Air Change Method (Basic : Airflow)
  - b. Air Change Method (ACH : air changes per hour)
  - c. ASHRAE Enhanced
2. Enhanced Model
3. Hygrothermal multiphysics CFD Analysis

The data shown in Table 5-2 is an excerpt of the hourly output for the southwest wall. It corresponds to the first 12 hours (midnight to noon) on January 1 and the last 12 hours (noon to midnight) of simulation flow time on January 31<sup>st</sup>. The full tabulated data is presented in Appendix A.

The plot in Chart 5-1 shows the calculated hourly output of sensible infiltration heat load on the SW wall for each of the 3 considered DOE-2/eQUEST methods. It is evident from the plot that the output is largely inconsistent among these different methods themselves. Also significantly different is the peak infiltration heat load reported by each method. The peak load obtained from the base Air Change method is 63.952 watts versus 97.002 watts obtained through Air Change method (ACH) and 238.63 from ASHRAE Enhanced. On the other hand, the peak hourly heat load calculated by the developed Enhanced Model is 1055.01 watts and compares very well against the peak hourly load of 1079.23 watts reported by the CFD analysis for the case of angled cracks.

### Hourly Southwest (SW) Wall Data (Watts)

hour	eUEST/DOE-2 Hourly Values (no reduction multiplier)			CFD Multiphysisc Simulation			
	Air Change	Air Change (ACH)	ASHRAE Enhanced	Enhanced Model	Angular Cracks	Mixed Cracks*	Straight Cracks*
1	27.841	12.382	78.440	562.563	1033.902	1001.086	990.942
2	28.263	12.570	79.632	764.879	1032.148	999.568	988.689
3	28.427	15.172	85.301	816.732	1031.288	997.784	987.061
4	33.504	14.901	103.464	868.444	1027.239	995.574	983.660
5	33.630	17.948	108.929	883.594	1025.149	993.470	981.911
6	42.192	11.259	136.746	858.155	1023.430	991.618	980.590
7	39.576	14.081	128.847	837.377	1021.008	989.738	980.309
8	45.585	20.274	151.554	830.891	1019.139	988.343	976.587
9	45.094	16.045	147.876	873.207	1020.458	991.931	979.906
10	37.357	16.615	122.458	881.855	1021.342	998.765	987.920
11	37.789	16.807	122.098	872.546	1025.298	1007.328	995.728
12	30.455	21.672	100.095	869.263	1027.725	1016.348	1005.657



733	14.610	19.493	55.866	1053.425	1030.938	1069.436	1064.581
734	11.944	19.123	51.364	1053.390	1034.757	1078.619	1076.438
735	13.016	19.683	54.011	1053.446	1035.416	1084.796	1083.577
736	15.210	20.294	58.740	1053.521	1036.224	1086.488	1084.065
737	20.371	19.932	68.917	1053.535	1034.587	1084.207	1081.982
738	20.063	19.631	68.312	1053.612	1031.302	1077.440	1075.818
739	35.181	12.518	106.956	1053.697	1030.366	1071.414	1069.026
740	37.148	9.913	112.348	1053.715	1027.498	1066.187	1062.234
741	39.079	6.952	117.834	1053.722	1026.245	1061.116	1057.834
742	40.683	10.856	124.034	1053.797	1023.751	1056.753	1053.215
743	41.173	14.649	127.170	1053.881	1023.359	1052.888	1048.771
744	33.906	18.096	107.430	1053.970	1020.565	1049.097	1045.088

**Table 5-2: Hourly Infiltration Heat Load Data for Southwest Wall**

Note\*: Last 12 Hourly CFD Data shown for Mixed and Straight Cracks in Table 5-2 are based on 15 Days of Flow time Simulation.

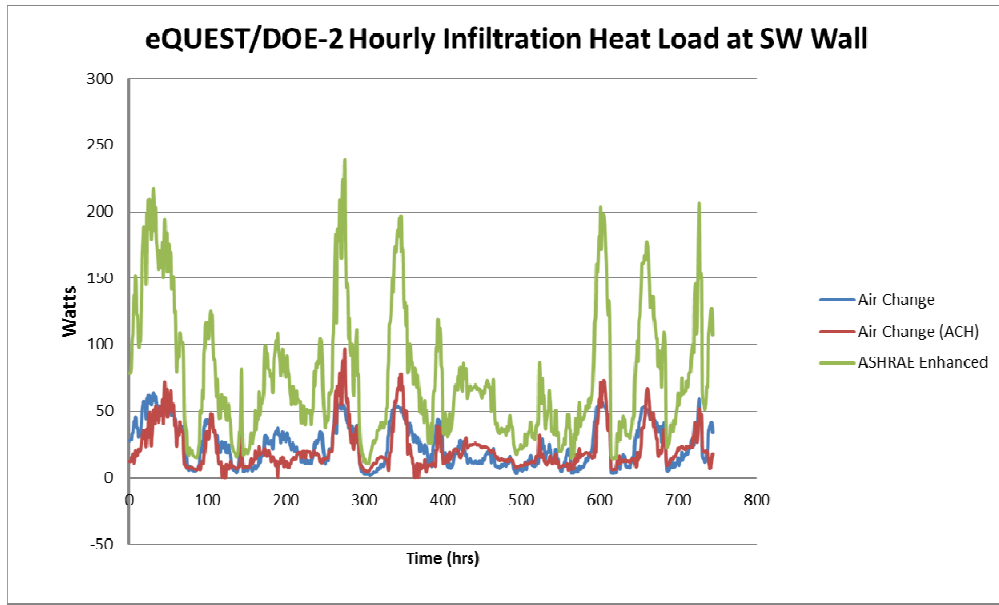


**Chart 5-1: Hourly Infiltration Heat Load at the Southwest Wall by Various DOE-2/eQUEST Methods**

Charts 5-2, 5-3 and 5-4 plot the hourly calculated infiltration heat load for the Southwest wall by the 5 previously stated methods. A separate chart is shown including each of the Three CFD cases (angled cracks, mixed cracks and straight cracks) versus the remaining models.

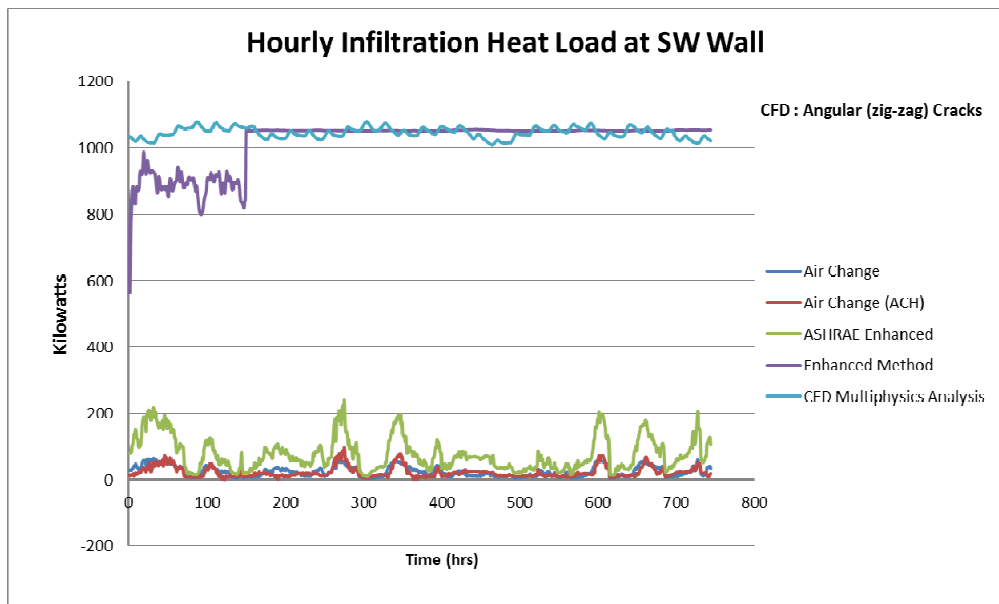


**Chart 5-2: Hourly Infiltration Heat Load at the Southwest Wall versus Angled (zig-zag) cracks CFD Output for the wall**

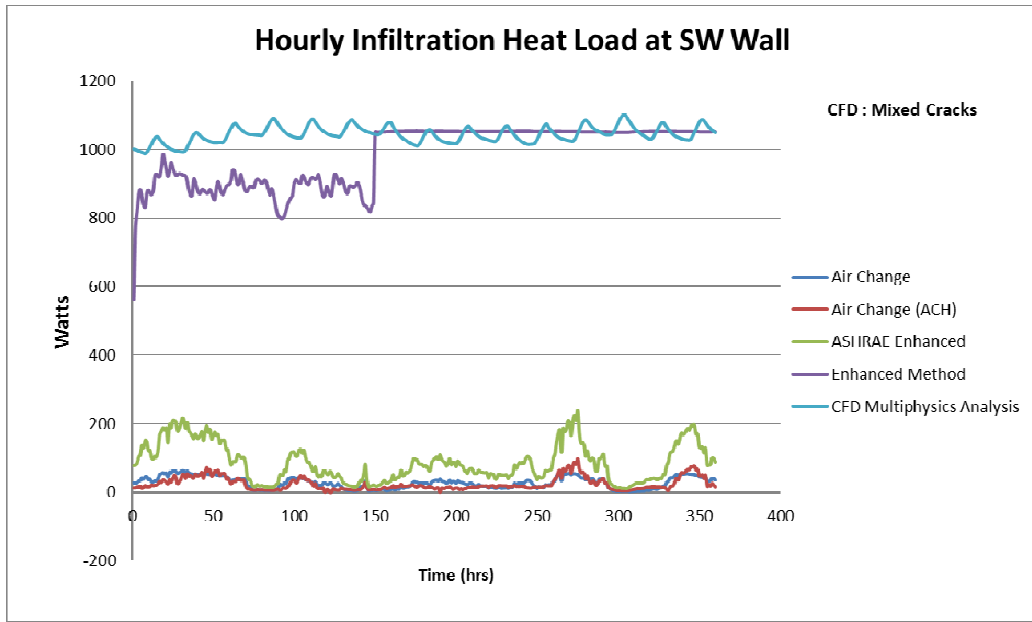


**Chart 5-3: Hourly Infiltration Heat Load at the Southwest Wall versus Mixed cracks CFD Output for the wall**

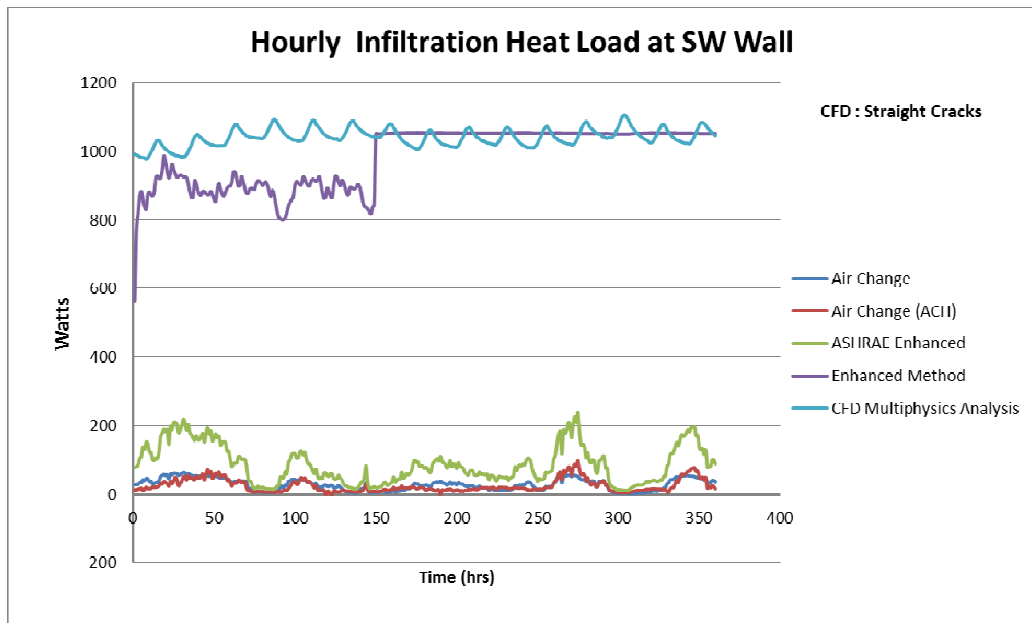


**Chart 5-4: Hourly Infiltration Heat Load at Southwest Wall versus Straight cracks CFD Output for the wall**

The output of the Enhanced Model is the same for the various types and combinations of cracks. Even though it is dependent on DOE-2/eQUEST hourly values, its output is independent of and invariable with the various DOE-2/eQUEST infiltration

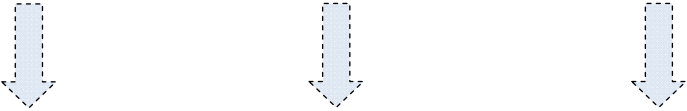
methods. The Enhanced Model was developed to be independent of previously existing infiltration heat load calculation methods. Also, as clear in the shown plots it is formulated to provide a highly accurate estimation of hourly infiltration loads without the need to specify or determine the type of cracks in the building envelope or the percentage of each type.

The cumulative heat load of infiltration is the major desired output and final objective of every energy analysis. It provides a quantifiable amount of the energy demand and expected energy costs over a measurable period of time. Table 5-3 presents an excerpt of the cumulative infiltration heat load calculated for the southwest wall by each of the methods and for the various crack types (CFD). A detailed hourly report is presented in Appendix A.

The plots in Charts 5-5, 5-6 and 5-7 reflect the cumulative infiltration load for the Southwest wall for the different DOE-2/eQUEST methods versus the CFD simulation results for the various crack types and versus the Enhanced Model output. From the charts shown, a major underestimation of the infiltration heat load by the DOE-2/eQUEST methods versus the CFD analysis is clearly observed. On the other hand, the output of the Enhanced Model is observed to be highly consistent with the results of the multiphysics hygrothermal CFD analysis. A summary of the cumulative results calculated by each method for the Southwest wall is shown in Table 5-4.

**Cumulative Southwest (SW) Wall Data (Watts)**

hour	eUEST/DOE-2 Hourly Values (no reduction multiplier)			CFD Multiphysics Simulation			
	Air Change	Air Change (ACH)	ASHRAE Enhanced	Enhanced Model	Angular Cracks	Mixed Cracks*	Straight Cracks*
1	27.841	12.382	78.440	562.563	1033.902	1001.086	990.942
2	56.104	24.952	158.072	1327.442	2066.050	2000.654	1979.632
3	84.531	40.124	243.374	2144.174	3097.338	2998.438	2966.693
4	118.035	55.025	346.837	3012.619	4124.577	3994.012	3950.352
5	151.665	72.973	455.766	3896.213	5149.727	4987.482	4932.263
6	193.857	84.232	592.512	4754.368	6173.157	5979.100	5912.853
7	233.433	98.314	721.360	5591.744	7194.165	6968.838	6893.162
8	279.017	118.587	872.913	6422.635	8213.304	7957.180	7869.749
9	324.112	134.632	1020.789	7295.842	9233.762	8949.111	8849.655
10	361.469	151.247	1143.247	8177.697	10255.104	9947.876	9837.575
11	399.258	168.054	1265.344	9050.244	11280.402	10955.204	10833.303
12	429.713	189.726	1365.440	9919.506	12308.128	11971.552	11838.960



733	17822.14	16273.10	55806.29	746490.21	766131.51	364067.22	362813.83
734	17834.09	16292.22	55857.66	747543.60	767166.27	365145.84	363890.27
735	17847.10	16311.90	55911.67	748597.04	768201.69	366230.64	364973.85
736	17862.31	16332.20	55970.41	749650.56	769237.91	367317.13	366057.91
737	17882.68	16352.13	56039.33	750704.10	770272.50	368401.33	367139.89
738	17902.75	16371.76	56107.64	751757.71	771303.80	369478.77	368215.71
739	17937.93	16384.28	56214.59	752811.41	772334.17	370550.19	369284.74
740	17975.07	16394.19	56326.94	753865.12	773361.66	371616.37	370346.97
741	18014.15	16401.14	56444.78	754918.84	774387.91	372677.49	371404.81
742	18054.84	16412.00	56568.81	755972.64	775411.66	373734.24	372458.02
743	18096.01	16426.65	56695.98	757026.52	776435.02	374787.13	373506.79
744	18129.92	16444.74	56803.41	758080.49	777455.58	375836.23	374551.88

**Table 5-3: Cumulative Infiltration Heat Load Data for Southwest Wall**

Note\*: Cumulative CFD Data for Mixed and Straight Cracks Simulation in Table 5-3 are based on 15 Days of Flow time Simulations.

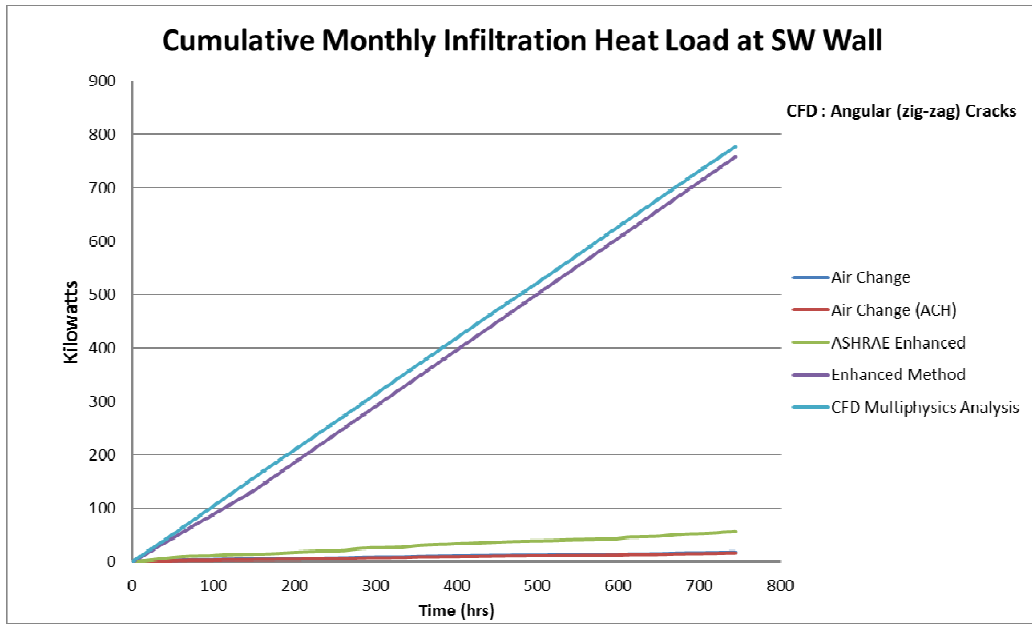


**Chart 5-5: Cumulative Monthly Infiltration Heat Load at Southwest Wall versus Angled (zig-zag) cracks CFD Output for the Wall**

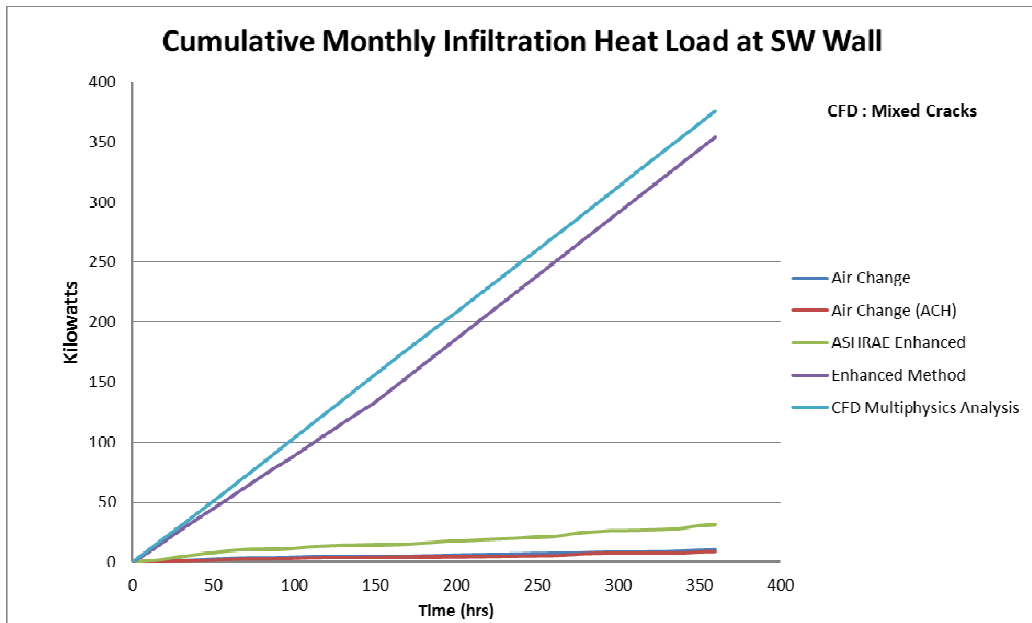


**Chart 5-6: Cumulative Monthly Infiltration Heat Load at Southwest Wall versus Mixed cracks CFD Output for the Wall**

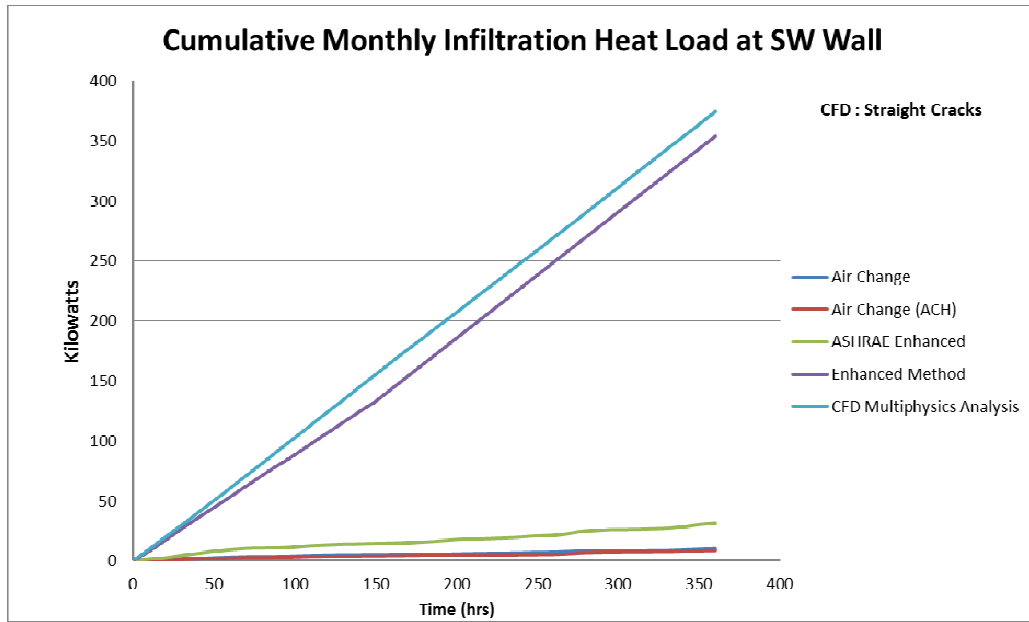


**Chart 5-7: Cumulative Monthly Infiltration Heat Load at Southwest Wall versus Straight cracks CFD Output for the Wall**

As shown in Table 5-4 a very high percentage of error in estimating the infiltration heat load is observed by the base Air Change method, Air Change (ACH), and ASHRAE Enhanced method. The underestimation error ranges between 91.66% and 97.88%. In contrast, the output of the Enhanced Model is highly accurate in comparison with the complex CFD analysis. The underestimation error of the Enhanced Model ranges between 2.49% and 5.48 % only. It is extremely important to note the capability of the Enhanced Model to very closely match the output of the complex CFD analysis while requiring less than 1 % of the time required for running a CFD analysis for the same building envelope. This advantage will be discussed with further detail in the following sections.



Table 5-4: Cumulative Monthly Heat Load on Southwest Wall

SW- Wall Full Month Summary								
		eQUEST/DOE-2 Infiltration Load V/s CFD Analysis			Enhanced eQUEST/DOE-2 Infiltration Load V/s CFD Analysis			
		DOE-2/eQUEST (watts)	Ansys (watts)	Uner/over Estimate	Enhanced Model (watts)	Ansys (watts)	Uner/over Estimate	
Angled (zig-zag)	Air Change (base)	18129.92	777455.58	Under Estimate 97.67%	758080.49	777455.58	Under Estimate 2.49%	Full Month Simulation
	Air Change (ACH)	16444.74	777455.58	Under Estimate 97.88%	758080.49	777455.58	Under Estimate 2.49%	
	ASHRAE Enhanced	56803.41	777455.58	Under Estimate 92.69%	758080.49	777455.58	Under Estimate by 2.49%	
Mixed Cracks	Air Change (base)	10177.45	375836.23	Under Estimate 97.29%	354017.23	375836.23	Under Estimate 5.81%	15 Days
	Air Change (ACH)	8829.61	375836.23	Under Estimate 97.65%	354017.23	375836.23	Under Estimate 5.81%	
	ASHRAE Enhanced	31247.49	375836.23	Under Estimate 91.69%	354017.23	375836.23	Under Estimate 5.81%	
Straight Cracks	Air Change (base)	10177.45	374551.88	Under Estimate 97.28%	354017.23	374551.88	Under Estimate 5.48%	15 Days
	Air Change (ACH)	8829.61	374551.88	Under Estimate 97.64%	354017.23	374551.88	Under Estimate 5.48%	
	ASHRAE Enhanced	31247.49	374551.88	Under Estimate 91.66%	354017.23	374551.88	Under Estimate 5.48%	

### **Northwest Wall (NW)**

Similar to the Southwest wall analyses discussed in the previous section in this section an analysis for the infiltration heat load calculations for the Northwest wall façade of the building envelope is presented. The data shown in Table 5-5 is an excerpt of the hourly infiltration heat load at the Northwest wall at the first 12 time steps and the final 12 time steps of each hourly analysis. The full hourly data is presented in appendix B.

The plot in Chart 5-8 shows the calculated hourly output of sensible infiltration heat load on the SW wall for each of the 3 considered DOE-2/eQUEST methods. As in the case of the Southwest wall, it is evident from the data plots that the output is largely inconsistent among these different methods themselves. Also significantly different is the peak infiltration heat load reported by each method. The peak load obtained from the base Air change method is 146 watts versus 344.31 watts obtained through Air Change (ACH) and 894.692 watts from ASHRAE Enhanced. On the other hand, the peak hourly load calculated by the developed Enhanced Model is 1055 watts and compares very well against the peak hourly load of 1007.212 watts reported by the CFD analysis for the case of angled cracks for example.

Charts 5-9, 5-10 and 5-11 plot the hourly calculated infiltration heat load for the Northwest wall by the 5 previously stated methods. A separate chart is shown including each of the Three CFD cases (angled cracks, mixed cracks and straight cracks) versus the remaining models.

### Hourly Northwest (NW) Wall Data (Watts)

hour	eUEST/DOE-2 Hourly Values (no reduction multiplier)			CFD Multiphysisc Simulation			
	Air Change	Air Change (ACH)	ASHRAE Enhanced	Enhanced Model	Angular Cracks	Mixed Cracks	Straight Cracks
1	56.029	24.919	157.860	525.783	954.536	867.704	916.750
2	54.852	24.395	154.544	746.408	953.216	866.990	915.432
3	65.523	34.970	196.614	805.611	951.399	865.908	914.195
4	60.664	26.981	187.338	805.096	950.079	864.373	912.754
5	69.586	37.138	225.392	821.346	946.745	862.458	909.881
6	42.192	11.259	136.746	826.700	944.771	860.788	908.104
7	58.600	20.850	190.787	823.588	942.659	859.075	906.221
8	45.585	20.274	151.554	819.754	941.388	857.656	905.070
9	45.094	16.045	147.876	818.078	942.205	860.151	907.145
10	64.774	28.809	212.331	841.410	944.555	864.975	912.290
11	59.864	26.625	193.424	854.493	947.400	871.483	918.960
12	74.712	53.166	245.551	862.263	950.602	878.035	926.349



733	103.980	138.737	397.612	1053.425	960.809	920.923	976.938
734	111.401	178.364	479.080	1053.390	963.164	927.357	982.118
735	110.269	166.744	457.551	1053.446	964.905	931.944	986.280
736	106.019	141.457	409.442	1053.521	964.809	933.747	986.164
737	91.655	89.681	310.087	1053.535	963.339	931.977	984.390
738	94.366	92.333	321.303	1053.612	960.226	927.629	979.750
739	54.141	19.264	164.595	1053.697	957.846	923.448	976.381
740	48.668	12.987	147.189	1053.715	957.264	919.926	972.738
741	43.294	7.702	130.546	1053.722	954.380	916.497	969.594
742	40.683	10.856	124.034	1053.797	953.315	912.969	967.552
743	41.173	14.649	127.170	1053.881	951.212	910.672	964.076
744	63.253	33.758	200.412	1053.970	951.220	907.971	961.581

**Table 5-5: Hourly Infiltration Heat Load Data for Northwest Wall**

Note\*: Last 12 Hourly CFD Data shown for Mixed and Straight Cracks in Table 5-5 are based on 15 Days of Flow time Simulations.

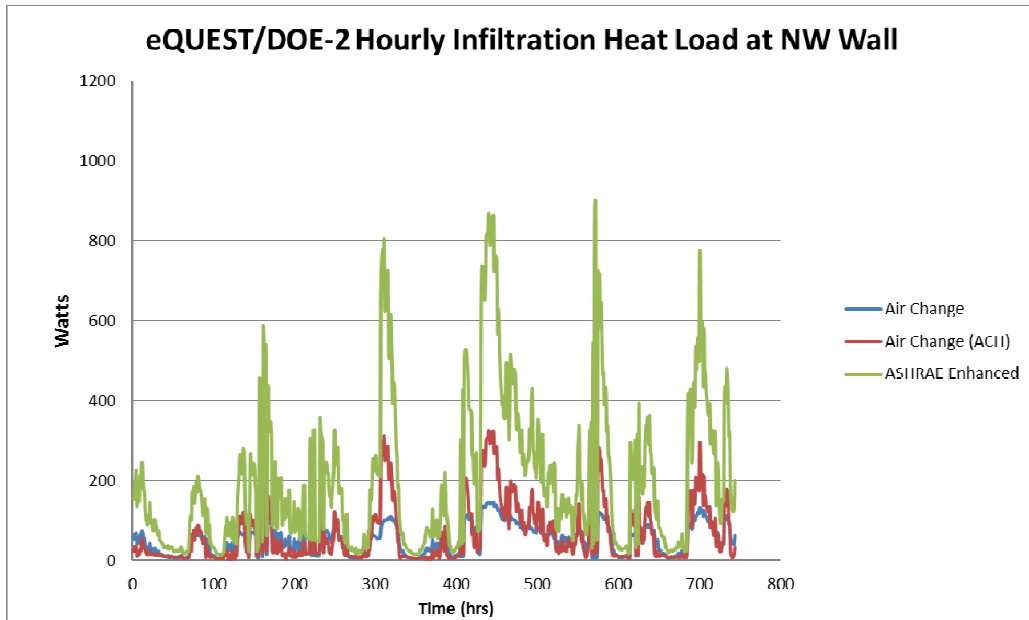


Chart 5-8: Hourly Infiltration Heat Load at Northwest Wall by Various DOE-2/eQUEST Methods

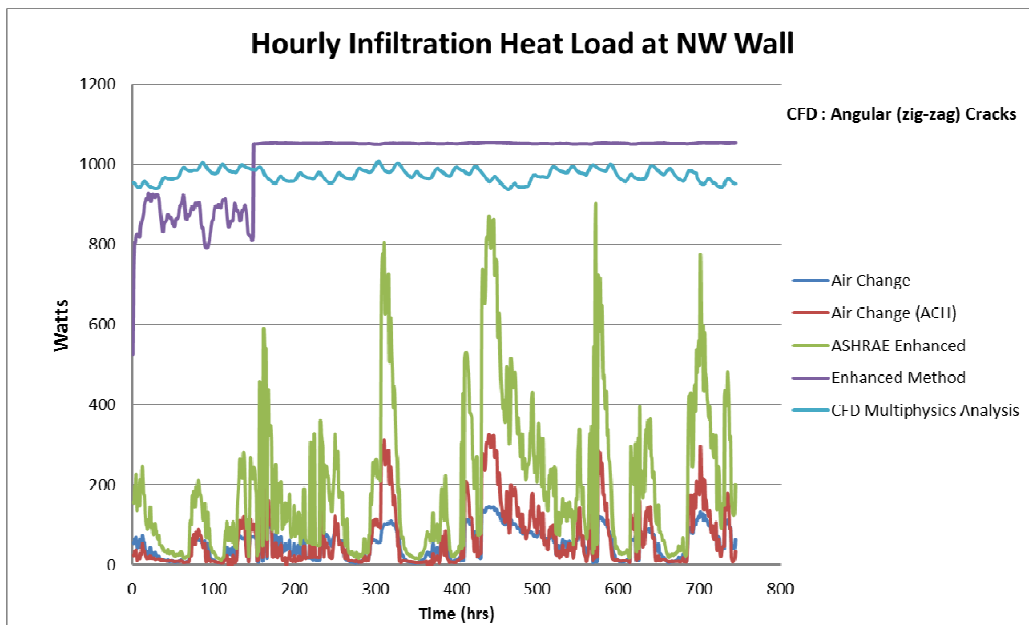


Chart 5-9: Hourly Infiltration Heat Load at Northwest Wall versus Angled (zig-zag) cracks CFD Output for the Wall

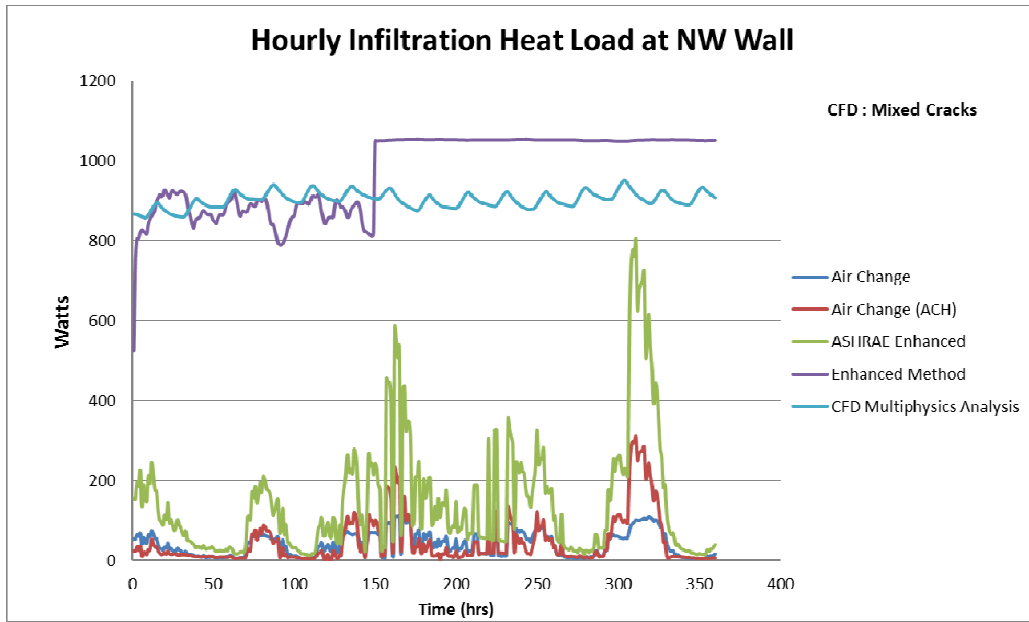


Chart 5-10: Hourly Infiltration Heat Load at Northwest Wall versus Mixed cracks CFD Output for the Wall

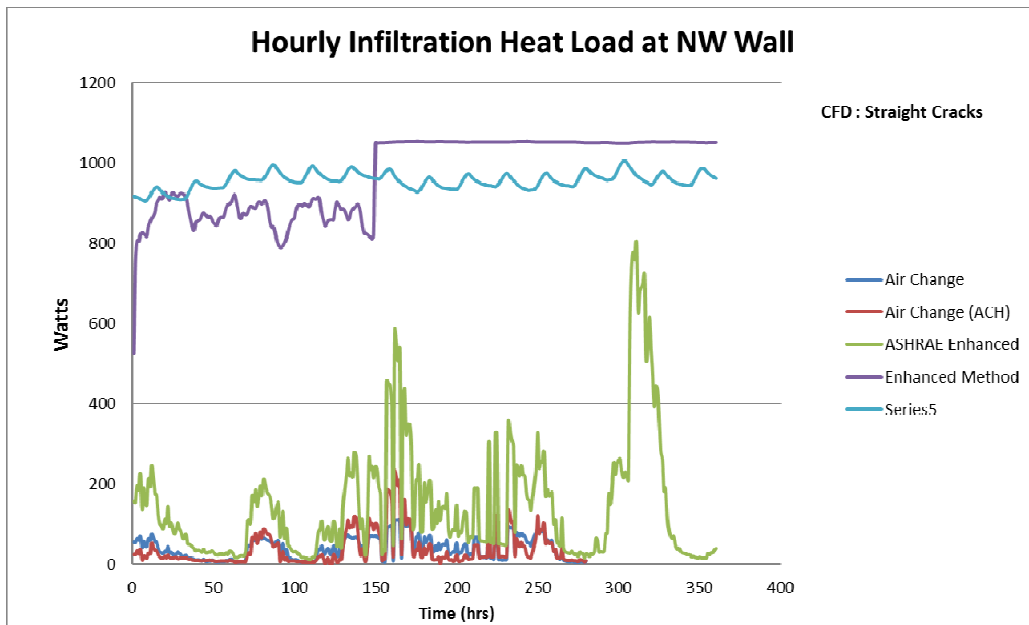


Chart 5-11: Hourly Infiltration Heat Load at Northwest Wall versus Straight cracks CFD Output for the Wall

### Cumulative Southwest (SW) Wall Data (Watts)

hour	eUEST/DOE-2 Hourly Values (no reduction multiplier)			CFD Multiphysisc Simulation			
	Air Change	Air Change (ACH)	ASHRAE Enhanced	Enhanced Model	Angular Cracks	Mixed Cracks*	Straight Cracks*
1	56.03	24.92	157.86	525.78	954.54	867.70	916.75
2	110.88	49.31	312.40	1272.19	1907.75	1734.69	1832.18
3	176.40	84.28	509.02	2077.80	2859.15	2600.60	2746.38
4	237.07	111.26	696.36	2882.90	3809.23	3464.98	3659.13
5	306.65	148.40	921.75	3704.24	4755.98	4327.43	4569.01
6	348.85	159.66	1058.49	4530.94	5700.75	5188.22	5477.12
7	407.45	180.51	1249.28	5354.53	6643.40	6047.30	6383.34
8	453.03	200.79	1400.84	6174.29	7584.79	6904.95	7288.41
9	498.12	216.83	1548.71	6992.36	8527.00	7765.10	8195.55
10	562.90	245.64	1761.04	7833.77	9471.55	8630.08	9107.84
11	622.76	272.26	1954.47	8688.27	10418.95	9501.56	10026.80
12	697.48	325.43	2200.02	9550.53	11369.55	10379.60	10953.15



733	39193.4	50492.8	147491.2	743970.2	713490.0	314865.5	333305.3
734	39304.8	50671.1	147970.3	745023.6	714453.2	315792.9	334287.5
735	39415.1	50837.9	148427.8	746077.1	715418.1	316724.8	335273.7
736	39521.1	50979.3	148837.3	747130.6	716382.9	317658.6	336259.9
737	39612.7	51069.0	149147.4	748184.1	717346.2	318590.5	337244.3
738	39707.1	51161.4	149468.7	749237.7	718306.5	319518.2	338224.0
739	39761.2	51180.6	149633.3	750291.4	719264.3	320441.6	339200.4
740	39809.9	51193.6	149780.4	751345.1	720221.6	321361.5	340173.2
741	39853.2	51201.3	149911.0	752398.9	721176.0	322278.0	341142.8
742	39893.9	51212.2	150035.0	753452.7	722129.3	323191.0	342110.3
743	39935.1	51226.8	150162.2	754506.5	723080.5	324101.7	343074.4
744	39998.3	51260.6	150362.6	755560.5	724031.7	325009.6	344036.0

**Table 5-6: Cumulative Infiltration Heat Load Data for Northwest Wall**

Note\*: Cumulative CFD Data for Mixed and Straight Cracks Simulation in Table 5-3 are based on 15 Days of Flow time Simulation.

Similar to what was presented for the Southwest wall, an excerpt of the cumulative infiltration heat load for the Northwest wall is shown in Table 5-6. The full data is presented in Appendix B. Charts 5-12, 5-13, and 5-14 present a plot of the cumulative DOE-2/eQUEST and Enhanced Model data in correspondence with the cumulative data for each crack type from the CFD models.

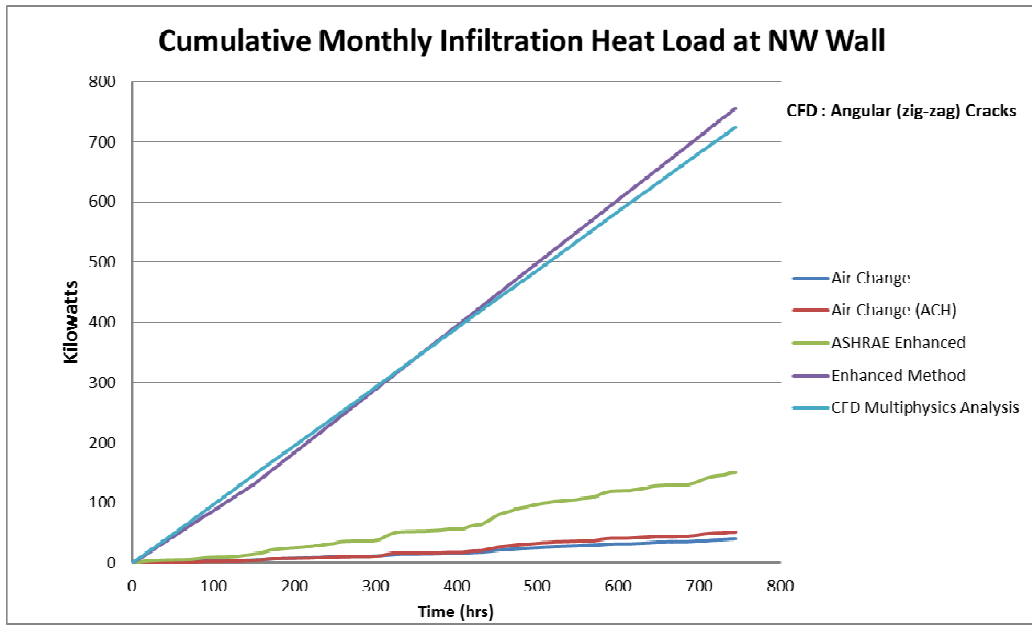


**Chart 5-12: Cumulative Monthly Infiltration Heat Load at Northwest Wall versus Angled (zig-zag) cracks CFD Output for the Wall**

From the cumulative charts a major underestimation of the infiltration heat load by the various DOE-2/eQUEST methods versus finite elements analysis is observed in this case too. The output of the Enhanced Model is however observed to be highly consistent and very close to that of the hygrothermal CFD analysis. A very slight overestimation is observed by the Enhanced Model. A summary of the cumulative results is shown in Table 5-7.

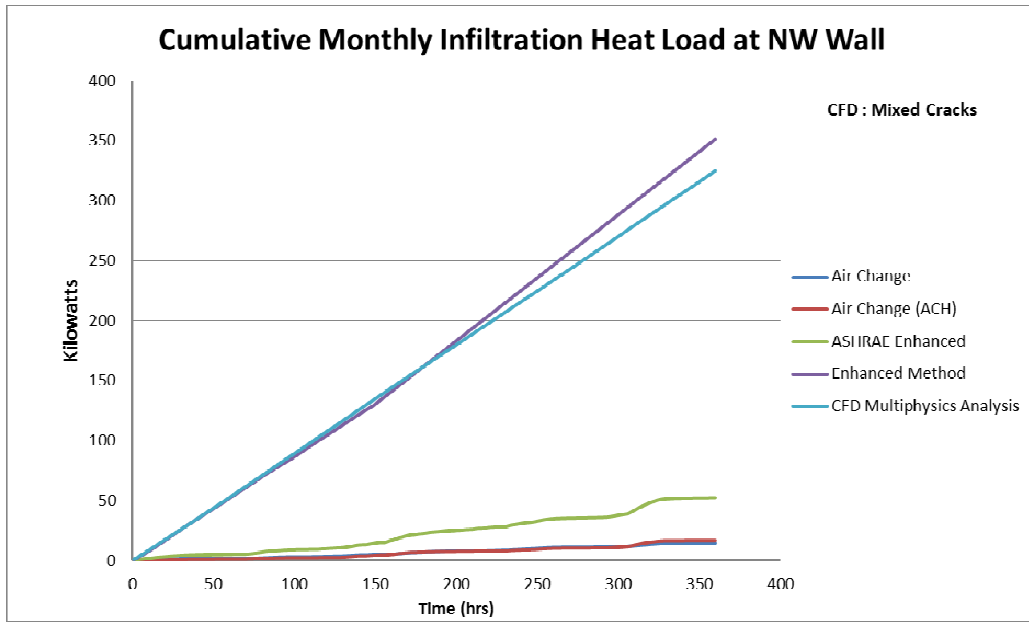


**Chart 5-13: Cumulative Monthly Infiltration Heat Load at Northwest Wall versus Mixed cracks CFD Output for the Wall**

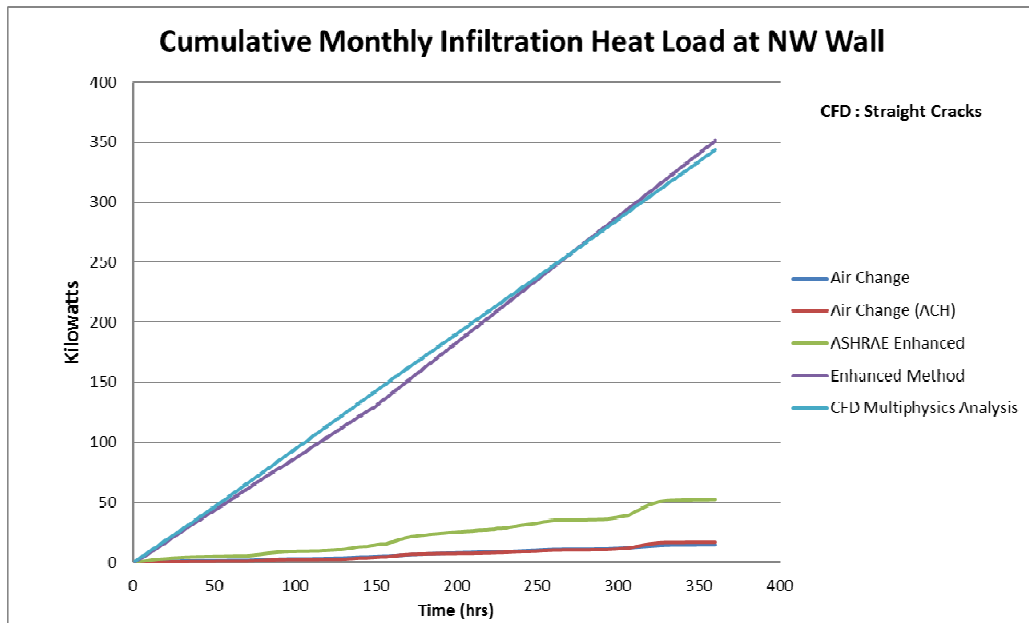


**Chart 5-14: Cumulative Monthly Infiltration Heat Load at Northwest Wall versus Straight cracks CFD Output for the Wall**



Table 5-7: Cumulative Monthly Heat Load on Northwest Wall

NW- Wall Full Month Summary								
		eQUEST/DOE-2 Infiltration Load V/s CFD Analysis			Enhanced eQUEST/DOE-2 Infiltration Load V/s CFD Analysis			
		DOE-2/eQUEST (watts)	Ansysis (watts)	Uner/over Estimate	Enhanced Model (watts)	Ansysis (watts)	Uner/over Estimate	
Angled (zig-zag)	Air Change (base)	39998.32	724031.70	Under Estimate 94.48%	755560.52	724031.70	Over Estimate 4.35%	Full Month Simulation
	Air Change (ACH)	51260.57	724031.70	Under Estimate 92.92%	755560.52	724031.70	Over Estimate 4.35%	
	ASHRAE Enhanced	150362.61	724031.70	Under Estimate 79.23%	755560.52	724031.70	Over Estimate 4.35%	
Mixed Cracks	Air Change (base)	14854.99	325009.64	Under Estimate 95.43%	351497.25	325009.64	Over Estimate 8.15%	15 Days
	Air Change (ACH)	17033.46	325009.64	Under Estimate 94.76%	351497.25	325009.64	Over Estimate 8.15%	
	ASHRAE Enhanced	52691.29	325009.64	Under Estimate 83.79%	351497.25	325009.64	Over Estimate 8.15%	
Straight Cracks	Air Change (base)	14854.99	344035.97	Under Estimate 95.68%	351497.25	344035.97	Over Estimate 2.17%	15 Days
	Air Change (ACH)	17033.46	344035.97	Under Estimate 95.05%	351497.25	344035.97	Over Estimate 2.17%	
	ASHRAE Enhanced	52691.29	344035.97	Under Estimate 84.68%	351497.25	344035.97	Over Estimate 2.17%	

As in the case of the Southwest wall, a very high percentage of error in estimating the infiltration heat load is observed for the various DOE-2/eQUEST methods. The underestimation error ranges between 83.79 % and 95.68%. Instead, the output of the Enhanced Model is highly accurate. It had a slight tendency to overestimate the CFD analysis results in this case. However, this overestimation is limited to a maximum of 8.15 %. This is while maintaining a high simulation speed and a high level of simplicity and ease of use.

### **Discussion of Results**

The previous sections closely examined the hourly and cumulative differences in infiltration heat load output for the same building envelope using different methods. The results show a vast underestimation by the different the DOE-2 engine methods in comparison with a complex multiphysics hygrothermal CFD analysis. The proposed Enhanced Model on the other hand performed very favorably and matched the CFD output with high accuracy. The sections below discuss various observations on the performance and aspects of the Enhanced Combined Heat and Air Infiltration Simulation Model. Charts 5-15 and 5-16 show for different walls the cumulative difference in kilowatts between the DOE-2/eQUEST methods, Enhanced Model, and the CFD analyses.

### **Heat Loading Error**

The foremost reason for performing a building energy analysis is to physically quantify with a good degree of accuracy the energy demands and associated expected energy costs of a building. In previous chapters we discussed the major problems that result from an inaccurate building energy analysis. Primarily, the impact it has on

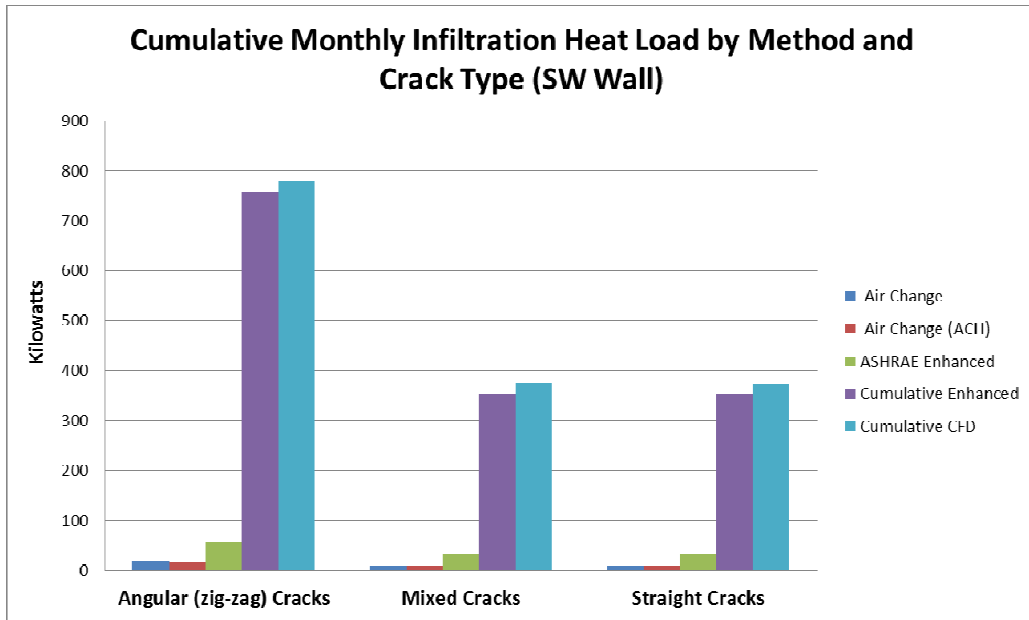


Chart 5-15: Comparison of Cumulative Monthly Infiltration Heat Load for the Southwest Wall

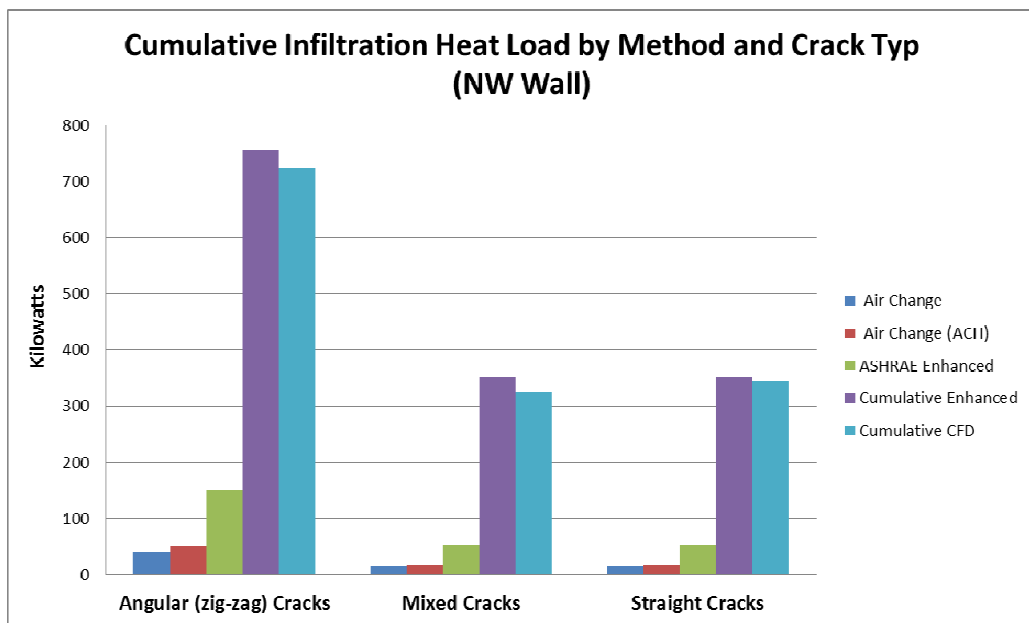


Chart 5-16: Comparison of Cumulative Monthly Infiltration Heat Load for the Northwest Wall

Note\*: Cumulative CFD Data for Mixed and Straight Cracks Simulation in Charts 5-15 and 5-16 are based on 15 Days of Flow time Simulations.

designing a building's HVAC system. As discussed, an oversized system results in higher than needed initial costs and in reduced efficiency during operation throughout the lifespan of a building. This results in large quantities of wasted energy and money. On the other side an underestimation of the building energy demands results in an undersized HVAC system. Consequently, the system has to run continuously in order to meet the building heating and cooling demands. In addition to the increased cost of non-stop operation, this mode of operation has a heavy toll on the mechanical aspects of the HVAC system. It results in an increased and repeated need for maintenance along with the associated increased costs. It also shortens the life span of the HVAC system and necessitates its overhaul and replacement more frequently than planned for the building's lifecycle. Table 5-8 shows in percentages and kilowatts the projected infiltration heat demand for the simulated building envelope over a month period (considering windward walls). The average overestimation error by the Enhanced Model ranges between 0.81 % and 4.5 %. While in DOE-2/eQUEST the error ranges between 85.70 % and 96.13 % of underestimation depending on the method used. In terms of watts, this represents a net error of 12.15 to 65.23 kilowatts versus an error of 1241.25 to 144.36 Kilowatts respectively.

The shown error in estimating the infiltration heat load is for a 6feet cubed building envelope. Extrapolating this error onto a full size building highlights the immense misvaluation of the building's energy demands that would be involved. For a full size family house or an office building the errors in estimating infiltration heat loads would therefore be immense. In particular when considering all the various material types, construction methods, and joints that are involved in a full size building. This error

reflects on the overall building energy analysis results and the dependent resulting HVAC system design. The proposed Enhanced Model gives users the accuracy of a complex multiphysics CFD analysis within a maximum error of 4.5 % while maintaining the high speed and ease of use of the common methods used in DOE-2 and other simulation engines.

### **Simulation Speed**

The Enhanced Model supersedes current methods by accuracy as was shown through output analysis. But the additional characteristic feature of this model is the combination of both high calculation speed and high accuracy. Accurate methods such as the finite element CFD models developed in this research for verification purposes already exist. However as shown, these methods are extremely complex. The complexity is in all of their modeling aspects: geometry construction (cracks modeling...etc.), meshing, simulation, and extraction of results and necessary data. In the CFD models used in this research upwards of 13 million mesh elements were necessary per model in order to obtain a good quality solution. This number of elements is just for a cube-shaped building envelope with 6ft by 6ft walls. Simulating a full size building with the potential number of millions of elements required and the computing power necessary is self-prohibitive and insurmountable. High Performance Computing (HPC) power was used in simulating the CFD models in this research. Nonetheless, 248 hours of simulation were required per model. With the same analogy, the required simulation and computing power for a full size building envelope multiphysics hygrothermal simulation would be immense and unaffordable. Such a simulation could easily require months and perhaps even years to complete depending on the building size. On the other hand escaping the

complexities of CFD analysis into faster and simplified methods has been shown to negatively affect the accuracy of simulation results and the overall building energy analysis validity in a drastic manner.

The Enhanced Model combines the accuracy of a CFD analysis and the speed of current DOE-2 infiltration calculation methods. It is able to maintain a higher than 96 % level of accuracy in comparison with complex CFD analysis while requiring less than 1% of the time required for a full CFD analysis. As shown in Table 5-9 the Enhanced Model is 892,800 times faster than a multiphysics CFD analysis while maintaining an error range of less than 4.5 % and resulting in 91.63% increase in accuracy over existing methods used in DOE-2 and other simulation engines, or the numerous software they power.

	<b>Simulation Time</b>	<b>Notes</b>
<b>CFD Analysis</b>	248 hours on HPC Computing	Excluding model geometry building & meshing time
<b>Enhanced Model</b>	< 1 minute	<ul style="list-style-type: none"> <li>- 892,800 times faster than CFD</li> <li>- Decreases Error by &gt; 91 %</li> </ul>

**Table 5-8: Simulation Speed Comparison**

Table 5-9: Cumulative Monthly Heat Load on Northwest Wall

Building Envelope Full Month Summary								
		eQUEST/DOE-2 Infiltration Load V/s CFD Analysis			Enhanced eQUEST/DOE-2 Infiltration Load V/s CFD Analysis			
		DOE-2/eQUEST (watts)	Ansysis (watts)	Uner/over Estimate	Enhanced Model (watts)	Ansysis (watts)	Uner/over Estimate	
Angled (zig-zag)	Air Change (base)	58128.23	1501487.28	Under Estimate 96.13%	1513641.01	1501487.28	Over Estimate 0.81%	Full Month Simulation
	Air Change (ACH)	67705.31	1501487.28	Under Estimate 95.49%	1513641.01	1501487.28	Over Estimate 0.81%	
	ASHRAE Enhanced	207166.02	1501487.28	Under Estimate 86.20%	1513641.01	1501487.28	Over Estimate 0.81%	
Mixed Cracks	Air Change (base)	58128.23	1448414.79	Under Estimate 95.99%	1513641.01	1448414.79	Over Estimate 4.50%	Extrapolated 15 Days
	Air Change (ACH)	67705.31	1448414.79	Under Estimate 95.33%	1513641.01	1448414.79	Over Estimate 4.50%	
	ASHRAE Enhanced	207166.02	1448414.79	Under Estimate 85.70%	1513641.01	1448414.79	Over Estimate 4.50%	
Straight Cracks	Air Change (base)	58128.23	1485081.55	Under Estimate 96.09%	1513641.01	1485081.55	Over Estimate 1.92%	Extrapolated 15 Days
	Air Change (ACH)	67705.31	1485081.55	Under Estimate 95.44%	1513641.01	1485081.55	Over Estimate 1.92%	
	ASHRAE Enhanced	207166.02	1485081.55	Under Estimate 86.05%	1513641.01	1485081.55	Over Estimate 1.92%	

### **Enhanced Model Ease of Use**

The advantage of DOE-2, eQUEST, energyPlus, energyPro and others is their ease of use. Especially easy are the software with a GUI interface such as eQUEST. This ease of use is a major driving force behind making these software extremely popular and widely used in building energy analysis and design.

The Enhanced Model as shown in Figure 5-1 and in previous figures has a very easy to use and user friendly interface. It only requires basic and readily available input coefficients. In contrast, other methods (such as ASHRAE Enhanced) require input that can only be obtained through costly experimental testing of the fully built building. For optimal benefit, building energy analysis is however usually performed during the design phase of a building rather than post construction. This drives users and designers to resort to a limited list of tabulated generic coefficients and data for use in analyses input. And results in dramatic inaccuracies in studying the building energy performance as has been demonstrated in this research.

In addition to the ease of use, simple interface, and quick simulation performance, the Enhanced Model can be easily integrated into existing simulation engines. The model's enhanced algorithm can be adopted and integrated into the hourly calculations of DOE-2, eQUEST and other similar programs as demonstrated in this research. Especially that all the hourly input values necessary for the Enhanced Model's calculations are already a part of the DOE-2 engine and other simulation engines' hourly calculations rather than being an added calculation load.



## **Infiltration Heat Recovery**

The phenomenon of infiltration heat recovery was discussed in Chapters 1 and 2. Conductive heat flowing through the building envelope interacts with air infiltrating through leakage paths in the envelope walls. This heat exchange allows the heating of cold infiltrating outside air as it leaks through the envelope into the building interior. This effect is reversed during the cooling season as discussed in Chapter 2. By the time the infiltrating air reaches the building interior its temperature is considerably warmer than its original outside air temperature.

The classical theory for evaluating infiltration heat loads was discussed in Chapters 1 and 2. It assumes that the temperature of infiltrating air remains equivalent to that of the outside air temperature. The outside ambient temperature is then used in calculating the inside/outside air temperature gradient used in calculating infiltration heat loads. However, due to the effect of heat recovery infiltrating air is expected to have a temperature closer to the indoor air temperature rather than the outside air temperature. Thus, using the outside air temperature in heat loading calculations results in errors in estimating the infiltration heat load. In our multiphysics hygrothermal CFD models we aimed at examining and validating the heat recovery phenomena. Our true multiphysics models allow a realistic evaluation of this phenomenon and its effect. Especially that these CFD simulations are of a full scale enclosed building envelope rather than of isolated portions of a standalone wall model.

The presence of heat recovery is clearly observed in the CFD simulations. All temperature contour plots taken at various lateral sections across each of the CFD models reveal the presence of air heating as air infiltrates through the building envelope. As

infiltrating air approaches the inner surface of the building envelope its temperature is observed to be significantly higher than its original outside ambient air temperature. In some instances it's observed to be very close and within few degrees from the indoor air temperature. A streamline is plot along the centerline of an individual straight crack across the building envelope. Chart 5-17 represents a plot of the rise in the infiltrating air temperature along this streamline as it flows across the building envelope. The variation in the flow velocity of the infiltrating air as it flows across the building envelope is shown in Chart 5-18. As shown in Chart 5-17, the air's temperature rises to within 5 degrees from the indoor air temperature.

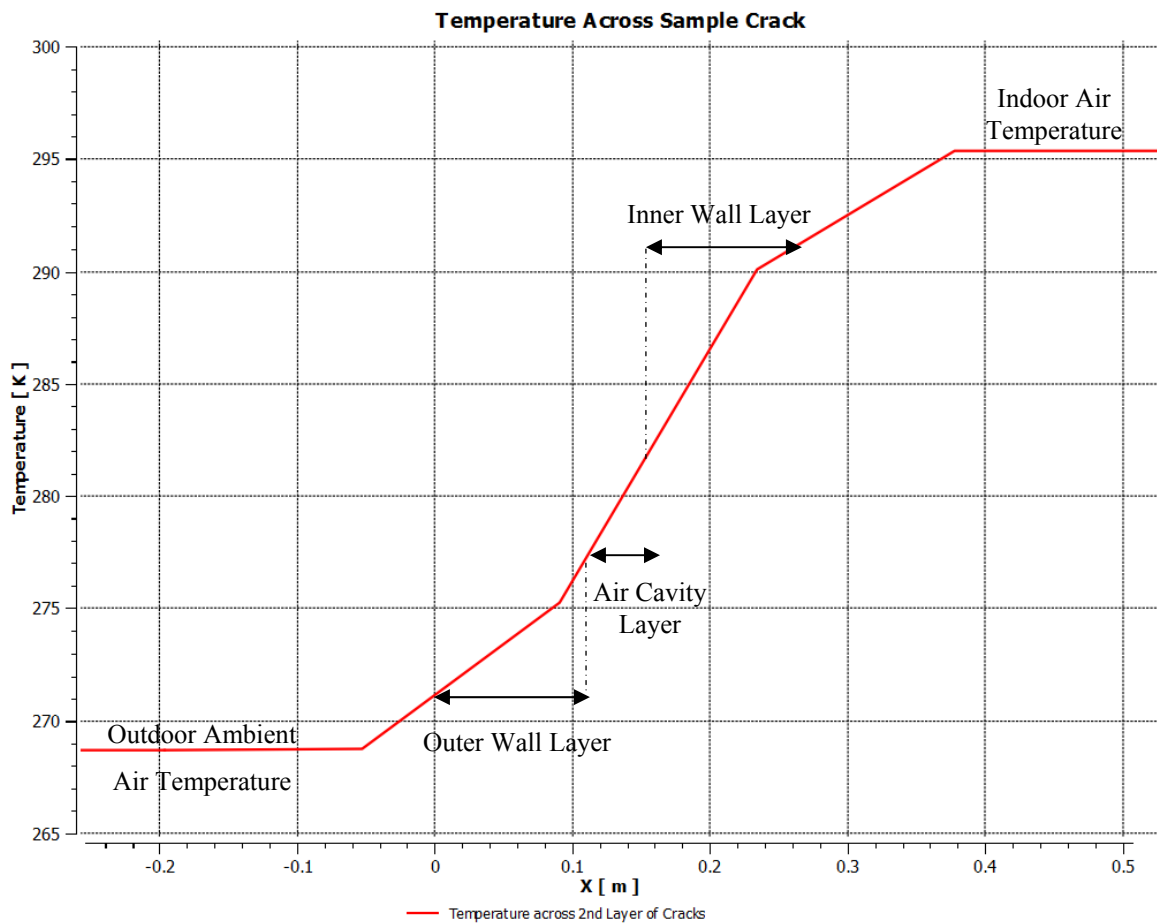


Chart 5-17: Infiltrating Air Temperature Rise Across the Building Envelope

Figures 5-1 to 5-3 are of temperature contour plots for various CFD models of various crack types and at various lateral section heights. Examining the air temperature variation as it flows through the leakage cracks reveals a gradual rise in the infiltrating air temperature. This is particularly observed as the air flows past the inner wall cavity and through the inner layer of the cavity wall. In parallel, Figures 5-4 to 5-7 show examples of the velocity and airflow vectors highlight air leakage flow through the cracks in the building envelope into the building interior. Both, Lateral and Vertical sample section plots are presented.

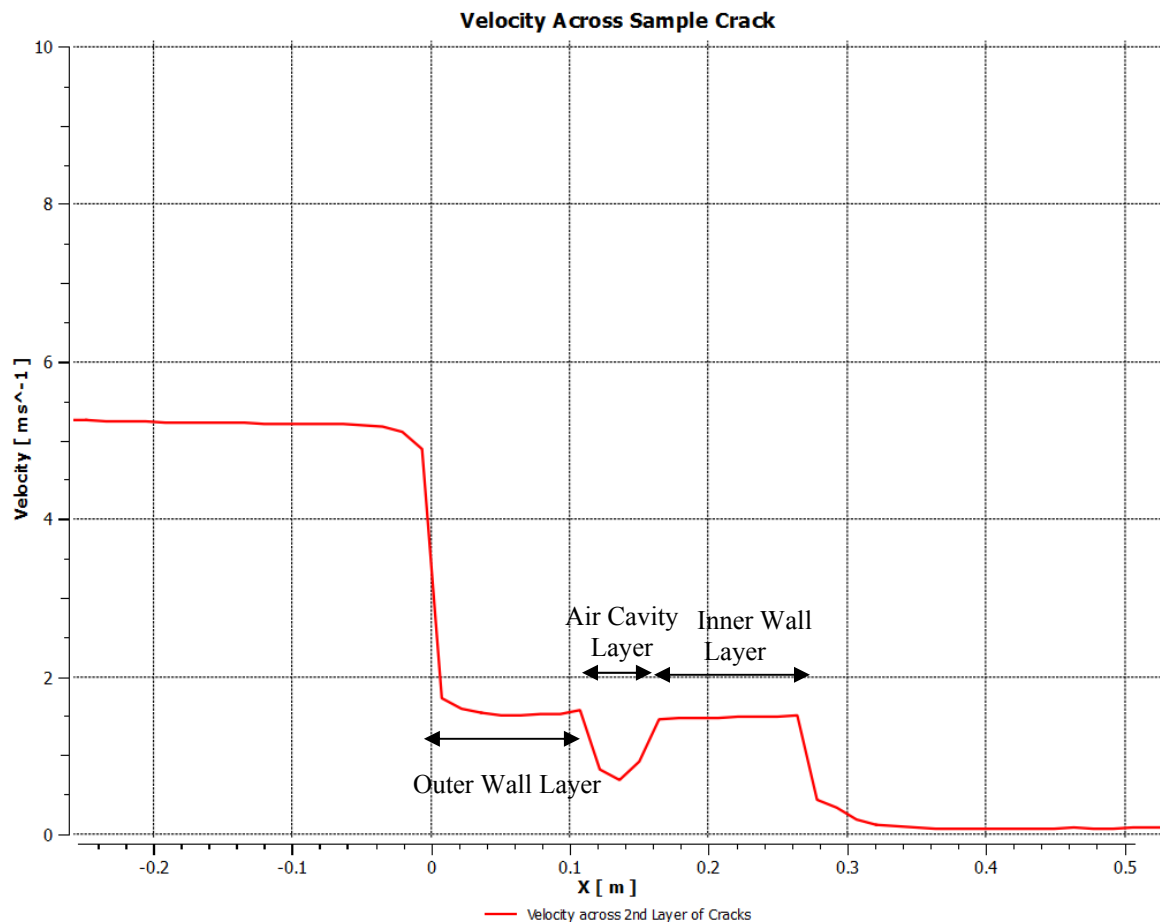


Chart 5-18: Infiltrating Air Velocity Drop Across the Building Envelope

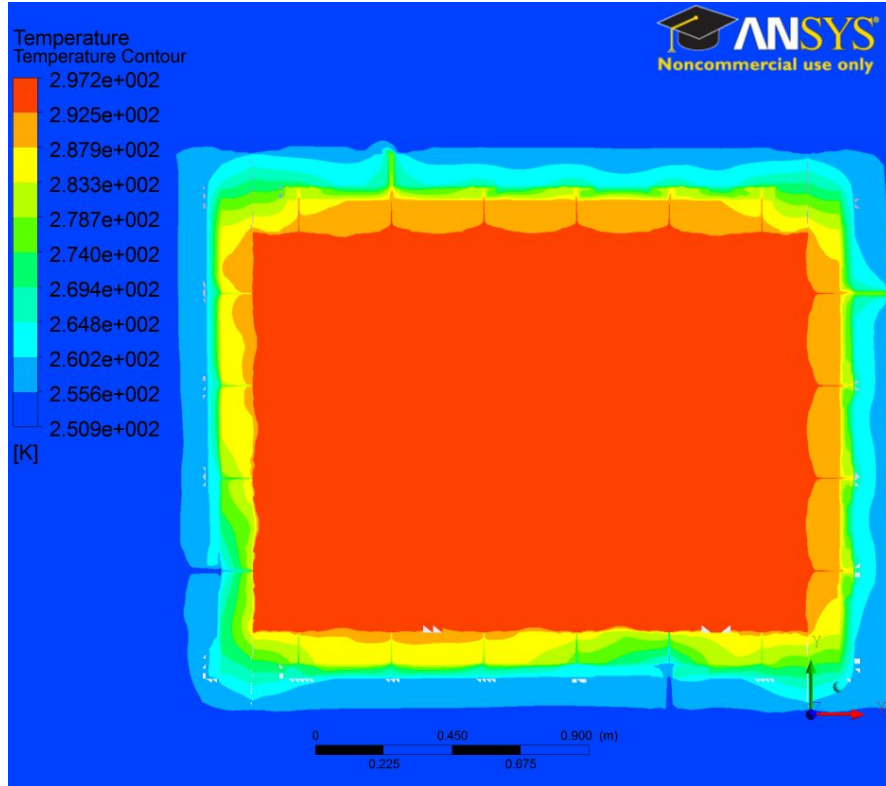


Figure 5-1: Lateral-Section Temperature Contour Plot Across a CFD Model with Angled (Zig-Zag) Cracks

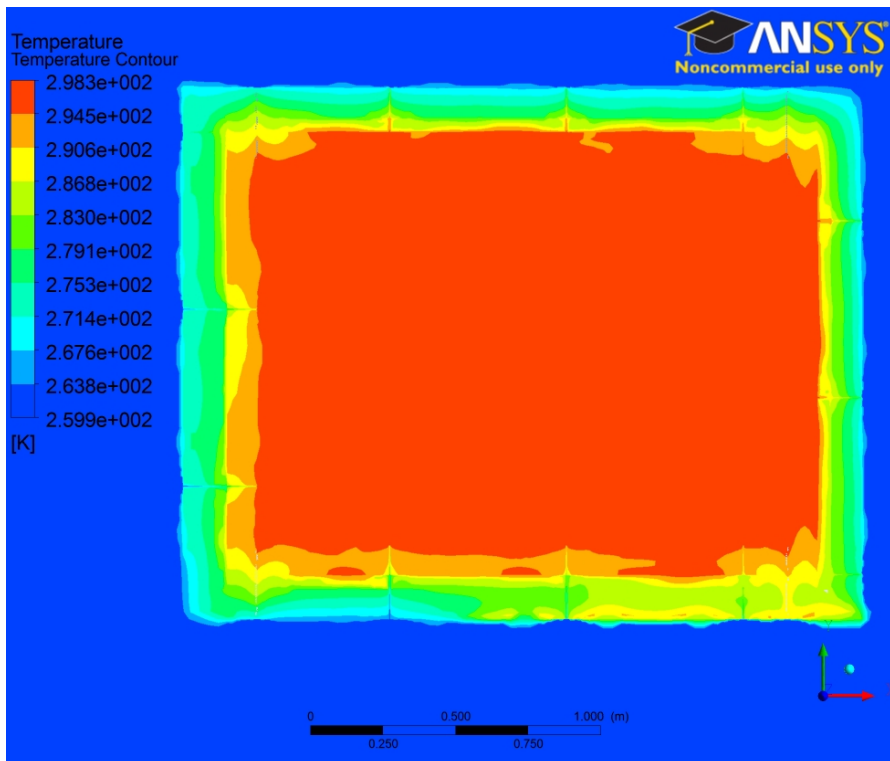


Figure 5-2: Lateral-Section Temperature Contour Plot Across a CFD Model with Mixed Cracks

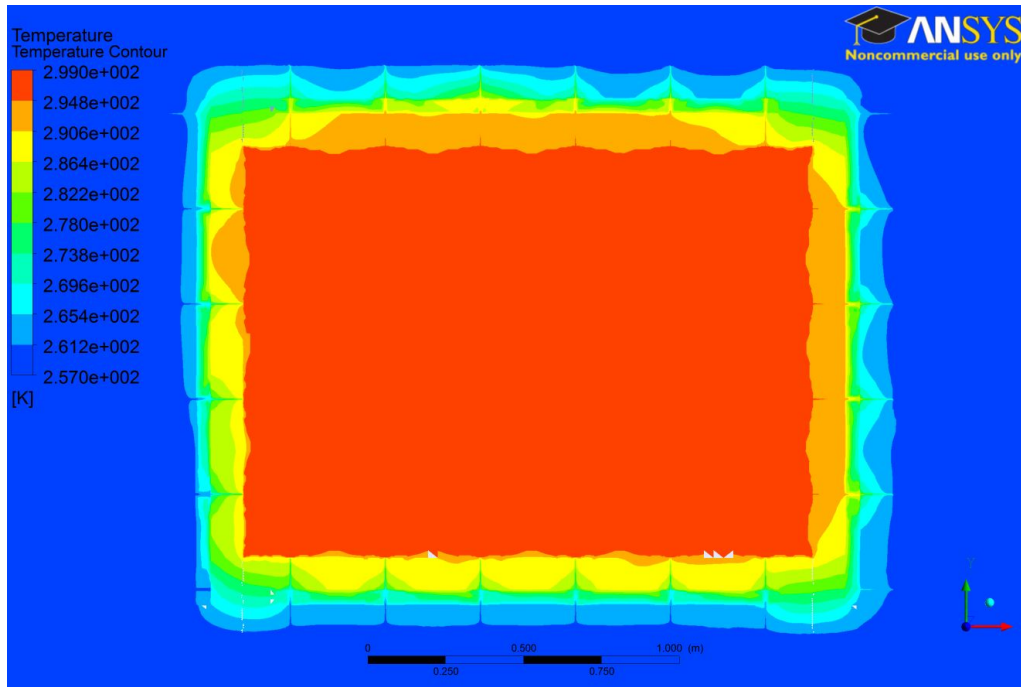


Figure 5-3: Lateral-Section Temperature Contour Plot Across a CFD Model with Straight Cracks

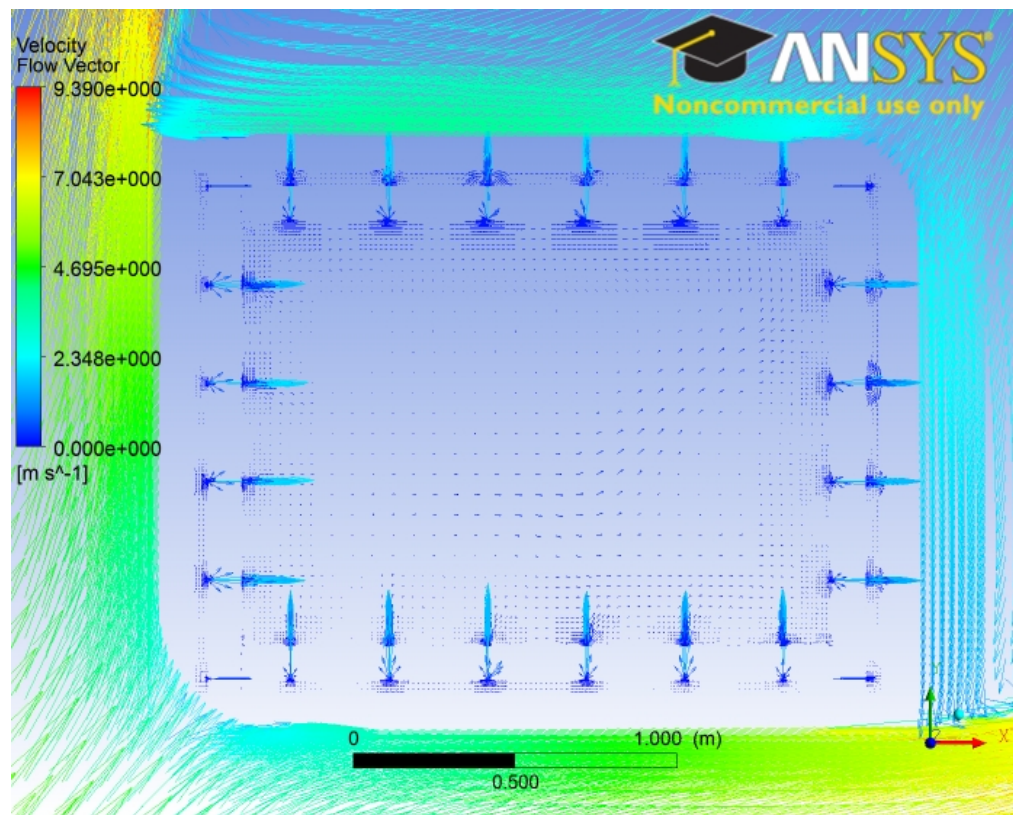


Figure 5-4: Lateral-Section Velocity Vector Plot Across a CFD Model with Angled (zig-zag) Cracks



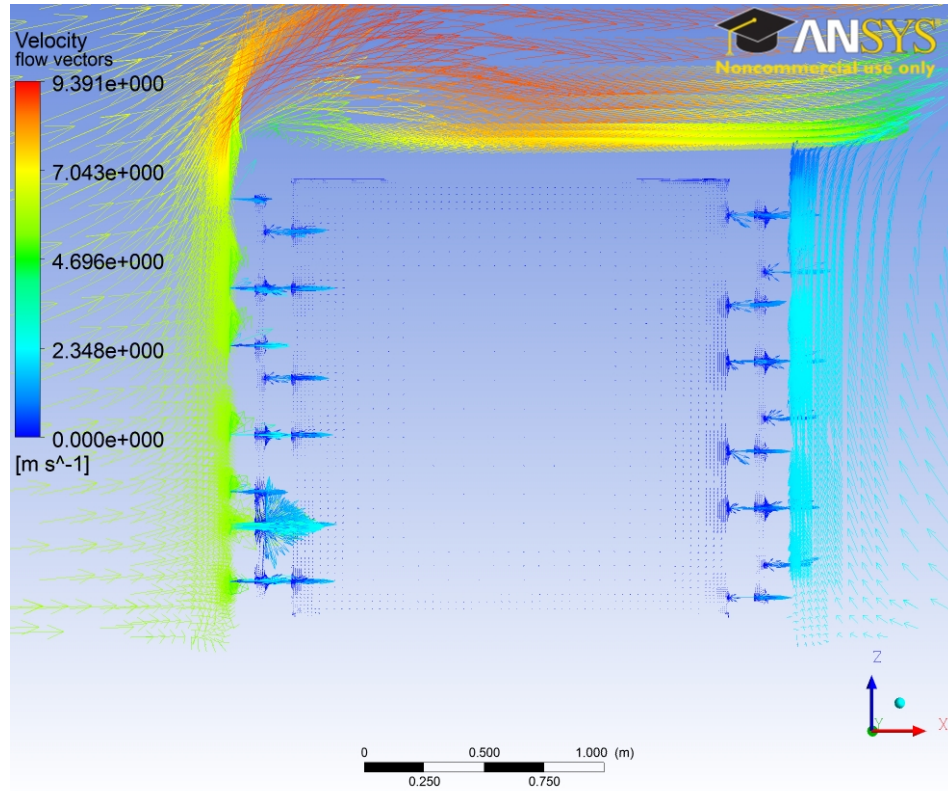


Figure 5-5: Vertical-Section Velocity Vector Plot Across a CFD Model with Mixed Straight and Angled Cracks

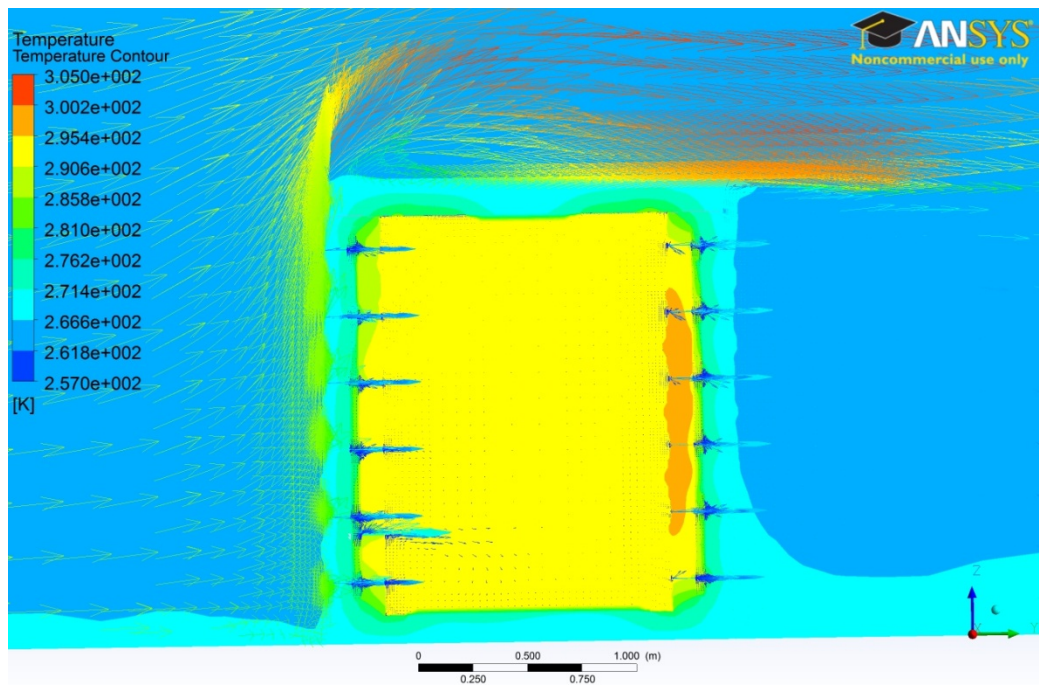


Figure 5-6: Vertical-Section Combined Velocity Vector and Temperature Contour Plot Across a CFD Model with Straight Cracks, with the Effect of Solar Heating Showing on the Envelope's Southern Wall

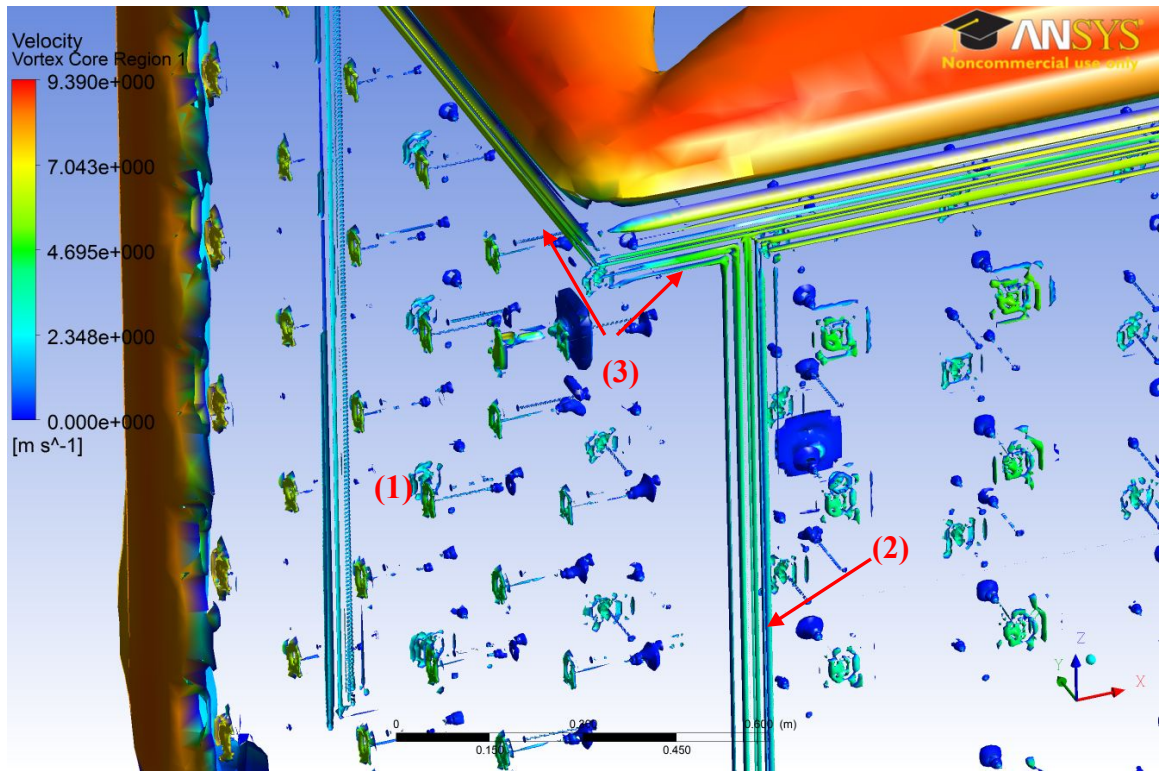


Figure 5-7: Vortex Plot Revealing Air Leakage Across In-wall Caracks (1), Corner Cracks (2) and Ceiling Joint Cracks (3)

## Chapter 6

### Conclusions and Recommended Future Work

Energy efficiency in general and building energy efficiency and design sustainability in particular continue to emerge as an increasingly critical concern. This is leading to an increasing need for tools to evaluate the energy demand and life span energy costs in buildings. As a result a large number of building energy analysis programs have been and continue to be developed and improved. These tools range between simple databases, component specific analysis tools, spreadsheets, and full building energy analysis programs. Advanced programs among these various tools provide detailed hourly energy analyses in buildings. In their analyses they account for various heat transfer phenomena including convection, conduction and incident solar heat. The ease of use and quick simulation speeds make them very popular among building energy modelers. They facilitate obtaining an energy demand analysis and facilitate performing parametric analyses that compare the energy efficiency of various design alternatives.

The primary reason for performing a building energy analysis is to obtain a solid understanding of a building's energy needs. This is particularly critical for designing an efficient HVAC system. As discussed in detail in Chapters 2 and 5, it is extremely critical and cost-wise significant to have a properly sized HVAC system. Expected life cycle energy costs are a leading driver of the need for a building energy analysis. The ability to study the efficiency of various design alternatives on energy demand is extremely essential for designers. It permits designers to reach a design that meets the building's



occupancy needs while optimizing its expected energy demand. This results in life time cost savings while insuring a comfortable living and working environment.

DOE-2 is a leading building energy analysis program. It is well known, widely used, and considered to be a standard for building energy simulation engines and software. DOE-2's powerful simulation engine has also been evolved to be incorporated into later and similarly popular energy simulation programs. A prominent example is eQUEST. It is based on the DOE-2 engine and coupled with wizards and graphics that facilitate its use through a GUI interface. The widespread use of these programs makes them of high significance and impact. Most importantly, it highlights the need for a high level of accuracy and reliability in their building energy simulations.

Building air leakage is a natural uncontrolled phenomenon in buildings. Air infiltration and leakage in buildings depends on various aspects of the building envelope. Construction materials and adopted construction methods are a primary factor. They provide the paths that allow air leakage through the building envelope. Air infiltration is primarily driven by the wind pressure on a building face and by other factors compiled as a driving stack pressure (stack effect). As discussed in Chapter 2, the energy toll of infiltration can represent as much as 50 % of the total energy demand in a building.

The experimentally proven significant energy impact of air infiltration was a driving reason for investigate current methods for calculating air infiltration energy loads on buildings. A primary source of interest are the methods utilized in widely used simulation engines such as DOE-2. After these methods' accuracy is evaluated, an enhanced infiltration load calculation method to improve accuracy was to be developed if

deemed necessary. The developed Enhanced Model would also be easy to adopt and incorporate into other software and energy simulation models.

In order to verify the accuracy of both the existing models and the proposed model's experimental data is necessary. Due to the lack of experimental data, a Multiphysics Hygrothermal CFD model was developed and used to provide the necessary verification data. The constructed model is based on actual experimentally obtained building properties and data. Hundreds of representative cracks were embedded into the various components of the building envelope. The cracks quantification is based on experimental databases such as the AIVC database, on data obtained from research on cracking in buildings, and on available ASHRAE data. Considered factors in the multiphysics CFD model include: solar radiation, variable outside temperature, wind velocity, variable material properties, thermostat settings, construction methods, and others. Three main CFD models are constructed reflecting the different variations of cracking patterns in building envelopes.

Transient hourly analysis on the CFD models versus DOE-2/eQUEST analyses results revealed large inaccuracies in calculated infiltration loading in these simulation engines. Several of the methods available in DOE-2 were simulated and compared with CFD analyses results. The methods ranged between the basic Air Change method and the more advanced ASHRAE Enhanced method. As discussed in detail in Chapter 5, underestimation of infiltration heat loading by these methods ranged between 85.70 % and 96.13 % (underestimation error).

Developing and enhanced infiltration load calculation model was therefore deemed necessary. The model has to improve infiltration heat loading calculations

accuracy. It also has to maintain the speed and ease of use advantage of current methods versus complex CFD analysis. A combined conduction, air infiltration, and solar radiation model was developed. The model accounts for heat recovery and exchange. This heat interaction occurs as air leaks through the walls of the building envelope. The Enhanced Model also considers the effect of solar air heat. Finally, it performs hourly heat load calculation in accordance with advanced full hourly building energy analysis programs such as DOE-2.

The Enhanced Model resulted in a 91.63% increase in the relative accuracy of calculated building infiltration loads. As discussed in details in Chapter 5, the relative error in heat loading calculations was reduced to a below 4.5 % when compared to all CFD analyses results. Another important aspect is the ability of the Enhanced Model to maintain the speed and ease of use characteristics of current methods. The Enhanced Model closely attains the simulation results of a complex multiphysics hygrothermal CFD analysis while requiring less than 1 % of the time necessary to run a CFD analysis.

In conclusion, the developed Enhanced Model for combined heat and air infiltration simulation is successful. It meets all the stated requirements of increased accuracy, ease of use, and speed of calculations. The developed algorithms are easy to apply into any other building energy simulation program in the same manner as demonstrated in this research on the DOE-2 engine through eQUEST.

Improving by 91.63 % the relative accuracy of calculating a component that represents 40 % to 50 % of the energy demand in buildings is extremely significant. This improvement in calculating building infiltration heat loads will help designers design more efficient building HVAC systems. It also paves the path for incorporating more

sustainable building design practices and components. Examples include controllable ventilation rates, optimal insulation distribution, effective utilization of solar energy, healthier building indoor environments, and others.

### **Fulfilled Research Objectives**

The main objective of this research was broken down into five specific objectives that needed to be fulfilled to meet the main objective of this work. In Chapter 2 a comprehensive review of infiltration and how it is accounted for in current models and in prominent building energy simulation software was performed. Also was a study of the latest research on studying the interaction between infiltration, conduction and solar radiation. Objective two was also met by developing a Mass Flow rate model in Chapter 3 and implementing it in the Visual Basic built program and interface we presented in Chapter 5. Similarly the third objective was met by building a Visual Basic program and interface based on the algorithms and equations of the Enhanced Model presented in Chapter 3. Another achievement of this research was to develop a geometry building technique, a meshing method, and a simulation approach for performing full 3D multiphysics hygrothermal CFD simulations of air leakage in building envelopes. This also allowed obtaining the data necessary to calibrate and validate the relative accuracy of the developed enhanced model in accordance with objective four of this research. In Chapter 5 the relative accuracy (versus the complex CFD analysis) of the developed Enhanced Model was compared to the relative accuracy of current DOE-2 methods in calculating infiltration heat loads. As discussed previously in detail, the Enhanced Model achieved less than 4.5% relative error versus the results of a complex CFD analysis while requiring less than 1 % of time necessary for performing a CFD analysis. This

represented up to 91.63 % improvement in relative accuracy versus currently available methods and a fulfillment of the fifth objective of this research.

### **Recommended Future Work**

In this research, the accuracy of the developed enhanced model was verified relative to a developed multiphysics hygrothermal CFD model. A critical follow up research to this work would be to perform experimental validation. The same test case simulated by the three models (DOE-2, Enhanced Model, and CFD) would be constructed with identical construction characteristics and material and then tested experimentally. The built envelope should be instrumented with necessary data collection devices to obtain all the required experimental data. This could be done in a full scale testing facility with capabilities to induce variable wind flow along with a heat source representing solar radiation. The Wall of Wind experimental testing facility at Florida International University is an ideal facility for performing these experimental tests. It allows subjecting a building envelope to a variable wind velocity, at variable wind angles (wind direction), with adjustable heat elements to represent solar radiation for variable longitudes and latitudes. The collected experimental data will help calibrate and validate the developed Enhanced Model. This is essential for supporting the use of the Enhanced Model as a new and more accurate method for evaluating infiltration heat loads. The experimental data can also be used to validate the CFD analyses performed. As discussed previously, special techniques for building, meshing and simulating 3D multiphysics hygrothermal CFD simulations of air infiltration were developed in this work. Experimentally validating this methodology for 3D CFD simulations of air infiltration

allows for higher confidence in the results of CFD analyses of air infiltration. Once validated experimentally these CFD analyses can be more confidently used in further research as a more cost and time efficient alternative to experimental testing.

Further research also should include testing the enhanced model and also performing CFD analyses for a test case located in a different climate. The current test case was located in Fargo, North Dakota in a cold, windy and snowy climate. The location for a future test case could be in a city with a warmer or subtropical weather. This will help validate the relative accuracy of the Enhanced Model in various climates. Most importantly, it will also highlight the role of the solar radiation as part of the interaction of the various heat phenomena, as discussed in this research and defined in the Enhanced Model's equations and algorithm.

## References

U.S. Energy Information Administration. (2009). Annual Energy Outlook 2010. Retrieved September 2010, from U.S. Energy Information Administration.

U.S. Energy Information Administration. (2010, September). Energy Overview. Retrieved September 2010, from U.S. Energy Information Administration/ Monthly Energy Review September 2010: <http://www.eia.doe.gov/mer/overview.html>

Achenbach, P. R., & Coblenz, C. W. (1963). Field Measurement of Air Infiltration in Ten Electrically Heated House. ASHRAE Transactions , 358-365.

Allard, F., & Herrlin, M. (1989). Wind-induced ventilation. ASHRAE Transactions , 95 (2), 722-728.

American Society of Heating, Refrigerating, and Air-Conditioning Engineers, Inc. (1977). Chapter 25. In R. a.-C. American Society of Heating, ASHRAE Handbook and Product Directory, 1977 Handbook of Fundamentals. New York, NY: American Society of Heating, Refrigerating, and Air-Conditioning Engineers, Inc.

American Society of Heating, Refrigeration, and Air-Conditioning Engineers. (1977). ASHRAE 1977 Hanbook of Fundamentals. New York: American Society of Heating, Refrigeration, and Air-Conditioning Engineers.

American Society of Heating, Refrigerating and Air-Conditioning Engineers. (2009). Chapter 16 : Ventilation and Infiltration. In 2009 ASHRAE Handbook - Funamentals (pp. 16.1 - 16.36). Atlanta, GA: American Society of Heating, Refrigerating and Air-Conditioning Engineers, Inc.

American Society of Heating, Refrigerating and Air-Conditioning Engineers. (2007). Chapter 43 : Building Envelopes. In 2007 ASHRAE Handbook - HVAC Applications (pp. 43.1 - 43.12). Atlanta, GA: American Society of Heating, Refrigerating and Air-Conditioning Engineers, Inc.

Anderlind, G. (1985). Energy consumption due to air infiltration. Proceedings of the 3rd ASHRAE/DOE/BTECC Conference on Thermal Performance of Exterior Envelopes of Buildings, (pp. 201-208). Clear Water Beach, FL.

Anon. (1937). Fireplace - Does it add to or subtract from the total heat ? Domestic Engineers , 149 (1), 85-93.

ANSYS® Academic Research, Release 14.0, Help System, ANSYS, Inc., 2011

Arasteh, D. K., Selkowitz, S., & Hartman, J. (1985). A versatile procedure for calculating heat transfer through windows. Proceedings of the 3rd ASHRAE/DOE/BTECC

Conference on Thermal Performance of Exterior Envelopes of Buildings, (pp. 830-845). Clear Water Beach, FL.

Arquis, E., & Langlais, C. (1986). What Scope for Dynamic Insulation ? *Batiment International Building Research and Practice* , 19, 84-93.

ASHRAE Task Group on Energy Requirements for Heating and Cooling of Buildings. Procedure for Determining Heating and Cooling Loads for Computerizing Energy Calculations. Algorithms for Building Heat Transfer Subroutines. (M. Lokmanhekim, Ed.) New York, NY: American Society of Heating, Refrigerating, and Air-Conditioning Engineers, Inc.

Automated Procedures for Engineering Consultants, Inc. (November 1967). HCC-Heating/Cooling Load Calculation Program. Dayton, Ohio.

Bailly, N. R. (1987). Dynamic Systems and Energy Conservation in Buildings. *ASHRAE Transactions* , 93 (1), 447-466.

Beyea, J., Dutt, G., & Wotecki, T. (1977). Critical Significance of Attics and Basements in the Energy Balance of Twin Rivers Townhouses. *Energy and Buildings* , 1, 261-269.

Bhattacharyya, S. (1999). Modelling and the phenomenon of infiltration heat exchange. *International journal of power & energy systems* , 19 (1), 87-91.

Bhattacharyya, S., & Claridge, D. E. (1995). Energy impact of air leakage through insulated walls. *Journal of Solar Energy Engineering* , 117 (3), 167-172.

Bhattacharyya, S., & Claridge, D. E. (1992). The energy impact of air leakage through insulated walls. *Solar Engineering* , 1, 451-458.

Blomsterberg, A. K., & Harrje, D. T. (1979). Approaches to evaluation of air infiltration energy losses in buildings. *ASHRAE Transactions* , 85 Part I, 797.

Blomsterberg, A. K., & Harrje, D. T. (1979). Reduction of Air Infiltration Due to Window and Door Retrofits in an Older Homes, Report PU/CEESS 85. Princeton University, Center of Environmental Studies.

Bobenhausen, W. (1994). Heat Loss from Buildings. In W. Bobenhausen, *Simplified Design of HVAC Systems* (pp. 63-93). U.S.A.: John Wiley & Sons, Inc.

Brownell, C. (2002). Infiltration Heat Recovery.

Buchanan, C. R., & Sherman, M. H. (2000). A Mathematical Model for Infiltration Heat Recovery, LBNL-44294. Lawrence Berkeley National laboratory, Indoor Environment Department.



Buchanan, C. R., & Sherman, M. H. (September 28-30, 1998). CFD Simulation of Infiltration Heat Recovery. Proceedings of the 19th AIVC Annual Conference on Ventilation Technologies in Urban Areas. Oslo, Norway.

Building Energy Software Tools Directory: DOE-2. (2008, Month August). Retrieved October 4, 2010, from DOE-2:  
[http://apps.1.eere.energy.gov/buildings/tools\\_directory/software.cfm/ID=34](http://apps.1.eere.energy.gov/buildings/tools_directory/software.cfm/ID=34)

Building Energy Software Tools Directory: eQuest. (2008, August 8). Retrieved October 4, 2010, from eQUEST:  
[http://apps.1.eere.energy.gov/buildings/tools\\_directory/software.cfm/ID=575](http://apps.1.eere.energy.gov/buildings/tools_directory/software.cfm/ID=575)

Boussa, H., Tognazzi-Lawrence, C., & La Borderie, C. (2001). A model for computation of leakage through damaged concrete structures. *Cement & Concrete Composites*, 23 (2001), 279-287

Building Technologies Program: Building Energy Software Tools Directory. (2010, September 9). Retrieved October 4, 2010, from  
[http://apps.eere.energy.gov/building/tools\\_directory](http://apps.eere.energy.gov/building/tools_directory)

Burns, P., & Deru, M. (2003). Infiltration and Natural Ventilation Model for Whole-Building Energy Simulation of Residential Buildings NREL/CP-550-33698. Midwest Research Institute. National Renewable Energy Laboratory.

Caffey, G. E. (1979). Residential Air Infiltration. *ASHRAE Transactions*, 85, 919-926.

Chebil, S., Galanis, N., & Zameureanu, R. (2003). Computer Simulation of Thermal Impact of Air Infiltration Through Multilayered Exterior Walls. Proceedings of the Eighth International IBPSA Conference. Eindhoven, Netherlands, 2003

Claridge, D. E., & Bhattacharyya, S. (1990). The Measured Energy Impact of "Infiltration" in a Test Cell. *ASME Journal of Solar Energy Engineering*, 112, 132-139.

Claridge, D. E., & Bhattacharyya, S. (April 1989). The measured energy impact of "infiltration" in a test cell. Proceedings of the Eleventh Annual ASME Solar Energy Conference. San Diego, CA.

Claridge, D. E., & Liu, M. (1996). The measured Energy Impact of Infiltration in an Outdoor Test Cell. *Journal of Solar Energy Engineering*, 118 (3), 162-167.

Claridge, D. E., Jeon, H., & Bida, M. (1985). A Comparison of Traditional Degree-Day and Variable-Base Degree-Day Prediction with Measured Consumption of 20 Houses in the Denver Area. *ASHRAE Transactions*, 91 (2), 865-874.

Claridge, D. E., Liu, M., & Bhattacharyya, S. (1995). Impact of air infiltration in frame walls on energy loads: taking advantage of the interaction between infiltration, solar radiation, and conduction. ASTM Special Technical Publication (1255), 178-196.

Clarke JA, Dempster WM and Negrao COR (1995) The implementation of a computational fluid dynamics algorithm within ESP-r system. Building Simulation 95 Conference, Madison, Wisconsin, USA, August 14–16.

Cole, J. T., Zawacki, T. S., Elkins, R. H., Zimmer, J. W., & Macriss, R. A. (1980). Application of a generalized model of air infiltration to existing homes. ASHRAE Transactions , 86 (2), 765.

Crall, C. (1983). Development of the Air Infiltration Model for the Energy Performance Design System. ASHRAE Transactions , 89 (2), 201-210.

Danko, G., & Bahrami, D. (July 2004). Heat and Moisture Flow Simulation with Multiflux. Proceedings of ASME Heat Transfer/Fluid Engineering. July 11-15, 2004, Charlotte, North Carolina, USA

Dickerhoff, D. J., Grimsrud, D. T., & Lipshutz, R. D. (1982). Component leakage testing in residential buildings, Report LBL 14735. Proceedings of the American Council for an Energy-Efficient Economy, 1982 Summer Study, Santa Cruz, CA, Lawrence Berkeley National Laboratory, Berkeley, CA.

Dickson, D. J. (1988). Infiltration rates in low energy house with a fireplace. The International Journal of Research, Development and Demonstration , 21 (4), 237-245.

DOE2.com Home Page. (2010). Retrieved October 4, 2010, from Welcome to DOE2.com The Home of DOE-2 Based Building Energy Use and Cost Analysis Software: <http://www.doe2.com>

Duffet-Smith, P. (1988). Practical astronomy with your calculator (Third Edition ed.). Cambridge, Great Britain: Cambridge University Press.

Elkins, R. H., & Wensman, C. E. (February 28- March 3, 1971). Natural Ventilation of Modern Tightly Constructed Homes. Paper presented at the American Gas Association - Institute of Gas Technology, Conference on Natural Gas Research and Technology. Chicago, Illinois.

eQUEST. (2010). Retrieved October 4, 2010, from eQUEST the Quick Energy Simulation Tool: <http://doe2.com/equest/index.html>

Etheridge, D. W. (1977). Crack flow equations and scale effect. Building and Environment , 12, 181.

- Etheridge, D. W. (1988). Modeling of air infiltration in single and multi-cell buildings. *Energy and Buildings* , 10 (3), 185-192.
- Etheridge, D. W., & Alexander, D. K. (1980). The British gas multi-cell model for calculating ventilation. *ASHRAE Transactions* , 86 (2), 808.
- Feustel, H. E., & Kendon, V. M. (1985). Infiltration Models for Multicellular Structures - A literature Review. *Energy and Buildings* , 8 (2), 123-136.
- Feustel, H. E., & Rayner-Hooson, A. (1990). COMIS Fundamentals, LBL-28560. Applied Science Division, Lawrence Berkeley National Laboratory, Berkeley, CA.
- Fuller, L. R. (1949). How to figure heating for store entrances. *Heating, piping and air conditioning* , 21 (4), 79-81.
- Grenville, Y. (2000). Air leakage through automatic doors. *ASHRAE Transactions* , 106, 145-160.
- Grot, R. A., & Clark, R. E. (1986). Measured air infiltration and ventilation rates in eight large office buildings, STP 904. In H. R. Treschel, & P. Lagus, *Measured air leakage of buildings* (p. 151). West Conshohocken, PA: American Society of Testing and Materials.
- Guo, J., & Liu, M. (August 1985). The energy saving effect of double frame windows. *Proceedings of the CLIMA 2000 World Congress in Heating, Ventilating and Air-Conditioning*, Vol. 2. Copenhagen.
- Haghighat, H., & Li, H. (2004). Building Airflow Movement-Validation of Three Airflow Models. *Journal of Architectural Planning Research*, 21 (4), 331-349
- Harrje, D. T., & Blomsterberg, A. K. (1979). Approaches to evaluation of air infiltration energy losses in buildings. *ASHRAE Transactions* , 85 (1), 797-815.
- Harrje, D. T., & Born, G. J. (1982). Cataloguing air leakage components in houses. *Proceedings of the American Council for an Energy-Efficient Economy, 1982 Summer Study*, Santa Cruz, CA. Washington, D.C.: American Council for an Energy-Efficient Economy.
- Harrje, J., Dutt, G., & Beyea, J. (1979). Locating and Elimination Obscure but Major Energy Losses in Residential Housing. *ASHRAE Transactions* , 85 (2), 521-559.
- Herrlin, M. K. (1985). MOVECOMP: A static-multicell-airflow-model. *ASHRAE Transactions* , 91 (2B), 1989.
- Hill, J. E., & Kusuda, T. (1975, June). Dynamic Characteristics of Air Infiltration. *ASHRAE REPORT #2337*, Presented at Boston, Mass., Annual Meeting .

- Hong, T., Mathew, P., Sator,D., & Yazdanian, M. (2009). Comparisons of HVAC Simulations between Energy Plus and DOE-2.2 for Data Centers. ASHRAE Transactiona , CH-09-039, 373-6381.
- Hopkins, L.P., & Hansford, B. (1974). Air flow through cracks. The Building Service Engineer, 42, 123-131
- Infiltration through doors. (1937). Heating and ventilating , 34 (8), 2-2.
- Jackman, P. (1974). Heat loss in buildings as a result of infiltration. The Building services engineer , 42, 6-15.
- James J. Hirsch & Associates. (April 2009). Q eQUEST Introductory Tutorial, version 3.63. Camarillo, CA: James J. Hirsch & Associates.
- James J. Hirsch & Associates. (May 2007). Q eQUEST Modeling Procedures Quick Reference Guide. Camarillo, CA: James J. Hirsch & Associates.
- Jayaraman B, Lorenzetti D and Gadgil A (2004) Coupled model for simulation of indoor airflow and pollutant transport. Lawrence Berkeley National laboratory, Berkeley, CA, USA.
- Jordon, R. C., Erickson, G. A., & Leonard, R. R. (1963). Infiltration Measurements in Two Research Houses. ASHRAE Report , Vol. 69, p. 344.
- Kerrisk, J. F., Moore, J.E., Schnurr, N.M. & Hunn, B. D. (1980). Passive Solar Design Calculations with the DOE-2 Computer Program, Los Alamos Scientific Laboratory , Fifthe National Passive Solar Conference, Amhert, Massachussets, October 19-26
- Kirkwood, R. C. (1977). Fuel consumption in industrial buildings. Building Services Engineer , 45.
- Klems, J. H. (1983). Methods of Estimating Air Infiltration through Windows. Energy and Buildings , 5 (4), 243-252.
- Kohonen, R. (1985). Thermal effects of airflows and moisture on exterior wall structures. Proceedings of the 3rd ASHRAE/DOE/BTECC conference on Thermal Performance of Exterior Envelopes of Buildings, (pp. 583-605). Florida.
- Kohonen, R., & Virtanem, M. (1987). Thermal coupling of leakage flows and heating load of buildings. ASHRAE Transactions , 93, 2303-2318.
- Kronvall, J. (1980). Correlating pressurization and infiltration rate data tests of an heuristic model. Lund, Sweden.

- Kusuda, T. (November 1974). NBSLD, Computer Program for Heating and Cooling Loads in Buildings. National Bureau of Standards, Washington, D.C.
- Lau, H., & Ayres, J. M. (1979). Building Energy Analysis Programs. Winter Simulation Conference, (pp. 283-289).
- Lawrence Berkeley National Laboratory ; James J. Hirsch & Associates. (March 2009). DOE-2.2 Building Energy Use and Cost Analysis Program (Vol. 2: Dictionary). Camarillo, CA.
- Liddament, M. (1983). The Air Infiltration Center's Program of Model Validation. ASHRAE transactions , 89 (2), 129-145.
- Liddament, M. W. (June 1986). Air Infiltration Calculation Techniques - An Application Guide. University of Warwick. Coventry, Great Britain: The Air Infiltration and Ventilation Center.
- Liddament, M., & Allen, C. (1983). The validation and comparison of mathematical models of air infiltration. Technical Note 11, International Energy Agency Air Infiltration and Ventilation Centre, Sint-Stevens-Woluwe, Belgium.
- Liu, D.L., & Nazaroff, W.W. (2001). Modeling Pollutant Penetration Across Building Envelopes, Atmospheric Environment, 35, 4451-4462
- Liu, D.L. (2002). Air Pollutant Penetration through Airflow Leaks into Building. Ph.D. Dissertation, Department of Civil and Environmental Engineering, University of California Berkeley
- Liu, M. (1992). Study of Air Infiltration Energy Consumption. Ph.D. Dissertation, Texas A&M University, Department of Mechanical Engineering.
- Liu, M. (1987). Thermal Techniques in Buildings. Harbin Architectural and Civil Engineering Institute Press, Harbin, China. pp 3.85-3.90.
- Liu, M., & Claridge, D. E. (1995). Heat flux error of steady-state method for building components under dynamic conditions. Journal of Solar Engineering , 1, 219-227.
- Liu, M., & Claridge, D. E. (1992). The energy impact of combined Solar-Radiation/Infiltration/Conduction effects in Walls and Attics. Thermal performance of the exterior envelopes of buildings V : proceedings of the ASHRAE/DOE/BTECC Conference, December 7-10, 1992, Clearwater Beach, Florida.
- Lokmanhekim, M.; et. al. (August 1971). Computer Program for Analysis of Energy Utilization in Postal Facilities. U.S. Postal Service Symposium, (pp. Vols. I, II and III). Washington, D.C.

- Los Alamos National Laboratory & Lawrence Berkeley Laboratory. (1982). DOE-2 ENGINEERS Manual, Version 2.1A. (D. A. York, & C. C. Cappiello, Eds.)
- Loutzenhiser, P.G., & Maxwell, G.M. (2006). Comparisons of DOE-2.1E Daylighting and HVAC System Interactions to Actual Building Performance. ASHRAE Transactions , QC-06-037, 409-417.
- McAdams, W. H. (1954). Heat Transmission. pp. 55-82 and 165-183. New York, NY: McGraw-Hill Book Co., Inc.
- McQuiston, F. C., Parker, J. D., & Spitler, J. D. (2000). Heating, ventilating and air conditioning - analysis and design. New York: John Wiley & Sons.
- Melden, R., and Winkelmann, F. (1998). Comparison of DOE-2 with Temperature Measurements in the Pala Test Houses. Energy and Buildings , 27 (1998), 69-81.
- Min, T. C., & Auburn, A. (1958). Winter Infiltration Through Swinging-Door Entrances in Multi-Story Buildings. Heating, Piping & Air Conditioning , 30 (2), 121-128.
- Mora, L., Gadgil, A.J., & Wurtz, E. (2003). Comparing zonal and CFD model predictions of isothermal indoor airflows to experimental data. Indoor Air, 13, 77-85.
- Murray, C. D., & Dermott, S. F. (1999). Solar System Dynamics. Cambridge: Cambridge University Press.
- Negrao COR (1998) Integration of computational fluid dynamics with building thermal and mass flow simulation. Energy and Buildings 27(2): 155–165
- Nevrala, D. J., & Etheridge, D. W. (1977). Natural ventilation in well-insulated houses. Proceedings of International Centre for Heat and Mass Transfer, International Seminar, UNESCO, Volume 3.
- NIST estimates nationwide energy impact of air leakage in U.S. buildings. (1996). Journal of Research of the NIST , 101 (3), 413.
- Orme, M., Liddament, M. W., & Wilson, A. (1998). Numerical Data for Air Infiltration & Natural Ventilation Calculations. International Energy Agency, Air Infiltration and Ventilation Centre. Technical Note AIVC 44. Coventry, Great Britain.
- Orme, M. S. (1994). Applications of the Air Infiltration and Ventilation Centre's Numerical Database. Air Infiltration and Ventilation Centre, University of Warwick Science Park, Coventry, United Kingdom.
- Paradis, R. (2010). Energy Analysis Tool : Whole Building Design Guide. Retrieved October 4, 2010, from Energy Analysis Tools: <http://www.wbdg.org/resources/energyanalysis.php>

- Persily, A. K., & Grot, R. A. (1986). Resserization testing of federal buildings, STP 904. In H. R. Treschel, & P. Lagus, Measured air leakage of buildings (p. 184). West Conshohocken, PA: American Society of Testing and Materials.
- Persily, A. (1982). Understanding Air Infiltration in Homes. Report PU/CEES # 129, Princeton University Center for Energy and Environmental Studies, Princeton, New Jersey.
- Peterson, J. (1979). ASHRAE Journal , 21, 60.
- Peterson, S. (n.d.). National Bureau of Standards.
- Reeves, G., McBride, M. F., & Sepsy, C. (1979). Air infiltration model for residences. ASHRAE Transactiona , 85 (1), 667-677.
- Robert, R. H., & Reinauer, R. H. (1981). SIZING OF RESIDENTIAL HEATING EQUIPMENT. Proceedings of the American Gas Association, Operating Section (pp. D. 73-D. 75). Atlanta, Ga and Anaheim, Calif, USA: American Gas Association.
- Ross, H. D., & Grimsrud, D. T. (1978). Air Infiltration in Buildings: Literature Survey and Proposed Research Agenda. Lawrence Berkeley Laboratory Report LBL-7822 .
- Schutrum, L. F., Ozisik, N., Humphreys, C. M., & Baker, J. T. (1961). Air infiltration through revolving doors. ASHRAE Journal , 3 (11).
- Selkowitz, S. E. (1979). Thermal performance of insulating window systems. ASHRAE Transaction , 85 (2), 669-685.
- Shaw, C. Y. (1981). A correlation between air infiltration and air tightness for a house in a developed residential area. ASHRAE Transactions , 87 (2), 333.
- Sherman, M. H., & Grimsrud, D. T. (1980). Infiltration-pressurization correlation: Simplified physical modeling. ASHRAE Transactions , 86 (2), 778.
- Sherman, M. H., & Modera, M. P. (1986). Comparison of Measured and Predicted Infiltration Using the LBL Infiltration Model. Proceedings Measured Air Leakage of Buildings (pp. 325-347). Philadelphia: ASTM STP 904 ASTMS.
- Sherman, M., & Matson, N. (1993). Ventilation-Energy liabilities in U.S. dwellings. Proceedings of the 14th AVIC Conference: Energy impact of ventilation and air infiltration, September 21-23, (pp. 23-41). Copenhagen.
- Sherman, M., & McWilliams, J. (2007). Air Leakage of U.S. Homes: Model Prediction. Lawrence Berkeley Natioanl Laborator Report LBNL-62078. Lawrence Berkeley Laboratory, Berkeley, CA.

- Simpson, A. M. (1936). Infiltration characteristics of entrance doors. *Refrigerating Engineering* , 31 (6), 345-350.
- Simpson, A. M. (1936, November). New data on entrance door infiltration with air conditioning. *American Architect and Architecture* , 85-88.
- Stam J (1999) Stable Fluids. Proceedings of the 26th international conference on computer graphics and interactive techniques, SIGGRAPH'99, Los Angeles
- Stamou,A., & Katsiris, I. (2006). Verification of a CFD model for indoor airflow and heat transfer. *Building and Environment*, 41 (2006), 1171-1181
- Stathopoulos, T., Dhiovitii, D., & Dodaro, L. (1994). Wind Shielding Effects of Trees on Low Buildings. *Building and Environments* , 29 (2), 141-150.
- Steeman, H.J., Janssens,A., Carmeliet,J., & De Paepe,M. (2009). Modeling indoor air and hygrothermal wall interaction in building simulation: Comparison between CFD and a well-mixed zonal model. *Building and Environment*, 44 (2009), 572-583
- Stephenson, D. G. (1965). Equations for Solar Heat Gain Through Windows. *Solar Energy* , 9 (2), 81.
- Stephenson, D. G., & Mitalas, G. P. (1967). Cooling Load Calculations by Thermal Response Factor Method. *ASHRAE Transactions* , 73 (1).
- Tamura, G. T. (1975). Measurement of air leakage characteristics of house enclosures. *ASHRAE Transactions* , 81, 202.
- Tamura, G. T., & Wilson, A. G. (1964). Air Leakage and Pressure Measurements on Two Occupied Houses. *ASHRAE Report #1869*, 20. p. 110.
- Threlkland, J. L., & Jordan, R. C. (1958). Direct Solar Radiation Available on Clear Days. *ASHRAE Transactions* , 64 (45).
- Vatistas, G. H., Chen, D., Chen, T.-F., & Lin, S. (2006). Prediction of infiltration rates through and automatic door. *Journal of Applied Thermal Engineering* , 27 (2007), 545-550.
- Walker, I. S., & Wilson, D. J. (1998). Field validation of algebraic equations for stack and wind driven air infiltration calculations. *International Journal of HVAC&R Research* , 4 (2), 119-140.
- Walton, G. (1982). Airflow and Multiroom Thermal Analysis. *ASHRAE Transactions* , 88 (2), 78-91.
- Walton, G. N. (1984). Computer Algorithm ForR Predicting Infiltration and Interrom Airflows. *ASHRAE Transactions* , 90 (pt 1B), 601-610.



- Walton, G., & Dols, W. S. (2003). CONTAM 2.1 supplemental user guide and program documentation. NISTIR Report 7049, National Institute of Standards, Gaithersburg, MD.
- Warren, P. R., & Webb, B. C. (1980). The relationship between tracer gas and pressurization techniques in dwellings. Proceedings of the 1st IEA Conference of the Air Infiltration Centre. London.
- Wang, L., & Chen, Q. (2006). Validation of Coupled Multizone-CFD Program for Building Airflow and Contaminant Transport Simulations. International Journal of HVAC&R Research , 13 (2), 267-281.
- Warren, P. (1982). Simple Method of Predicting Infiltration Rates In Housing. Energy Conservation in the Built Environment, Proceedings of CIB W67 3rd International Symposium (pp. 6. A. 85-6. A. 104). Dublin, Ireland: An Foras Forbartha.
- Weidt, J. L., & Weidt, J. (1980). Field air leakage of newly installed residential windows. LBL Report 11111. Lawrence Berkeley Laboratory, Berkeley, CA.
- Weidt, J. L., Weidt, J., & Selkowitz, S. (1979). Field Air Leakage of Newly Installed Residential Windows Report LBL-9937. Lawrence Berkeley Laboratory.
- Wilson, D. J., & Kiel, D. E. (1990). Gravity Driven Counterflow Through an Open Door in a Sealed Room. Building and Environment , 25 (4), 379-388.
- York, D. A., & Tucker, E. F. (May 1980). DOE-2 Reference Manual (Version 2.1), Los Alamos Scientific Laboratory report LA-7689-M (Report LBL-8706, Rev.1, Lawrence Berkeley Laboratory).
- Yuill, G. K. (1996). Impact of high use automatic doors on infiltration, ASHRAE Research Project 763-TRP. Atlanta: American Society of Heating, Refrigerating and Air-Conditioning Engineers, Inc.
- Yuill, G. K., Upham, R., & Chen, H. (2000). Air leakage through automatic doors. ASHRAE Transactiona , 106 (2), 145-160.
- Zmeureanu, R., Stathopoulos, T., Schopmeijer, M. E., Siret, F., & Payer, J. (2001). Measurements of Air Leakage Through Revolving Doors of Institutional Building. Journal of Architectural Engineering , 131-137.
- Zuo, W., & Chen, Q. (2010). Fast and informative flow simulations in a building by using fast fluid dynamics model on graphics processing unit. Building and Environment, 45 (2010), 747-757

## **APPENDICES**

## **Appendix A**

### **Hourly and Cumulative Data for Southwest Wall Obtained from the DOE-2/eQUEST, CFD Analyses, and Enhanced Model Simulations**

Supporting Data for Charts 5-1 to 5-7

## Hourly Data for Southwest Wall

<b>Hourly Southwest (SW) Wall Data (Watts)</b>
--

hour	eUEST/DOE-2 Hourly Values (no reduction multiplier)			CFD Multiphysisc Simulation			
	Air Change	Air Change (ACH)	ASHRAE Enhanced	Enhanced Model	Angular Cracks	Mixed Cracks	Straight Cracks
1	27.841	12.382	78.440	562.563	1033.902	1001.086	990.942
2	28.263	12.570	79.632	764.879	1032.148	999.568	988.689
3	28.427	15.172	85.301	816.732	1031.288	997.784	987.061
4	33.504	14.901	103.464	868.444	1027.239	995.574	983.660
5	33.630	17.948	108.929	883.594	1025.149	993.470	981.911
6	42.192	11.259	136.746	858.155	1023.430	991.618	980.590
7	39.576	14.081	128.847	837.377	1021.008	989.738	980.309
8	45.585	20.274	151.554	830.891	1019.139	988.343	976.587
9	45.094	16.045	147.876	873.207	1020.458	991.931	979.906
10	37.357	16.615	122.458	881.855	1021.342	998.765	987.920
11	37.789	16.807	122.098	872.546	1025.298	1007.328	995.728
12	30.455	21.672	100.095	869.263	1027.725	1016.348	1005.657
13	31.003	19.304	98.090	879.652	1032.188	1025.572	1016.419
14	33.623	20.936	104.793	923.966	1034.425	1033.401	1026.598
15	33.140	20.635	102.502	928.111	1035.710	1037.293	1032.240
16	39.703	24.721	123.741	920.548	1035.179	1036.331	1030.898
17	51.670	32.172	167.101	921.072	1030.190	1029.530	1024.118
18	54.900	29.300	177.824	945.536	1029.099	1023.798	1017.510
19	57.359	35.715	188.161	986.180	1026.581	1018.225	1010.697
20	54.216	33.758	181.594	967.011	1022.710	1013.398	1005.666
21	56.467	30.136	186.845	940.164	1022.880	1009.544	1001.527
22	44.114	23.544	144.947	921.302	1019.865	1006.109	997.716
23	58.983	36.726	197.562	936.365	1017.847	1003.242	994.831
24	56.467	30.136	186.845	961.769	1017.517	1000.521	991.415
25	61.865	38.521	208.631	948.632	1016.081	999.027	991.520
26	61.651	49.355	209.315	933.645	1016.429	997.093	987.507
27	60.742	43.224	205.166	924.793	1014.335	995.630	986.987
28	55.205	24.553	179.668	926.249	1014.685	994.700	986.410
29	57.022	30.433	184.697	930.246	1014.577	993.881	984.306

hour	Air Change	Air Change (ACH)	ASHRAE Enhanced	Enhanced Model	Angular Cracks	Mixed Cracks	Straight Cracks
32	62.718	50.209	210.129	923.967	1013.996	992.880	984.674
33	57.345	40.807	185.834	922.689	1017.099	997.799	989.897
34	61.202	54.439	202.888	906.037	1021.823	1006.194	998.177
35	57.077	45.693	179.542	882.402	1025.969	1016.055	1008.670
36	54.767	48.715	172.951	864.225	1031.606	1026.018	1018.344
37	53.876	43.130	163.216	865.180	1035.119	1035.913	1031.268
38	52.581	42.094	156.828	913.238	1039.699	1043.261	1041.314
39	54.355	53.184	170.758	906.145	1041.136	1048.039	1047.856
40	52.562	46.754	158.789	885.759	1043.459	1049.599	1049.267
41	52.562	46.754	158.789	873.139	1041.362	1044.810	1042.675
42	53.656	52.500	167.368	871.524	1040.436	1039.970	1039.282
43	54.593	58.273	176.333	883.176	1038.711	1035.615	1033.630
44	51.278	41.051	150.520	882.670	1037.512	1031.985	1029.686
45	54.593	58.273	176.333	877.086	1038.150	1029.415	1025.853
46	54.008	72.060	194.144	872.217	1038.134	1027.226	1023.854
47	52.604	60.829	174.187	873.195	1037.653	1025.492	1022.282
48	53.352	66.440	183.927	883.424	1037.824	1023.542	1018.953
49	51.883	46.150	155.542	872.970	1037.013	1022.393	1018.989
50	52.955	51.815	164.001	858.710	1037.343	1021.213	1017.146
51	53.348	61.689	175.542	852.861	1037.407	1020.802	1015.986
52	51.105	59.095	164.966	887.296	1038.832	1020.960	1015.333
53	48.917	65.268	169.290	906.999	1038.689	1021.063	1016.116
54	46.985	50.152	142.594	889.213	1040.386	1021.163	1015.570
55	47.721	55.182	151.052	874.585	1040.425	1021.291	1016.310
56	47.721	55.182	151.052	868.966	1039.887	1021.293	1015.687
57	47.721	55.182	151.052	879.986	1043.882	1025.786	1020.501
58	44.474	39.560	123.990	891.985	1045.917	1033.622	1028.856
59	44.049	43.100	125.473	897.105	1050.950	1043.149	1037.060
60	38.033	33.831	101.514	897.750	1054.659	1053.101	1048.097
61	33.399	23.767	79.647	908.796	1060.105	1062.876	1060.499
62	34.925	31.066	89.013	939.435	1062.846	1070.106	1070.323
63	36.231	32.228	90.584	939.104	1066.339	1074.922	1076.928
64	36.231	32.228	90.584	918.288	1065.999	1075.554	1079.379
65	39.020	41.650	108.992	897.708	1063.702	1069.626	1069.800
66	39.814	38.956	107.923	900.724	1061.814	1064.381	1063.913
67	39.021	34.709	101.338	926.201	1060.793	1059.829	1059.282
68	39.021	34.709	101.338	912.169	1059.575	1055.667	1053.394
69	39.021	34.709	101.338	891.739	1058.219	1051.624	1049.742

hour	Air Change	Air Change (ACH)	ASHRAE Enhanced	Enhanced Model	Angular Cracks	Mixed Cracks	Straight Cracks
70	35.905	19.163	84.802	878.612	1057.242	1048.471	1044.954
71	19.072	10.179	45.044	877.880	1056.849	1046.456	1043.551
72	16.263	10.127	38.032	887.916	1056.539	1044.808	1040.812
73	15.608	8.330	34.726	893.023	1056.217	1043.985	1040.622
74	7.529	8.036	20.530	891.277	1058.003	1043.882	1039.399
75	6.758	7.214	17.979	888.099	1057.828	1043.591	1039.478
76	5.638	7.021	16.730	903.968	1058.293	1042.632	1038.205
77	9.135	8.126	22.617	912.507	1058.472	1042.167	1037.599
78	7.269	7.759	19.660	911.357	1058.177	1041.672	1037.676
79	6.075	7.566	18.271	906.798	1058.290	1041.130	1036.522
80	7.529	8.036	20.530	901.171	1059.016	1040.834	1036.411
81	5.585	7.451	17.732	906.733	1061.681	1045.357	1040.873
82	5.178	6.909	16.247	910.173	1063.046	1052.685	1047.467
83	5.424	6.754	15.987	900.871	1066.891	1061.776	1056.596
84	5.213	6.491	15.261	883.197	1071.209	1070.837	1065.964
85	5.253	6.542	15.276	867.753	1074.840	1079.853	1076.733
86	5.776	6.166	14.855	886.048	1076.772	1086.399	1087.372
87	6.792	6.041	15.478	875.963	1078.106	1089.497	1093.414
88	7.645	6.800	17.990	848.479	1078.038	1088.511	1090.917
89	9.501	8.451	23.522	823.820	1074.751	1081.165	1083.912
90	10.461	9.306	26.663	807.704	1070.313	1074.321	1075.268
91	22.729	6.065	50.207	803.538	1068.490	1068.159	1066.724
92	21.750	7.738	49.124	799.680	1064.325	1061.736	1060.435
93	19.297	12.015	48.684	800.593	1062.282	1056.774	1054.707
94	27.544	12.250	66.112	806.198	1059.537	1052.257	1048.950
95	24.657	10.966	59.850	820.664	1056.533	1047.988	1045.467
96	37.321	16.599	92.590	840.110	1055.169	1044.670	1040.912
97	39.324	20.987	99.162	850.459	1052.304	1041.619	1037.555
98	43.275	30.794	115.343	859.202	1052.184	1039.470	1035.540
99	43.348	34.703	116.819	866.632	1050.675	1037.432	1032.500
100	43.348	34.703	116.819	900.801	1050.910	1036.054	1032.481
101	40.788	29.025	104.609	911.522	1049.445	1034.891	1031.238
102	41.557	29.572	105.524	907.667	1049.718	1034.066	1028.978
103	43.349	42.415	122.490	903.244	1049.338	1034.002	1030.044
104	41.818	48.357	125.350	902.529	1050.703	1033.889	1030.173
105	41.575	40.679	113.656	923.514	1051.441	1038.200	1032.917
106	41.070	47.492	122.244	920.919	1057.215	1046.523	1041.714
107	37.540	40.070	103.196	907.708	1059.660	1056.447	1052.080

hour	Air Change	Air Change (ACH)	ASHRAE Enhanced	Enhanced Model	Angular Cracks	Mixed Cracks	Straight Cracks
108	34.754	34.006	88.559	900.302	1064.218	1066.303	1060.956
109	33.793	36.071	89.153	897.949	1068.897	1076.005	1072.583
110	32.545	31.843	80.646	911.648	1073.158	1083.300	1083.475
111	29.156	25.934	67.888	918.789	1073.714	1087.343	1090.343
112	29.430	18.324	60.750	916.893	1074.411	1086.789	1090.055
113	31.488	25.208	73.840	913.315	1069.697	1079.704	1080.191
114	23.609	12.600	52.528	917.520	1067.957	1073.520	1074.042
115	19.686	10.507	44.344	926.085	1064.662	1067.488	1067.047
116	21.107	11.265	49.278	905.707	1062.812	1062.199	1061.457
117	19.072	10.179	45.044	879.893	1060.086	1057.634	1055.539
118	26.560	11.813	62.303	861.595	1058.402	1053.460	1050.164
119	27.052	0.000	62.325	866.511	1057.629	1049.949	1047.157
120	23.191	8.251	54.317	892.801	1056.921	1046.943	1042.964
121	22.281	7.928	52.185	882.472	1053.779	1044.573	1040.624
122	26.560	0.000	60.444	868.698	1053.363	1042.755	1038.664
123	26.069	0.000	58.586	863.975	1052.716	1041.156	1037.081
124	19.072	10.179	45.044	900.734	1053.171	1039.949	1036.123
125	18.704	8.319	42.844	927.398	1052.774	1039.109	1034.968
126	21.003	7.473	46.846	924.035	1051.847	1038.336	1036.256
127	25.023	6.678	55.275	910.097	1052.073	1037.368	1032.032
128	20.568	7.318	46.455	899.465	1051.122	1036.664	1032.069
129	17.153	12.206	42.238	914.128	1053.739	1040.895	1036.091
130	12.233	9.793	30.544	910.370	1055.681	1048.061	1042.674
131	8.975	9.580	25.266	893.660	1059.733	1056.269	1051.432
132	7.562	9.417	23.496	877.231	1063.063	1065.487	1059.327
133	5.786	8.749	20.874	871.702	1066.389	1074.349	1071.319
134	6.002	8.009	19.285	893.844	1069.647	1081.091	1082.208
135	5.616	7.993	18.930	894.610	1070.738	1085.421	1086.806
136	5.215	7.422	17.392	891.513	1072.259	1085.946	1089.152
137	3.750	6.671	15.454	891.307	1068.928	1080.125	1082.305
138	4.177	7.060	16.390	895.441	1068.509	1074.893	1074.595
139	5.863	7.822	18.615	903.994	1066.046	1069.760	1069.904
140	11.604	8.257	26.759	895.992	1065.213	1065.439	1063.515
141	15.947	8.511	34.590	877.015	1063.452	1061.736	1059.742
142	13.695	12.182	33.907	851.519	1063.510	1058.919	1056.057
143	22.134	19.688	54.798	837.728	1062.602	1056.241	1053.529
144	33.028	29.379	81.770	837.163	1061.209	1053.774	1049.564
145	14.105	12.547	35.265	831.130	1061.456	1052.100	1048.774

hour	Air Change	Air Change (ACH)	ASHRAE Enhanced	Enhanced Model	Angular Cracks	Mixed Cracks	Straight Cracks
146	4.592	7.353	17.228	823.873	1059.562	1050.326	1046.819
147	5.540	7.885	18.774	817.371	1060.471	1048.721	1044.083
148	5.739	8.167	19.550	836.587	1057.826	1047.001	1043.026
149	6.986	8.700	21.567	844.487	1058.090	1045.889	1042.531
150	5.739	8.167	19.550	1050.527	1058.321	1045.177	1041.557
151	5.344	7.606	18.014	1050.381	1058.271	1044.184	1040.661
152	7.118	8.230	20.586	1050.429	1057.374	1043.534	1038.511
153	7.792	8.317	21.420	1050.429	1059.282	1046.261	1041.730
154	8.714	10.076	25.203	1050.429	1061.593	1052.698	1047.078
155	9.451	13.450	32.878	1050.786	1061.683	1060.090	1055.594
156	6.835	13.984	33.835	1051.056	1063.767	1067.077	1061.481
157	5.207	10.652	25.976	1051.329	1064.860	1073.647	1070.954
158	5.859	11.465	28.087	1051.532	1065.437	1077.645	1077.523
159	6.772	12.649	31.307	1051.795	1064.653	1078.904	1080.910
160	8.662	13.869	35.206	1051.993	1061.788	1076.558	1078.198
161	9.436	20.144	50.561	1052.326	1056.299	1067.927	1068.814
162	6.789	14.493	36.464	1052.463	1052.455	1059.969	1060.682
163	8.177	16.001	40.692	1052.718	1048.320	1052.717	1051.730
164	9.650	17.167	44.416	1052.913	1045.828	1046.542	1045.257
165	9.085	16.970	43.607	1052.958	1042.459	1041.201	1040.219
166	16.611	23.641	64.774	1052.979	1039.794	1036.566	1033.093
167	11.698	17.690	47.511	1052.988	1038.449	1032.413	1028.702
168	12.219	18.478	50.057	1053.134	1035.735	1028.780	1025.137
169	17.190	18.348	58.825	1053.230	1034.409	1026.775	1022.778
170	15.912	18.400	56.303	1053.252	1032.699	1023.189	1019.386
171	16.872	19.511	60.045	1053.334	1030.825	1020.396	1016.050
172	19.996	19.565	67.216	1053.421	1028.990	1018.059	1013.548
173	27.537	22.045	87.884	1053.439	1027.365	1015.509	1011.025
174	31.740	19.763	98.924	1053.590	1026.774	1013.416	1008.694
175	30.277	16.159	93.769	1053.687	1024.190	1011.607	1006.244
176	30.277	16.159	93.769	1053.710	1024.542	1010.301	1005.288
177	26.116	18.584	82.819	1053.649	1024.339	1013.959	1008.700
178	25.550	20.454	81.543	1053.500	1027.657	1020.786	1016.113
179	26.414	18.796	81.290	1053.331	1031.422	1029.557	1023.501
180	25.490	15.872	75.788	1053.155	1035.592	1038.550	1033.693
181	27.841	12.382	78.440	1052.903	1038.205	1047.261	1044.651
182	26.179	13.972	74.699	1052.852	1041.171	1053.957	1053.518
183	21.841	15.542	64.099	1052.758	1042.661	1058.173	1060.358



hour	Air Change	Air Change (ACH)	ASHRAE Enhanced	Enhanced Model	Angular Cracks	Mixed Cracks	Straight Cracks
184	21.841	15.542	64.099	1052.737	1041.751	1058.245	1061.026
185	31.127	13.844	88.482	1052.870	1040.000	1051.877	1052.858
186	33.079	11.770	94.014	1052.960	1036.327	1045.536	1045.289
187	34.475	9.200	100.000	1053.193	1034.379	1039.767	1038.840
188	35.036	12.466	103.073	1053.307	1032.402	1035.032	1032.247
189	32.901	11.706	96.792	1053.338	1031.523	1030.796	1029.114
190	37.742	0.000	108.941	1053.280	1029.880	1027.599	1024.636
191	33.268	11.837	96.217	1053.203	1029.871	1024.902	1020.858
192	31.782	11.308	91.124	1053.118	1028.468	1023.035	1019.920
193	30.814	10.964	86.797	1052.958	1029.368	1021.926	1018.388
194	26.638	14.217	76.669	1052.928	1027.951	1020.696	1017.455
195	30.017	13.350	85.327	1052.914	1029.057	1019.473	1015.720
196	34.750	15.455	97.031	1052.766	1027.689	1018.489	1013.411
197	28.699	12.764	80.135	1052.740	1028.504	1017.739	1013.219
198	32.194	8.591	88.494	1052.729	1027.810	1017.284	1012.448
199	31.126	11.075	85.301	1052.653	1028.789	1016.756	1011.951
200	27.319	12.150	75.592	1052.639	1029.206	1016.508	1011.617
201	33.742	12.005	91.605	1052.562	1031.332	1021.009	1015.986
202	30.904	8.247	82.552	1052.477	1033.767	1028.396	1023.926
203	29.663	10.554	78.998	1052.388	1039.281	1037.474	1033.407
204	29.318	7.824	76.782	1052.297	1042.321	1046.954	1040.400
205	24.608	10.944	64.294	1052.135	1046.055	1056.258	1054.619
206	23.673	10.529	60.612	1051.961	1049.021	1063.365	1063.984
207	21.086	13.129	55.369	1051.853	1050.931	1067.175	1068.674
208	25.401	13.557	67.351	1052.039	1049.422	1067.525	1069.975
209	25.875	13.809	69.269	1052.132	1048.101	1061.107	1062.738
210	24.719	15.391	68.028	1052.225	1046.338	1055.336	1054.738
211	19.761	14.062	55.601	1052.245	1042.765	1050.072	1049.939
212	19.761	14.062	55.601	1052.254	1042.343	1045.507	1042.717
213	19.761	14.062	55.601	1052.258	1041.148	1041.504	1039.608
214	23.223	16.526	65.343	1052.260	1040.776	1038.392	1036.300
215	19.132	18.720	58.823	1052.261	1038.301	1035.611	1031.759
216	19.132	18.720	58.823	1052.261	1037.982	1033.269	1029.259
217	17.933	19.142	57.151	1052.262	1038.182	1031.984	1029.074
218	17.933	19.142	57.151	1052.262	1037.201	1030.473	1026.450
219	17.933	19.142	57.151	1052.262	1037.216	1028.771	1023.845
220	12.062	15.021	41.583	1052.262	1035.632	1027.130	1023.318
221	15.790	19.664	54.436	1052.262	1035.231	1025.865	1021.819

hour	Air Change	Air Change (ACH)	ASHRAE Enhanced	Enhanced Model	Angular Cracks	Mixed Cracks	Straight Cracks
222	15.790	19.664	54.436	1052.262	1036.176	1024.858	1020.734
223	13.152	19.888	51.565	1052.262	1036.033	1023.981	1019.944
224	11.191	14.932	40.230	1052.262	1034.871	1023.321	1017.530
225	11.191	14.932	40.230	1052.262	1036.806	1026.334	1021.905
226	13.152	19.888	51.565	1052.262	1038.037	1032.930	1027.867
227	13.152	19.888	51.565	1052.262	1042.457	1041.289	1035.067
228	11.082	19.715	49.637	1052.262	1044.594	1050.572	1045.133
229	12.177	19.497	49.698	1052.190	1049.393	1059.294	1056.135
230	11.885	19.029	48.308	1052.108	1049.812	1065.267	1065.166
231	12.913	19.526	50.399	1052.163	1052.195	1068.423	1070.633
232	10.664	15.178	40.216	1052.309	1049.905	1067.708	1068.816
233	13.234	16.481	46.678	1052.548	1046.970	1060.350	1061.141
234	14.593	16.875	49.833	1052.664	1043.655	1053.897	1054.187
235	16.107	17.193	53.408	1052.766	1040.396	1047.427	1046.049
236	25.744	20.610	79.791	1053.005	1038.617	1041.889	1040.384
237	22.121	17.709	69.073	1053.122	1035.729	1036.503	1034.297
238	25.249	17.967	78.893	1053.367	1033.875	1031.833	1029.202
239	27.729	17.266	85.767	1053.486	1030.159	1027.676	1024.265
240	26.116	18.584	82.819	1053.590	1030.285	1024.323	1021.654
241	28.181	17.547	87.830	1053.616	1028.228	1021.514	1016.522
242	27.729	17.266	85.767	1053.556	1025.805	1018.921	1014.716
243	32.546	14.475	98.931	1053.621	1024.682	1016.764	1012.256
244	34.695	12.344	104.629	1053.630	1023.184	1015.037	1010.845
245	34.208	12.171	102.324	1053.562	1024.741	1014.718	1010.748
246	32.293	11.490	91.779	1053.125	1024.349	1015.063	1011.302
247	24.774	13.222	69.457	1052.768	1025.895	1015.572	1010.256
248	20.030	14.254	57.335	1052.548	1027.683	1016.204	1011.201
249	16.092	14.314	47.871	1052.348	1030.602	1021.462	1016.809
250	10.503	14.014	37.556	1052.229	1033.895	1028.992	1022.876
251	15.042	14.718	45.912	1052.196	1037.433	1039.049	1034.139
252	13.532	14.444	42.540	1052.110	1042.786	1048.093	1041.782
253	13.532	14.444	42.540	1052.093	1045.973	1058.073	1054.035
254	13.263	16.516	45.192	1052.085	1048.553	1066.684	1063.928
255	21.813	19.403	63.880	1052.081	1050.203	1072.488	1070.800
256	20.627	20.183	62.496	1052.080	1050.611	1074.268	1073.297
257	21.813	19.403	63.880	1052.079	1048.142	1066.333	1064.053
258	22.257	19.797	65.695	1052.150	1045.603	1059.295	1057.117
259	23.046	20.500	69.092	1052.304	1045.159	1053.394	1051.825

hour	Air Change	Air Change (ACH)	ASHRAE Enhanced	Enhanced Model	Angular Cracks	Mixed Cracks	Straight Cracks
260	32.840	32.133	101.706	1052.331	1040.939	1047.877	1044.006
261	33.331	38.542	111.750	1052.415	1039.907	1043.118	1039.267
262	48.038	42.730	147.326	1052.574	1038.576	1039.273	1036.500
263	50.987	58.959	172.006	1052.533	1037.743	1036.162	1031.240
264	51.945	64.688	182.184	1052.535	1035.960	1033.475	1029.424
265	33.331	41.507	116.235	1052.465	1037.069	1031.631	1028.154
266	51.470	68.674	186.006	1052.382	1034.978	1030.427	1025.203
267	53.314	61.650	177.646	1052.366	1035.848	1028.627	1024.048
268	53.352	66.440	183.927	1052.288	1034.114	1027.142	1022.375
269	55.339	78.759	208.685	1052.345	1035.017	1026.134	1021.330
270	54.584	77.685	204.836	1052.278	1035.115	1025.208	1021.060
271	51.746	55.234	164.908	1052.269	1033.734	1024.381	1018.729
272	54.584	77.685	204.836	1052.265	1034.643	1023.895	1019.161
273	54.943	87.969	224.237	1052.192	1035.858	1028.337	1023.158
274	53.727	81.243	208.759	1052.109	1039.719	1036.686	1030.919
275	51.942	97.025	238.627	1051.807	1044.074	1046.685	1040.339
276	46.649	70.541	176.368	1051.612	1049.808	1056.266	1051.671
277	42.675	56.940	143.610	1051.280	1053.604	1067.322	1063.441
278	41.796	59.484	146.162	1051.072	1057.538	1076.558	1076.077
279	42.004	56.044	138.146	1050.878	1060.802	1083.161	1082.370
280	37.246	39.757	104.860	1050.761	1061.509	1085.683	1086.063
281	38.572	48.034	119.850	1050.730	1061.087	1082.304	1083.616
282	37.632	33.473	95.912	1050.644	1059.524	1076.125	1073.160
283	37.627	26.775	91.681	1050.841	1057.308	1070.328	1067.430
284	39.418	31.556	100.394	1050.938	1056.866	1065.428	1062.444
285	36.798	32.732	96.450	1050.890	1055.308	1061.472	1058.106
286	25.085	22.313	65.750	1050.888	1055.738	1058.186	1054.855
287	24.101	21.438	62.010	1050.745	1054.150	1054.988	1050.965
288	36.798	32.732	96.450	1050.865	1053.451	1052.201	1050.122
289	37.417	33.282	98.972	1050.949	1053.380	1050.567	1049.009
290	38.378	37.552	105.802	1050.966	1053.030	1047.619	1042.382
291	39.651	38.796	111.131	1051.116	1051.214	1045.315	1041.792
292	27.052	26.469	76.440	1051.213	1050.784	1043.766	1039.132
293	26.560	28.351	77.701	1051.164	1050.779	1042.728	1037.116
294	13.759	15.911	41.532	1051.021	1051.377	1042.968	1039.130
295	10.186	9.967	26.668	1050.570	1052.778	1043.095	1038.680
296	7.690	9.577	23.281	1050.421	1053.106	1043.638	1038.562
297	4.782	8.082	18.690	1050.161	1056.220	1049.153	1044.367

hour	Air Change	Air Change (ACH)	ASHRAE Enhanced	Enhanced Model	Angular Cracks	Mixed Cracks	Straight Cracks
298	4.730	7.573	17.366	1049.964	1060.990	1057.716	1052.511
299	3.172	5.643	12.892	1049.775	1064.180	1067.612	1062.755
300	2.836	5.298	12.121	1049.661	1070.256	1077.478	1072.025
301	3.054	5.977	13.715	1049.559	1072.741	1087.613	1084.737
302	2.765	4.919	11.123	1049.463	1076.902	1095.383	1096.541
303	2.967	5.014	11.287	1049.441	1077.693	1100.210	1104.110
304	2.765	4.919	11.123	1049.431	1079.233	1101.777	1105.658
305	2.810	4.749	10.691	1049.426	1075.880	1097.303	1100.219
306	3.170	5.076	11.441	1049.495	1073.643	1089.352	1092.070
307	1.986	6.005	15.269	1050.147	1069.883	1081.827	1083.297
308	2.273	7.279	18.881	1050.680	1067.024	1074.829	1072.902
309	2.515	8.052	20.945	1051.009	1062.811	1068.235	1066.907
310	3.008	9.098	23.428	1051.308	1059.779	1062.172	1061.214
311	3.294	9.962	25.737	1051.594	1056.972	1057.046	1054.541
312	4.471	11.135	27.860	1051.731	1054.502	1053.003	1050.852
313	3.942	10.518	26.542	1051.700	1053.380	1049.345	1044.662
314	4.058	10.828	27.364	1051.778	1053.030	1046.045	1042.067
315	4.175	11.141	28.199	1051.863	1051.214	1042.636	1038.776
316	4.415	11.781	29.906	1052.024	1050.784	1039.256	1035.073
317	7.233	14.154	35.483	1052.268	1050.779	1036.375	1033.670
318	7.002	14.324	35.958	1052.387	1051.377	1033.757	1030.741
319	6.430	14.299	36.006	1052.490	1052.778	1031.134	1025.620
320	7.793	15.251	38.563	1052.587	1053.106	1029.073	1024.598
321	8.789	15.636	39.910	1052.610	1055.049	1032.197	1025.818
322	10.434	15.778	41.457	1052.549	1058.983	1037.850	1032.753
323	9.139	15.445	39.595	1052.542	1061.396	1046.837	1041.719
324	8.701	14.706	37.420	1052.397	1066.705	1054.916	1048.792
325	10.408	14.812	39.057	1052.301	1068.556	1064.648	1061.041
326	12.792	14.793	42.093	1052.208	1072.184	1072.361	1070.321
327	13.012	13.889	40.904	1052.116	1072.585	1077.654	1076.917
328	19.030	13.542	52.611	1052.095	1073.813	1078.049	1077.985
329	18.903	13.451	52.723	1052.157	1071.435	1072.815	1073.103
330	30.077	8.026	80.343	1052.378	1069.820	1065.515	1061.427
331	32.673	5.813	87.795	1052.487	1066.545	1058.545	1055.875
332	42.020	14.951	115.159	1052.586	1064.093	1052.877	1049.023
333	42.509	18.906	116.541	1052.538	1060.230	1047.507	1043.346
334	43.555	19.371	121.617	1052.680	1057.500	1043.205	1039.587
335	48.599	30.260	137.370	1052.560	1054.956	1039.724	1034.863

hour	Air Change	Air Change (ACH)	ASHRAE Enhanced	Enhanced Model	Angular Cracks	Mixed Cracks	Straight Cracks
336	51.278	41.051	150.520	1052.476	1052.714	1037.044	1032.664
337	49.142	34.969	139.468	1052.387	1051.289	1035.569	1030.551
338	51.883	46.150	155.542	1052.368	1049.070	1033.757	1029.199
339	53.872	57.504	172.847	1052.360	1047.403	1031.587	1026.748
340	53.150	56.733	169.382	1052.285	1044.372	1030.066	1025.227
341	53.538	57.147	170.618	1052.272	1043.298	1028.687	1023.398
342	54.282	62.769	179.743	1052.266	1041.380	1027.977	1023.259
343	54.331	67.658	186.217	1052.193	1039.509	1027.399	1022.662
344	53.240	66.300	181.414	1052.109	1038.332	1027.176	1021.716
345	52.962	75.376	194.868	1051.949	1038.391	1031.077	1026.243
346	52.697	74.998	193.893	1051.919	1041.157	1039.444	1033.804
347	51.492	77.865	196.476	1051.763	1043.268	1049.463	1043.348
348	49.364	65.865	169.893	1051.592	1046.637	1058.666	1053.999
349	48.146	68.522	171.873	1051.414	1049.550	1069.436	1064.581
350	45.506	48.574	134.125	1051.305	1051.998	1078.619	1076.438
351	43.988	46.953	127.717	1051.134	1053.440	1084.796	1083.577
352	43.494	50.294	131.286	1051.028	1052.038	1086.488	1084.065
353	41.863	40.961	114.444	1050.929	1050.818	1084.207	1081.982
354	42.721	49.401	128.056	1050.906	1046.854	1077.440	1075.818
355	33.825	18.052	78.970	1050.967	1045.344	1071.414	1069.026
356	31.984	22.760	79.581	1051.045	1043.247	1066.187	1062.234
357	34.406	18.363	81.260	1051.059	1041.061	1061.116	1057.834
358	40.583	25.269	100.272	1051.208	1039.445	1056.753	1053.215
359	40.133	21.419	99.083	1051.376	1038.345	1052.888	1048.771
360	35.876	15.956	88.044	1051.481	1038.961	1049.097	1045.088
361	34.194	15.208	86.648	1051.721	1036.854		
362	31.408	11.175	81.182	1051.981	1036.367		
363	27.247	9.694	70.425	1052.035	1036.676		
364	31.971	0.000	82.380	1052.130	1035.286		
365	31.895	8.511	82.693	1052.153	1036.497		
366	30.987	0.000	78.191	1052.020	1035.639		
367	26.763	9.522	68.469	1052.001	1035.552		
368	30.428	10.826	77.038	1051.922	1036.387		
369	29.020	0.000	70.077	1051.693	1037.357		
370	26.227	9.332	63.583	1051.582	1042.053		
371	19.960	10.653	49.806	1051.552	1044.943		
372	25.649	6.844	60.259	1051.397	1051.088		
373	21.039	7.486	48.108	1051.154	1053.484		

hour	Air Change	Air Change (ACH)	ASHRAE Enhanced	Enhanced Model	Angular Cracks	Mixed Cracks	Straight Cracks
374	21.750	7.738	49.124	1051.037	1057.787		
375	22.238	9.890	50.939	1051.005	1058.970		
376	18.171	9.698	41.930	1050.919	1061.352		
377	25.085	13.388	57.882	1050.902	1059.615		
378	20.386	7.254	45.471	1050.894	1059.052		
379	23.465	4.174	50.866	1050.819	1055.883		
380	19.915	7.086	43.855	1050.806	1054.829		
381	10.703	9.521	27.797	1050.801	1053.890		
382	9.259	9.884	26.273	1050.798	1052.974		
383	11.448	10.183	30.007	1050.868	1051.610		
384	10.029	9.813	27.418	1050.879	1049.547		
385	17.328	9.248	40.457	1050.955	1047.317		
386	8.642	9.993	26.086	1050.968	1047.225		
387	12.679	11.278	34.747	1051.259	1043.537		
388	23.207	10.321	58.807	1051.663	1042.282		
389	26.088	9.282	65.354	1051.741	1042.174		
390	26.717	9.506	65.494	1051.633	1041.740		
391	32.446	8.658	78.016	1051.555	1041.261		
392	39.687	21.181	97.982	1051.469	1040.451		
393	39.094	20.865	95.479	1051.380	1042.918		
394	43.696	38.868	118.714	1051.290	1046.681		
395	42.035	33.651	109.145	1051.199	1049.823		
396	42.272	37.601	112.828	1051.107	1055.054		
397	41.001	32.823	104.424	1051.016	1057.498		
398	36.492	19.476	84.204	1050.924	1060.458		
399	35.877	19.147	81.802	1050.833	1063.394		
400	13.310	10.656	33.235	1050.812	1063.531		
401	12.977	11.543	34.014	1050.874	1062.639		
402	11.864	11.608	32.707	1050.953	1061.771		
403	18.886	13.440	48.437	1051.252	1059.980		
404	12.769	15.901	41.721	1051.375	1058.283		
405	10.185	16.307	40.376	1051.481	1057.326		
406	8.486	12.078	30.604	1051.508	1056.564		
407	10.398	17.574	43.719	1051.733	1056.445		
408	7.405	13.173	32.826	1051.915	1053.916		
409	10.873	19.343	48.535	1052.097	1054.715		
410	7.233	14.154	35.483	1052.280	1051.904		
411	7.605	14.881	37.521	1052.464	1050.652		

hour	Air Change	Air Change (ACH)	ASHRAE Enhanced	Enhanced Model	Angular Cracks	Mixed Cracks	Straight Cracks
412	8.878	16.583	42.482	1052.789	1048.159		
413	10.092	17.954	46.766	1053.067	1047.707		
414	12.453	19.939	53.977	1053.414	1047.099		
415	15.069	21.447	61.247	1053.701	1047.116		
416	18.907	21.863	69.596	1053.839	1045.974		
417	18.907	21.863	69.596	1053.879	1049.177		
418	18.563	21.465	67.953	1053.826	1051.279		
419	18.221	21.070	66.331	1053.752	1054.891		
420	23.765	19.026	76.393	1053.596	1058.956		
421	22.293	17.847	70.639	1053.425	1061.865		
422	27.967	14.926	83.241	1053.319	1065.293		
423	25.365	15.793	76.026	1053.220	1066.891		
424	21.489	17.203	67.099	1053.197	1066.728		
425	20.429	18.172	65.437	1053.187	1064.972		
426	27.087	21.685	85.828	1053.325	1061.988		
427	19.406	25.892	74.575	1053.417	1059.519		
428	20.507	27.362	79.977	1053.651	1057.168		
429	16.266	28.937	77.408	1053.837	1054.721		
430	17.769	30.031	81.896	1054.021	1053.139		
431	11.950	22.322	59.696	1054.134	1049.613		
432	11.330	23.179	61.631	1054.377	1049.426		
433	12.423	24.311	65.418	1054.567	1045.502		
434	12.423	24.311	65.418	1054.611	1044.247		
435	14.167	25.203	69.426	1054.702	1040.668		
436	13.379	24.992	68.053	1054.722	1039.207		
437	11.583	24.729	66.078	1054.802	1035.742		
438	11.798	25.186	67.462	1054.888	1033.082		
439	11.798	25.186	67.462	1054.907	1029.231		
440	11.416	25.386	67.880	1054.986	1028.350		
441	12.014	25.647	68.860	1055.001	1027.557		
442	12.660	25.901	69.940	1055.008	1030.229		
443	12.014	25.647	68.860	1055.010	1032.011		
444	11.209	24.927	66.505	1054.940	1035.544		
445	11.798	25.186	67.462	1054.930	1037.735		
446	11.209	24.927	66.505	1054.925	1040.420		
447	12.655	24.765	66.822	1054.780	1041.541		
448	12.059	23.598	63.676	1054.756	1041.882		
449	11.202	22.917	61.249	1054.675	1038.812		



hour	Air Change	Air Change (ACH)	ASHRAE Enhanced	Enhanced Model	Angular Cracks	Mixed Cracks	Straight Cracks
450	10.992	22.487	59.946	1054.587	1035.987		
451	14.463	23.157	65.141	1054.497	1032.473		
452	13.408	23.853	65.073	1054.478	1030.656		
453	13.592	22.972	63.533	1054.469	1027.269		
454	16.463	23.430	69.015	1054.465	1025.028		
455	17.374	23.182	69.407	1054.250	1023.100		
456	18.603	23.167	71.859	1054.215	1021.411		
457	19.601	22.666	72.945	1054.128	1019.266		
458	17.941	22.342	68.598	1054.039	1016.465		
459	19.623	20.946	70.044	1053.948	1015.191		
460	19.270	20.568	68.379	1053.857	1012.768		
461	17.878	20.673	65.445	1053.836	1011.399		
462	11.648	18.650	50.291	1053.542	1010.069		
463	13.558	20.502	56.737	1053.635	1009.209		
464	16.962	21.123	63.856	1053.708	1007.326		
465	22.098	19.656	73.748	1053.719	1008.717		
466	16.559	19.149	59.269	1053.510	1009.359		
467	9.189	16.348	42.297	1053.122	1013.682		
468	8.773	15.608	40.109	1052.909	1016.218		
469	9.361	15.820	40.708	1052.712	1019.240		
470	8.494	14.356	36.666	1052.523	1020.711		
471	7.768	13.819	34.913	1052.408	1023.496		
472	7.113	13.288	33.303	1052.307	1022.709		
473	7.573	13.472	33.920	1052.282	1021.898		
474	9.257	13.998	36.292	1052.271	1019.006		
475	10.503	14.014	37.556	1052.194	1017.477		
476	8.848	13.379	34.378	1052.110	1015.751		
477	9.508	13.532	35.333	1052.092	1015.273		
478	9.987	13.325	35.327	1052.013	1014.597		
479	11.401	13.184	36.803	1051.927	1013.927		
480	9.732	12.985	34.240	1051.909	1013.570		
481	8.791	12.512	32.186	1051.830	1014.120		
482	12.574	13.422	38.710	1051.815	1012.879		
483	11.114	12.851	35.643	1051.809	1013.197		
484	11.114	12.851	35.643	1051.806	1014.794		
485	14.747	13.117	42.498	1051.876	1014.904		
486	15.996	14.228	46.844	1052.029	1014.810		
487	14.164	13.859	42.914	1052.057	1015.411		



hour	Air Change	Air Change (ACH)	ASHRAE Enhanced	Enhanced Model	Angular Cracks	Mixed Cracks	Straight Cracks
488	12.390	13.225	38.412	1051.926	1014.456		
489	12.390	13.225	38.412	1051.909	1018.800		
490	9.458	11.778	31.092	1051.616	1021.610		
491	6.413	10.268	25.105	1051.354	1026.390		
492	5.841	9.353	22.579	1051.085	1032.285		
493	3.794	8.099	19.420	1050.812	1035.933		
494	3.273	7.278	17.497	1050.681	1040.534		
495	5.381	8.615	20.447	1050.643	1042.017		
496	5.786	8.749	20.874	1050.626	1044.936		
497	6.746	9.001	21.931	1050.619	1044.057		
498	5.985	9.050	21.696	1050.687	1042.249		
499	8.490	9.818	25.270	1050.768	1041.228		
500	6.560	9.336	22.821	1050.855	1040.019		
501	5.092	9.059	21.729	1050.944	1040.317		
502	6.029	9.654	23.405	1051.035	1039.191		
503	6.029	9.654	23.405	1051.055	1040.008		
504	7.552	10.076	25.269	1051.064	1038.797		
505	11.703	11.451	33.068	1051.210	1040.234		
506	8.188	10.197	26.098	1051.092	1039.376		
507	6.340	10.151	24.610	1051.080	1039.502		
508	11.679	10.388	31.172	1051.075	1039.295		
509	12.860	10.295	33.074	1051.073	1038.441		
510	12.803	11.388	34.782	1051.214	1038.487		
511	12.803	11.388	34.782	1051.236	1038.450		
512	16.544	11.773	41.587	1051.175	1037.759		
513	16.544	11.773	41.587	1051.168	1041.709		
514	9.628	11.990	30.494	1051.022	1044.758		
515	11.579	12.359	33.619	1051.070	1049.911		
516	8.936	11.923	29.731	1050.999	1054.599		
517	9.342	11.634	29.403	1050.917	1060.124		
518	8.668	11.565	28.672	1050.900	1061.972		
519	10.495	15.870	38.407	1050.893	1064.917		
520	13.385	15.478	40.121	1050.890	1066.697		
521	10.808	16.344	39.739	1050.960	1066.194		
522	12.126	17.258	42.846	1051.113	1062.247		
523	27.544	31.851	85.455	1051.283	1060.365		
524	28.036	24.938	77.498	1051.389	1059.867		
525	21.535	15.324	56.318	1051.487	1056.845		

hour	Air Change	Air Change (ACH)	ASHRAE Enhanced	Enhanced Model	Angular Cracks	Mixed Cracks	Straight Cracks
526	22.456	15.980	59.855	1051.653	1057.027		
527	29.020	18.069	74.713	1051.614	1054.459		
528	21.995	15.652	58.074	1051.618	1053.350		
529	24.448	13.048	61.650	1051.619	1052.860		
530	17.375	12.364	44.562	1051.406	1053.566		
531	14.038	11.239	36.798	1051.301	1051.052		
532	16.957	10.558	41.897	1051.275	1051.676		
533	18.637	9.947	45.020	1051.263	1049.729		
534	19.736	12.289	50.304	1051.472	1049.901		
535	19.059	11.867	49.557	1051.646	1049.577		
536	25.409	13.561	65.400	1051.754	1049.439		
537	22.456	15.980	59.855	1051.710	1051.167		
538	19.891	15.924	53.118	1051.497	1054.137		
539	13.263	11.797	35.081	1051.108	1057.503		
540	14.905	10.607	35.932	1050.894	1059.870		
541	14.517	12.913	36.648	1050.626	1063.558		
542	11.965	12.771	32.626	1050.425	1066.436		
543	14.654	11.731	34.738	1050.377	1067.540		
544	21.642	17.325	50.751	1050.284	1067.581		
545	14.230	11.392	33.369	1050.263	1065.257		
546	11.592	12.374	31.353	1050.254	1062.214		
547	13.695	12.182	33.907	1050.321	1059.175		
548	7.269	7.759	19.660	1050.259	1057.241		
549	7.595	8.107	20.543	1050.252	1053.853		
550	5.196	8.320	19.662	1050.463	1053.475		
551	5.193	8.776	20.853	1050.638	1050.643		
552	5.023	8.935	21.284	1050.746	1049.978		
553	8.490	9.818	25.270	1050.774	1048.519		
554	8.875	9.473	25.181	1050.786	1048.562		
555	11.811	9.456	29.492	1050.792	1047.816		
556	8.875	9.473	25.181	1050.794	1047.903		
557	14.888	9.270	35.214	1050.866	1048.024		
558	16.896	9.017	38.986	1050.878	1046.272		
559	20.633	11.012	47.609	1050.883	1044.884		
560	21.638	5.774	47.178	1050.814	1044.131		
561	21.833	7.768	47.455	1050.733	1047.309		
562	16.832	8.983	37.449	1050.646	1049.544		
563	15.668	11.149	35.716	1050.414	1054.976		

hour	Air Change	Air Change (ACH)	ASHRAE Enhanced	Enhanced Model	Angular Cracks	Mixed Cracks	Straight Cracks
564	3.602	6.407	14.792	1050.087	1058.329		
565	3.877	7.241	17.039	1050.379	1063.490		
566	4.766	7.207	16.872	1050.265	1065.961		
567	3.504	6.856	16.135	1050.326	1068.826		
568	5.320	13.251	32.761	1050.974	1070.498		
569	5.226	11.622	28.750	1051.577	1070.685		
570	7.423	17.827	44.658	1051.917	1067.523		
571	4.459	12.693	32.730	1052.292	1065.327		
572	4.494	13.192	34.280	1052.520	1064.322		
573	7.695	20.533	52.672	1052.651	1063.734		
574	9.208	22.115	56.352	1052.832	1063.016		
575	6.396	15.360	39.139	1052.872	1059.676		
576	7.430	16.523	42.165	1053.032	1059.150		
577	7.218	16.694	42.719	1053.134	1058.631		
578	8.966	17.546	45.135	1053.159	1057.842		
579	8.020	17.121	43.813	1053.170	1056.804		
580	9.504	17.754	45.906	1053.174	1056.044		
581	11.443	18.321	48.822	1053.177	1054.178		
582	11.692	18.720	50.084	1053.249	1054.329		
583	14.313	19.097	54.459	1053.261	1052.891		
584	14.008	18.690	53.564	1053.337	1052.968		
585	13.052	18.576	51.854	1053.351	1055.480		
586	17.190	18.348	58.825	1053.286	1059.732		
587	15.274	17.662	53.417	1053.134	1063.238		
588	19.033	16.930	60.105	1053.037	1067.692		
589	18.285	16.265	56.914	1052.871	1070.457		
590	20.103	16.093	60.430	1052.767	1072.654		
591	23.282	14.497	66.383	1052.669	1072.555		
592	29.157	15.561	81.013	1052.575	1069.314		
593	34.311	15.260	94.938	1052.625	1066.789		
594	41.642	22.224	116.746	1052.627	1060.729		
595	43.555	19.371	121.617	1052.699	1055.542		
596	53.229	42.613	160.012	1052.711	1053.287		
597	51.423	41.167	154.581	1052.716	1047.766		
598	52.853	47.013	163.303	1052.718	1046.435		
599	55.187	58.907	181.804	1052.719	1041.679		
600	56.439	55.223	181.056	1052.791	1039.443		
601	57.594	71.723	203.143	1052.660	1037.923		

hour	Air Change	Air Change (ACH)	ASHRAE Enhanced	Enhanced Model	Angular Cracks	Mixed Cracks	Straight Cracks
602	54.798	53.617	172.149	1052.571	1036.603		
603	56.134	64.911	189.368	1052.552	1034.118		
604	56.094	69.854	195.616	1052.472	1033.461		
605	54.749	73.050	197.858	1052.386	1030.843		
606	54.008	72.060	194.144	1052.297	1029.755		
607	53.352	66.440	183.927	1052.277	1029.193		
608	52.054	60.193	171.283	1052.197	1027.453		
609	50.511	53.916	158.789	1052.111	1028.825		
610	46.557	37.272	131.109	1052.022	1030.770		
611	44.639	35.736	122.472	1051.788	1034.850		
612	44.841	47.864	133.148	1051.461	1038.647		
613	41.070	47.492	122.244	1050.969	1041.828		
614	34.714	27.790	82.290	1050.517	1044.122		
615	3.640	7.123	16.527	1050.061	1046.727		
616	3.703	6.259	14.364	1049.961	1045.457		
617	3.703	6.259	14.364	1049.916	1045.764		
618	3.456	6.148	14.144	1049.896	1042.213		
619	4.635	6.597	15.212	1049.887	1040.193		
620	3.979	6.372	14.611	1049.883	1038.055		
621	3.843	6.837	15.949	1050.167	1037.375		
622	11.751	12.544	33.084	1050.567	1036.232		
623	8.399	11.206	28.424	1051.071	1034.600		
624	7.452	11.268	27.914	1051.244	1034.867		
625	12.277	16.380	42.252	1051.443	1033.636		
626	6.444	11.464	28.078	1051.491	1034.020		
627	14.553	12.945	41.258	1051.654	1032.249		
628	12.260	13.086	37.475	1051.686	1033.826		
629	14.553	12.945	41.258	1051.701	1032.612		
630	17.406	12.386	46.394	1051.707	1033.781		
631	14.553	12.945	41.258	1051.710	1033.021		
632	15.905	12.733	43.637	1051.711	1034.374		
633	10.707	13.334	35.842	1051.783	1035.989		
634	8.345	12.618	31.840	1051.723	1040.733		
635	8.966	12.761	32.663	1051.717	1044.887		
636	7.785	12.464	31.121	1051.714	1050.838		
637	7.785	12.464	31.121	1051.713	1055.925		
638	9.401	12.544	32.536	1051.641	1062.173		
639	7.412	11.868	29.633	1051.701	1065.049		

hour	Air Change	Air Change (ACH)	ASHRAE Enhanced	Enhanced Model	Angular Cracks	Mixed Cracks	Straight Cracks
640	10.431	12.989	34.708	1051.707	1068.894		
641	11.886	13.744	38.368	1051.852	1068.096		
642	15.100	13.431	43.868	1051.947	1068.412		
643	15.455	13.747	45.259	1052.041	1066.426		
644	16.092	14.314	47.871	1052.204	1065.868		
645	26.433	11.756	72.469	1052.450	1062.450		
646	31.270	8.345	85.151	1052.569	1061.539		
647	33.444	8.925	91.929	1052.673	1058.604		
648	35.781	19.097	102.987	1052.842	1056.493		
649	30.527	13.577	87.538	1052.947	1053.916		
650	41.381	18.404	117.629	1052.903	1052.934		
651	42.665	15.180	121.258	1052.974	1050.379		
652	46.151	20.526	134.636	1053.128	1049.049		
653	49.076	26.192	146.070	1053.228	1046.681		
654	52.727	37.521	161.029	1053.180	1047.368		
655	52.727	37.521	161.029	1053.179	1044.831		
656	52.727	37.521	161.029	1053.179	1045.366		
657	53.877	43.132	166.985	1053.107	1046.249		
658	52.853	47.013	163.303	1052.811	1049.717		
659	51.746	55.234	164.908	1052.404	1051.094		
660	52.056	64.826	177.381	1052.182	1055.656		
661	50.430	67.287	176.457	1051.911	1056.832		
662	49.893	66.570	172.669	1051.709	1059.536		
663	47.614	59.294	156.528	1051.588	1061.337		
664	46.259	53.492	144.487	1051.484	1061.341		
665	44.746	43.782	128.480	1051.458	1057.561		
666	44.746	43.782	128.480	1051.446	1055.141		
667	45.558	48.629	136.274	1051.441	1051.005		
668	45.558	48.629	136.274	1051.439	1049.463		
669	43.801	38.962	121.078	1051.438	1046.081		
670	43.126	38.361	118.189	1051.366	1043.170		
671	42.048	33.662	111.254	1051.355	1041.736		
672	40.788	29.025	104.609	1051.350	1038.913		
673	40.788	29.025	104.609	1051.347	1037.519		
674	34.484	18.404	84.220	1051.346	1035.861		
675	35.700	15.878	85.689	1051.346	1032.950		
676	39.094	20.865	95.479	1051.346	1032.826		
677	33.955	18.122	82.023	1051.274	1031.112		

hour	Air Change	Air Change (ACH)	ASHRAE Enhanced	Enhanced Model	Angular Cracks	Mixed Cracks	Straight Cracks
678	33.955	18.122	82.023	1051.263	1029.214		
679	27.052	19.250	68.693	1051.258	1028.803		
680	38.721	24.110	95.671	1051.256	1028.604		
681	39.531	28.130	99.371	1051.183	1031.378		
682	41.085	36.545	109.659	1051.100	1034.238		
683	40.400	35.936	106.862	1051.013	1039.627		
684	37.627	26.775	91.681	1050.923	1044.149		
685	16.806	13.454	41.963	1050.832	1048.406		
686	5.551	9.381	22.464	1050.883	1052.913		
687	4.931	9.649	23.368	1051.171	1053.910		
688	5.576	10.416	25.375	1051.359	1056.079		
689	5.912	11.044	27.077	1051.545	1056.424		
690	8.174	12.360	31.332	1051.729	1053.460		
691	12.891	13.760	39.966	1051.842	1053.227		
692	12.186	14.091	39.589	1051.943	1050.624		
693	7.804	13.883	34.834	1052.110	1050.633		
694	8.705	14.712	37.715	1052.428	1048.820		
695	11.200	15.941	43.059	1052.631	1049.805		
696	8.445	15.776	40.413	1052.823	1047.576		
697	11.162	17.872	47.815	1053.153	1037.927		
698	11.391	19.252	51.572	1053.503	1033.927		
699	12.108	20.463	55.407	1053.792	1031.863		
700	14.948	22.604	63.871	1054.001	1027.229		
701	9.425	20.959	54.812	1054.054	1025.137		
702	12.422	22.099	59.507	1054.077	1023.313		
703	13.705	23.162	63.610	1054.230	1022.090		
704	13.340	22.545	62.136	1054.328	1019.936		
705	19.273	24.001	75.200	1054.352	1021.254		
706	13.705	23.162	63.610	1054.291	1023.000		
707	15.294	21.767	62.999	1054.142	1026.658		
708	15.658	22.284	64.211	1054.045	1028.431		
709	17.252	21.484	65.963	1054.022	1032.026		
710	17.286	21.527	65.417	1053.869	1034.074		
711	19.250	23.972	72.467	1053.771	1035.878		
712	18.895	23.531	70.763	1053.676	1035.523		
713	17.722	23.646	68.778	1053.654	1035.353		
714	23.047	22.550	78.472	1053.645	1031.738		
715	22.330	23.835	79.239	1053.783	1029.401		

hour	Air Change	Air Change (ACH)	ASHRAE Enhanced	Enhanced Model	Angular Cracks	Mixed Cracks	Straight Cracks
716	22.330	23.835	79.239	1053.804	1027.134		
717	26.348	23.437	89.680	1053.956	1025.392		
718	28.570	22.872	95.719	1054.054	1023.658		
719	27.999	29.887	99.944	1053.934	1022.119		
720	24.996	31.127	94.591	1053.851	1021.979		
721	41.173	36.624	139.230	1053.905	1017.068		
722	41.663	40.766	145.453	1053.980	1017.738		
723	31.706	28.202	108.613	1054.065	1015.237		
724	33.630	26.923	113.428	1054.153	1015.482		
725	43.134	30.694	143.734	1054.243	1013.184		
726	55.128	39.230	184.956	1054.334	1013.092		
727	58.738	52.248	205.074	1054.355	1012.557		
728	42.644	41.725	150.703	1054.221	1014.883		
729	41.663	48.178	154.208	1054.059	1015.244		
730	40.683	47.044	148.928	1053.886	1019.472		
731	16.643	23.686	67.032	1053.707	1022.938		
732	14.202	20.213	56.942	1053.597	1028.775		
733	14.610	19.493	55.866	1053.425	1030.938		
734	11.944	19.123	51.364	1053.390	1034.757		
735	13.016	19.683	54.011	1053.446	1035.416		
736	15.210	20.294	58.740	1053.521	1036.224		
737	20.371	19.932	68.917	1053.535	1034.587		
738	20.063	19.631	68.312	1053.612	1031.302		
739	35.181	12.518	106.956	1053.697	1030.366		
740	37.148	9.913	112.348	1053.715	1027.498		
741	39.079	6.952	117.834	1053.722	1026.245		
742	40.683	10.856	124.034	1053.797	1023.751		
743	41.173	14.649	127.170	1053.881	1023.359		
744	33.906	18.096	107.430	1053.970	1020.565		

## Cumulative Data for Southwest Wall

### Cumulative Southwest (SW) Wall Data (Watts)

hour	eUEST/DOE-2 Hourly Values (no reduction multiplier)			CFD Multiphysisc Simulation			
	Air Change	Air Change (ACH)	ASHRAE Enhanced	Enhanced Model	Angular Cracks	Mixed Cracks	Straight Cracks
1	27.84	12.38	78.44	562.56	1033.90	1001.09	990.94
2	56.10	24.95	158.07	1327.44	2066.05	2000.65	1979.63
3	84.53	40.12	243.37	2144.17	3097.34	2998.44	2966.69
4	118.03	55.02	346.84	3012.62	4124.58	3994.01	3950.35
5	151.66	72.97	455.77	3896.21	5149.73	4987.48	4932.26
6	193.86	84.23	592.51	4754.37	6173.16	5979.10	5912.85
7	233.43	98.31	721.36	5591.74	7194.17	6968.84	6893.16
8	279.02	118.59	872.91	6422.64	8213.30	7957.18	7869.75
9	324.11	134.63	1020.79	7295.84	9233.76	8949.11	8849.66
10	361.47	151.25	1143.25	8177.70	10255.10	9947.88	9837.58
11	399.26	168.05	1265.34	9050.24	11280.40	10955.20	10833.30
12	429.71	189.73	1365.44	9919.51	12308.13	11971.55	11838.96
13	460.72	209.03	1463.53	10799.16	13340.32	12997.12	12855.38
14	494.34	229.97	1568.32	11723.12	14374.74	14030.52	13881.98
15	527.48	250.60	1670.82	12651.24	15410.45	15067.82	14914.22
16	567.18	275.32	1794.57	13571.78	16445.63	16104.15	15945.12
17	618.85	307.49	1961.67	14492.86	17475.82	17133.68	16969.23
18	673.75	336.79	2139.49	15438.39	18504.92	18157.48	17986.74
19	731.11	372.51	2327.65	16424.57	19531.50	19175.70	18997.44
20	785.33	406.27	2509.25	17391.58	20554.21	20189.10	20003.11
21	841.79	436.40	2696.09	18331.75	21577.09	21198.64	21004.63
22	885.91	459.95	2841.04	19253.05	22596.96	22204.75	22002.35
23	944.89	496.67	3038.60	20189.41	23614.80	23207.99	22997.18
24	1001.36	526.81	3225.44	21151.18	24632.32	24208.52	23988.59
25	1063.22	565.33	3434.07	22099.81	25648.40	25207.54	24980.11
26	1124.87	614.68	3643.39	23033.46	26664.83	26204.64	25967.62
27	1185.62	657.91	3848.56	23958.25	27679.17	27200.27	26954.61
28	1240.82	682.46	4028.22	24884.50	28693.85	28194.97	27941.02
29	1297.84	712.89	4212.92	25814.74	29708.43	29188.85	28925.32



hour	Air Change	Air Change (ACH)	ASHRAE Enhanced	Enhanced Model	Angular Cracks	Mixed Cracks	Straight Cracks
30	1358.02	750.37	4411.73	26743.47	30723.26	30181.91	29909.18
31	1421.98	801.56	4628.86	27669.47	31737.88	31174.62	30893.38
32	1484.69	851.77	4838.99	28593.44	32751.87	32167.50	31878.06
33	1542.04	892.58	5024.82	29516.13	33768.97	33165.30	32867.95
34	1603.24	947.02	5227.71	30422.17	34790.80	34171.50	33866.13
35	1660.32	992.71	5407.25	31304.57	35816.77	35187.55	34874.80
36	1715.08	1041.43	5580.20	32168.79	36848.37	36213.57	35893.15
37	1768.96	1084.56	5743.42	33033.97	37883.49	37249.48	36924.41
38	1821.54	1126.65	5900.25	33947.21	38923.19	38292.74	37965.73
39	1875.90	1179.84	6071.01	34853.36	39964.33	39340.78	39013.58
40	1928.46	1226.59	6229.79	35739.11	41007.79	40390.38	40062.85
41	1981.02	1273.34	6388.58	36612.25	42049.15	41435.19	41105.53
42	2034.68	1325.84	6555.95	37483.78	43089.58	42475.16	42144.81
43	2089.27	1384.12	6732.29	38366.95	44128.29	43510.78	43178.44
44	2140.55	1425.17	6882.81	39249.62	45165.81	44542.76	44208.12
45	2195.14	1483.44	7059.14	40126.71	46203.96	45572.18	45233.98
46	2249.15	1555.50	7253.28	40998.93	47242.09	46599.40	46257.83
47	2301.75	1616.33	7427.47	41872.12	48279.74	47624.89	47280.11
48	2355.10	1682.77	7611.40	42755.54	49317.57	48648.44	48299.07
49	2406.98	1728.92	7766.94	43628.51	50354.58	49670.83	49318.05
50	2459.94	1780.73	7930.94	44487.22	51391.92	50692.04	50335.20
51	2513.29	1842.42	8106.48	45340.09	52429.33	51712.84	51351.19
52	2564.39	1901.52	8271.45	46227.38	53468.16	52733.80	52366.52
53	2613.31	1966.78	8440.74	47134.38	54506.85	53754.87	53382.64
54	2660.29	2016.94	8583.33	48023.59	55547.24	54776.03	54398.20
55	2708.01	2072.12	8734.38	48898.18	56587.66	55797.32	55414.51
56	2755.74	2127.30	8885.43	49767.14	57627.55	56818.61	56430.20
57	2803.46	2182.48	9036.49	50647.13	58671.43	57844.40	57450.70
58	2847.93	2222.04	9160.48	51539.12	59717.35	58878.02	58479.56
59	2891.98	2265.14	9285.95	52436.22	60768.30	59921.17	59516.62
60	2930.01	2298.97	9387.46	53333.97	61822.96	60974.27	60564.71
61	2963.41	2322.74	9467.11	54242.77	62883.06	62037.15	61625.21
62	2998.34	2353.81	9556.12	55182.20	63945.91	63107.25	62695.54
63	3034.57	2386.03	9646.71	56121.31	65012.25	64182.17	63772.46
64	3070.80	2418.26	9737.29	57039.59	66078.25	65257.73	64851.84
65	3109.82	2459.91	9846.28	57937.30	67141.95	66327.35	65921.64
66	3149.63	2498.87	9954.21	58838.03	68203.76	67391.74	66985.56
67	3188.65	2533.58	10055.55	59764.23	69264.55	68451.56	68044.84

hour	Air Change	Air Change (ACH)	ASHRAE Enhanced	Enhanced Model	Angular Cracks	Mixed Cracks	Straight Cracks
68	3227.67	2568.29	10156.88	60676.40	70324.13	69507.23	69098.23
69	3266.70	2603.00	10258.22	61568.13	71382.35	70558.86	70147.97
70	3302.60	2622.16	10343.02	62446.75	72439.59	71607.33	71192.93
71	3321.67	2632.34	10388.07	63324.63	73496.44	72653.78	72236.48
72	3337.94	2642.46	10426.10	64212.54	74552.98	73698.59	73277.29
73	3353.54	2650.79	10460.83	65105.57	75609.20	74742.57	74317.91
74	3361.07	2658.83	10481.36	65996.84	76667.20	75786.46	75357.31
75	3367.83	2666.04	10499.34	66884.94	77725.03	76830.05	76396.79
76	3373.47	2673.07	10516.07	67788.91	78783.32	77872.68	77434.99
77	3382.60	2681.19	10538.68	68701.42	79841.79	78914.85	78472.59
78	3389.87	2688.95	10558.34	69612.77	80899.97	79956.52	79510.27
79	3395.95	2696.52	10576.61	70519.57	81958.26	80997.65	80546.79
80	3403.48	2704.55	10597.14	71420.74	83017.27	82038.48	81583.20
81	3409.06	2712.00	10614.87	72327.48	84078.96	83083.84	82624.08
82	3414.24	2718.91	10631.12	73237.65	85142.00	84136.53	83671.54
83	3419.66	2725.67	10647.11	74138.52	86208.89	85198.30	84728.14
84	3424.88	2732.16	10662.37	75021.72	87280.10	86269.14	85794.10
85	3430.13	2738.70	10677.65	75889.47	88354.94	87348.99	86870.83
86	3435.91	2744.86	10692.50	76775.52	89431.71	88435.39	87958.21
87	3442.70	2750.91	10707.98	77651.48	90509.82	89524.89	89051.62
88	3450.34	2757.71	10725.97	78499.96	91587.86	90613.40	90142.54
89	3459.84	2766.16	10749.49	79323.78	92662.61	91694.56	91226.45
90	3470.31	2775.46	10776.15	80131.48	93732.92	92768.89	92301.72
91	3493.03	2781.53	10826.36	80935.02	94801.41	93837.05	93368.44
92	3514.78	2789.27	10875.48	81734.70	95865.74	94898.78	94428.88
93	3534.08	2801.28	10924.17	82535.29	96928.02	95955.56	95483.58
94	3561.62	2813.53	10990.28	83341.49	97987.56	97007.81	96532.53
95	3586.28	2824.50	11050.13	84162.16	99044.09	98055.80	97578.00
96	3623.60	2841.10	11142.72	85002.27	100099.26	99100.47	98618.91
97	3662.93	2862.08	11241.88	85852.73	101151.56	100142.09	99656.47
98	3706.20	2892.88	11357.22	86711.93	102203.75	101181.56	100692.01
99	3749.55	2927.58	11474.04	87578.56	103254.42	102218.99	101724.51
100	3792.90	2962.28	11590.86	88479.36	104305.33	103255.05	102756.99
101	3833.69	2991.31	11695.47	89390.88	105354.78	104289.94	103788.22
102	3875.24	3020.88	11800.99	90298.55	106404.50	105324.00	104817.20
103	3918.59	3063.30	11923.48	91201.79	107453.83	106358.00	105847.25
104	3960.41	3111.65	12048.83	92104.32	108504.54	107391.89	106877.42
105	4001.99	3152.33	12162.49	93027.84	109555.98	108430.09	107910.34

hour	Air Change	Air Change (ACH)	ASHRAE Enhanced	Enhanced Model	Angular Cracks	Mixed Cracks	Straight Cracks
106	4043.06	3199.82	12284.73	93948.76	110613.19	109476.62	108952.05
107	4080.60	3239.89	12387.93	94856.46	111672.85	110533.06	110004.13
108	4115.35	3273.90	12476.49	95756.77	112737.07	111599.37	111065.09
109	4149.14	3309.97	12565.64	96654.72	113805.97	112675.37	112137.67
110	4181.69	3341.81	12646.29	97566.36	114879.13	113758.67	113221.14
111	4210.84	3367.75	12714.18	98485.15	115952.84	114846.02	114311.49
112	4240.27	3386.07	12774.93	99402.05	117027.25	115932.80	115401.54
113	4271.76	3411.28	12848.77	100315.36	118096.95	117012.51	116481.73
114	4295.37	3423.88	12901.29	101232.88	119164.91	118086.03	117555.78
115	4315.06	3434.39	12945.64	102158.97	120229.57	119153.52	118622.82
116	4336.16	3445.65	12994.92	103064.67	121292.38	120215.72	119684.28
117	4355.23	3455.83	13039.96	103944.57	122352.47	121273.35	120739.82
118	4381.80	3467.64	13102.26	104806.16	123410.87	122326.81	121789.98
119	4408.85	3467.64	13164.59	105672.67	124468.50	123376.76	122837.14
120	4432.04	3475.90	13218.90	106565.47	125525.42	124423.70	123880.10
121	4454.32	3483.82	13271.09	107447.95	126579.20	125468.27	124920.73
122	4480.88	3483.82	13331.53	108316.64	127632.56	126511.03	125959.39
123	4506.95	3483.82	13390.12	109180.62	128685.28	127552.18	126996.47
124	4526.02	3494.00	13435.16	110081.35	129738.45	128592.13	128032.60
125	4544.72	3502.32	13478.01	111008.75	130791.22	129631.24	129067.56
126	4565.73	3509.79	13524.85	111932.78	131843.07	130669.58	130103.82
127	4590.75	3516.47	13580.13	112842.88	132895.14	131706.95	131135.85
128	4611.32	3523.79	13626.58	113742.35	133946.26	132743.61	132167.92
129	4628.47	3535.99	13668.82	114656.47	135000.00	133784.51	133204.01
130	4640.70	3545.79	13699.37	115566.84	136055.68	134832.57	134246.69
131	4649.68	3555.37	13724.63	116460.50	137115.42	135888.84	135298.12
132	4657.24	3564.78	13748.13	117337.74	138178.48	136954.32	136357.45
133	4663.03	3573.53	13769.00	118209.44	139244.87	138028.67	137428.76
134	4669.03	3581.54	13788.29	119103.28	140314.51	139109.76	138510.97
135	4674.64	3589.53	13807.22	119997.89	141385.25	140195.18	139597.78
136	4679.86	3596.96	13824.61	120889.41	142457.51	141281.13	140686.93
137	4683.61	3603.63	13840.06	121780.71	143526.44	142361.25	141769.24
138	4687.79	3610.69	13856.45	122676.15	144594.95	143436.15	142843.83
139	4693.65	3618.51	13875.07	123580.15	145660.99	144505.91	143913.73
140	4705.25	3626.77	13901.83	124476.14	146726.21	145571.35	144977.25
141	4721.20	3635.28	13936.42	125353.15	147789.66	146633.08	146036.99
142	4734.90	3647.46	13970.33	126204.67	148853.17	147692.00	147093.05
143	4757.03	3667.15	14025.12	127042.40	149915.77	148748.24	148146.58

hour	Air Change	Air Change (ACH)	ASHRAE Enhanced	Enhanced Model	Angular Cracks	Mixed Cracks	Straight Cracks
144	4790.06	3696.53	14106.89	127879.57	150976.98	149802.02	149196.14
145	4804.16	3709.07	14142.16	128710.70	152038.44	150854.11	150244.92
146	4808.75	3716.43	14159.39	129534.57	153098.00	151904.44	151291.74
147	4814.29	3724.31	14178.16	130351.94	154158.47	152953.16	152335.82
148	4820.03	3732.48	14197.71	131188.53	155216.30	154000.16	153378.85
149	4827.02	3741.18	14219.28	132033.01	156274.39	155046.05	154421.38
150	4832.76	3749.34	14238.83	133083.54	157332.71	156091.23	155462.93
151	4838.10	3756.95	14256.84	134133.92	158390.98	157135.41	156503.59
152	4845.22	3765.18	14277.43	135184.35	159448.35	158178.95	157542.10
153	4853.01	3773.50	14298.85	136234.78	160507.63	159225.21	158583.84
154	4861.72	3783.57	14324.05	137285.21	161569.23	160277.91	159630.91
155	4871.18	3797.02	14356.93	138335.99	162630.91	161338.00	160686.51
156	4878.01	3811.01	14390.76	139387.05	163694.68	162405.07	161747.99
157	4883.22	3821.66	14416.74	140438.38	164759.54	163478.72	162818.94
158	4889.08	3833.13	14444.83	141489.91	165824.97	164556.36	163896.47
159	4895.85	3845.77	14476.13	142541.71	166889.63	165635.27	164977.38
160	4904.51	3859.64	14511.34	143593.70	167951.41	166711.83	166055.57
161	4913.95	3879.79	14561.90	144646.02	169007.71	167779.75	167124.39
162	4920.73	3894.28	14598.36	145698.49	170060.17	168839.72	168185.07
163	4928.91	3910.28	14639.06	146751.21	171108.49	169892.44	169236.80
164	4938.56	3927.45	14683.47	147804.12	172154.32	170938.98	170282.06
165	4947.65	3944.42	14727.08	148857.08	173196.78	171980.18	171322.28
166	4964.26	3968.06	14791.85	149910.06	174236.57	173016.75	172355.37
167	4975.96	3985.75	14839.36	150963.04	175275.02	174049.16	173384.07
168	4988.17	4004.23	14889.42	152016.18	176310.75	175077.94	174409.21
169	5005.36	4022.58	14948.25	153069.41	177345.16	176104.72	175431.99
170	5021.28	4040.98	15004.55	154122.66	178377.86	177127.91	176451.37
171	5038.15	4060.49	15064.59	155175.99	179408.69	178148.30	177467.42
172	5058.15	4080.05	15131.81	156229.41	180437.68	179166.36	178480.97
173	5085.68	4102.10	15219.69	157282.85	181465.04	180181.87	179492.00
174	5117.42	4121.86	15318.62	158336.44	182491.82	181195.29	180500.69
175	5147.70	4138.02	15412.39	159390.13	183516.01	182206.89	181506.93
176	5177.98	4154.18	15506.16	160443.84	184540.55	183217.19	182512.22
177	5204.09	4172.76	15588.98	161497.49	185564.89	184231.15	183520.92
178	5229.64	4193.22	15670.52	162550.99	186592.54	185251.94	184537.03
179	5256.06	4212.01	15751.81	163604.32	187623.97	186281.49	185560.54
180	5281.55	4227.88	15827.60	164657.47	188659.56	187320.04	186594.23
181	5309.39	4240.27	15906.04	165710.38	189697.76	188367.31	187638.88

hour	Air Change	Air Change (ACH)	ASHRAE Enhanced	Enhanced Model	Angular Cracks	Mixed Cracks	Straight Cracks
182	5335.57	4254.24	15980.74	166763.23	190738.93	189421.26	188692.40
183	5357.41	4269.78	16044.84	167815.99	191781.59	190479.44	189752.75
184	5379.25	4285.32	16108.94	168868.73	192823.34	191537.68	190813.78
185	5410.37	4299.16	16197.42	169921.60	193863.34	192589.56	191866.64
186	5443.45	4310.93	16291.43	170974.56	194899.67	193635.09	192911.93
187	5477.93	4320.13	16391.43	172027.75	195934.05	194674.86	193950.77
188	5512.96	4332.60	16494.50	173081.06	196966.45	195709.89	194983.01
189	5545.86	4344.31	16591.30	174134.39	197997.98	196740.69	196012.13
190	5583.61	4344.31	16700.24	175187.67	199027.85	197768.29	197036.76
191	5616.87	4356.14	16796.45	176240.88	200057.73	198793.19	198057.62
192	5648.66	4367.45	16887.58	177293.99	201086.19	199816.23	199077.54
193	5679.47	4378.41	16974.37	178346.95	202115.56	200838.15	200095.93
194	5706.11	4392.63	17051.04	179399.88	203143.51	201858.85	201113.38
195	5736.12	4405.98	17136.37	180452.79	204172.57	202878.32	202129.10
196	5770.87	4421.44	17233.40	181505.56	205200.26	203896.81	203142.52
197	5799.57	4434.20	17313.54	182558.30	206228.76	204914.55	204155.73
198	5831.77	4442.79	17402.03	183611.03	207256.57	205931.83	205168.18
199	5862.89	4453.87	17487.33	184663.68	208285.36	206948.59	206180.13
200	5890.21	4466.02	17562.92	185716.32	209314.57	207965.10	207191.75
201	5923.95	4478.02	17654.53	186768.88	210345.90	208986.10	208207.74
202	5954.86	4486.27	17737.08	187821.36	211379.67	210014.50	209231.66
203	5984.52	4496.82	17816.08	188873.75	212418.95	211051.97	210265.07
204	6013.84	4504.65	17892.86	189926.04	213461.27	212098.93	211305.47
205	6038.45	4515.59	17957.15	190978.18	214507.32	213155.19	212360.09
206	6062.12	4526.12	18017.77	192030.14	215556.35	214218.55	213424.07
207	6083.21	4539.25	18073.14	193081.99	216607.28	215285.73	214492.75
208	6108.61	4552.80	18140.49	194134.03	217656.70	216353.25	215562.72
209	6134.48	4566.61	18209.76	195186.17	218704.80	217414.36	216625.46
210	6159.20	4582.01	18277.78	196238.39	219751.14	218469.70	217680.20
211	6178.96	4596.07	18333.38	197290.63	220793.90	219519.77	218730.14
212	6198.72	4610.13	18388.99	198342.89	221836.25	220565.27	219772.85
213	6218.48	4624.19	18444.59	199395.15	222877.39	221606.78	220812.46
214	6241.71	4640.72	18509.93	200447.41	223918.17	222645.17	221848.76
215	6260.84	4659.44	18568.75	201499.67	224956.47	223680.78	222880.52
216	6279.97	4678.16	18627.58	202551.93	225994.45	224714.05	223909.78
217	6297.90	4697.30	18684.73	203604.19	227032.64	225746.03	224938.86
218	6315.84	4716.44	18741.88	204656.45	228069.84	226776.51	225965.31
219	6333.77	4735.58	18799.03	205708.72	229107.05	227805.28	226989.15

hour	Air Change	Air Change (ACH)	ASHRAE Enhanced	Enhanced Model	Angular Cracks	Mixed Cracks	Straight Cracks
220	6345.83	4750.61	18840.61	206760.98	230142.68	228832.41	228012.47
221	6361.62	4770.27	18895.05	207813.24	231177.92	229858.27	229034.29
222	6377.41	4789.93	18949.49	208865.50	232214.09	230883.13	230055.02
223	6390.57	4809.82	19001.05	209917.76	233250.12	231907.11	231074.97
224	6401.76	4824.75	19041.28	210970.02	234285.00	232930.43	232092.50
225	6412.95	4839.69	19081.51	212022.29	235321.80	233956.77	233114.40
226	6426.10	4859.57	19133.07	213074.55	236359.84	234989.70	234142.27
227	6439.25	4879.46	19184.64	214126.81	237402.29	236030.98	235177.34
228	6450.34	4899.18	19234.28	215179.07	238446.89	237081.56	236222.47
229	6462.51	4918.67	19283.97	216231.26	239496.28	238140.85	237278.60
230	6474.40	4937.70	19332.28	217283.37	240546.09	239206.12	238343.77
231	6487.31	4957.23	19382.68	218335.53	241598.29	240274.54	239414.40
232	6497.97	4972.41	19422.90	219387.84	242648.19	241342.25	240483.22
233	6511.21	4988.89	19469.58	220440.39	243695.16	242402.60	241544.36
234	6525.80	5005.76	19519.41	221493.05	244738.82	243456.49	242598.55
235	6541.91	5022.95	19572.82	222545.82	245779.22	244503.92	243644.60
236	6567.65	5043.56	19652.61	223598.83	246817.83	245545.81	244684.98
237	6589.77	5061.27	19721.68	224651.95	247853.56	246582.31	245719.28
238	6615.02	5079.24	19800.57	225705.31	248887.44	247614.15	246748.48
239	6642.75	5096.51	19886.34	226758.80	249917.59	248641.82	247772.74
240	6668.87	5115.09	19969.16	227812.39	250947.88	249666.15	248794.40
241	6697.05	5132.64	20056.99	228866.01	251976.11	250687.66	249810.92
242	6724.78	5149.90	20142.75	229919.56	253001.91	251706.58	250825.64
243	6757.32	5164.38	20241.69	230973.19	254026.59	252723.34	251837.89
244	6792.02	5176.72	20346.31	232026.82	255049.78	253738.38	252848.74
245	6826.23	5188.89	20448.64	233080.38	256074.52	254753.10	253859.49
246	6858.52	5200.38	20540.42	234133.50	257098.87	255768.16	254870.79
247	6883.29	5213.61	20609.87	235186.27	258124.76	256783.73	255881.05
248	6903.32	5227.86	20667.21	236238.82	259152.45	257799.94	256892.25
249	6919.42	5242.17	20715.08	237291.17	260183.05	258821.40	257909.06
250	6929.92	5256.19	20752.64	238343.39	261216.94	259850.39	258931.93
251	6944.96	5270.91	20798.55	239395.59	262254.38	260889.44	259966.07
252	6958.49	5285.35	20841.09	240447.70	263297.16	261937.53	261007.85
253	6972.03	5299.79	20883.63	241499.79	264343.14	262995.61	262061.89
254	6985.29	5316.31	20928.82	242551.88	265391.69	264062.29	263125.82
255	7007.10	5335.71	20992.70	243603.96	266441.89	265134.78	264196.62
256	7027.73	5355.90	21055.20	244656.04	267492.50	266209.05	265269.91
257	7049.54	5375.30	21119.08	245708.12	268540.64	267275.38	266333.97



hour	Air Change	Air Change (ACH)	ASHRAE Enhanced	Enhanced Model	Angular Cracks	Mixed Cracks	Straight Cracks
258	7071.80	5395.10	21184.77	246760.27	269586.25	268334.67	267391.08
259	7094.85	5415.60	21253.87	247812.57	270631.41	269388.07	268442.91
260	7127.69	5447.73	21355.57	248864.90	271672.34	270435.95	269486.92
261	7161.02	5486.27	21467.32	249917.32	272712.25	271479.06	270526.18
262	7209.05	5529.00	21614.65	250969.89	273750.83	272518.34	271562.68
263	7260.04	5587.96	21786.65	252022.43	274788.57	273554.50	272593.92
264	7311.99	5652.65	21968.84	253074.96	275824.53	274587.97	273623.35
265	7345.32	5694.16	22085.07	254127.43	276861.60	275619.60	274651.50
266	7396.79	5762.83	22271.08	255179.81	277896.58	276650.03	275676.70
267	7450.10	5824.48	22448.72	256232.17	278932.43	277678.66	276700.75
268	7503.45	5890.92	22632.65	257284.46	279966.54	278705.80	277723.13
269	7558.79	5969.68	22841.34	258336.81	281001.56	279731.93	278744.46
270	7613.38	6047.36	23046.17	259389.08	282036.67	280757.14	279765.52
271	7665.12	6102.60	23211.08	260441.35	283070.41	281781.52	280784.25
272	7719.71	6180.28	23415.92	261493.62	284105.05	282805.42	281803.41
273	7774.65	6268.25	23640.15	262545.81	285140.91	283833.75	282826.56
274	7828.38	6349.49	23848.91	263597.92	286180.63	284870.44	283857.48
275	7880.32	6446.52	24087.54	264649.73	287224.70	285917.13	284897.82
276	7926.97	6517.06	24263.91	265701.34	288274.51	286973.39	285949.49
277	7969.64	6574.00	24407.52	266752.62	289328.11	288040.71	287012.94
278	8011.44	6633.48	24553.68	267803.69	290385.65	289117.27	288089.01
279	8053.44	6689.53	24691.83	268854.57	291446.45	290200.43	289171.38
280	8090.69	6729.28	24796.69	269905.33	292507.96	291286.12	290257.45
281	8129.26	6777.32	24916.54	270956.06	293569.05	292368.42	291341.06
282	8166.89	6810.79	25012.45	272006.70	294628.57	293444.55	292414.22
283	8204.52	6837.57	25104.13	273057.54	295685.88	294514.87	293481.65
284	8243.94	6869.12	25204.52	274108.48	296742.75	295580.30	294544.10
285	8280.73	6901.85	25300.97	275159.37	297798.05	296641.77	295602.20
286	8305.82	6924.17	25366.72	276210.26	298853.79	297699.96	296657.06
287	8329.92	6945.61	25428.73	277261.01	299907.94	298754.95	297708.02
288	8366.72	6978.34	25525.18	278311.87	300961.39	299807.15	298758.14
289	8404.13	7011.62	25624.15	279362.82	302014.77	300857.71	299807.15
290	8442.51	7049.17	25729.96	280413.78	303067.80	301905.33	300849.53
291	8482.16	7087.97	25841.09	281464.90	304119.02	302950.65	301891.33
292	8509.21	7114.44	25917.53	282516.11	305169.80	303994.41	302930.46
293	8535.77	7142.79	25995.23	283567.28	306220.58	305037.14	303967.57
294	8549.53	7158.70	26036.76	284618.30	307271.96	306080.11	305006.70
295	8559.72	7168.66	26063.43	285668.87	308324.73	307123.20	306045.38

hour	Air Change	Air Change (ACH)	ASHRAE Enhanced	Enhanced Model	Angular Cracks	Mixed Cracks	Straight Cracks
296	8567.41	7178.24	26086.71	286719.29	309377.84	308166.84	307083.95
297	8572.19	7186.32	26105.40	287769.45	310434.06	309216.00	308128.31
298	8576.92	7193.90	26122.77	288819.42	311495.05	310273.71	309180.82
299	8580.09	7199.54	26135.66	289869.19	312559.23	311341.32	310243.58
300	8582.93	7204.84	26147.78	290918.85	313629.48	312418.80	311315.60
301	8585.99	7210.81	26161.49	291968.41	314702.22	313506.41	312400.34
302	8588.75	7215.73	26172.62	293017.87	315779.13	314601.80	313496.88
303	8591.72	7220.75	26183.90	294067.31	316856.82	315702.01	314600.99
304	8594.48	7225.67	26195.03	295116.74	317936.05	316803.78	315706.65
305	8597.29	7230.42	26205.72	296166.17	319011.93	317901.09	316806.87
306	8600.46	7235.49	26217.16	297215.67	320085.58	318990.44	317898.94
307	8602.45	7241.50	26232.43	298265.81	321155.46	320072.27	318982.24
308	8604.72	7248.78	26251.31	299316.49	322222.48	321147.10	320055.14
309	8607.24	7256.83	26272.26	300367.50	323285.29	322215.33	321122.05
310	8610.24	7265.93	26295.68	301418.81	324345.07	323277.50	322183.26
311	8613.54	7275.89	26321.42	302470.40	325402.05	324334.55	323237.80
312	8618.01	7287.02	26349.28	303522.13	326456.55	325387.55	324288.65
313	8621.95	7297.54	26375.82	304573.83	327509.93	326436.90	325333.31
314	8626.01	7308.37	26403.19	305625.61	328562.96	327482.94	326375.38
315	8630.18	7319.51	26431.39	306677.48	329614.17	328525.58	327414.16
316	8634.60	7331.29	26461.29	307729.50	330664.95	329564.83	328449.23
317	8641.83	7345.45	26496.77	308781.77	331715.73	330601.21	329482.90
318	8648.83	7359.77	26532.73	309834.15	332767.11	331634.97	330513.64
319	8655.26	7374.07	26568.74	310886.64	333819.89	332666.10	331539.26
320	8663.06	7389.32	26607.30	311939.23	334872.99	333695.17	332563.86
321	8671.84	7404.96	26647.21	312991.84	335928.04	334727.37	333589.68
322	8682.28	7420.73	26688.67	314044.39	336987.03	335765.22	334622.43
323	8691.42	7436.18	26728.26	315096.93	338048.42	336812.06	335664.15
324	8700.12	7450.88	26765.68	316149.33	339115.13	337866.97	336712.94
325	8710.53	7465.70	26804.74	317201.63	340183.68	338931.62	337773.98
326	8723.32	7480.49	26846.83	318253.84	341255.87	340003.98	338844.31
327	8736.33	7494.38	26887.74	319305.95	342328.45	341081.64	339921.22
328	8755.36	7507.92	26940.35	320358.05	343402.26	342159.69	340999.21
329	8774.26	7521.37	26993.07	321410.21	344473.70	343232.50	342072.31
330	8804.34	7529.40	27073.42	322462.59	345543.52	344298.02	343133.74
331	8837.01	7535.21	27161.21	323515.07	346610.06	345356.56	344189.61
332	8879.03	7550.16	27276.37	324567.66	347674.16	346409.44	345238.64
333	8921.54	7569.07	27392.91	325620.20	348734.39	347456.94	346281.98



hour	Air Change	Air Change (ACH)	ASHRAE Enhanced	Enhanced Model	Angular Cracks	Mixed Cracks	Straight Cracks
334	8965.10	7588.44	27514.53	326672.88	349791.89	348500.15	347321.57
335	9013.70	7618.70	27651.90	327725.44	350846.84	349539.87	348356.43
336	9064.97	7659.75	27802.42	328777.91	351899.56	350576.92	349389.10
337	9114.12	7694.72	27941.89	329830.30	352950.85	351612.49	350419.65
338	9166.00	7740.87	28097.43	330882.67	353999.92	352646.24	351448.85
339	9219.87	7798.37	28270.27	331935.03	355047.32	353677.83	352475.59
340	9273.02	7855.11	28439.66	332987.31	356091.69	354707.90	353500.82
341	9326.56	7912.25	28610.27	334039.58	357134.99	355736.58	354524.22
342	9380.84	7975.02	28790.02	335091.85	358176.37	356764.56	355547.48
343	9435.17	8042.68	28976.23	336144.04	359215.88	357791.96	356570.14
344	9488.41	8108.98	29157.65	337196.15	360254.21	358819.14	357591.86
345	9541.37	8184.36	29352.52	338248.10	361292.60	359850.21	358618.10
346	9594.07	8259.35	29546.41	339300.02	362333.76	360889.66	359651.90
347	9645.56	8337.22	29742.89	340351.78	363377.03	361939.12	360695.25
348	9694.93	8403.08	29912.78	341403.38	364423.66	362997.79	361749.25
349	9743.07	8471.61	30084.65	342454.79	365473.21	364067.22	362813.83
350	9788.58	8520.18	30218.78	343506.09	366525.21	365145.84	363890.27
351	9832.57	8567.13	30346.49	344557.23	367578.65	366230.64	364973.85
352	9876.06	8617.43	30477.78	345608.26	368630.69	367317.13	366057.91
353	9917.92	8658.39	30592.22	346659.19	369681.51	368401.33	367139.89
354	9960.64	8707.79	30720.28	347710.09	370728.36	369478.77	368215.71
355	9994.47	8725.84	30799.25	348761.06	371773.71	370550.19	369284.74
356	10026.45	8748.60	30878.83	349812.10	372816.95	371616.37	370346.97
357	10060.86	8766.96	30960.09	350863.16	373858.01	372677.49	371404.81
358	10101.44	8792.23	31060.36	351914.37	374897.46	373734.24	372458.02
359	10141.58	8813.65	31159.45	352965.75	375935.80	374787.13	373506.79
360	10177.45	8829.61	31247.49	354017.23	376974.76	375836.23	374551.88
361	10211.64	8844.81	31334.14	355068.95	378011.62		
362	10243.05	8855.99	31415.32	356120.93	379047.98		
363	10270.30	8865.68	31485.75	357172.97	380084.66		
364	10302.27	8865.68	31568.13	358225.10	381119.95		
365	10334.17	8874.20	31650.82	359277.25	382156.44		
366	10365.15	8874.20	31729.01	360329.27	383192.08		
367	10391.92	8883.72	31797.48	361381.27	384227.63		
368	10422.34	8894.54	31874.52	362433.19	385264.02		
369	10451.36	8894.54	31944.59	363484.89	386301.38		
370	10477.59	8903.88	32008.18	364536.47	387343.43		
371	10497.55	8914.53	32057.98	365588.02	388388.37		

hour	Air Change	Air Change (ACH)	ASHRAE Enhanced	Enhanced Model	Angular Cracks	Mixed Cracks	Straight Cracks
372	10523.20	8921.37	32118.24	366639.42	389439.46		
373	10544.24	8928.86	32166.35	367690.57	390492.95		
374	10565.99	8936.60	32215.47	368741.61	391550.73		
375	10588.23	8946.49	32266.41	369792.61	392609.70		
376	10606.40	8956.19	32308.34	370843.53	393671.05		
377	10631.48	8969.57	32366.23	371894.43	394730.67		
378	10651.87	8976.83	32411.70	372945.33	395789.72		
379	10675.33	8981.00	32462.56	373996.15	396845.61		
380	10695.25	8988.09	32506.42	375046.95	397900.43		
381	10705.95	8997.61	32534.21	376097.75	398954.32		
382	10715.21	9007.49	32560.49	377148.55	400007.30		
383	10726.66	9017.67	32590.49	378199.42	401058.91		
384	10736.69	9027.49	32617.91	379250.30	402108.46		
385	10754.02	9036.74	32658.37	380301.25	403155.77		
386	10762.66	9046.73	32684.45	381352.22	404203.00		
387	10775.34	9058.01	32719.20	382403.48	405246.53		
388	10798.54	9068.33	32778.01	383455.14	406288.82		
389	10824.63	9077.61	32843.36	384506.88	407330.99		
390	10851.35	9087.12	32908.86	385558.52	408372.73		
391	10883.80	9095.77	32986.87	386610.07	409413.99		
392	10923.48	9116.96	33084.86	387661.54	410454.44		
393	10962.58	9137.82	33180.33	388712.92	411497.36		
394	11006.27	9176.69	33299.05	389764.21	412544.04		
395	11048.31	9210.34	33408.19	390815.41	413593.86		
396	11090.58	9247.94	33521.02	391866.52	414648.92		
397	11131.58	9280.76	33625.45	392917.53	415706.42		
398	11168.07	9300.24	33709.65	393968.46	416766.87		
399	11203.95	9319.39	33791.45	395019.29	417830.27		
400	11217.26	9330.04	33824.69	396070.10	418893.80		
401	11230.24	9341.59	33858.70	397120.98	419956.44		
402	11242.10	9353.19	33891.41	398171.93	421018.21		
403	11260.99	9366.63	33939.84	399223.18	422078.19		
404	11273.76	9382.54	33981.57	400274.56	423136.47		
405	11283.94	9398.84	34021.94	401326.04	424193.80		
406	11292.43	9410.92	34052.55	402377.55	425250.36		
407	11302.83	9428.49	34096.27	403429.28	426306.81		
408	11310.23	9441.67	34129.09	404481.19	427360.72		
409	11321.10	9461.01	34177.63	405533.29	428415.44		

hour	Air Change	Air Change (ACH)	ASHRAE Enhanced	Enhanced Model	Angular Cracks	Mixed Cracks	Straight Cracks
410	11328.34	9475.16	34213.11	406585.57	429467.34		
411	11335.94	9490.05	34250.63	407638.03	430517.99		
412	11344.82	9506.63	34293.11	408690.82	431566.15		
413	11354.91	9524.58	34339.88	409743.89	432613.86		
414	11367.36	9544.52	34393.85	410797.30	433660.96		
415	11382.43	9565.97	34455.10	411851.01	434708.07		
416	11401.34	9587.83	34524.70	412904.84	435754.05		
417	11420.25	9609.69	34594.30	413958.72	436803.23		
418	11438.81	9631.16	34662.25	415012.55	437854.50		
419	11457.03	9652.23	34728.58	416066.30	438909.39		
420	11480.80	9671.26	34804.97	417119.90	439968.35		
421	11503.09	9689.10	34875.61	418173.32	441030.22		
422	11531.06	9704.03	34958.85	419226.64	442095.51		
423	11556.42	9719.82	35034.88	420279.86	443162.40		
424	11577.91	9737.02	35101.98	421333.06	444229.13		
425	11598.34	9755.20	35167.41	422386.25	445294.10		
426	11625.43	9776.88	35253.24	423439.57	446356.09		
427	11644.83	9802.77	35327.82	424492.99	447415.61		
428	11665.34	9830.13	35407.79	425546.64	448472.77		
429	11681.60	9859.07	35485.20	426600.47	449527.50		
430	11699.37	9889.10	35567.10	427654.50	450580.63		
431	11711.32	9911.42	35626.79	428708.63	451630.25		
432	11722.65	9934.60	35688.42	429763.01	452679.67		
433	11735.08	9958.92	35753.84	430817.57	453725.18		
434	11747.50	9983.23	35819.26	431872.19	454769.42		
435	11761.67	10008.43	35888.69	432926.89	455810.09		
436	11775.05	10033.42	35956.74	433981.61	456849.30		
437	11786.63	10058.15	36022.82	435036.41	457885.04		
438	11798.43	10083.34	36090.28	436091.30	458918.12		
439	11810.22	10108.52	36157.74	437146.21	459947.35		
440	11821.64	10133.91	36225.62	438201.19	460975.70		
441	11833.65	10159.56	36294.48	439256.19	462003.26		
442	11846.31	10185.46	36364.42	440311.20	463033.49		
443	11858.33	10211.10	36433.28	441366.21	464065.50		
444	11869.54	10236.03	36499.79	442421.15	465101.04		
445	11881.34	10261.22	36567.25	443476.08	466138.78		
446	11892.54	10286.14	36633.75	444531.01	467179.20		
447	11905.20	10310.91	36700.58	445585.79	468220.74		

hour	Air Change	Air Change (ACH)	ASHRAE Enhanced	Enhanced Model	Angular Cracks	Mixed Cracks	Straight Cracks
448	11917.26	10334.51	36764.25	446640.54	469262.62		
449	11928.46	10357.42	36825.50	447695.22	470301.43		
450	11939.45	10379.91	36885.45	448749.80	471337.42		
451	11953.91	10403.07	36950.59	449804.30	472369.89		
452	11967.32	10426.92	37015.66	450858.78	473400.55		
453	11980.91	10449.89	37079.19	451913.25	474427.82		
454	11997.38	10473.32	37148.21	452967.71	475452.85		
455	12014.75	10496.50	37217.62	454021.96	476475.95		
456	12033.36	10519.67	37289.47	455076.18	477497.36		
457	12052.96	10542.34	37362.42	456130.31	478516.62		
458	12070.90	10564.68	37431.02	457184.34	479533.09		
459	12090.52	10585.62	37501.06	458238.29	480548.28		
460	12109.79	10606.19	37569.44	459292.15	481561.05		
461	12127.67	10626.86	37634.89	460345.99	482572.45		
462	12139.32	10645.52	37685.18	461399.53	483582.52		
463	12152.87	10666.02	37741.91	462453.16	484591.72		
464	12169.84	10687.14	37805.77	463506.87	485599.05		
465	12191.93	10706.80	37879.52	464560.59	486607.77		
466	12208.49	10725.95	37938.79	465614.10	487617.13		
467	12217.68	10742.29	37981.08	466667.22	488630.81		
468	12226.46	10757.90	38021.19	467720.13	489647.03		
469	12235.82	10773.72	38061.90	468772.84	490666.27		
470	12244.31	10788.08	38098.57	469825.37	491686.98		
471	12252.08	10801.90	38133.48	470877.78	492710.47		
472	12259.19	10815.18	38166.78	471930.08	493733.18		
473	12266.77	10828.66	38200.70	472982.36	494755.08		
474	12276.02	10842.65	38237.00	474034.63	495774.09		
475	12286.53	10856.67	38274.55	475086.83	496791.56		
476	12295.37	10870.05	38308.93	476138.94	497807.31		
477	12304.88	10883.58	38344.26	477191.03	498822.59		
478	12314.87	10896.91	38379.59	478243.04	499837.18		
479	12326.27	10910.09	38416.39	479294.97	500851.11		
480	12336.00	10923.07	38450.63	480346.88	501864.68		
481	12344.79	10935.59	38482.82	481398.71	502878.80		
482	12357.37	10949.01	38521.53	482450.53	503891.68		
483	12368.48	10961.86	38557.17	483502.33	504904.88		
484	12379.60	10974.71	38592.82	484554.14	505919.67		
485	12394.34	10987.83	38635.31	485606.02	506934.57		

hour	Air Change	Air Change (ACH)	ASHRAE Enhanced	Enhanced Model	Angular Cracks	Mixed Cracks	Straight Cracks
486	12410.34	11002.06	38682.16	486658.05	507949.38		
487	12424.50	11015.92	38725.07	487710.10	508964.80		
488	12436.89	11029.14	38763.48	488762.03	509979.25		
489	12449.28	11042.37	38801.90	489813.94	510998.05		
490	12458.74	11054.14	38832.99	490865.55	512019.66		
491	12465.15	11064.41	38858.09	491916.91	513046.05		
492	12470.99	11073.76	38880.67	492967.99	514078.34		
493	12474.79	11081.86	38900.09	494018.80	515114.27		
494	12478.06	11089.14	38917.59	495069.49	516154.80		
495	12483.44	11097.76	38938.04	496120.13	517196.82		
496	12489.23	11106.50	38958.91	497170.76	518241.76		
497	12495.97	11115.51	38980.84	498221.37	519285.81		
498	12501.96	11124.56	39002.54	499272.06	520328.06		
499	12510.45	11134.37	39027.81	500322.83	521369.29		
500	12517.01	11143.71	39050.63	501373.68	522409.31		
501	12522.10	11152.77	39072.36	502424.63	523449.63		
502	12528.13	11162.42	39095.76	503475.66	524488.82		
503	12534.16	11172.08	39119.17	504526.72	525528.83		
504	12541.71	11182.15	39144.44	505577.78	526567.62		
505	12553.41	11193.60	39177.50	506628.99	527607.86		
506	12561.60	11203.80	39203.60	507680.08	528647.23		
507	12567.94	11213.95	39228.21	508731.16	529686.73		
508	12579.62	11224.34	39259.38	509782.24	530726.03		
509	12592.48	11234.63	39292.46	510833.31	531764.47		
510	12605.28	11246.02	39327.24	511884.52	532802.96		
511	12618.09	11257.41	39362.02	512935.76	533841.41		
512	12634.63	11269.18	39403.61	513986.93	534879.16		
513	12651.17	11280.96	39445.20	515038.10	535920.87		
514	12660.80	11292.95	39475.69	516089.13	536965.63		
515	12672.38	11305.30	39509.31	517140.19	538015.54		
516	12681.32	11317.23	39539.04	518191.19	539070.14		
517	12690.66	11328.86	39568.44	519242.11	540130.27		
518	12699.33	11340.43	39597.12	520293.01	541192.24		
519	12709.82	11356.30	39635.52	521343.90	542257.15		
520	12723.21	11371.78	39675.64	522394.79	543323.85		
521	12734.02	11388.12	39715.38	523445.75	544390.05		
522	12746.14	11405.38	39758.23	524496.87	545452.29		
523	12773.69	11437.23	39843.68	525548.15	546512.66		

hour	Air Change	Air Change (ACH)	ASHRAE Enhanced	Enhanced Model	Angular Cracks	Mixed Cracks	Straight Cracks
524	12801.72	11462.17	39921.18	526599.54	547572.52		
525	12823.26	11477.49	39977.50	527651.03	548629.37		
526	12845.71	11493.47	40037.36	528702.68	549686.40		
527	12874.73	11511.54	40112.07	529754.29	550740.86		
528	12896.73	11527.19	40170.14	530805.91	551794.21		
529	12921.18	11540.24	40231.79	531857.53	552847.07		
530	12938.55	11552.60	40276.35	532908.94	553900.63		
531	12952.59	11563.84	40313.15	533960.24	554951.68		
532	12969.55	11574.40	40355.05	535011.51	556003.36		
533	12988.18	11584.35	40400.07	536062.78	557053.09		
534	13007.92	11596.64	40450.37	537114.25	558102.99		
535	13026.98	11608.50	40499.93	538165.89	559152.57		
536	13052.39	11622.06	40565.33	539217.65	560202.01		
537	13074.84	11638.04	40625.19	540269.36	561253.17		
538	13094.73	11653.97	40678.30	541320.85	562307.31		
539	13108.00	11665.76	40713.38	542371.96	563364.81		
540	13122.90	11676.37	40749.32	543422.86	564424.68		
541	13137.42	11689.28	40785.96	544473.48	565488.24		
542	13149.38	11702.06	40818.59	545523.91	566554.68		
543	13164.04	11713.79	40853.33	546574.28	567622.22		
544	13185.68	11731.11	40904.08	547624.57	568689.80		
545	13199.91	11742.50	40937.45	548674.83	569755.05		
546	13211.50	11754.88	40968.80	549725.08	570817.27		
547	13225.20	11767.06	41002.71	550775.41	571876.44		
548	13232.47	11774.82	41022.37	551825.67	572933.68		
549	13240.06	11782.93	41042.91	552875.92	573987.54		
550	13245.26	11791.25	41062.57	553926.38	575041.01		
551	13250.45	11800.02	41083.43	554977.02	576091.65		
552	13255.47	11808.96	41104.71	556027.76	577141.63		
553	13263.96	11818.77	41129.98	557078.54	578190.15		
554	13272.84	11828.25	41155.16	558129.32	579238.71		
555	13284.65	11837.70	41184.65	559180.12	580286.53		
556	13293.52	11847.18	41209.84	560230.91	581334.43		
557	13308.41	11856.45	41245.05	561281.78	582382.46		
558	13325.31	11865.46	41284.04	562332.65	583428.73		
559	13345.94	11876.48	41331.64	563383.54	584473.61		
560	13367.58	11882.25	41378.82	564434.35	585517.74		
561	13389.41	11890.02	41426.28	565485.08	586565.05		

hour	Air Change	Air Change (ACH)	ASHRAE Enhanced	Enhanced Model	Angular Cracks	Mixed Cracks	Straight Cracks
562	13406.24	11899.00	41463.73	566535.73	587614.60		
563	13421.91	11910.15	41499.44	567586.14	588669.57		
564	13425.51	11916.56	41514.23	568636.23	589727.90		
565	13429.39	11923.80	41531.27	569686.61	590791.39		
566	13434.16	11931.01	41548.15	570736.87	591857.35		
567	13437.66	11937.86	41564.28	571787.20	592926.18		
568	13442.98	11951.11	41597.04	572838.17	593996.68		
569	13448.21	11962.74	41625.79	573889.75	595067.36		
570	13455.63	11980.56	41670.45	574941.67	596134.88		
571	13460.09	11993.26	41703.18	575993.96	597200.21		
572	13464.58	12006.45	41737.46	577046.48	598264.53		
573	13472.28	12026.98	41790.13	578099.13	599328.27		
574	13481.49	12049.10	41846.48	579151.96	600391.28		
575	13487.88	12064.46	41885.62	580204.83	601450.96		
576	13495.31	12080.98	41927.79	581257.87	602510.11		
577	13502.53	12097.67	41970.51	582311.00	603568.74		
578	13511.50	12115.22	42015.64	583364.16	604626.58		
579	13519.52	12132.34	42059.45	584417.33	605683.39		
580	13529.02	12150.09	42105.36	585470.50	606739.43		
581	13540.46	12168.42	42154.18	586523.68	607793.61		
582	13552.15	12187.14	42204.27	587576.93	608847.94		
583	13566.47	12206.23	42258.73	588630.19	609900.83		
584	13580.48	12224.92	42312.29	589683.53	610953.79		
585	13593.53	12243.50	42364.14	590736.88	612009.27		
586	13610.72	12261.85	42422.97	591790.16	613069.01		
587	13625.99	12279.51	42476.38	592843.30	614132.24		
588	13645.02	12296.44	42536.49	593896.33	615199.94		
589	13663.31	12312.70	42593.40	594949.20	616270.39		
590	13683.41	12328.80	42653.83	596001.97	617343.05		
591	13706.69	12343.29	42720.22	597054.64	618415.60		
592	13735.85	12358.86	42801.23	598107.22	619484.92		
593	13770.16	12374.12	42896.17	599159.84	620551.71		
594	13811.80	12396.34	43012.91	600212.47	621612.43		
595	13855.36	12415.71	43134.53	601265.17	622667.98		
596	13908.59	12458.32	43294.54	602317.88	623721.26		
597	13960.01	12499.49	43449.12	603370.59	624769.03		
598	14012.86	12546.50	43612.43	604423.31	625815.46		
599	14068.05	12605.41	43794.23	605476.03	626857.14		



hour	Air Change	Air Change (ACH)	ASHRAE Enhanced	Enhanced Model	Angular Cracks	Mixed Cracks	Straight Cracks
600	14124.49	12660.63	43975.29	606528.82	627896.59		
601	14182.08	12732.36	44178.43	607581.48	628934.51		
602	14236.88	12785.97	44350.58	608634.05	629971.11		
603	14293.02	12850.88	44539.95	609686.60	631005.23		
604	14349.11	12920.74	44735.56	610739.08	632038.69		
605	14403.86	12993.79	44933.42	611791.46	633069.53		
606	14457.87	13065.85	45127.56	612843.76	634099.29		
607	14511.22	13132.29	45311.49	613896.04	635128.48		
608	14563.27	13192.48	45482.77	614948.23	636155.93		
609	14613.78	13246.40	45641.56	616000.34	637184.76		
610	14660.34	13283.67	45772.67	617052.37	638215.53		
611	14704.98	13319.40	45895.14	618104.15	639250.38		
612	14749.82	13367.27	46028.29	619155.62	640289.03		
613	14790.89	13414.76	46150.54	620206.58	641330.85		
614	14825.60	13442.55	46232.83	621257.10	642374.98		
615	14829.24	13449.67	46249.35	622307.16	643421.70		
616	14832.95	13455.93	46263.72	623357.12	644467.16		
617	14836.65	13462.19	46278.08	624407.04	645512.92		
618	14840.11	13468.34	46292.22	625456.94	646555.14		
619	14844.74	13474.94	46307.44	626506.82	647595.33		
620	14848.72	13481.31	46322.05	627556.71	648633.39		
621	14852.56	13488.14	46338.00	628606.87	649670.76		
622	14864.32	13500.69	46371.08	629657.44	650706.99		
623	14872.72	13511.89	46399.51	630708.51	651741.59		
624	14880.17	13523.16	46427.42	631759.76	652776.46		
625	14892.44	13539.54	46469.67	632811.20	653810.10		
626	14898.89	13551.01	46497.75	633862.69	654844.12		
627	14913.44	13563.95	46539.01	634914.34	655876.36		
628	14925.70	13577.04	46576.48	635966.03	656910.19		
629	14940.25	13589.98	46617.74	637017.73	657942.80		
630	14957.66	13602.37	46664.13	638069.44	658976.58		
631	14972.21	13615.31	46705.39	639121.15	660009.60		
632	14988.12	13628.05	46749.03	640172.86	661043.98		
633	14998.82	13641.38	46784.87	641224.64	662079.97		
634	15007.17	13654.00	46816.71	642276.36	663120.70		
635	15016.14	13666.76	46849.37	643328.08	664165.59		
636	15023.92	13679.22	46880.49	644379.79	665216.42		
637	15031.70	13691.69	46911.62	645431.51	666272.35		



hour	Air Change	Air Change (ACH)	ASHRAE Enhanced	Enhanced Model	Angular Cracks	Mixed Cracks	Straight Cracks
638	15041.11	13704.23	46944.15	646483.15	667334.52		
639	15048.52	13716.10	46973.78	647534.85	668399.57		
640	15058.95	13729.09	47008.49	648586.56	669468.46		
641	15070.84	13742.83	47046.86	649638.41	670536.56		
642	15085.93	13756.26	47090.73	650690.36	671604.97		
643	15101.39	13770.01	47135.99	651742.40	672671.40		
644	15117.48	13784.33	47183.86	652794.60	673737.27		
645	15143.91	13796.08	47256.33	653847.05	674799.72		
646	15175.19	13804.43	47341.48	654899.62	675861.25		
647	15208.63	13813.35	47433.41	655952.29	676919.86		
648	15244.41	13832.45	47536.39	657005.14	677976.35		
649	15274.94	13846.02	47623.93	658058.08	679030.27		
650	15316.32	13864.43	47741.56	659110.99	680083.20		
651	15358.98	13879.61	47862.82	660163.96	681133.58		
652	15405.14	13900.14	47997.46	661217.09	682182.63		
653	15454.21	13926.33	48143.53	662270.32	683229.31		
654	15506.94	13963.85	48304.56	663323.50	684276.68		
655	15559.67	14001.37	48465.58	664376.67	685321.51		
656	15612.39	14038.89	48626.61	665429.85	686366.88		
657	15666.27	14082.02	48793.60	666482.96	687413.13		
658	15719.12	14129.04	48956.90	667535.77	688462.84		
659	15770.87	14184.27	49121.81	668588.17	689513.94		
660	15822.93	14249.10	49299.19	669640.36	690569.59		
661	15873.36	14316.38	49475.65	670692.27	691626.42		
662	15923.25	14382.95	49648.32	671743.98	692685.96		
663	15970.86	14442.25	49804.84	672795.56	693747.30		
664	16017.12	14495.74	49949.33	673847.05	694808.64		
665	16061.87	14539.52	50077.81	674898.51	695866.20		
666	16106.61	14583.30	50206.29	675949.95	696921.34		
667	16152.17	14631.93	50342.57	677001.39	697972.35		
668	16197.73	14680.56	50478.84	678052.83	699021.81		
669	16241.53	14719.52	50599.92	679104.27	700067.89		
670	16284.66	14757.88	50718.11	680155.64	701111.06		
671	16326.71	14791.54	50829.36	681206.99	702152.80		
672	16367.49	14820.57	50933.97	682258.34	703191.71		
673	16408.28	14849.59	51038.58	683309.69	704229.23		
674	16442.77	14868.00	51122.80	684361.04	705265.09		
675	16478.47	14883.88	51208.49	685412.38	706298.04		

hour	Air Change	Air Change (ACH)	ASHRAE Enhanced	Enhanced Model	Angular Cracks	Mixed Cracks	Straight Cracks
676	16517.56	14904.74	51303.97	686463.73	707330.86		
677	16551.52	14922.86	51385.99	687515.00	708361.98		
678	16585.47	14940.99	51468.01	688566.26	709391.19		
679	16612.52	14960.24	51536.71	689617.52	710419.99		
680	16651.24	14984.35	51632.38	690668.78	711448.60		
681	16690.78	15012.48	51731.75	691719.96	712479.98		
682	16731.86	15049.02	51841.41	692771.06	713514.21		
683	16772.26	15084.96	51948.27	693822.07	714553.84		
684	16809.89	15111.73	52039.95	694873.00	715597.99		
685	16826.69	15125.19	52081.91	695923.83	716646.40		
686	16832.24	15134.57	52104.38	696974.71	717699.31		
687	16837.17	15144.22	52127.74	698025.88	718753.22		
688	16842.75	15154.63	52153.12	699077.24	719809.30		
689	16848.66	15165.68	52180.20	700128.79	720865.72		
690	16856.84	15178.04	52211.53	701180.52	721919.18		
691	16869.73	15191.80	52251.49	702232.36	722972.41		
692	16881.91	15205.89	52291.08	703284.30	724023.03		
693	16889.72	15219.77	52325.92	704336.41	725073.67		
694	16898.42	15234.48	52363.63	705388.84	726122.49		
695	16909.62	15250.42	52406.69	706441.47	727172.29		
696	16918.07	15266.20	52447.11	707494.29	728219.87		
697	16929.23	15284.07	52494.92	708547.45	729257.79		
698	16940.62	15303.32	52546.49	709600.95	730291.72		
699	16952.73	15323.79	52601.90	710654.74	731323.58		
700	16967.68	15346.39	52665.77	711708.74	732350.81		
701	16977.10	15367.35	52720.58	712762.80	733375.95		
702	16989.53	15389.45	52780.09	713816.87	734399.26		
703	17003.23	15412.61	52843.70	714871.10	735421.35		
704	17016.57	15435.16	52905.84	715925.43	736441.29		
705	17035.84	15459.16	52981.04	716979.78	737462.54		
706	17049.55	15482.32	53044.65	718034.07	738485.54		
707	17064.84	15504.09	53107.64	719088.22	739512.20		
708	17080.50	15526.37	53171.86	720142.26	740540.63		
709	17097.75	15547.85	53237.82	721196.28	741572.66		
710	17115.04	15569.38	53303.24	722250.15	742606.73		
711	17134.29	15593.35	53375.70	723303.92	743642.61		
712	17153.18	15616.88	53446.47	724357.60	744678.13		
713	17170.90	15640.53	53515.24	725411.25	745713.49		

hour	Air Change	Air Change (ACH)	ASHRAE Enhanced	Enhanced Model	Angular Cracks	Mixed Cracks	Straight Cracks
714	17193.95	15663.08	53593.72	726464.90	746745.22		
715	17216.28	15686.91	53672.95	727518.68	747774.62		
716	17238.61	15710.75	53752.19	728572.48	748801.76		
717	17264.96	15734.19	53841.87	729626.44	749827.15		
718	17293.53	15757.06	53937.59	730680.49	750850.81		
719	17321.53	15786.94	54037.54	731734.43	751872.93		
720	17346.52	15818.07	54132.13	732788.28	752894.91		
721	17387.70	15854.69	54271.36	733842.18	753911.97		
722	17429.36	15895.46	54416.81	734896.16	754929.71		
723	17461.07	15923.66	54525.42	735950.23	755944.95		
724	17494.70	15950.59	54638.85	737004.38	756960.43		
725	17537.83	15981.28	54782.59	738058.62	757973.62		
726	17592.96	16020.51	54967.54	739112.96	758986.71		
727	17651.70	16072.76	55172.62	740167.31	759999.26		
728	17694.34	16114.48	55323.32	741221.53	761014.15		
729	17736.00	16162.66	55477.53	742275.59	762029.39		
730	17776.69	16209.70	55626.45	743329.48	763048.86		
731	17793.33	16233.39	55693.49	744383.18	764071.80		
732	17807.53	16253.60	55750.43	745436.78	765100.58		
733	17822.14	16273.10	55806.29	746490.21	766131.51		
734	17834.09	16292.22	55857.66	747543.60	767166.27		
735	17847.10	16311.90	55911.67	748597.04	768201.69		
736	17862.31	16332.20	55970.41	749650.56	769237.91		
737	17882.68	16352.13	56039.33	750704.10	770272.50		
738	17902.75	16371.76	56107.64	751757.71	771303.80		
739	17937.93	16384.28	56214.59	752811.41	772334.17		
740	17975.07	16394.19	56326.94	753865.12	773361.66		
741	18014.15	16401.14	56444.78	754918.84	774387.91		
742	18054.84	16412.00	56568.81	755972.64	775411.66		
743	18096.01	16426.65	56695.98	757026.52	776435.02		
744	18129.92	16444.74	56803.41	758080.49	777455.58		

## **Appendix B**

### **Hourly and Cumulative Data for Northwest Wall Obtained from the DOE-2/eQUEST, CFD Analyses, and Enhanced Model Simulations**

Supporting Data for Charts 5-8 to 5-14

## Hourly Data for Northwest Wall

### Hourly Northwest (NW) Wall Data (Watts)

hour	eUEST/DOE-2 Hourly Values (no reduction multiplier)			CFD Multiphysisc Simulation			
	Air Change	Air Change (ACH)	ASHRAE Enhanced	Enhanced Model	Angular Cracks	Mixed Cracks	Straight Cracks
1	56.029	24.919	157.860	525.783	954.536	867.704	916.750
2	54.852	24.395	154.544	746.408	953.216	866.990	915.432
3	65.523	34.970	196.614	805.611	951.399	865.908	914.195
4	60.664	26.981	187.338	805.096	950.079	864.373	912.754
5	69.586	37.138	225.392	821.346	946.745	862.458	909.881
6	42.192	11.259	136.746	826.700	944.771	860.788	908.104
7	58.600	20.850	190.787	823.588	942.659	859.075	906.221
8	45.585	20.274	151.554	819.754	941.388	857.656	905.070
9	45.094	16.045	147.876	818.078	942.205	860.151	907.145
10	64.774	28.809	212.331	841.410	944.555	864.975	912.290
11	59.864	26.625	193.424	854.493	947.400	871.483	918.960
12	74.712	53.166	245.551	862.263	950.602	878.035	926.349
13	67.624	42.106	213.952	868.778	953.916	884.995	932.466
14	56.624	35.257	176.479	877.865	956.870	890.961	938.016
15	56.113	34.939	173.557	899.262	957.854	894.329	940.576
16	39.703	24.721	123.741	906.931	956.940	894.628	939.172
17	31.480	19.601	101.808	914.507	954.134	889.560	933.638
18	29.937	15.978	96.969	910.030	951.371	885.008	929.334
19	27.180	16.924	89.162	914.855	948.677	880.678	925.349
20	33.825	21.061	113.295	927.686	948.055	876.501	922.078
21	31.300	16.705	103.571	921.476	945.406	873.477	919.130
22	44.114	23.544	144.947	913.276	944.517	870.692	916.915
23	28.478	17.732	95.387	907.334	942.667	868.363	914.771
24	31.300	16.705	103.571	920.200	941.435	866.306	912.772
25	26.285	16.367	88.643	925.721	941.842	865.147	912.357
26	22.367	17.906	75.939	921.773	940.196	863.722	911.316
27	25.466	18.122	86.016	918.444	940.068	862.233	910.127
28	31.675	14.088	103.090	917.329	939.593	861.620	909.504
29	27.558	14.708	89.261	921.973	939.384	860.834	909.065

hour	Air Change	Air Change (ACH)	ASHRAE Enhanced	Enhanced Model	Angular Cracks	Mixed Cracks	Straight Cracks
30	25.054	15.600	82.765	923.959	939.520	860.380	908.712
31	19.786	15.840	67.177	923.155	940.121	860.105	909.373
32	19.090	15.282	63.957	921.372	940.145	860.240	909.215
33	23.037	16.393	74.654	914.168	943.046	863.867	913.357
34	15.591	13.869	51.686	896.036	946.949	870.127	920.039
35	16.057	12.855	50.510	874.360	951.813	877.950	928.547
36	15.529	13.813	49.039	857.968	956.320	885.531	936.222
37	14.448	11.567	43.771	841.326	961.226	892.898	944.449
38	13.821	11.064	41.221	831.687	963.997	899.484	951.081
39	10.791	10.559	33.900	849.936	966.618	903.758	953.925
40	11.762	10.463	35.535	855.459	967.685	905.847	954.231
41	11.762	10.463	35.535	857.480	967.015	902.294	950.331
42	10.535	10.308	32.861	861.351	965.634	898.644	947.806
43	9.484	10.124	30.635	871.802	965.724	895.416	945.376
44	13.202	10.569	38.754	874.792	963.386	892.458	943.665
45	9.484	10.124	30.635	871.686	964.258	890.748	941.589
46	8.061	10.756	28.978	867.954	963.588	888.903	940.572
47	9.636	11.142	31.906	865.702	963.586	887.446	939.213
48	8.796	10.954	30.324	867.023	962.475	886.138	938.394
49	11.484	10.215	34.429	861.357	963.982	885.271	937.656
50	10.281	10.060	31.840	851.339	963.030	884.315	937.350
51	7.996	9.246	26.310	848.488	964.697	884.066	937.272
52	7.381	8.536	23.827	844.254	965.418	884.392	937.377
53	6.705	8.946	23.203	856.770	965.494	884.468	937.900
54	8.871	9.469	26.924	864.491	965.777	884.734	938.305
55	8.046	9.304	25.469	865.169	966.023	884.796	938.524
56	8.046	9.304	25.469	865.127	967.091	884.825	938.663
57	8.046	9.304	25.469	872.848	968.891	888.363	942.551
58	10.643	9.467	29.673	888.357	972.688	894.168	948.342
59	9.034	8.839	25.732	896.172	976.470	901.230	955.606
60	12.650	11.252	33.763	898.358	981.472	909.246	963.791
61	13.673	9.729	32.605	902.750	984.998	916.299	972.140
62	10.918	9.712	27.828	913.144	989.081	922.753	977.473
63	7.366	6.552	18.417	922.061	990.873	927.443	981.056
64	7.366	6.552	18.417	907.839	991.661	928.308	980.373
65	6.326	6.752	17.669	890.289	989.341	923.778	975.554
66	7.522	7.360	20.391	866.384	987.478	919.932	972.671
67	8.412	7.482	21.845	862.035	986.230	916.426	968.874

hour	Air Change	Air Change (ACH)	ASHRAE Enhanced	Enhanced Model	Angular Cracks	Mixed Cracks	Straight Cracks
68	8.412	7.482	21.845	873.034	985.480	913.243	966.444
69	8.412	7.482	21.845	872.977	983.763	910.223	963.600
70	15.036	8.025	35.512	871.356	983.056	907.742	961.256
71	45.542	24.306	107.562	874.179	983.178	905.770	960.018
72	47.776	29.748	111.724	885.444	983.099	904.683	958.977
73	45.878	24.485	102.074	892.412	982.846	904.001	958.720
74	62.783	67.015	171.199	891.404	983.819	903.871	958.870
75	59.345	63.346	157.880	887.864	985.016	903.904	959.116
76	62.464	77.787	185.362	887.729	985.138	903.304	958.512
77	58.312	51.869	144.368	897.420	985.313	903.134	958.236
78	61.646	65.801	166.733	902.696	985.060	902.865	958.107
79	64.968	80.904	195.379	901.718	984.837	902.532	957.881
80	62.783	67.015	171.199	898.385	985.406	902.418	957.734
81	66.334	88.506	210.618	902.173	987.667	905.716	961.046
82	63.743	85.049	199.989	905.398	991.063	911.208	966.760
83	61.199	76.212	180.394	896.181	994.065	917.995	973.693
84	59.926	74.626	175.452	877.663	998.385	924.914	980.976
85	57.952	72.169	168.527	851.815	1000.959	931.507	987.767
86	54.635	58.318	140.502	840.118	1004.137	937.154	992.953
87	49.948	44.429	113.829	841.821	1004.240	940.607	995.234
88	53.156	47.282	125.082	828.233	1003.737	940.117	993.192
89	57.294	50.963	141.848	810.639	999.289	934.412	986.988
90	60.203	53.551	153.440	796.296	997.050	929.261	981.769
91	31.641	8.444	69.893	790.532	993.335	924.095	977.159
92	36.229	12.890	81.827	789.929	990.621	919.239	972.356
93	52.360	32.602	132.100	793.831	988.078	915.027	968.278
94	27.544	12.250	66.112	801.292	985.426	911.450	964.798
95	37.439	16.651	90.875	811.065	983.085	907.946	961.748
96	19.710	8.766	48.897	828.908	981.946	905.307	958.581
97	17.463	9.320	44.035	843.348	979.618	902.870	956.360
98	14.076	10.016	37.517	854.863	978.354	900.754	954.382
99	11.906	9.532	32.086	860.670	977.676	899.034	953.595
100	11.906	9.532	32.086	862.017	977.558	897.739	951.837
101	12.690	9.030	32.547	882.990	976.725	896.929	951.371
102	10.785	7.674	27.385	892.812	976.309	896.179	950.638
103	8.775	8.586	24.794	895.311	977.424	896.231	950.888
104	6.318	7.306	18.938	894.903	977.247	896.011	951.003
105	6.591	6.449	18.018	892.141	979.616	899.419	954.099

hour	Air Change	Air Change (ACH)	ASHRAE Enhanced	Enhanced Model	Angular Cracks	Mixed Cracks	Straight Cracks
106	6.113	7.069	18.196	898.847	983.294	905.367	960.659
107	5.899	6.296	16.216	896.794	988.757	912.788	968.490
108	5.892	5.765	15.014	894.501	991.859	920.499	975.894
109	4.883	5.212	12.883	891.079	996.714	927.541	983.347
110	5.240	5.127	12.985	899.424	998.982	933.792	989.427
111	7.997	7.113	18.621	910.328	1001.090	937.877	993.074
112	8.734	5.438	18.028	911.537	1000.347	938.429	990.991
113	10.599	8.485	24.856	909.831	996.933	932.814	985.312
114	23.609	12.600	52.528	911.207	994.534	928.334	980.465
115	36.389	19.421	81.968	914.198	992.575	923.357	976.407
116	38.017	20.290	88.759	895.264	989.526	919.179	972.760
117	45.542	24.306	107.562	871.610	988.098	915.476	968.919
118	26.560	11.813	62.303	854.984	985.489	911.853	965.596
119	27.052	0.000	62.325	843.055	984.927	909.166	963.151
120	37.799	13.449	88.532	849.075	982.596	906.610	960.706
121	40.332	14.350	94.465	857.616	981.810	904.957	958.990
122	26.560	0.000	60.444	858.589	981.162	903.305	957.582
123	26.069	0.000	58.586	859.912	980.451	902.340	956.447
124	45.542	24.306	107.562	859.054	980.681	901.071	955.771
125	44.705	19.883	102.403	884.846	980.523	900.510	955.124
126	21.003	7.473	46.846	902.204	980.082	899.702	954.809
127	20.575	5.491	45.449	898.389	979.625	899.036	954.114
128	39.517	14.060	89.254	891.877	979.401	898.603	953.423
129	17.153	12.206	42.238	883.783	981.194	901.541	956.869
130	58.995	47.228	147.304	885.382	984.187	906.850	961.964
131	66.202	70.665	186.381	880.069	986.862	912.945	968.187
132	70.135	87.339	217.922	870.799	991.400	920.129	975.576
133	73.218	110.716	264.166	859.157	993.813	926.456	982.813
134	68.892	91.920	221.348	862.443	996.222	932.218	987.110
135	68.107	96.931	229.575	877.823	999.295	936.116	990.189
136	65.501	93.222	218.450	884.583	998.798	937.349	990.136
137	67.718	120.472	279.079	888.605	996.850	933.085	985.359
138	68.390	115.583	268.348	893.309	995.008	928.925	982.057
139	65.559	87.473	208.159	897.776	993.722	925.047	978.256
140	53.302	37.930	122.913	889.597	992.402	921.562	975.500
141	41.214	21.996	89.397	870.388	991.201	918.958	972.807
142	45.620	40.579	112.944	844.273	990.674	916.572	970.887
143	22.134	19.688	54.798	826.535	990.071	914.371	969.161



hour	Air Change	Air Change (ACH)	ASHRAE Enhanced	Enhanced Model	Angular Cracks	Mixed Cracks	Straight Cracks
144	9.915	8.820	24.548	824.220	989.873	912.617	968.002
145	46.340	41.220	115.857	821.787	988.619	911.144	966.185
146	70.956	113.609	266.192	818.448	988.166	909.779	964.958
147	70.179	99.880	237.818	815.049	987.178	908.515	963.665
148	71.487	101.741	243.536	810.595	987.607	907.316	962.716
149	69.876	87.017	215.722	820.211	986.000	906.247	961.961
150	71.487	101.741	243.536	1050.527	987.070	905.857	961.166
151	68.864	98.007	232.125	1050.381	986.071	905.196	961.156
152	65.789	76.075	190.281	1050.429	985.341	904.362	960.002
153	63.911	68.219	175.691	1050.429	987.235	906.844	962.170
154	8.714	10.076	25.203	1050.429	988.519	911.423	967.191
155	9.451	13.450	32.878	1050.786	990.934	917.024	971.956
156	6.835	13.984	33.835	1051.056	991.288	922.012	977.551
157	91.576	187.352	456.876	1051.329	992.741	926.548	981.189
158	93.483	182.939	448.171	1051.532	992.141	929.805	984.263
159	96.525	180.304	446.252	1051.795	990.979	931.613	984.076
160	94.986	152.082	386.073	1051.993	988.078	929.807	981.303
161	9.436	20.144	50.561	1052.326	983.969	923.031	973.717
162	109.059	232.820	585.774	1052.463	978.981	916.742	967.163
163	110.759	216.746	551.210	1052.718	975.509	910.584	961.733
164	110.368	196.345	507.995	1052.913	973.013	905.616	957.174
165	111.941	209.101	537.331	1052.958	969.689	901.094	952.914
166	16.611	23.641	64.774	1052.979	967.880	897.422	949.547
167	104.666	158.271	425.081	1052.988	965.082	893.785	946.020
168	106.925	161.687	438.022	1053.134	963.141	891.216	942.985
169	94.945	101.345	324.914	1053.230	962.213	889.247	941.439
170	98.500	113.901	348.522	1053.252	960.012	886.378	938.751
171	97.683	112.956	347.628	1053.334	959.503	884.110	936.405
172	90.842	88.885	305.362	1053.421	956.934	882.197	934.647
173	27.537	22.045	87.884	1053.439	955.745	880.220	932.801
174	31.740	19.763	98.924	1053.590	954.097	878.460	931.171
175	67.792	36.181	209.954	1053.687	953.380	876.882	928.929
176	67.792	36.181	209.954	1053.710	951.926	875.577	927.877
177	77.519	55.163	245.831	1053.649	953.772	878.036	930.359
178	25.550	20.454	81.543	1053.500	955.711	883.371	935.841
179	26.414	18.796	81.290	1053.331	960.171	889.952	942.897
180	68.133	42.423	202.574	1053.155	963.315	897.013	949.741
181	56.029	24.919	157.860	1052.903	966.621	903.194	956.688

hour	Air Change	Air Change (ACH)	ASHRAE Enhanced	Enhanced Model	Angular Cracks	Mixed Cracks	Straight Cracks
182	60.654	32.371	173.073	1052.852	969.357	909.041	961.727
183	70.874	50.434	208.005	1052.758	970.240	913.192	965.358
184	70.874	50.434	208.005	1052.737	969.863	913.604	963.897
185	31.127	13.844	88.482	1052.870	967.036	908.552	958.859
186	33.079	11.770	94.014	1052.960	965.082	903.557	953.514
187	46.836	12.498	135.856	1053.193	962.833	899.139	949.543
188	35.036	12.466	103.073	1053.307	960.815	895.198	946.029
189	53.070	18.882	156.126	1053.338	959.373	891.879	942.880
190	37.742	0.000	108.941	1053.280	959.281	889.175	941.160
191	48.341	17.200	139.810	1053.203	957.546	887.091	938.916
192	50.623	18.012	145.146	1053.118	957.701	885.794	937.659
193	49.609	17.651	139.740	1052.958	957.109	884.734	937.374
194	61.231	32.679	176.237	1052.928	957.793	883.683	936.446
195	30.017	13.350	85.327	1052.914	957.223	882.868	935.982
196	24.563	10.924	68.586	1052.766	958.376	882.151	935.119
197	28.699	12.764	80.135	1052.740	957.185	881.567	934.488
198	32.194	8.591	88.494	1052.729	958.038	881.252	934.475
199	31.126	11.075	85.301	1052.653	957.556	881.091	934.352
200	53.771	23.915	148.784	1052.639	958.605	880.613	934.002
201	26.407	9.396	71.690	1052.562	960.097	884.245	937.818
202	30.904	8.247	82.552	1052.477	963.217	889.633	943.398
203	29.663	10.554	78.998	1052.388	967.107	896.792	950.578
204	40.791	10.885	106.829	1052.297	970.553	903.944	958.003
205	50.604	22.506	132.216	1052.135	974.456	910.906	964.981
206	49.483	22.008	126.698	1051.961	977.809	917.019	970.614
207	21.086	13.129	55.369	1051.853	978.455	920.721	973.342
208	25.401	13.557	67.351	1052.039	978.100	921.378	972.298
209	25.875	13.809	69.269	1052.132	975.813	916.363	967.256
210	24.719	15.391	68.028	1052.225	973.592	911.647	962.584
211	67.390	47.955	189.612	1052.245	972.057	907.674	959.171
212	67.390	47.955	189.612	1052.254	970.430	904.063	956.309
213	67.390	47.955	189.612	1052.258	970.298	901.095	953.312
214	23.223	16.526	65.343	1052.260	968.492	898.397	951.318
215	19.132	18.720	58.823	1052.261	968.440	896.302	949.064
216	19.132	18.720	58.823	1052.261	966.952	894.706	947.926
217	17.933	19.142	57.151	1052.262	966.676	893.325	946.730
218	17.933	19.142	57.151	1052.262	966.605	892.158	945.716
219	17.933	19.142	57.151	1052.262	965.682	891.177	944.229

hour	Air Change	Air Change (ACH)	ASHRAE Enhanced	Enhanced Model	Angular Cracks	Mixed Cracks	Straight Cracks
220	88.819	110.606	306.195	1052.262	965.850	889.877	943.163
221	15.790	19.664	54.436	1052.262	964.850	888.826	943.499
222	15.790	19.664	54.436	1052.262	964.470	888.160	941.576
223	13.152	19.888	51.565	1052.262	964.293	887.511	941.491
224	91.242	121.740	327.992	1052.262	964.608	886.712	940.607
225	91.242	121.740	327.992	1052.262	965.485	889.224	943.000
226	13.152	19.888	51.565	1052.262	968.524	894.259	948.206
227	13.152	19.888	51.565	1052.262	970.874	900.442	953.790
228	11.082	19.715	49.637	1052.262	973.874	907.326	961.125
229	12.177	19.497	49.698	1052.190	976.583	913.718	968.051
230	11.885	19.029	48.308	1052.108	979.789	918.816	972.237
231	12.913	19.526	50.399	1052.163	979.157	922.138	974.427
232	94.563	134.583	356.599	1052.309	978.172	921.862	972.501
233	92.974	115.781	327.931	1052.548	974.246	916.353	966.283
234	91.046	105.282	310.911	1052.664	971.598	910.989	961.538
235	88.686	94.664	294.059	1052.766	968.818	905.878	956.717
236	25.744	20.610	79.791	1053.005	966.348	901.320	952.937
237	79.366	63.537	247.822	1053.122	964.487	897.079	948.356
238	76.222	54.240	238.161	1053.367	961.603	893.245	945.003
239	71.173	44.316	220.136	1053.486	959.255	889.872	941.637
240	77.519	55.163	245.831	1053.590	957.706	887.077	939.372
241	71.772	44.689	223.689	1053.616	956.222	884.805	936.584
242	71.173	44.316	220.136	1053.556	955.368	882.539	935.053
243	59.623	26.517	181.238	1053.621	953.608	881.050	933.852
244	53.641	19.086	161.767	1053.630	953.180	879.288	931.535
245	53.141	18.908	158.955	1053.562	953.197	879.055	931.548
246	47.345	16.846	134.559	1053.125	955.144	879.311	932.319
247	60.854	32.478	170.607	1052.768	955.311	879.636	932.552
248	70.349	50.061	201.366	1052.548	956.724	880.102	933.750
249	77.602	69.028	230.857	1052.348	959.761	884.535	938.066
250	91.721	122.379	327.956	1052.229	963.253	890.151	943.600
251	79.088	77.384	241.392	1052.196	967.328	897.729	951.831
252	81.430	86.918	255.984	1052.110	971.529	904.965	958.662
253	81.430	86.918	255.984	1052.093	974.350	911.294	965.515
254	82.180	102.340	280.028	1052.085	977.620	917.183	971.711
255	58.382	51.931	170.971	1052.081	978.468	921.473	974.599
256	61.682	60.353	186.881	1052.080	978.964	922.833	974.376
257	58.382	51.931	170.971	1052.079	976.415	917.366	969.038

hour	Air Change	Air Change (ACH)	ASHRAE Enhanced	Enhanced Model	Angular Cracks	Mixed Cracks	Straight Cracks
258	59.008	52.488	174.174	1052.150	973.342	912.848	964.171
259	60.101	53.460	180.180	1052.304	972.287	908.368	960.099
260	32.840	32.133	101.706	1052.331	970.898	904.332	956.857
261	33.331	38.542	111.750	1052.415	968.293	901.260	953.313
262	18.916	16.826	58.014	1052.574	967.294	898.327	951.434
263	14.568	16.846	49.146	1052.533	966.292	895.760	948.824
264	13.494	16.804	47.326	1052.535	965.944	893.907	946.951
265	33.331	41.507	116.235	1052.465	964.986	892.581	946.051
266	11.947	15.941	43.177	1052.382	965.450	891.485	944.892
267	9.879	11.423	32.916	1052.366	964.263	890.423	943.736
268	8.796	10.954	30.324	1052.288	964.821	889.322	943.100
269	7.608	10.828	28.689	1052.345	963.853	888.560	942.977
270	7.415	10.553	27.825	1052.278	964.289	888.040	941.752
271	10.597	11.312	33.773	1052.269	964.127	887.365	941.205
272	7.415	10.553	27.825	1052.265	963.687	886.983	940.902
273	6.207	9.939	25.334	1052.192	966.448	890.269	944.230
274	6.528	9.871	25.364	1052.109	969.298	896.355	950.617
275	4.356	8.136	20.010	1051.807	973.565	903.618	958.095
276	8.204	12.406	31.019	1051.612	978.277	911.496	966.426
277	8.487	11.324	28.560	1051.280	982.371	918.946	975.248
278	7.386	10.513	25.831	1051.072	986.175	925.794	980.813
279	5.066	6.760	16.663	1050.878	988.953	930.465	985.110
280	9.359	9.989	26.347	1050.761	989.826	932.755	985.777
281	7.872	9.803	24.460	1050.730	989.571	930.675	983.375
282	7.883	7.012	20.091	1050.644	988.147	926.594	979.414
283	11.019	7.841	26.849	1050.841	986.182	922.474	975.524
284	10.053	8.048	25.604	1050.938	986.231	919.086	973.067
285	11.949	10.628	31.319	1050.890	984.332	916.448	969.933
286	25.085	22.313	65.750	1050.888	984.348	914.042	968.620
287	24.101	21.438	62.010	1050.745	983.893	911.978	966.309
288	11.949	10.628	31.319	1050.865	982.599	909.977	965.175
289	12.298	10.939	32.529	1050.949	982.628	908.952	963.400
290	11.219	10.977	30.929	1050.966	981.132	906.740	962.114
291	11.879	11.623	33.295	1051.116	980.313	905.084	959.646
292	27.052	26.469	76.440	1051.213	979.843	903.817	958.690
293	26.560	28.351	77.701	1051.164	979.707	902.863	957.843
294	58.468	67.610	176.486	1051.021	980.667	903.267	958.607
295	57.247	56.014	149.875	1050.570	981.155	903.276	959.008

hour	Air Change	Air Change (ACH)	ASHRAE Enhanced	Enhanced Model	Angular Cracks	Mixed Cracks	Straight Cracks
296	62.333	77.624	188.699	1050.421	983.855	904.050	959.519
297	64.846	109.594	253.461	1050.161	985.684	908.539	963.998
298	61.269	98.099	224.965	1049.964	989.631	915.222	971.300
299	61.884	110.092	251.523	1049.775	994.294	922.829	979.089
300	60.956	113.864	260.493	1049.661	997.971	930.589	987.373
301	58.489	114.457	262.616	1049.559	1002.672	938.214	994.554
302	57.433	102.175	231.040	1049.463	1005.163	944.179	1000.589
303	56.873	96.118	216.386	1049.441	1006.867	949.336	1004.492
304	57.433	102.175	231.040	1049.431	1007.212	951.432	1005.206
305	57.308	96.855	218.043	1049.426	1005.797	948.132	1001.141
306	58.167	93.132	209.929	1049.495	1001.680	942.443	994.823
307	78.212	236.536	601.449	1050.147	997.964	936.430	989.354
308	88.576	283.640	735.742	1050.680	995.636	930.625	984.042
309	93.487	299.364	778.677	1051.009	991.446	925.455	979.098
310	97.695	295.460	760.817	1051.308	988.251	920.269	974.044
311	102.482	309.939	800.701	1051.594	985.411	916.109	969.276
312	101.068	251.721	629.815	1051.731	983.086	912.338	966.457
313	100.680	268.665	677.989	1051.700	982.628	909.227	962.932
314	102.218	272.770	689.356	1051.778	981.132	906.409	960.449
315	103.752	276.863	700.731	1051.863	980.313	903.800	958.392
316	106.806	285.015	723.500	1052.024	979.843	901.014	954.365
317	104.114	203.742	510.763	1052.268	979.707	898.467	952.355
318	106.612	218.114	547.530	1052.387	980.667	896.289	950.313
319	110.056	244.740	616.250	1052.490	981.155	894.128	947.417
320	108.117	211.576	534.989	1052.587	983.855	892.173	945.943
321	105.345	187.410	478.347	1052.610	984.585	894.457	947.679
322	98.913	149.573	393.018	1052.549	987.759	898.479	952.208
323	102.518	173.261	444.177	1052.542	991.701	904.695	958.747
324	100.027	169.051	430.164	1052.397	994.683	910.967	966.233
325	93.423	132.960	350.585	1052.301	998.799	917.317	971.185
326	85.350	98.695	280.844	1052.208	1000.823	922.425	976.582
327	82.878	88.465	260.538	1052.116	1002.179	926.366	979.332
328	66.127	47.056	182.815	1052.095	1002.260	926.703	978.308
329	68.343	48.633	190.619	1052.157	1001.770	923.239	973.859
330	42.387	11.311	113.226	1052.378	998.254	918.179	969.134
331	32.673	5.813	87.795	1052.487	995.002	912.773	963.876
332	25.665	9.132	70.336	1052.586	993.055	908.315	960.420
333	24.077	10.708	66.009	1052.538	989.195	904.488	956.393

hour	Air Change	Air Change (ACH)	ASHRAE Enhanced	Enhanced Model	Angular Cracks	Mixed Cracks	Straight Cracks
334	24.984	11.112	69.762	1052.680	986.276	901.269	953.493
335	17.247	10.739	48.750	1052.560	983.677	898.819	951.877
336	13.202	10.569	38.754	1052.476	981.559	896.868	949.592
337	14.558	10.360	41.318	1052.387	979.275	895.611	949.228
338	11.484	10.215	34.429	1052.368	978.196	894.229	947.415
339	9.253	9.876	29.686	1052.360	976.010	892.964	946.646
340	9.023	9.631	28.754	1052.285	973.465	891.631	945.116
341	8.588	9.167	27.368	1052.272	972.294	890.764	944.664
342	7.754	8.966	25.675	1052.266	969.894	890.210	943.925
343	6.894	8.585	23.627	1052.193	968.426	889.970	943.800
344	7.073	8.809	24.103	1052.109	966.877	890.016	943.733
345	5.298	7.541	19.495	1051.949	967.887	893.004	946.850
346	5.596	7.964	20.589	1051.919	969.125	899.141	953.354
347	4.859	7.348	18.541	1051.763	972.230	906.325	960.922
348	5.159	6.884	17.756	1051.592	974.882	913.931	968.579
349	4.438	6.316	15.843	1051.414	978.005	920.923	976.938
350	6.355	6.784	18.732	1051.305	980.406	927.357	982.118
351	5.972	6.374	17.338	1051.134	981.084	931.944	986.280
352	5.482	6.339	16.548	1051.028	981.045	933.747	986.164
353	6.268	6.133	17.134	1050.929	978.333	931.977	984.390
354	5.305	6.135	15.902	1050.906	975.600	927.629	979.750
355	12.077	6.445	28.195	1050.967	973.017	923.448	976.381
356	9.603	6.834	23.894	1051.045	971.400	919.926	972.738
357	12.426	6.632	29.347	1051.059	969.347	916.497	969.594
358	11.878	7.396	29.347	1051.208	968.037	912.969	967.552
359	14.469	7.722	35.723	1051.376	967.400	910.672	964.076
360	16.578	7.373	40.684	1051.481	966.500	907.971	961.581
361	18.340	8.157	46.474	1051.721	966.184		
362	24.166	8.598	62.462	1051.981	966.003		
363	27.247	9.694	70.425	1052.035	965.345		
364	31.971	0.000	82.380	1052.130	965.180		
365	27.303	7.286	70.787	1052.153	965.251		
366	30.987	0.000	78.191	1052.020	964.611		
367	26.763	9.522	68.469	1052.001	965.786		
368	23.232	8.266	58.818	1051.922	965.422		
369	29.020	0.000	70.077	1051.693	967.051		
370	34.930	12.428	84.681	1051.582	971.077		
371	52.375	27.953	130.693	1051.552	974.943		

hour	Air Change	Air Change (ACH)	ASHRAE Enhanced	Enhanced Model	Angular Cracks	Mixed Cracks	Straight Cracks
372	25.649	6.844	60.259	1051.397	978.812		
373	40.067	14.256	91.620	1051.154	982.781		
374	36.229	12.890	81.827	1051.037	986.186		
375	34.869	15.508	79.872	1051.005	988.088		
376	44.327	23.657	102.282	1050.919	988.945		
377	25.085	13.388	57.882	1050.902	989.726		
378	38.162	13.578	85.119	1050.894	986.618		
379	27.733	4.934	60.118	1050.819	985.751		
380	37.613	13.383	82.829	1050.806	984.022		
381	63.252	56.262	164.266	1050.801	982.944		
382	67.270	71.805	190.873	1050.798	981.253		
383	63.039	56.073	165.232	1050.868	980.152		
384	66.988	65.545	183.131	1050.879	977.886		
385	48.534	25.903	113.312	1050.955	976.890		
386	72.711	84.080	219.479	1050.968	974.804		
387	68.919	61.303	188.876	1051.259	973.332		
388	48.920	21.757	123.963	1051.663	971.656		
389	40.901	14.553	102.462	1051.741	970.968		
390	35.428	12.605	86.848	1051.633	970.779		
391	24.134	6.440	58.029	1051.555	970.212		
392	14.969	7.989	36.957	1051.469	970.204		
393	14.591	7.787	35.635	1051.380	972.498		
394	8.385	7.459	22.782	1051.290	974.901		
395	9.205	7.369	23.902	1051.199	979.805		
396	7.895	7.023	21.074	1051.107	982.974		
397	8.278	6.627	21.084	1051.016	986.866		
398	12.291	6.560	28.362	1050.924	989.353		
399	11.938	6.371	27.219	1050.833	991.900		
400	13.310	10.656	33.235	1050.812	992.861		
401	12.977	11.543	34.014	1050.874	991.382		
402	11.864	11.608	32.707	1050.953	989.330		
403	18.886	13.440	48.437	1051.252	987.927		
404	12.769	15.901	41.721	1051.375	987.864		
405	10.185	16.307	40.376	1051.481	985.805		
406	84.309	119.989	304.042	1051.508	985.072		
407	10.398	17.574	43.719	1051.733	984.445		
408	96.624	171.895	428.352	1051.915	984.294		
409	10.873	19.343	48.535	1052.097	983.117		



hour	Air Change	Air Change (ACH)	ASHRAE Enhanced	Enhanced Model	Angular Cracks	Mixed Cracks	Straight Cracks
410	104.114	203.742	510.763	1052.280	981.667		
411	106.788	208.975	526.900	1052.464	979.291		
412	110.663	206.713	529.546	1052.789	978.125		
413	112.845	200.752	522.910	1053.067	976.575		
414	113.692	182.033	492.784	1053.414	976.487		
415	111.973	159.361	455.095	1053.701	975.462		
416	103.146	119.274	379.682	1053.839	975.894		
417	103.146	119.274	379.682	1053.879	977.336		
418	102.250	118.237	374.305	1053.826	980.011		
419	101.347	117.194	368.942	1053.752	983.927		
420	82.206	65.811	264.247	1053.596	987.297		
421	82.595	66.122	261.710	1053.425	990.935		
422	64.949	34.663	193.313	1053.319	993.133		
423	70.337	43.796	210.824	1053.220	994.658		
424	81.125	64.945	253.315	1053.197	994.747		
425	84.074	74.785	269.302	1053.187	993.446		
426	27.087	21.685	85.828	1053.325	989.834		
427	19.406	25.892	74.575	1053.417	987.615		
428	20.507	27.362	79.977	1053.651	984.827		
429	16.266	28.937	77.408	1053.837	984.102		
430	17.769	30.031	81.896	1054.021	980.772		
431	128.073	239.236	639.781	1054.134	978.916		
432	135.363	276.934	736.342	1054.377	976.516		
433	136.027	266.193	716.285	1054.567	974.642		
434	136.027	266.193	716.285	1054.611	972.216		
435	133.029	236.659	651.923	1054.702	970.229		
436	135.221	252.587	687.791	1054.722	966.980		
437	142.074	303.301	810.465	1054.802	964.630		
438	143.331	305.986	819.589	1054.888	961.421		
439	143.331	305.986	819.589	1054.907	958.781		
440	146.249	325.224	869.623	1054.986	956.273		
441	144.585	308.661	828.726	1055.001	956.650		
442	142.785	292.120	788.799	1055.008	957.952		
443	144.585	308.661	828.726	1055.010	960.816		
444	144.970	322.378	860.111	1054.940	963.344		
445	143.331	305.986	819.589	1054.930	965.880		
446	144.970	322.378	860.111	1054.925	968.052		
447	137.237	268.562	724.664	1054.780	969.819		



hour	Air Change	Air Change (ACH)	ASHRAE Enhanced	Enhanced Model	Angular Cracks	Mixed Cracks	Straight Cracks
448	138.896	271.808	733.421	1054.756	969.485		
449	139.428	285.250	762.380	1054.675	967.843		
450	138.158	282.653	753.489	1054.587	964.423		
451	126.642	202.768	570.399	1054.497	961.552		
452	129.578	230.522	628.883	1054.478	958.685		
453	129.065	218.128	603.277	1054.469	956.886		
454	121.076	172.316	507.573	1054.465	953.828		
455	112.975	150.738	451.307	1054.250	951.599		
456	109.555	136.430	423.181	1054.215	949.018		
457	104.924	121.329	390.477	1054.128	948.162		
458	107.690	134.107	411.758	1054.039	945.770		
459	101.153	107.972	361.067	1053.948	943.727		
460	100.283	107.043	355.860	1053.857	942.335		
461	104.157	120.442	381.287	1053.836	940.839		
462	114.077	182.650	492.521	1053.542	939.210		
463	112.470	170.072	470.649	1053.635	937.735		
464	104.851	130.571	394.724	1053.708	937.164		
465	90.555	80.549	302.210	1053.719	937.495		
466	100.408	116.108	359.383	1053.510	939.590		
467	111.649	198.625	513.894	1053.122	942.176		
468	109.098	194.087	498.769	1052.909	945.635		
469	103.754	175.352	451.209	1052.712	947.763		
470	102.458	173.160	442.266	1052.523	949.754		
471	102.624	182.570	461.246	1052.408	950.811		
472	102.592	191.638	480.307	1052.307	951.975		
473	101.313	180.236	453.793	1052.282	949.397		
474	96.627	146.115	378.838	1052.271	947.717		
475	91.721	122.379	327.956	1052.194	946.193		
476	94.468	142.851	367.065	1052.110	944.903		
477	92.630	131.831	344.214	1052.092	943.521		
478	89.436	119.331	316.366	1052.013	943.539		
479	83.640	96.717	269.990	1051.927	943.193		
480	88.284	117.794	310.599	1051.909	943.532		
481	89.042	126.726	325.993	1051.830	942.911		
482	78.513	83.806	241.703	1051.815	943.197		
483	82.579	95.491	264.842	1051.809	943.393		
484	82.579	95.491	264.842	1051.806	943.599		
485	74.328	66.115	214.206	1051.876	944.989		

hour	Air Change	Air Change (ACH)	ASHRAE Enhanced	Enhanced Model	Angular Cracks	Mixed Cracks	Straight Cracks
486	74.573	66.333	218.387	1052.029	944.710		
487	79.671	77.954	241.384	1052.057	944.938		
488	80.887	86.339	250.770	1051.926	945.559		
489	80.887	86.339	250.770	1051.909	947.670		
490	81.605	101.623	268.273	1051.616	952.700		
491	84.497	135.289	330.786	1051.354	956.135		
492	80.506	128.899	311.183	1051.085	961.056		
493	80.622	172.113	412.700	1050.812	965.886		
494	80.211	178.371	428.838	1050.681	968.914		
495	74.344	119.034	282.511	1050.643	972.953		
496	73.218	110.716	264.166	1050.626	972.752		
497	70.544	94.124	229.331	1050.619	973.306		
498	74.524	112.692	270.157	1050.687	970.894		
499	69.412	80.265	206.602	1050.768	970.243		
500	76.645	109.082	266.643	1050.855	969.268		
501	82.591	146.930	352.437	1050.944	969.370		
502	81.843	131.039	317.697	1051.035	969.297		
503	81.843	131.039	317.697	1051.055	968.765		
504	77.605	103.546	259.674	1051.064	968.594		
505	69.774	68.271	197.156	1051.210	968.747		
506	75.834	94.437	241.706	1051.092	969.422		
507	80.979	129.656	314.343	1051.080	969.155		
508	66.119	58.813	176.476	1051.075	968.481		
509	62.831	50.299	161.586	1051.073	968.376		
510	66.713	59.342	181.246	1051.214	967.535		
511	66.713	59.342	181.246	1051.236	967.376		
512	54.439	38.739	136.846	1051.175	967.250		
513	54.439	38.739	136.846	1051.168	970.594		
514	69.966	87.130	221.601	1051.022	974.032		
515	66.398	70.873	192.783	1051.070	978.699		
516	71.892	95.922	239.183	1050.999	984.427		
517	68.900	85.802	216.845	1050.917	987.891		
518	70.778	94.436	234.131	1050.900	991.613		
519	65.692	99.336	240.398	1050.893	993.586		
520	57.649	66.663	172.802	1050.890	995.715		
521	66.681	100.832	245.167	1050.960	993.470		
522	66.735	94.978	235.802	1051.113	992.377		
523	27.544	31.851	85.455	1051.283	989.374		

hour	Air Change	Air Change (ACH)	ASHRAE Enhanced	Enhanced Model	Angular Cracks	Mixed Cracks	Straight Cracks
524	28.036	24.938	77.498	1051.389	987.853		
525	47.992	34.151	125.508	1051.487	986.590		
526	49.148	34.974	130.998	1051.653	984.897		
527	29.020	18.069	74.713	1051.614	984.257		
528	48.571	34.564	128.245	1051.618	982.333		
529	41.743	22.278	105.262	1051.619	982.001		
530	55.847	39.741	143.228	1051.406	981.682		
531	63.273	50.654	165.856	1051.301	981.494		
532	55.151	34.340	136.267	1051.275	980.016		
533	50.474	26.938	121.926	1051.263	980.063		
534	52.997	32.999	135.079	1051.472	978.698		
535	58.605	36.491	152.388	1051.646	979.023		
536	42.792	22.838	110.142	1051.754	978.378		
537	49.148	34.974	130.998	1051.710	980.115		
538	50.705	40.592	135.405	1051.497	982.630		
539	59.850	53.237	158.310	1051.108	986.037		
540	51.556	36.688	124.287	1050.894	989.060		
541	47.054	41.855	118.785	1050.626	991.875		
542	50.436	53.836	137.532	1050.425	994.232		
543	42.951	34.385	101.818	1050.377	995.424		
544	21.642	17.325	50.751	1050.284	995.089		
545	42.272	33.841	99.129	1050.263	993.622		
546	49.613	52.957	134.187	1050.254	989.983		
547	45.620	40.579	112.944	1050.321	988.436		
548	61.646	65.801	166.733	1050.259	984.972		
549	60.737	64.831	164.275	1050.252	983.019		
550	72.997	116.875	276.206	1050.463	981.110		
551	76.728	129.675	308.120	1050.638	980.584		
552	79.063	140.653	335.036	1050.746	978.411		
553	69.412	80.265	206.602	1050.774	978.230		
554	68.341	72.948	193.910	1050.786	977.474		
555	60.168	48.168	150.235	1050.792	977.781		
556	68.341	72.948	193.910	1050.794	976.999		
557	53.464	33.290	126.453	1050.866	976.200		
558	47.878	25.552	110.476	1050.878	976.206		
559	37.477	20.001	86.476	1050.883	974.692		
560	32.816	8.757	71.549	1050.814	973.653		
561	30.415	10.822	66.110	1050.733	975.753		

hour	Air Change	Air Change (ACH)	ASHRAE Enhanced	Enhanced Model	Angular Cracks	Mixed Cracks	Straight Cracks
562	42.473	22.668	94.497	1050.646	979.670		
563	40.129	28.556	91.476	1050.414	983.118		
564	66.270	117.895	272.164	1050.087	987.661		
565	74.809	139.740	328.814	1050.379	991.805		
566	68.611	103.751	242.875	1050.265	995.938		
567	73.986	144.784	340.728	1050.326	997.327		
568	5.320	13.251	32.761	1050.974	998.961		
569	98.965	220.074	544.382	1051.577	997.993		
570	7.423	17.827	44.658	1051.917	995.859		
571	113.688	323.603	834.452	1052.292	995.339		
572	117.299	344.317	894.692	1052.520	993.118		
573	7.695	20.533	52.672	1052.651	992.997		
574	9.208	22.115	56.352	1052.832	990.320		
575	117.571	282.365	719.510	1052.872	989.812		
576	118.400	263.294	671.897	1053.032	987.717		
577	120.844	279.479	715.184	1053.134	987.558		
578	115.979	226.960	583.815	1053.159	986.306		
579	118.613	253.216	647.974	1053.170	985.808		
580	114.481	213.847	552.943	1053.174	984.325		
581	109.087	174.660	465.436	1053.177	984.102		
582	110.246	176.516	472.250	1053.249	983.004		
583	102.952	137.365	391.721	1053.261	983.138		
584	105.657	140.973	404.022	1053.337	982.488		
585	108.315	154.155	430.307	1053.351	984.586		
586	94.945	101.345	324.914	1053.286	988.572		
587	96.569	111.668	337.726	1053.134	992.466		
588	84.252	74.943	266.064	1053.037	995.287		
589	82.623	73.494	257.169	1052.871	998.577		
590	75.711	60.611	227.594	1052.767	1000.722		
591	65.008	40.477	185.354	1052.669	1000.231		
592	46.801	24.978	130.036	1052.575	997.603		
593	34.311	15.260	94.938	1052.625	993.447		
594	26.089	13.924	73.142	1052.627	988.676		
595	24.984	11.112	69.762	1052.699	984.011		
596	14.133	11.314	42.486	1052.711	979.934		
597	16.159	12.936	48.576	1052.716	976.954		
598	14.555	12.947	44.972	1052.718	973.049		
599	11.938	12.743	39.329	1052.719	971.099		

hour	Air Change	Air Change (ACH)	ASHRAE Enhanced	Enhanced Model	Angular Cracks	Mixed Cracks	Straight Cracks
600	11.574	11.324	37.128	1052.791	967.608		
601	8.198	10.209	28.916	1052.660	966.640		
602	10.294	10.073	32.340	1052.571	964.605		
603	8.796	10.172	29.674	1052.552	962.690		
604	7.801	9.715	27.206	1052.472	961.802		
605	8.269	11.033	29.884	1052.386	960.363		
606	8.061	10.756	28.978	1052.297	959.104		
607	8.796	10.954	30.324	1052.277	957.584		
608	9.447	10.924	31.087	1052.197	956.084		
609	10.134	10.817	31.856	1052.111	957.612		
610	13.525	10.827	38.086	1052.022	960.132		
611	12.546	10.044	34.421	1051.788	963.112		
612	8.145	8.694	24.185	1051.461	967.103		
613	6.113	7.069	18.196	1050.969	969.650		
614	8.025	6.424	19.023	1050.517	973.614		
615	64.303	125.835	291.970	1050.061	973.942		
616	64.126	108.377	248.719	1049.961	975.538		
617	64.126	108.377	248.719	1049.916	973.346		
618	64.815	115.306	265.265	1049.896	970.824		
619	61.532	87.573	201.934	1049.887	968.799		
620	63.358	101.443	232.633	1049.883	966.994		
621	71.181	126.631	295.394	1050.167	965.827		
622	11.751	12.544	33.084	1050.567	964.802		
623	78.970	105.366	267.254	1051.071	963.655		
624	83.467	126.215	312.664	1051.244	962.822		
625	12.277	16.380	42.252	1051.443	963.499		
626	89.993	160.099	392.119	1051.491	962.347		
627	71.146	63.284	201.699	1051.654	962.319		
628	77.528	82.754	236.982	1051.686	962.126		
629	71.146	63.284	201.699	1051.701	963.398		
630	63.204	44.976	168.462	1051.707	962.496		
631	71.146	63.284	201.699	1051.710	963.340		
632	67.383	53.944	184.872	1051.711	963.072		
633	83.710	104.245	280.221	1051.783	966.542		
634	88.425	133.712	337.396	1051.723	969.511		
635	86.695	123.384	315.812	1051.717	974.181		
636	89.983	144.073	359.728	1051.714	979.452		
637	89.983	144.073	359.728	1051.713	986.304		

hour	Air Change	Air Change (ACH)	ASHRAE Enhanced	Enhanced Model	Angular Cracks	Mixed Cracks	Straight Cracks
638	83.623	111.574	289.398	1051.641	990.464		
639	91.020	145.733	363.871	1051.701	994.681		
640	82.619	102.886	274.916	1051.707	996.419		
641	82.291	95.157	265.635	1051.852	997.197		
642	75.207	66.897	218.493	1051.947	996.213		
643	76.079	67.672	222.796	1052.041	995.747		
644	77.602	69.028	230.857	1052.204	993.715		
645	54.382	24.187	149.092	1052.450	991.931		
646	42.773	11.414	116.474	1052.569	989.193		
647	38.578	10.295	106.042	1052.673	987.004		
648	35.781	19.097	102.987	1052.842	984.426		
649	52.261	23.243	149.864	1052.947	983.706		
650	29.501	13.121	83.860	1052.903	980.672		
651	29.101	10.354	82.707	1052.974	979.343		
652	27.271	12.129	79.556	1053.128	977.603		
653	25.031	13.359	74.501	1053.228	976.943		
654	19.896	14.158	60.762	1053.180	975.305		
655	19.896	14.158	60.762	1053.179	974.557		
656	19.896	14.158	60.762	1053.179	974.481		
657	17.566	14.063	54.445	1053.107	975.823		
658	14.555	12.947	44.972	1052.811	977.791		
659	10.597	11.312	33.773	1052.404	980.901		
660	8.401	10.462	28.626	1052.182	983.105		
661	7.094	9.465	24.822	1051.911	986.041		
662	5.609	7.484	19.413	1051.709	987.555		
663	7.122	8.869	23.414	1051.588	989.396		
664	7.599	8.787	23.734	1051.484	987.994		
665	9.295	9.095	26.690	1051.458	985.914		
666	9.295	9.095	26.690	1051.446	982.188		
667	8.385	8.950	25.080	1051.441	979.963		
668	8.385	8.950	25.080	1051.439	976.528		
669	10.355	9.211	28.623	1051.438	974.173		
670	10.069	8.956	27.594	1051.366	971.679		
671	11.277	9.028	29.839	1051.355	969.332		
672	12.690	9.030	32.547	1051.350	967.662		
673	12.690	9.030	32.547	1051.347	966.046		
674	19.761	10.546	48.262	1051.346	963.862		
675	18.396	8.182	44.156	1051.346	962.252		

hour	Air Change	Air Change (ACH)	ASHRAE Enhanced	Enhanced Model	Angular Cracks	Mixed Cracks	Straight Cracks
676	14.591	7.787	35.635	1051.346	960.573		
677	19.310	10.306	46.646	1051.274	960.207		
678	19.310	10.306	46.646	1051.263	958.861		
679	27.052	19.250	68.693	1051.258	957.592		
680	13.966	8.696	34.507	1051.256	957.934		
681	12.013	8.549	30.199	1051.183	960.287		
682	9.227	8.208	24.628	1051.100	964.088		
683	8.952	7.963	23.680	1051.013	968.178		
684	11.019	7.841	26.849	1050.923	972.904		
685	46.266	37.038	115.522	1050.832	977.645		
686	79.453	134.280	321.530	1050.883	980.613		
687	88.622	173.426	420.000	1051.171	983.724		
688	90.548	169.141	412.067	1051.359	984.516		
689	93.334	174.343	427.436	1051.545	984.689		
690	90.761	137.245	347.893	1051.729	982.536		
691	79.492	84.851	246.446	1051.842	980.977		
692	83.317	96.344	270.685	1051.943	979.975		
693	99.235	176.539	442.962	1052.110	978.941		
694	103.726	175.303	449.410	1052.428	978.536		
695	100.488	143.016	386.316	1052.631	977.831		
696	111.866	208.961	535.304	1052.823	977.617		
697	111.721	178.877	478.565	1053.153	965.331		
698	118.501	200.274	536.486	1053.503	963.073		
699	122.070	206.306	558.616	1053.792	958.890		
700	117.873	178.243	503.645	1054.001	957.002		
701	133.247	296.310	774.924	1054.054	954.030		
702	124.904	222.206	598.338	1054.077	952.671		
703	125.044	211.331	580.390	1054.230	949.916		
704	127.913	216.180	595.799	1054.328	949.421		
705	111.399	138.726	434.657	1054.352	949.711		
706	125.044	211.331	580.390	1054.291	951.936		
707	116.911	166.389	481.577	1054.142	954.840		
708	114.044	162.308	467.684	1054.045	957.324		
709	109.608	136.496	419.093	1054.022	960.182		
710	105.803	131.757	400.387	1053.869	963.137		
711	98.484	122.643	370.757	1053.771	963.845		
712	97.615	121.561	365.563	1053.676	964.517		
713	100.882	134.602	391.520	1053.654	963.188		

hour	Air Change	Air Change (ACH)	ASHRAE Enhanced	Enhanced Model	Angular Cracks	Mixed Cracks	Straight Cracks
714	86.060	84.206	293.024	1053.645	960.630		
715	91.765	97.950	325.632	1053.783	957.751		
716	91.765	97.950	325.632	1053.804	955.556		
717	84.289	74.976	286.890	1053.956	954.029		
718	79.961	64.013	267.898	1054.054	952.245		
719	77.839	83.086	277.847	1053.934	951.344		
720	84.345	105.035	319.186	1053.851	950.072		
721	41.173	36.624	139.230	1053.905	947.405		
722	41.663	40.766	145.453	1053.980	946.151		
723	71.232	63.361	244.016	1054.065	945.744		
724	67.731	54.222	228.442	1054.153	944.196		
725	43.134	30.694	143.734	1054.243	943.939		
726	30.721	21.862	103.071	1054.334	942.475		
727	26.673	23.726	93.123	1054.355	943.127		
728	42.644	41.725	150.703	1054.221	943.502		
729	41.663	48.178	154.208	1054.059	946.290		
730	40.683	47.044	148.928	1053.886	948.855		
731	103.885	147.850	418.420	1053.707	953.136		
732	108.824	154.879	436.319	1053.597	957.078		
733	103.980	138.737	397.612	1053.425	960.809		
734	111.401	178.364	479.080	1053.390	963.164		
735	110.269	166.744	457.551	1053.446	964.905		
736	106.019	141.457	409.442	1053.521	964.809		
737	91.655	89.681	310.087	1053.535	963.339		
738	94.366	92.333	321.303	1053.612	960.226		
739	54.141	19.264	164.595	1053.697	957.846		
740	48.668	12.987	147.189	1053.715	957.264		
741	43.294	7.702	130.546	1053.722	954.380		
742	40.683	10.856	124.034	1053.797	953.315		
743	41.173	14.649	127.170	1053.881	951.212		
744	63.253	33.758	200.412	1053.970	951.220		



### Cumulative Data for Northwest Wall

<b>Cumulative Northwest (NW) Wall Data (Watts)</b>
--

hour	eUEST/DOE-2 Hourly Values			Enhanced Model	CFD Multiphysics Simulation		
	(no reduction multiplier)				Angular Cracks	Mixed Cracks	Straight Cracks
	Air Change	Air Change (ACH)	ASHRAE Enhanced				
1	56.03	24.92	157.86	525.78	954.54	867.70	916.75
2	110.88	49.31	312.40	1272.19	1907.75	1734.69	1832.18
3	176.40	84.28	509.02	2077.80	2859.15	2600.60	2746.38
4	237.07	111.26	696.36	2882.90	3809.23	3464.98	3659.13
5	306.65	148.40	921.75	3704.24	4755.98	4327.43	4569.01
6	348.85	159.66	1058.49	4530.94	5700.75	5188.22	5477.12
7	407.45	180.51	1249.28	5354.53	6643.40	6047.30	6383.34
8	453.03	200.79	1400.84	6174.29	7584.79	6904.95	7288.41
9	498.12	216.83	1548.71	6992.36	8527.00	7765.10	8195.55
10	562.90	245.64	1761.04	7833.77	9471.55	8630.08	9107.84
11	622.76	272.26	1954.47	8688.27	10418.95	9501.56	10026.80
12	697.48	325.43	2200.02	9550.53	11369.55	10379.60	10953.15
13	765.10	367.54	2413.97	10419.31	12323.47	11264.59	11885.62
14	821.72	402.79	2590.45	11297.17	13280.34	12155.55	12823.63
15	877.84	437.73	2764.01	12196.44	14238.19	13049.88	13764.21
16	917.54	462.45	2887.75	13103.37	15195.13	13944.51	14703.38
17	949.02	482.05	2989.55	14017.87	16149.27	14834.07	15637.02
18	978.96	498.03	3086.52	14927.90	17100.64	15719.08	16566.35
19	1006.14	514.96	3175.69	15842.76	18049.32	16599.75	17491.70
20	1039.96	536.02	3288.98	16770.44	18997.37	17476.26	18413.78
21	1071.26	552.72	3392.55	17691.92	19942.78	18349.73	19332.91
22	1115.38	576.27	3537.50	18605.20	20887.29	19220.42	20249.82
23	1143.86	594.00	3632.89	19512.53	21829.96	20088.79	21164.59
24	1175.16	610.70	3736.46	20432.73	22771.40	20955.09	22077.37
25	1201.44	627.07	3825.10	21358.45	23713.24	21820.24	22989.72
26	1223.81	644.98	3901.04	22280.22	24653.43	22683.96	23901.04
27	1249.27	663.10	3987.05	23198.67	25593.50	23546.20	24811.17
28	1280.95	677.19	4090.14	24116.00	26533.10	24407.82	25720.67

hour	Air Change	Air Change (ACH)	ASHRAE Enhanced	Enhanced Model	Angular Cracks	Mixed Cracks	Straight Cracks
29	1308.51	691.89	4179.41	25037.97	27472.48	25268.65	26629.73
30	1333.56	707.49	4262.17	25961.93	28412.00	26129.03	27538.45
31	1353.35	723.33	4329.35	26885.09	29352.12	26989.13	28447.82
32	1372.44	738.61	4393.31	27806.46	30292.27	27849.37	29357.03
33	1395.47	755.01	4467.96	28720.63	31235.31	28713.24	30270.39
34	1411.06	768.88	4519.65	29616.66	32182.26	29583.37	31190.43
35	1427.12	781.73	4570.16	30491.02	33134.07	30461.32	32118.98
36	1442.65	795.54	4619.19	31348.99	34090.39	31346.85	33055.20
37	1457.10	807.11	4662.97	32190.32	35051.62	32239.75	33999.65
38	1470.92	818.17	4704.19	33022.00	36015.62	33139.23	34950.73
39	1481.71	828.73	4738.09	33871.94	36982.23	34042.99	35904.65
40	1493.47	839.20	4773.62	34727.40	37949.92	34948.84	36858.88
41	1505.24	849.66	4809.16	35584.88	38916.93	35851.13	37809.22
42	1515.77	859.97	4842.02	36446.23	39882.57	36749.77	38757.02
43	1525.25	870.09	4872.65	37318.03	40848.29	37645.19	39702.40
44	1538.46	880.66	4911.41	38192.82	41811.68	38537.65	40646.06
45	1547.94	890.78	4942.04	39064.51	42775.94	39428.40	41587.65
46	1556.00	901.54	4971.02	39932.46	43739.52	40317.30	42528.23
47	1565.64	912.68	5002.92	40798.17	44703.11	41204.75	43467.44
48	1574.43	923.64	5033.25	41665.19	45665.59	42090.88	44405.83
49	1585.92	933.85	5067.68	42526.55	46629.57	42976.15	45343.49
50	1596.20	943.91	5099.52	43377.88	47592.60	43860.47	46280.84
51	1604.20	953.16	5125.83	44226.37	48557.29	44744.53	47218.11
52	1611.58	961.69	5149.66	45070.63	49522.71	45628.93	48155.49
53	1618.28	970.64	5172.86	45927.40	50488.21	46513.40	49093.39
54	1627.15	980.11	5199.78	46791.89	51453.98	47398.13	50031.69
55	1635.20	989.41	5225.25	47657.06	52420.01	48282.93	50970.22
56	1643.25	998.72	5250.72	48522.18	53387.10	49167.75	51908.88
57	1651.29	1008.02	5276.19	49395.03	54355.99	50056.11	52851.43
58	1661.93	1017.49	5305.86	50283.39	55328.68	50950.28	53799.77
59	1670.97	1026.33	5331.59	51179.56	56305.15	51851.51	54755.38
60	1683.62	1037.58	5365.36	52077.92	57286.62	52760.76	55719.17
61	1697.29	1047.31	5397.96	52980.67	58271.62	53677.06	56691.31
62	1708.21	1057.02	5425.79	53893.81	59260.70	54599.81	57668.78
63	1715.58	1063.57	5444.21	54815.87	60251.57	55527.25	58649.84
64	1722.94	1070.12	5462.62	55723.71	61243.23	56455.56	59630.21
65	1729.27	1076.88	5480.29	56614.00	62232.57	57379.34	60605.77

hour	Air Change	Air Change (ACH)	ASHRAE Enhanced	Enhanced Model	Angular Cracks	Mixed Cracks	Straight Cracks
66	1736.79	1084.24	5500.68	57480.38	63220.05	58299.27	61578.44
67	1745.20	1091.72	5522.53	58342.42	64206.28	59215.70	62547.31
68	1753.61	1099.20	5544.37	59215.45	65191.76	60128.94	63513.76
69	1762.02	1106.68	5566.22	60088.43	66175.52	61039.16	64477.36
70	1777.06	1114.71	5601.73	60959.79	67158.58	61946.91	65438.61
71	1822.60	1139.01	5709.29	61833.97	68141.76	62852.68	66398.63
72	1870.38	1168.76	5821.02	62719.41	69124.86	63757.36	67357.61
73	1916.26	1193.25	5923.09	63611.82	70107.70	64661.36	68316.33
74	1979.04	1260.26	6094.29	64503.23	71091.52	65565.23	69275.20
75	2038.39	1323.61	6252.17	65391.09	72076.54	66469.13	70234.31
76	2100.85	1401.39	6437.53	66278.82	73061.68	67372.44	71192.82
77	2159.16	1453.26	6581.90	67176.24	74046.99	68275.57	72151.06
78	2220.81	1519.06	6748.63	68078.93	75032.05	69178.44	73109.17
79	2285.78	1599.97	6944.01	68980.65	76016.89	70080.97	74067.05
80	2348.56	1666.98	7115.21	69879.04	77002.29	70983.39	75024.78
81	2414.89	1755.49	7325.83	70781.21	77989.96	71889.10	75985.83
82	2478.63	1840.54	7525.82	71686.61	78981.02	72800.31	76952.59
83	2539.83	1916.75	7706.21	72582.79	79975.09	73718.31	77926.28
84	2599.76	1991.38	7881.66	73460.45	80973.47	74643.22	78907.26
85	2657.71	2063.54	8050.19	74312.27	81974.43	75574.73	79895.03
86	2712.35	2121.86	8190.69	75152.38	82978.57	76511.88	80887.98
87	2762.29	2166.29	8304.52	75994.21	83982.81	77452.49	81883.21
88	2815.45	2213.57	8429.60	76822.44	84986.54	78392.60	82876.41
89	2872.74	2264.54	8571.45	77633.08	85985.83	79327.02	83863.39
90	2932.95	2318.09	8724.89	78429.37	86982.88	80256.28	84845.16
91	2964.59	2326.53	8794.79	79219.90	87976.22	81180.37	85822.32
92	3000.82	2339.42	8876.61	80009.83	88966.84	82099.61	86794.68
93	3053.18	2372.02	9008.71	80803.67	89954.92	83014.64	87762.95
94	3080.72	2384.27	9074.82	81604.96	90940.34	83926.09	88727.75
95	3118.16	2400.93	9165.70	82416.02	91923.43	84834.03	89689.50
96	3137.87	2409.69	9214.60	83244.93	92905.38	85739.34	90648.08
97	3155.33	2419.01	9258.63	84088.28	93884.99	86642.21	91604.44
98	3169.41	2429.03	9296.15	84943.14	94863.35	87542.96	92558.82
99	3181.32	2438.56	9328.24	85803.81	95841.02	88442.00	93512.42
100	3193.22	2448.09	9360.32	86665.83	96818.58	89339.74	94464.26
101	3205.91	2457.12	9392.87	87548.82	97795.31	90236.66	95415.63
102	3216.70	2464.80	9420.25	88441.63	98771.61	91132.84	96366.26

hour	Air Change	Air Change (ACH)	ASHRAE Enhanced	Enhanced Model	Angular Cracks	Mixed Cracks	Straight Cracks
103	3225.47	2473.38	9445.05	89336.94	99749.04	92029.07	97317.15
104	3231.79	2480.69	9463.99	90231.84	100726.29	92925.09	98268.16
105	3238.38	2487.14	9482.00	91123.98	101705.90	93824.50	99222.25
106	3244.49	2494.21	9500.20	92022.83	102689.20	94729.87	100182.91
107	3250.39	2500.50	9516.42	92919.62	103677.95	95642.66	101151.40
108	3256.28	2506.27	9531.43	93814.13	104669.81	96563.16	102127.30
109	3261.17	2511.48	9544.31	94705.20	105666.53	97490.70	103110.64
110	3266.41	2516.61	9557.30	95604.63	106665.51	98424.49	104100.07
111	3274.41	2523.72	9575.92	96514.96	107666.60	99362.37	105093.15
112	3283.14	2529.16	9593.95	97426.49	108666.94	100300.80	106084.14
113	3293.74	2537.64	9618.80	98336.33	109663.88	101233.61	107069.45
114	3317.35	2550.24	9671.33	99247.53	110658.41	102161.95	108049.91
115	3353.74	2569.66	9753.30	100161.73	111650.98	103085.30	109026.32
116	3391.75	2589.95	9842.06	101057.00	112640.51	104004.48	109999.08
117	3437.30	2614.26	9949.62	101928.61	113628.61	104919.96	110968.00
118	3463.86	2626.07	10011.92	102783.59	114614.10	105831.81	111933.59
119	3490.91	2626.07	10074.25	103626.64	115599.02	106740.98	112896.75
120	3528.71	2639.52	10162.78	104475.72	116581.62	107647.59	113857.45
121	3569.04	2653.87	10257.24	105333.33	117563.43	108552.54	114816.44
122	3595.60	2653.87	10317.69	106191.92	118544.59	109455.85	115774.02
123	3621.67	2653.87	10376.27	107051.84	119525.04	110358.19	116730.47
124	3667.21	2678.18	10483.84	107910.89	120505.72	111259.26	117686.24
125	3711.92	2698.06	10586.24	108795.74	121486.25	112159.77	118641.37
126	3732.92	2705.53	10633.09	109697.94	122466.33	113059.47	119596.17
127	3753.49	2711.02	10678.54	110596.33	123445.95	113958.51	120550.29
128	3793.01	2725.08	10767.79	111488.21	124425.36	114857.11	121503.71
129	3810.16	2737.29	10810.03	112371.99	125406.55	115758.65	122460.58
130	3869.16	2784.52	10957.33	113257.37	126390.74	116665.50	123422.54
131	3935.36	2855.18	11143.71	114137.44	127377.60	117578.45	124390.73
132	4005.50	2942.52	11361.63	115008.24	128369.00	118498.58	125366.31
133	4078.71	3053.24	11625.80	115867.40	129362.81	119425.03	126349.12
134	4147.61	3145.16	11847.15	116729.84	130359.03	120357.25	127336.23
135	4215.71	3242.09	12076.72	117607.66	131358.33	121293.36	128326.42
136	4281.21	3335.31	12295.17	118492.24	132357.13	122230.71	129316.56
137	4348.93	3455.78	12574.25	119380.85	133353.98	123163.80	130301.91
138	4417.32	3571.37	12842.60	120274.16	134348.99	124092.72	131283.97
139	4482.88	3658.84	13050.76	121171.93	135342.71	125017.77	132262.23

hour	Air Change	Air Change (ACH)	ASHRAE Enhanced	Enhanced Model	Angular Cracks	Mixed Cracks	Straight Cracks
140	4536.18	3696.77	13173.67	122061.53	136335.11	125939.33	133237.73
141	4577.40	3718.77	13263.07	122931.92	137326.31	126858.29	134210.54
142	4623.02	3759.35	13376.02	123776.19	138316.99	127774.86	135181.42
143	4645.15	3779.03	13430.81	124602.73	139307.06	128689.23	136150.58
144	4655.07	3787.85	13455.36	125426.95	140296.93	129601.85	137118.59
145	4701.41	3829.07	13571.22	126248.73	141285.55	130512.99	138084.77
146	4772.36	3942.68	13837.41	127067.18	142273.71	131422.77	139049.73
147	4842.54	4042.56	14075.23	127882.23	143260.89	132331.29	140013.39
148	4914.03	4144.30	14318.76	128692.83	144248.50	133238.60	140976.11
149	4983.91	4231.32	14534.49	129513.04	145234.50	134144.85	141938.07
150	5055.39	4333.06	14778.02	130563.57	146221.57	135050.71	142899.24
151	5124.26	4431.07	15010.15	131613.95	147207.64	135955.90	143860.39
152	5190.05	4507.14	15200.43	132664.38	148192.98	136860.27	144820.40
153	5253.96	4575.36	15376.12	133714.80	149180.22	137767.11	145782.57
154	5262.67	4585.44	15401.32	134765.23	150168.74	138678.53	146749.76
155	5272.12	4598.89	15434.20	135816.02	151159.67	139595.56	147721.71
156	5278.96	4612.87	15468.04	136867.08	152150.96	140517.57	148699.26
157	5370.53	4800.23	15924.91	137918.40	153143.70	141444.12	149680.45
158	5464.02	4983.16	16373.08	138969.94	154135.84	142373.92	150664.72
159	5560.54	5163.47	16819.33	140021.73	155126.82	143305.54	151648.79
160	5655.53	5315.55	17205.41	141073.72	156114.90	144235.34	152630.10
161	5664.96	5335.69	17255.97	142126.05	157098.87	145158.37	153603.81
162	5774.02	5568.51	17841.74	143178.51	158077.85	146075.11	154570.98
163	5884.78	5785.26	18392.95	144231.23	159053.36	146985.70	155532.71
164	5995.15	5981.60	18900.95	145284.14	160026.37	147891.31	156489.88
165	6107.09	6190.71	19438.28	146337.10	160996.06	148792.41	157442.80
166	6123.70	6214.35	19503.05	147390.08	161963.94	149689.83	158392.34
167	6228.37	6372.62	19928.13	148443.07	162929.02	150583.62	159338.36
168	6335.29	6534.31	20366.15	149496.20	163892.16	151474.83	160281.35
169	6430.24	6635.65	20691.07	150549.43	164854.38	152364.08	161222.79
170	6528.74	6749.55	21039.59	151602.68	165814.39	153250.46	162161.54
171	6626.42	6862.51	21387.22	152656.02	166773.89	154134.57	163097.94
172	6717.26	6951.39	21692.58	153709.44	167730.82	155016.77	164032.59
173	6744.80	6973.44	21780.46	154762.88	168686.57	155896.98	164965.39
174	6776.54	6993.20	21879.39	155816.47	169640.67	156775.44	165896.56
175	6844.33	7029.38	22089.34	156870.15	170594.05	157652.33	166825.49
176	6912.12	7065.56	22299.30	157923.86	171545.97	158527.90	167753.37

hour	Air Change	Air Change (ACH)	ASHRAE Enhanced	Enhanced Model	Angular Cracks	Mixed Cracks	Straight Cracks
177	6989.64	7120.72	22545.13	158977.51	172499.74	159405.94	168683.73
178	7015.19	7141.18	22626.67	160031.01	173455.45	160289.31	169619.57
179	7041.60	7159.97	22707.96	161084.34	174415.63	161179.26	170562.46
180	7109.74	7202.40	22910.53	162137.50	175378.94	162076.28	171512.21
181	7165.77	7227.32	23068.40	163190.40	176345.56	162979.47	172468.89
182	7226.42	7259.69	23241.47	164243.25	177314.92	163888.51	173430.62
183	7297.29	7310.12	23449.47	165296.01	178285.16	164801.70	174395.98
184	7368.17	7360.56	23657.48	166348.75	179255.02	165715.31	175359.88
185	7399.29	7374.40	23745.96	167401.62	180222.06	166623.86	176318.73
186	7432.37	7386.17	23839.97	168454.58	181187.14	167527.42	177272.25
187	7479.21	7398.67	23975.83	169507.77	182149.97	168426.56	178221.79
188	7514.25	7411.13	24078.90	170561.08	183110.79	169321.75	179167.82
189	7567.32	7430.02	24235.03	171614.42	184070.16	170213.63	180110.70
190	7605.06	7430.02	24343.97	172667.70	185029.44	171102.81	181051.86
191	7653.40	7447.22	24483.78	173720.90	185986.99	171989.90	181990.78
192	7704.02	7465.23	24628.93	174774.02	186944.69	172875.69	182928.44
193	7753.63	7482.88	24768.67	175826.98	187901.80	173760.43	183865.81
194	7814.86	7515.56	24944.90	176879.90	188859.59	174644.11	184802.26
195	7844.88	7528.91	25030.23	177932.82	189816.81	175526.98	185738.24
196	7869.44	7539.83	25098.82	178985.58	190775.19	176409.13	186673.36
197	7898.14	7552.60	25178.95	180038.32	191732.38	177290.70	187607.84
198	7930.33	7561.19	25267.45	181091.05	192690.41	178171.95	188542.32
199	7961.46	7572.26	25352.75	182143.71	193647.97	179053.04	189476.67
200	8015.23	7596.18	25501.53	183196.35	194606.57	179933.65	190410.67
201	8041.64	7605.57	25573.22	184248.91	195566.67	180817.90	191348.49
202	8072.54	7613.82	25655.77	185301.38	196529.89	181707.53	192291.89
203	8102.20	7624.37	25734.77	186353.77	197496.99	182604.32	193242.47
204	8142.99	7635.26	25841.60	187406.07	198467.55	183508.27	194200.47
205	8193.60	7657.77	25973.82	188458.20	199442.00	184419.17	195165.45
206	8243.08	7679.77	26100.51	189510.16	200419.81	185336.19	196136.07
207	8264.17	7692.90	26155.88	190562.02	201398.27	186256.91	197109.41
208	8289.57	7706.46	26223.23	191614.06	202376.37	187178.29	198081.71
209	8315.44	7720.27	26292.50	192666.19	203352.18	188094.65	199048.96
210	8340.16	7735.66	26360.53	193718.41	204325.77	189006.30	200011.55
211	8407.55	7783.62	26550.14	194770.66	205297.83	189913.97	200970.72
212	8474.94	7831.57	26739.75	195822.91	206268.26	190818.04	201927.03
213	8542.33	7879.53	26929.37	196875.17	207238.56	191719.13	202880.34

hour	Air Change	Air Change (ACH)	ASHRAE Enhanced	Enhanced Model	Angular Cracks	Mixed Cracks	Straight Cracks
214	8565.56	7896.05	26994.71	197927.43	208207.05	192617.53	203831.66
215	8584.69	7914.77	27053.53	198979.69	209175.49	193513.83	204780.72
216	8603.82	7933.49	27112.36	200031.96	210142.44	194408.54	205728.65
217	8621.75	7952.63	27169.51	201084.22	211109.12	195301.86	206675.38
218	8639.69	7971.78	27226.66	202136.48	212075.73	196194.02	207621.09
219	8657.62	7990.92	27283.81	203188.74	213041.41	197085.20	208565.32
220	8746.44	8101.52	27590.00	204241.00	214007.26	197975.07	209508.48
221	8762.23	8121.19	27644.44	205293.26	214972.11	198863.90	210451.98
222	8778.02	8140.85	27698.88	206345.53	215936.58	199752.06	211393.56
223	8791.17	8160.74	27750.44	207397.79	216900.87	200639.57	212335.05
224	8882.41	8282.48	28078.43	208450.05	217865.48	201526.28	213275.66
225	8973.66	8404.22	28406.43	209502.31	218830.96	202415.51	214218.66
226	8986.81	8424.11	28457.99	210554.57	219799.49	203309.77	215166.86
227	8999.96	8444.00	28509.56	211606.83	220770.36	204210.21	216120.65
228	9011.04	8463.71	28559.19	212659.10	221744.24	205117.53	217081.78
229	9023.22	8483.21	28608.89	213711.29	222720.82	206031.25	218049.83
230	9035.10	8502.24	28657.20	214763.39	223700.61	206950.07	219022.07
231	9048.02	8521.76	28707.60	215815.56	224679.77	207872.21	219996.49
232	9142.58	8656.35	29064.20	216867.87	225657.94	208794.07	220968.99
233	9235.55	8772.13	29392.13	217920.41	226632.18	209710.42	221935.28
234	9326.60	8877.41	29703.04	218973.08	227603.78	210621.41	222896.81
235	9415.29	8972.07	29997.10	220025.84	228572.60	211527.29	223853.53
236	9441.03	8992.68	30076.89	221078.85	229538.95	212428.61	224806.47
237	9520.40	9056.22	30324.71	222131.97	230503.43	213325.69	225754.82
238	9596.62	9110.46	30562.87	223185.34	231465.04	214218.93	226699.83
239	9667.79	9154.78	30783.01	224238.83	232424.29	215108.80	227641.46
240	9745.31	9209.94	31028.84	225292.42	233382.00	215995.88	228580.84
241	9817.08	9254.63	31252.53	226346.03	234338.22	216880.69	229517.42
242	9888.25	9298.94	31472.66	227399.59	235293.59	217763.22	230452.47
243	9947.88	9325.46	31653.90	228453.21	236247.20	218644.27	231386.32
244	10001.52	9344.55	31815.67	229506.84	237200.38	219523.56	232317.86
245	10054.66	9363.45	31974.62	230560.40	238153.57	220402.62	233249.41
246	10102.00	9380.30	32109.18	231613.53	239108.72	221281.93	234181.73
247	10162.86	9412.78	32279.79	232666.30	240064.03	222161.56	235114.28
248	10233.21	9462.84	32481.16	233718.84	241020.75	223041.67	236048.03
249	10310.81	9531.87	32712.01	234771.19	241980.51	223926.20	236986.09
250	10402.53	9654.24	33039.97	235823.42	242943.77	224816.35	237929.69



hour	Air Change	Air Change (ACH)	ASHRAE Enhanced	Enhanced Model	Angular Cracks	Mixed Cracks	Straight Cracks
251	10481.62	9731.63	33281.36	236875.62	243911.09	225714.08	238881.53
252	10563.05	9818.55	33537.35	237927.73	244882.62	226619.05	239840.19
253	10644.48	9905.47	33793.33	238979.82	245856.97	227530.34	240805.70
254	10726.66	10007.80	34073.36	240031.90	246834.59	228447.52	241777.41
255	10785.04	10059.74	34244.33	241083.98	247813.06	229369.00	242752.01
256	10846.72	10120.09	34431.21	242136.06	248792.02	230291.83	243726.39
257	10905.10	10172.02	34602.18	243188.14	249768.44	231209.20	244695.43
258	10964.11	10224.51	34776.35	244240.29	250741.78	232122.04	245659.60
259	11024.21	10277.97	34956.53	245292.60	251714.07	233030.41	246619.70
260	11057.05	10310.10	35058.24	246344.93	252684.97	233934.74	247576.55
261	11090.38	10348.64	35169.99	247397.34	253653.26	234836.00	248529.87
262	11109.30	10365.47	35228.00	248449.92	254620.55	235734.33	249481.30
263	11123.87	10382.31	35277.15	249502.45	255586.84	236630.09	250430.12
264	11137.36	10399.12	35324.48	250554.99	256552.79	237524.00	251377.08
265	11170.69	10440.63	35440.71	251607.45	257517.77	238416.58	252323.13
266	11182.64	10456.57	35483.89	252659.83	258483.22	239308.06	253268.02
267	11192.52	10467.99	35516.80	253712.20	259447.49	240198.49	254211.75
268	11201.31	10478.94	35547.13	254764.49	260412.31	241087.81	255154.85
269	11208.92	10489.77	35575.82	255816.83	261376.16	241976.37	256097.83
270	11216.34	10500.32	35603.64	256869.11	262340.45	242864.41	257039.58
271	11226.93	10511.64	35637.42	257921.38	263304.58	243751.77	257980.79
272	11234.35	10522.19	35665.24	258973.64	264268.27	244638.76	258921.69
273	11240.55	10532.13	35690.57	260025.84	265234.71	245529.03	259865.92
274	11247.08	10542.00	35715.94	261077.94	266204.01	246425.38	260816.54
275	11251.44	10550.13	35735.95	262129.75	267177.58	247329.00	261774.63
276	11259.64	10562.54	35766.97	263181.36	268155.85	248240.49	262741.06
277	11268.13	10573.86	35795.53	264232.64	269138.22	249159.44	263716.31
278	11275.52	10584.38	35821.36	265283.72	270124.40	250085.23	264697.12
279	11280.58	10591.14	35838.02	266334.59	271113.35	251015.70	265682.23
280	11289.94	10601.13	35864.37	267385.35	272103.18	251948.46	266668.01
281	11297.81	10610.93	35888.83	268436.08	273092.75	252879.13	267651.38
282	11305.70	10617.94	35908.92	269486.73	274080.90	253805.72	268630.79
283	11316.71	10625.78	35935.77	270537.57	275067.08	254728.20	269606.32
284	11326.77	10633.83	35961.37	271588.51	276053.31	255647.28	270579.39
285	11338.72	10644.46	35992.69	272639.40	277037.64	256563.73	271549.32
286	11363.80	10666.77	36058.44	273690.28	278021.99	257477.77	272517.94
287	11387.90	10688.21	36120.45	274741.03	279005.88	258389.75	273484.25



hour	Air Change	Air Change (ACH)	ASHRAE Enhanced	Enhanced Model	Angular Cracks	Mixed Cracks	Straight Cracks
288	11399.85	10698.84	36151.77	275791.90	279988.48	259299.73	274449.42
289	11412.15	10709.78	36184.30	276842.84	280971.11	260208.68	275412.82
290	11423.37	10720.75	36215.23	277893.81	281952.24	261115.42	276374.94
291	11435.25	10732.38	36248.52	278944.93	282932.55	262020.51	277334.58
292	11462.30	10758.85	36324.96	279996.14	283912.39	262924.32	278293.27
293	11488.86	10787.20	36402.66	281047.30	284892.10	263827.19	279251.12
294	11547.33	10854.81	36579.15	282098.32	285872.77	264730.45	280209.72
295	11604.57	10910.82	36729.02	283148.89	286853.92	265633.73	281168.73
296	11666.91	10988.44	36917.72	284199.31	287837.78	266537.78	282128.25
297	11731.75	11098.04	37171.18	285249.48	288823.46	267446.32	283092.25
298	11793.02	11196.14	37396.15	286299.44	289813.09	268361.54	284063.55
299	11854.91	11306.23	37647.67	287349.22	290807.39	269284.37	285042.64
300	11915.86	11420.09	37908.17	288398.88	291805.36	270214.96	286030.01
301	11974.35	11534.55	38170.78	289448.44	292808.03	271153.17	287024.56
302	12031.79	11636.72	38401.82	290497.90	293813.19	272097.35	288025.15
303	12088.66	11732.84	38618.21	291547.34	294820.06	273046.69	289029.65
304	12146.09	11835.02	38849.25	292596.77	295827.27	273998.12	290034.85
305	12203.40	11931.87	39067.29	293646.20	296833.07	274946.25	291035.99
306	12261.57	12025.00	39277.22	294695.69	297834.75	275888.69	292030.82
307	12339.78	12261.54	39878.67	295745.84	298832.71	276825.13	293020.17
308	12428.36	12545.18	40614.41	296796.52	299828.35	277755.75	294004.21
309	12521.84	12844.54	41393.09	297847.53	300819.80	278681.20	294983.31
310	12619.54	13140.00	42153.90	298898.84	301808.05	279601.47	295957.35
311	12722.02	13449.94	42954.60	299950.43	302793.46	280517.58	296926.63
312	12823.09	13701.67	43584.42	301002.16	303776.54	281429.92	297893.09
313	12923.77	13970.33	44262.41	302053.86	304759.17	282339.15	298856.02
314	13025.99	14243.10	44951.76	303105.64	305740.30	283245.56	299816.47
315	13129.74	14519.96	45652.49	304157.50	306720.62	284149.36	300774.86
316	13236.54	14804.98	46375.99	305209.52	307700.46	285050.37	301729.22
317	13340.66	15008.72	46886.76	306261.79	308680.17	285948.84	302681.58
318	13447.27	15226.83	47434.29	307314.18	309660.83	286845.13	303631.89
319	13557.33	15471.57	48050.54	308366.67	310641.99	287739.25	304579.31
320	13665.44	15683.15	48585.53	309419.26	311625.84	288631.43	305525.25
321	13770.79	15870.56	49063.87	310471.87	312610.43	289525.88	306472.93
322	13869.70	16020.13	49456.89	311524.42	313598.19	290424.36	307425.14
323	13972.22	16193.39	49901.07	312576.96	314589.89	291329.06	308383.89
324	14072.25	16362.44	50331.23	313629.35	315584.57	292240.03	309350.12

hour	Air Change	Air Change (ACH)	ASHRAE Enhanced	Enhanced Model	Angular Cracks	Mixed Cracks	Straight Cracks
325	14165.67	16495.40	50681.82	314681.66	316583.37	293157.34	310321.31
326	14251.02	16594.10	50962.66	315733.86	317584.19	294079.77	311297.89
327	14333.90	16682.56	51223.20	316785.98	318586.37	295006.13	312277.22
328	14400.02	16729.62	51406.01	317838.07	319588.63	295932.84	313255.53
329	14468.37	16778.25	51596.63	318890.23	320590.40	296856.07	314229.39
330	14510.75	16789.56	51709.86	319942.61	321588.66	297774.25	315198.52
331	14543.43	16795.38	51797.65	320995.10	322583.66	298687.03	316162.40
332	14569.09	16804.51	51867.99	322047.68	323576.71	299595.34	317122.82
333	14593.17	16815.22	51934.00	323100.22	324565.91	300499.83	318079.21
334	14618.15	16826.33	52003.76	324152.90	325552.18	301401.10	319032.70
335	14635.40	16837.07	52052.51	325205.46	326535.86	302299.92	319984.58
336	14648.60	16847.64	52091.26	326257.94	327517.42	303196.79	320934.17
337	14663.16	16858.00	52132.58	327310.32	328496.69	304092.40	321883.40
338	14674.64	16868.21	52167.01	328362.69	329474.89	304986.63	322830.82
339	14683.90	16878.09	52196.70	329415.05	330450.90	305879.59	323777.46
340	14692.92	16887.72	52225.45	330467.34	331424.37	306771.22	324722.58
341	14701.51	16896.89	52252.82	331519.61	332396.66	307661.98	325667.24
342	14709.26	16905.85	52278.50	332571.87	333366.55	308552.19	326611.17
343	14716.15	16914.44	52302.12	333624.07	334334.98	309442.16	327554.97
344	14723.23	16923.24	52326.23	334676.18	335301.86	310332.18	328498.70
345	14728.52	16930.79	52345.72	335728.13	336269.74	311225.18	329445.55
346	14734.12	16938.75	52366.31	336780.04	337238.87	312124.32	330398.90
347	14738.98	16946.10	52384.85	337831.81	338211.10	313030.65	331359.83
348	14744.14	16952.98	52402.61	338883.40	339185.98	313944.58	332328.41
349	14748.58	16959.30	52418.45	339934.81	340163.99	314865.50	333305.34
350	14754.93	16966.08	52437.18	340986.12	341144.39	315792.86	334287.46
351	14760.90	16972.46	52454.52	342037.25	342125.48	316724.80	335273.74
352	14766.39	16978.80	52471.07	343088.28	343106.52	317658.55	336259.91
353	14772.65	16984.93	52488.20	344139.21	344084.85	318590.53	337244.30
354	14777.96	16991.06	52504.11	345190.12	345060.45	319518.16	338224.05
355	14790.04	16997.51	52532.30	346241.08	346033.47	320441.61	339200.43
356	14799.64	17004.34	52556.19	347292.13	347004.87	321361.53	340173.16
357	14812.06	17010.97	52585.54	348343.19	347974.22	322278.03	341142.76
358	14823.94	17018.37	52614.89	349394.40	348942.26	323191.00	342110.31
359	14838.41	17026.09	52650.61	350445.77	349909.66	324101.67	343074.39
360	14854.99	17033.46	52691.30	351497.25	350876.16	325009.64	344035.97
361	14873.33	17041.62	52737.77	352548.98	351842.34		

hour	Air Change	Air Change (ACH)	ASHRAE Enhanced	Enhanced Model	Angular Cracks	Mixed Cracks	Straight Cracks
362	14897.50	17050.22	52800.23	353600.96	352808.34		
363	14924.74	17059.91	52870.66	354652.99	353773.69		
364	14956.71	17059.91	52953.04	355705.12	354738.87		
365	14984.02	17067.20	53023.82	356757.27	355704.12		
366	15015.00	17067.20	53102.01	357809.29	356668.73		
367	15041.77	17076.72	53170.48	358861.30	357634.52		
368	15065.00	17084.99	53229.30	359913.22	358599.94		
369	15094.02	17084.99	53299.38	360964.91	359566.99		
370	15128.95	17097.42	53384.06	362016.49	360538.06		
371	15181.32	17125.37	53514.75	363068.04	361513.01		
372	15206.97	17132.21	53575.01	364119.44	362491.82		
373	15247.04	17146.47	53666.63	365170.60	363474.60		
374	15283.27	17159.36	53748.46	366221.63	364460.79		
375	15318.14	17174.87	53828.33	367272.64	365448.87		
376	15362.46	17198.52	53930.61	368323.56	366437.82		
377	15387.55	17211.91	53988.49	369374.46	367427.55		
378	15425.71	17225.49	54073.61	370425.35	368414.16		
379	15453.44	17230.42	54133.73	371476.17	369399.91		
380	15491.06	17243.81	54216.56	372526.98	370383.94		
381	15554.31	17300.07	54380.83	373577.78	371366.88		
382	15621.58	17371.87	54571.70	374628.58	372348.13		
383	15684.62	17427.95	54736.93	375679.44	373328.29		
384	15751.61	17493.49	54920.06	376730.32	374306.17		
385	15800.14	17519.40	55033.38	377781.28	375283.06		
386	15872.85	17603.48	55252.85	378832.25	376257.87		
387	15941.77	17664.78	55441.73	379883.50	377231.20		
388	15990.69	17686.54	55565.69	380935.17	378202.85		
389	16031.59	17701.09	55668.15	381986.91	379173.82		
390	16067.02	17713.69	55755.00	383038.54	380144.60		
391	16091.15	17720.13	55813.03	384090.10	381114.81		
392	16106.12	17728.12	55849.99	385141.57	382085.02		
393	16120.71	17735.91	55885.62	386192.95	383057.51		
394	16129.10	17743.37	55908.41	387244.24	384032.42		
395	16138.30	17750.74	55932.31	388295.44	385012.22		
396	16146.20	17757.76	55953.38	389346.54	385995.19		
397	16154.48	17764.39	55974.46	390397.56	386982.06		
398	16166.77	17770.95	56002.83	391448.48	387971.41		

hour	Air Change	Air Change (ACH)	ASHRAE Enhanced	Enhanced Model	Angular Cracks	Mixed Cracks	Straight Cracks
399	16178.70	17777.32	56030.05	392499.31	388963.31		
400	16192.01	17787.98	56063.28	393550.13	389956.17		
401	16204.99	17799.52	56097.30	394601.00	390947.55		
402	16216.86	17811.13	56130.00	395651.95	391936.89		
403	16235.74	17824.57	56178.44	396703.21	392924.81		
404	16248.51	17840.47	56220.16	397754.58	393912.68		
405	16258.70	17856.77	56260.54	398806.06	394898.48		
406	16343.00	17976.76	56564.58	399857.57	395883.55		
407	16353.40	17994.34	56608.30	400909.30	396868.00		
408	16450.03	18166.23	57036.65	401961.22	397852.29		
409	16460.90	18185.58	57085.19	403013.32	398835.41		
410	16565.01	18389.32	57595.95	404065.60	399817.08		
411	16671.80	18598.29	58122.85	405118.06	400796.37		
412	16782.47	18805.01	58652.40	406170.85	401774.49		
413	16895.31	19005.76	59175.31	407223.92	402751.07		
414	17009.00	19187.79	59668.09	408277.33	403727.55		
415	17120.97	19347.15	60123.18	409331.03	404703.02		
416	17224.12	19466.43	60502.87	410384.87	405678.91		
417	17327.27	19585.70	60882.55	411438.75	406656.25		
418	17429.52	19703.94	61256.85	412492.57	407636.26		
419	17530.86	19821.13	61625.80	413546.33	408620.18		
420	17613.07	19886.94	61890.04	414599.92	409607.48		
421	17695.67	19953.06	62151.75	415653.35	410598.42		
422	17760.61	19987.73	62345.07	416706.67	411591.55		
423	17830.95	20031.52	62555.89	417759.89	412586.21		
424	17912.08	20096.47	62809.21	418813.08	413580.95		
425	17996.15	20171.25	63078.51	419866.27	414574.40		
426	18023.24	20192.94	63164.34	420919.59	415564.23		
427	18042.64	20218.83	63238.91	421973.01	416551.85		
428	18063.15	20246.19	63318.89	423026.66	417536.68		
429	18079.42	20275.13	63396.30	424080.50	418520.78		
430	18097.19	20305.16	63478.19	425134.52	419501.55		
431	18225.26	20544.39	64117.97	426188.65	420480.47		
432	18360.62	20821.33	64854.31	427243.03	421456.98		
433	18496.65	21087.52	65570.60	428297.60	422431.62		
434	18632.68	21353.71	66286.88	429352.21	423403.84		
435	18765.71	21590.37	66938.81	430406.91	424374.07		

hour	Air Change	Air Change (ACH)	ASHRAE Enhanced	Enhanced Model	Angular Cracks	Mixed Cracks	Straight Cracks
436	18900.93	21842.96	67626.60	431461.63	425341.05		
437	19043.00	22146.26	68437.06	432516.44	426305.68		
438	19186.33	22452.25	69256.65	433571.32	427267.10		
439	19329.66	22758.23	70076.24	434626.23	428225.88		
440	19475.91	23083.46	70945.86	435681.22	429182.15		
441	19620.50	23392.12	71774.59	436736.22	430138.80		
442	19763.28	23684.24	72563.39	437791.22	431096.76		
443	19907.87	23992.90	73392.11	438846.24	432057.57		
444	20052.84	24315.28	74252.22	439901.18	433020.92		
445	20196.17	24621.26	75071.81	440956.11	433986.80		
446	20341.14	24943.64	75931.92	442011.03	434954.85		
447	20478.37	25212.20	76656.59	443065.81	435924.67		
448	20617.27	25484.01	77390.01	444120.57	436894.15		
449	20756.70	25769.26	78152.39	445175.24	437861.99		
450	20894.86	26051.91	78905.88	446229.83	438826.42		
451	21021.50	26254.68	79476.28	447284.33	439787.97		
452	21151.08	26485.20	80105.16	448338.80	440746.65		
453	21280.14	26703.33	80708.44	449393.27	441703.54		
454	21401.22	26875.65	81216.01	450447.74	442657.37		
455	21514.19	27026.38	81667.32	451501.99	443608.97		
456	21623.75	27162.81	82090.50	452556.20	444557.98		
457	21728.67	27284.14	82480.97	453610.33	445506.15		
458	21836.36	27418.25	82892.73	454664.37	446451.92		
459	21937.51	27526.22	83253.80	455718.32	447395.64		
460	22037.80	27633.26	83609.66	456772.17	448337.98		
461	22141.95	27753.71	83990.95	457826.01	449278.82		
462	22256.03	27936.36	84483.47	458879.55	450218.03		
463	22368.50	28106.43	84954.12	459933.19	451155.76		
464	22473.35	28237.00	85348.84	460986.90	452092.93		
465	22563.91	28317.55	85651.05	462040.61	453030.42		
466	22664.32	28433.66	86010.43	463094.13	453970.01		
467	22775.97	28632.28	86524.33	464147.25	454912.19		
468	22885.06	28826.37	87023.10	465200.16	455857.82		
469	22988.82	29001.72	87474.30	466252.87	456805.59		
470	23091.28	29174.88	87916.57	467305.39	457755.34		
471	23193.90	29357.45	88377.82	468357.80	458706.15		
472	23296.49	29549.09	88858.12	469410.11	459658.13		

hour	Air Change	Air Change (ACH)	ASHRAE Enhanced	Enhanced Model	Angular Cracks	Mixed Cracks	Straight Cracks
473	23397.80	29729.32	89311.92	470462.39	460607.52		
474	23494.43	29875.44	89690.75	471514.66	461555.24		
475	23586.15	29997.82	90018.71	472566.85	462501.43		
476	23680.62	30140.67	90385.78	473618.96	463446.33		
477	23773.25	30272.50	90729.99	474671.06	464389.86		
478	23862.69	30391.83	91046.36	475723.07	465333.39		
479	23946.33	30488.55	91316.35	476775.00	466276.59		
480	24034.61	30606.34	91626.94	477826.91	467220.12		
481	24123.65	30733.07	91952.94	478878.74	468163.03		
482	24202.17	30816.87	92194.64	479930.55	469106.23		
483	24284.74	30912.36	92459.48	480982.36	470049.62		
484	24367.32	31007.85	92724.32	482034.17	470993.22		
485	24441.65	31073.97	92938.53	483086.04	471938.21		
486	24516.22	31140.30	93156.92	484138.07	472882.92		
487	24595.90	31218.26	93398.30	485190.13	473827.86		
488	24676.78	31304.60	93649.07	486242.05	474773.42		
489	24757.67	31390.94	93899.84	487293.96	475721.09		
490	24839.27	31492.56	94168.11	488345.58	476673.79		
491	24923.77	31627.85	94498.90	489396.93	477629.92		
492	25004.28	31756.75	94810.08	490448.02	478590.98		
493	25084.90	31928.86	95222.78	491498.83	479556.86		
494	25165.11	32107.23	95651.62	492549.51	480525.78		
495	25239.46	32226.27	95934.13	493600.15	481498.73		
496	25312.67	32336.98	96198.30	494650.78	482471.48		
497	25383.22	32431.11	96427.63	495701.40	483444.79		
498	25457.74	32543.80	96697.78	496752.09	484415.68		
499	25527.15	32624.06	96904.39	497802.85	485385.93		
500	25603.80	32733.14	97171.03	498853.71	486355.19		
501	25686.39	32880.07	97523.47	499904.65	487324.56		
502	25768.23	33011.11	97841.16	500955.69	488293.86		
503	25850.08	33142.15	98158.86	502006.74	489262.63		
504	25927.68	33245.70	98418.53	503057.81	490231.22		
505	25997.45	33313.97	98615.69	504109.02	491199.97		
506	26073.29	33408.41	98857.40	505160.11	492169.39		
507	26154.27	33538.06	99171.74	506211.19	493138.54		
508	26220.39	33596.88	99348.22	507262.26	494107.02		
509	26283.22	33647.18	99509.80	508313.33	495075.40		

hour	Air Change	Air Change (ACH)	ASHRAE Enhanced	Enhanced Model	Angular Cracks	Mixed Cracks	Straight Cracks
510	26349.93	33706.52	99691.05	509364.55	496042.94		
511	26416.64	33765.86	99872.29	510415.79	497010.31		
512	26471.08	33804.60	100009.14	511466.96	497977.56		
513	26525.52	33843.34	100145.99	512518.13	498948.16		
514	26595.49	33930.47	100367.59	513569.15	499922.19		
515	26661.89	34001.34	100560.37	514620.22	500900.89		
516	26733.78	34097.26	100799.55	515671.22	501885.32		
517	26802.68	34183.06	101016.40	516722.14	502873.21		
518	26873.46	34277.50	101250.53	517773.04	503864.82		
519	26939.15	34376.84	101490.93	518823.93	504858.41		
520	26996.80	34443.50	101663.73	519874.82	505854.12		
521	27063.48	34544.33	101908.90	520925.78	506847.59		
522	27130.21	34639.31	102144.70	521976.89	507839.97		
523	27157.76	34671.16	102230.15	523028.17	508829.34		
524	27185.79	34696.10	102307.65	524079.56	509817.19		
525	27233.78	34730.25	102433.16	525131.05	510803.78		
526	27282.93	34765.22	102564.16	526182.70	511788.68		
527	27311.95	34783.29	102638.87	527234.32	512772.94		
528	27360.52	34817.86	102767.12	528285.94	513755.27		
529	27402.27	34840.13	102872.38	529337.55	514737.27		
530	27458.11	34879.87	103015.61	530388.96	515718.96		
531	27521.39	34930.53	103181.46	531440.26	516700.45		
532	27576.54	34964.87	103317.73	532491.54	517680.47		
533	27627.01	34991.81	103439.65	533542.80	518660.53		
534	27680.01	35024.81	103574.73	534594.27	519639.23		
535	27738.61	35061.30	103727.12	535645.92	520618.25		
536	27781.41	35084.13	103837.26	536697.67	521596.63		
537	27830.55	35119.11	103968.26	537749.38	522576.74		
538	27881.26	35159.70	104103.67	538800.88	523559.37		
539	27941.11	35212.94	104261.98	539851.99	524545.41		
540	27992.67	35249.62	104386.26	540902.88	525534.47		
541	28039.72	35291.48	104505.05	541953.51	526526.35		
542	28090.16	35345.32	104642.58	543003.93	527520.58		
543	28133.11	35379.70	104744.40	544054.31	528516.00		
544	28154.75	35397.03	104795.15	545104.59	529511.09		
545	28197.02	35430.87	104894.28	546154.86	530504.71		
546	28246.63	35483.82	105028.47	547205.11	531494.70		



hour	Air Change	Air Change (ACH)	ASHRAE Enhanced	Enhanced Model	Angular Cracks	Mixed Cracks	Straight Cracks
547	28292.25	35524.40	105141.41	548255.43	532483.13		
548	28353.90	35590.20	105308.14	549305.69	533468.10		
549	28414.64	35655.03	105472.42	550355.94	534451.12		
550	28487.63	35771.91	105748.62	551406.41	535432.23		
551	28564.36	35901.59	106056.74	552457.04	536412.82		
552	28643.42	36042.24	106391.78	553507.79	537391.23		
553	28712.84	36122.50	106598.38	554558.56	538369.46		
554	28781.18	36195.45	106792.29	555609.35	539346.93		
555	28841.34	36243.62	106942.53	556660.14	540324.71		
556	28909.69	36316.57	107136.44	557710.93	541301.71		
557	28963.15	36349.86	107262.89	558761.80	542277.91		
558	29011.03	36375.41	107373.37	559812.68	543254.12		
559	29048.50	36395.41	107459.84	560863.56	544228.81		
560	29081.32	36404.17	107531.39	561914.38	545202.46		
561	29111.73	36414.99	107597.50	562965.11	546178.22		
562	29154.21	36437.66	107692.00	564015.76	547157.89		
563	29194.34	36466.21	107783.47	565066.17	548141.00		
564	29260.61	36584.11	108055.64	566116.26	549128.66		
565	29335.42	36723.85	108384.45	567166.63	550120.47		
566	29404.03	36827.60	108627.33	568216.90	551116.41		
567	29478.01	36972.38	108968.05	569267.23	552113.74		
568	29483.33	36985.63	109000.81	570318.20	553112.70		
569	29582.30	37205.71	109545.20	571369.78	554110.69		
570	29589.72	37223.53	109589.85	572421.69	555106.55		
571	29703.41	37547.14	110424.31	573473.99	556101.89		
572	29820.71	37891.45	111319.00	574526.50	557095.01		
573	29828.40	37911.99	111371.67	575579.16	558088.00		
574	29837.61	37934.10	111428.02	576631.99	559078.32		
575	29955.18	38216.47	112147.53	577684.86	560068.13		
576	30073.58	38479.76	112819.43	578737.89	561055.85		
577	30194.43	38759.24	113534.61	579791.03	562043.41		
578	30310.40	38986.20	114118.43	580844.18	563029.71		
579	30429.02	39239.42	114766.40	581897.35	564015.52		
580	30543.50	39453.26	115319.35	582950.53	564999.85		
581	30652.59	39627.92	115784.78	584003.70	565983.95		
582	30762.83	39804.44	116257.03	585056.95	566966.95		
583	30865.78	39941.80	116648.75	586110.21	567950.09		



hour	Air Change	Air Change (ACH)	ASHRAE Enhanced	Enhanced Model	Angular Cracks	Mixed Cracks	Straight Cracks
584	30971.44	40082.78	117052.77	587163.55	568932.58		
585	31079.76	40236.93	117483.08	588216.90	569917.17		
586	31174.70	40338.28	117808.00	589270.19	570905.74		
587	31271.27	40449.94	118145.72	590323.32	571898.20		
588	31355.52	40524.89	118411.79	591376.36	572893.49		
589	31438.14	40598.38	118668.95	592429.23	573892.07		
590	31513.86	40658.99	118896.55	593482.00	574892.79		
591	31578.86	40699.47	119081.90	594534.67	575893.02		
592	31625.66	40724.45	119211.94	595587.24	576890.62		
593	31659.98	40739.71	119306.88	596639.87	577884.07		
594	31686.06	40753.63	119380.02	597692.49	578872.75		
595	31711.05	40764.74	119449.78	598745.19	579856.76		
596	31725.18	40776.06	119492.26	599797.90	580836.69		
597	31741.34	40788.99	119540.84	600850.62	581813.65		
598	31755.90	40801.94	119585.81	601903.34	582786.70		
599	31767.83	40814.68	119625.14	602956.06	583757.79		
600	31779.41	40826.01	119662.27	604008.85	584725.40		
601	31787.61	40836.22	119691.19	605061.51	585692.04		
602	31797.90	40846.29	119723.53	606114.08	586656.65		
603	31806.70	40856.46	119753.20	607166.63	587619.34		
604	31814.50	40866.18	119780.41	608219.10	588581.14		
605	31822.77	40877.21	119810.29	609271.49	589541.50		
606	31830.83	40887.96	119839.27	610323.78	590500.61		
607	31839.62	40898.92	119869.59	611376.06	591458.19		
608	31849.07	40909.84	119900.68	612428.26	592414.27		
609	31859.21	40920.66	119932.53	613480.37	593371.89		
610	31872.73	40931.49	119970.62	614532.39	594332.02		
611	31885.28	40941.53	120005.04	615584.18	595295.13		
612	31893.42	40950.22	120029.23	616635.64	596262.23		
613	31899.53	40957.29	120047.42	617686.61	597231.88		
614	31907.56	40963.72	120066.45	618737.13	598205.50		
615	31971.86	41089.55	120358.42	619787.19	599179.44		
616	32035.99	41197.93	120607.14	620837.15	600154.98		
617	32100.11	41306.31	120855.86	621887.06	601128.32		
618	32164.93	41421.61	121121.12	622936.96	602099.15		
619	32226.46	41509.19	121323.06	623986.85	603067.95		
620	32289.82	41610.63	121555.69	625036.73	604034.94		

hour	Air Change	Air Change (ACH)	ASHRAE Enhanced	Enhanced Model	Angular Cracks	Mixed Cracks	Straight Cracks
621	32361.00	41737.26	121851.08	626086.90	605000.77		
622	32372.75	41749.80	121884.17	627137.47	605965.57		
623	32451.72	41855.17	122151.42	628188.54	606929.22		
624	32535.19	41981.38	122464.08	629239.78	607892.05		
625	32547.46	41997.76	122506.34	630291.22	608855.55		
626	32637.46	42157.86	122898.45	631342.71	609817.89		
627	32708.60	42221.15	123100.15	632394.37	610780.21		
628	32786.13	42303.90	123337.14	633446.05	611742.34		
629	32857.28	42367.19	123538.83	634497.75	612705.74		
630	32920.48	42412.16	123707.30	635549.46	613668.23		
631	32991.63	42475.45	123909.00	636601.17	614631.57		
632	33059.01	42529.39	124093.87	637652.88	615594.64		
633	33142.72	42633.64	124374.09	638704.67	616561.19		
634	33231.14	42767.35	124711.49	639756.39	617530.70		
635	33317.84	42890.73	125027.30	640808.11	618504.88		
636	33407.82	43034.81	125387.02	641859.82	619484.33		
637	33497.81	43178.88	125746.75	642911.53	620470.63		
638	33581.43	43290.45	126036.15	643963.17	621461.10		
639	33672.45	43436.18	126400.02	645014.87	622455.78		
640	33755.07	43539.07	126674.94	646066.58	623452.20		
641	33837.36	43634.23	126940.57	647118.43	624449.40		
642	33912.56	43701.12	127159.07	648170.38	625445.61		
643	33988.64	43768.80	127381.86	649222.42	626441.36		
644	34066.24	43837.82	127612.72	650274.63	627435.07		
645	34120.63	43862.01	127761.81	651327.08	628427.00		
646	34163.40	43873.43	127878.28	652379.65	629416.20		
647	34201.98	43883.72	127984.33	653432.32	630403.20		
648	34237.76	43902.82	128087.31	654485.16	631387.63		
649	34290.02	43926.06	128237.18	655538.11	632371.33		
650	34319.52	43939.18	128321.04	656591.01	633352.00		
651	34348.62	43949.54	128403.74	657643.98	634331.35		
652	34375.89	43961.66	128483.30	658697.11	635308.95		
653	34400.92	43975.02	128557.80	659750.34	636285.89		
654	34420.82	43989.18	128618.56	660803.52	637261.20		
655	34440.72	44003.34	128679.32	661856.70	638235.75		
656	34460.61	44017.50	128740.09	662909.88	639210.24		
657	34478.18	44031.56	128794.53	663962.99	640186.06		

hour	Air Change	Air Change (ACH)	ASHRAE Enhanced	Enhanced Model	Angular Cracks	Mixed Cracks	Straight Cracks
658	34492.73	44044.51	128839.50	665015.80	641163.85		
659	34503.33	44055.82	128873.28	666068.20	642144.75		
660	34511.73	44066.28	128901.90	667120.38	643127.86		
661	34518.83	44075.75	128926.72	668172.29	644113.90		
662	34524.44	44083.23	128946.14	669224.00	645101.45		
663	34531.56	44092.10	128969.55	670275.59	646090.85		
664	34539.16	44100.89	128993.28	671327.07	647078.84		
665	34548.45	44109.98	129019.97	672378.53	648064.76		
666	34557.75	44119.08	129046.66	673429.98	649046.95		
667	34566.13	44128.03	129071.74	674481.42	650026.91		
668	34574.52	44136.98	129096.82	675532.86	651003.44		
669	34584.87	44146.19	129125.45	676584.30	651977.61		
670	34594.94	44155.14	129153.04	677635.66	652949.29		
671	34606.22	44164.17	129182.88	678687.02	653918.62		
672	34618.91	44173.20	129215.43	679738.37	654886.28		
673	34631.60	44182.23	129247.97	680789.71	655852.33		
674	34651.36	44192.78	129296.23	681841.06	656816.19		
675	34669.75	44200.96	129340.39	682892.41	657778.44		
676	34684.35	44208.75	129376.02	683943.75	658739.02		
677	34703.66	44219.05	129422.67	684995.03	659699.22		
678	34722.97	44229.36	129469.32	686046.29	660658.08		
679	34750.02	44248.61	129538.01	687097.55	661615.67		
680	34763.98	44257.30	129572.52	688148.80	662573.61		
681	34776.00	44265.85	129602.71	689199.99	663533.90		
682	34785.22	44274.06	129627.34	690251.09	664497.98		
683	34794.18	44282.02	129651.02	691302.10	665466.16		
684	34805.20	44289.87	129677.87	692353.02	666439.07		
685	34851.46	44326.90	129793.39	693403.85	667416.71		
686	34930.91	44461.18	130114.92	694454.74	668397.32		
687	35019.54	44634.61	130534.92	695505.91	669381.05		
688	35110.09	44803.75	130946.99	696557.27	670365.56		
689	35203.42	44978.09	131374.43	697608.81	671350.25		
690	35294.18	45115.34	131722.32	698660.54	672332.79		
691	35373.67	45200.19	131968.77	699712.38	673313.77		
692	35456.99	45296.53	132239.45	700764.33	674293.74		
693	35556.22	45473.07	132682.41	701816.44	675272.68		
694	35659.95	45648.38	133131.82	702868.86	676251.22		

hour	Air Change	Air Change (ACH)	ASHRAE Enhanced	Enhanced Model	Angular Cracks	Mixed Cracks	Straight Cracks
695	35760.44	45791.39	133518.14	703921.50	677229.05		
696	35872.30	46000.35	134053.44	704974.32	678206.67		
697	35984.02	46179.23	134532.01	706027.47	679172.00		
698	36102.53	46379.50	135068.49	707080.98	680135.07		
699	36224.60	46585.81	135627.11	708134.77	681093.96		
700	36342.47	46764.05	136130.76	709188.77	682050.96		
701	36475.72	47060.36	136905.68	710242.82	683004.99		
702	36600.62	47282.57	137504.02	711296.90	683957.66		
703	36725.66	47493.90	138084.41	712351.13	684907.58		
704	36853.58	47710.08	138680.21	713405.46	685857.00		
705	36964.98	47848.81	139114.86	714459.81	686806.71		
706	37090.02	48060.14	139695.25	715514.10	687758.65		
707	37206.93	48226.53	140176.83	716568.24	688713.49		
708	37320.97	48388.83	140644.51	717622.29	689670.81		
709	37430.58	48525.33	141063.61	718676.31	690630.99		
710	37536.38	48657.09	141463.99	719730.18	691594.13		
711	37634.87	48779.73	141834.75	720783.95	692557.98		
712	37732.48	48901.29	142200.31	721837.62	693522.49		
713	37833.37	49035.89	142591.83	722891.28	694485.68		
714	37919.43	49120.10	142884.86	723944.92	695446.31		
715	38011.19	49218.05	143210.49	724998.70	696404.06		
716	38102.96	49316.00	143536.12	726052.51	697359.62		
717	38187.24	49390.97	143823.01	727106.46	698313.65		
718	38267.21	49454.99	144090.91	728160.52	699265.89		
719	38345.04	49538.07	144368.76	729214.45	700217.24		
720	38429.39	49643.11	144687.94	730268.30	701167.31		
721	38470.56	49679.73	144827.17	731322.21	702114.71		
722	38512.23	49720.50	144972.63	732376.19	703060.87		
723	38583.46	49783.86	145216.64	733430.25	704006.61		
724	38651.19	49838.08	145445.08	734484.40	704950.81		
725	38694.32	49868.78	145588.82	735538.65	705894.75		
726	38725.04	49890.64	145691.89	736592.98	706837.22		
727	38751.72	49914.36	145785.01	737647.34	707780.35		
728	38794.36	49956.09	145935.71	738701.56	708723.85		
729	38836.02	50004.27	146089.92	739755.62	709670.14		
730	38876.71	50051.31	146238.85	740809.50	710618.99		
731	38980.59	50199.16	146657.27	741863.21	711572.13		

hour	Air Change	Air Change (ACH)	ASHRAE Enhanced	Enhanced Model	Angular Cracks	Mixed Cracks	Straight Cracks
732	39089.42	50354.04	147093.59	742916.81	712529.21		
733	39193.40	50492.78	147491.20	743970.23	713490.02		
734	39304.80	50671.14	147970.28	745023.62	714453.18		
735	39415.07	50837.89	148427.83	746077.07	715418.09		
736	39521.09	50979.34	148837.27	747130.59	716382.90		
737	39612.74	51069.02	149147.36	748184.12	717346.24		
738	39707.11	51161.36	149468.66	749237.73	718306.46		
739	39761.25	51180.62	149633.26	750291.43	719264.31		
740	39809.92	51193.61	149780.45	751345.15	720221.57		
741	39853.21	51201.31	149911.00	752398.87	721175.95		
742	39893.89	51212.16	150035.03	753452.67	722129.27		
743	39935.07	51226.81	150162.20	754506.55	723080.48		
744	39998.32	51260.57	150362.61	755560.52	724031.70		

## VITA

### CHADI YOUNES

Born, Lebanon

- 2006 B.E. Civil Engineering  
Lebanese American University  
Byblos, Lebanon
- 2008 M.S. Civil Engineering  
Florida International University  
Miami, Florida
- 2012 Doctoral Candidate  
Florida International University  
Miami, Florida

### PUBLICATIONS, CONFERENCE PAPERS, AND PRESENTATIONS

Younes, C., Abi Shdid, C. & Bitsuamlak, G. , Air Infiltration In Building Envelopes: A Review, *Journal of Building Physics*. 35, No. 3, January 2012.

Younes, C., Abi Shdid, C., Developing an Enhanced Model for Combined Heat and Air Infiltration Energy Simulation, *Journal of Building Physics*. In review

Younes, C., Abi Shdid, C. & Bitsuamlak, G., Thermal Simulation Approach in DOE-2: Outline & Methodology Fundamentals. *Journal of Computer Aided Design*. In review.

Younes C. and Abi Shdid, C., “True Multiphysics Simulation of Air Leakage in Building Envelopes”. *Proceedings of the 2012 Engineering Mechanics Institute and 11th ASCE Joint Specialty Conference on Probabilistic Mechanics and Structural Reliability (EMI/PMC 2012)*, pp 16, June 2012.

Issa, Camille A., and Younis, Chadi, “ Integrating Virtual Reality with Structural Aided Design System”, *Proceedings of 6th International Conference on Construction Applications of Virtual Reality*, August 3- 4, 2006, Orlando, FL, USA

USGBC & LEED Overview, Miami, April 2011

eQUEST, Building Energy Simulation, Miami, April 2011

Air Infiltration Modeling For Building Energy Simulation, Miami, March 2011